

An **IPRF** Research Report
Innovative Pavement Research Foundation
for the Federal Aviation Administration

Report DOT/FAA-01-G-002-2

**Improved Concrete Overlay
Design Parameters
For
Airfield Pavements**

Prepared by

ERES Consultants
A Division of Applied Research Associates, Inc.
505 W. University Avenue
Champaign, IL 61820

Dr. Lev Khazanovich, Principal Investigator

Programs Management Office
1010 Massachusetts Avenue, N.W.
Suite 200
Washington, DC 2001

This document has been prepared for

**Federal Aviation Administration
Airport Technology R&D Branch, AAR-410
William J. Hughes Technical Center
Atlantic City International Airport
New Jersey 08405**

This report was prepared for the Federal Aviation Administration by the Innovative Pavement Research Foundation under the Airport Concrete Pavement Technology Program. Funding is provided by the Federal Aviation Administration under Cooperative Agreement Number 01-G-002. Dr. Satish Agrawal is the Manager of the FAA Airport Technology R&D Branch and the Technical Manager of the Cooperative Agreement.

The Innovative Pavement Research Foundation and the Federal Aviation Administration thanks the Technical Panel that willingly gave of their expertise and time. They were responsible for the oversight and the technical direction provided to the research team for the development of this report. The names of those individuals on the Technical Panel follow.

Dr. Earnest J. Barenberg, P.E.
Dr. Raymond S. Rollings, P.E.
Mr. Robert McChord
Mr. Jim Mack, P.E.
Dr. Gordon F. Hayhoe

Professor Emeritus, University of Illinois
US Army Corps of Engineers
Vice-President, APAC-Georgia, Inc.
American Concrete Pavement Assoc.
FAA Project Technical Advisor

The contents of this report reflect the views of the authors who are responsible for the facts and the accuracy of the data presented within. The contents do not necessarily reflect the official views and policies of the Federal Aviation Administration. This report does not constitute a standard, specification, or regulation.

NOTICE

This document is disseminated under the sponsorship of the U.S. Department of Transportation in the interest of information exchange. The United States Government assumes no liability for the contents or use thereof. The United States Government does not endorse products or manufacturers. Trade or manufacturer's names appear herein solely because they are considered essential to the objective of this report. This document does not constitute FAA certification policy. Consult your local FAA aircraft certification office as to its use.

This report is available at the Federal Aviation Administration William J. Hughes Technical Center's Full-Text Technical Reports page: actlibrary.act.faa.gov in Adobe Acrobat portable document format (PDF).

TABLE OF CONTENTS

	Page
EXECUTIVE SUMMARY	xiv
1. INTRODUCTION	1
1.1 RESEARCH OBJECTIVES	2
1.2 SCOPE OF WORK	2
1.3 ASSUMPTIONS	2
1.4 REPORT ORGANIZATION	2
2. CRITICAL FACTORS FOR PERFORMANCE OF PCC OVERLAY	4
2.1 SITE CONDITIONS	5
2.1.1 Traffic Loading	5
2.1.2 Climate	7
2.1.3 Subgrade	10
2.2 EXISTING PCC PAVEMENT	12
2.2.1 Existing Pavement Design Parameters	12
2.2.2 Existing Pavement Conditions	13
2.3 EXISTING AC PAVEMENTS	20
2.3.1 Existing Pavement Design Parameters	20
2.3.2 Existing Pavement Conditions	21
2.4 DESIGN FEATURES THAT AFFECT PERFORMANCE OF PCC OVERLAYS	21
2.4.1 Preoverlay Repair	21
2.4.2 Overlay Thickness	22
2.4.3 Overlay Type	22
2.4.4 Overlay Materials	23
2.4.5 Interlayer	24
2.4.6 Joint Design (JPCP/JRCP)	24
2.5 RECOMMENDATIONS	25
3. EXPERIMENTAL PROGRAM – OVERVIEW	27
3.1 EXPERIMENTAL PLAN OVERVIEW	27

3.1.1	Structural Model Verification	27
3.1.2	Verification of Pavement Deterioration Mechanism	29
3.1.3	Existing Pavement Condition Characterization and Structural Contribution	30
3.1.4	Performance Model Calibration	31
3.1.5	Development of Design Recommendations	31
3.2	EXPERIMENTAL PAVEMENT STRUCTURE	32
3.2.1	Existing Pavement Parameters	32
3.2.2	AC Interlayer Parameters	34
3.2.3	Overlay Parameters	34
3.2.4	Overlay Design Using LEDFAA	35
3.2.5	Overlay Design Using Navy Design	36
3.2.6	Mechanistic Analysis of Unbonded PCC Overlay	41
3.2.7	Final Pavement Structure	51
3.3	PCC MIX PROPERTIES	51
3.3.1	Water-Cement Ratio	53
3.3.2	Moisture Content	53
3.3.3	Cement Type and Amount	53
3.3.4	Aggregate Properties	54
3.3.5	Aggregate Gradation	55
3.3.6	Water-reducing Admixtures	56
3.3.7	Fly Ash Admixture	56
3.3.8	Air Entrainment Admixtures	56
3.3.9	Shrinkage Reducing Agents	57
4.	EXPERIMENTAL DESIGN	59
4.1	INTRODUCTION	59
4.1.1	Coordinates	59
4.2	TEST PLAN DETAILS	60
4.2.1	Joint/Crack Alignment	60
4.2.2	Transverse Joints	60
4.2.3	Longitudinal Joints	63
4.2.4	Shattered Slabs	64
4.2.5	Joint Sealing	64
4.2.6	Spalling	64
4.2.7	Transition Slabs	64
4.2.8	Wheel Load and Configuration	65
4.2.9	Shoulders	65

4.3	DESCRIPTION OF TEST CELLS	67
4.4	CONSTRUCTION OF TEST SECTIONS	70
4.4.1	PCC Mixing	70
4.4.2	Method of Mixture Handling	71
4.4.3	Preparation of Existing (Underlying) Pavement Surface	71
4.4.4	Transporting and Handling	72
4.4.5	PCC Placement	73
4.4.6	Weather at Time of Placement	74
4.4.7	PCC Surface Finishing	74
4.4.8	Consolidation	75
4.4.9	Curing	76
4.4.10	Sawing Joints	77
5.	INSTRUMENTATION AND DATA ACQUISITION FOR THE NAPTF TEST	79
5.1	SENSORS	79
5.1.1	Humidity Gages	80
5.1.2	Thermocouples – Type T (static)	82
5.1.3	LVDT – Joint Gages	83
5.1.4	Linear Potentiometers (Slab lift-off measurement)	84
5.1.5	Concrete Strain Gages	84
5.1.6	Thermocouples –Type T (dynamic)	86
5.1.7	Multi-depth Deflectometer	87
5.1.8	LVDT – Surface Deflections	88
5.1.9	Accessories	89
5.2	SENSOR PLACEMENT	90
5.2.1	Slab Lift-off Gages	115
5.2.2	Thermocouples	116
5.2.3	Humidity Gages	117
5.2.4	Joint Gages	118
5.2.5	MDD	119
5.2.6	Strain Gage – S-gages	120
5.2.7	S-gages in the Underlying Slab	120
5.2.8	S-gages in the Overlay	121
5.2.9	Strain Gage Rosettes – RS	121
5.2.10	RS in the Underlying Slabs	122
5.2.11	RS in the Overlay	123
5.3	ADEQUACY OF DATA ACQUISITION SYSTEM	125
5.3.1	Static Data Logger	125

5.3.2	High-Speed Data Acquisition System for Dynamic Sensor	125
5.4	COST ESTIMATE	125
6.	COST ESTIMATE	127
6.1	INTRODUCTION	127
6.2	CONSTRUCTION COST ESTIMATE	127
7.	CONSTRUCTION SCHEDULE	129
7.1	INTRODUCTION	129
7.2	CONSTRUCTION SCHEDULE	129
7.3	COORDINATION REQUIREMENTS FOR SPECIAL TESTING	130
7.4	CONTRACTOR'S SCHEDULE REQUIREMENTS	130
7.5	SUBMITTALS AND SHOP DRAWINGS	132
7.6	DRAWING INDEX	133
8.	CONSTRUCTION MATERIALS QC/QA PLAN AND SPECIFICATIONS	135
8.1	INTRODUCTION	135
8.2	CONSTRUCTION MATERIALS SPECIFICATIONS	135
8.3	QC/QA PLAN AND SPECIFICATIONS	137
8.4	SPECIAL CONDITIONS FOR QC/QA	143
8.4.1	Inspection and Testing	143
8.4.2	Protection of Existing Layers During Construction	143
8.4.3	Drawing Index	143
8.4.4	Errors and Omissions	144
8.4.5	QC/QA Testing	144
8.4.6	Auxiliary Sampling and Testing	144
8.4.7	Final Acceptance	144
9.	DATA COLLECTION PLAN	145
9.1	INTRODUCTION	145
9.2	DATA COLLECTION BEFORE FULL-SCALE TESTING	145
9.2.1	Subgrade Testing Prior to Construction of Base Layer	145
9.2.2	Base Testing Prior to Construction of Base Layer	146
9.2.3	Existing Pavement Testing	146
9.2.4	PCC Material Properties	147
9.2.5	HWD Testing	147
9.2.6	Static Load Test	149
9.2.7	Slow Rolling Load Test	149
9.2.8	Traffic Load Test	150
9.2.9	Interlayer Properties	152

9.2.10	PCC Overlay Testing	152
9.2.11	PCC Overlay Material Properties Testing	152
9.2.12	Surface Profile Measurement	153
9.2.13	HWD Testing	153
9.3	DATA COLLECTION DURING ACCELERATED LOAD TESTING	156
9.3.1	Traffic testing	156
9.3.2	HWD Testing	160
9.3.3	Profile Measurement	161
9.4	DATA COLLECTION AFTER ACCELERATED LOAD TESTING	161
9.4.1	HWD Testing	161
9.4.2	Post-traffic testing evaluation	161
10.	DATA ANALYSIS PLAN	173
10.1	DATA ACQUISITION QA/QC	173
10.2	RELIMINARY DATA ANALYSIS	173
10.2.1	Data Review	173
10.2.2	Development of Computed Parameters Tables	174
10.2.3	Side-by-side Analysis	174
10.2.4	Statistical Analysis	177
10.3	CALIBRATION OF PERFORMANCE PREDICTION MODELS	182
10.3.1	Calibration/Verification of LEDFAA	182
10.3.2	Verification of Gear Configuration Modeling	184
10.3.3	Calibration of PCC Overlay Fatigue Models	184
10.4	DEVELOPMENT OF IMPROVED STRUCTURAL MODELS	187
10.4.1	Degree of Composite Behavior (Friction)	187
10.4.2	Effects of Distresses in the Existing Pavements on Overlay Responses	189
10.4.3	Effects of Joint Mismatching	190
10.4.4	Effect of Slab Curling/Warping	190
10.4.5	Evaluation of Slab Built-in Curling	191
10.5	CONCLUDING REMARKS	193
11.	SUMMARY AND RECOMMENDATIONS	195
12.	REFERENCES	199
APPENDICES		

- A - Test Pavement Plan and Profile
- B - Itemized Cost Estimate
- C - Detailed Construction Schedule
- D - Material Specifications
- E - Quality Control (QC) Specifications

LIST OF FIGURES

Figure	Page	
1	“ROADMAP” FOR THE DEVELOPMENT OF FAA PAVEMENT DESIGN PROCEDURE (FAA WEBSITE)	1
2	TEMPERATURE PROFILE IN A PCC SLAB	8
3	DEVELOPMENT OF VOID UNDER UNBONDED CONCRETE OVERLAY DUE TO DAY TIME CURLING	8
4	DEVELOPMENT OF VOID UNDER UNBONDED CONCRETE OVERLAY DUE TO NIGHT TIME CURLING	9
5	EFFECT OF SUBGRADE TYPE ON UNBONDED PCC OVERLAY THICKNESS REQUIRED BY LEDFAA	11
6	EFFECT OF SUBGRADE TYPE ON UNBONDED PCC OVERLAY THICKNESS REQUIRED BY NAVY DESIGN PROGRAM (CENTER LOADING).	11
7	EFFECT OF SUBGRADE TYPE ON UNBONDED PCC OVERLAY THICKNESS REQUIRED BY NAVY DESIGN PROGRAM (EDGE LOADING).	12
8	EFFECT OF CONDITION OF THE EXISTING PAVEMENT ON THE OVERLAY THICKNESS (LEDFAA).	16
9	EFFECT OF CONDITION OF THE EXISTING PAVEMENT ON THE OVERLAY THICKNESS (NAVY DESIGN – CENTER LOADING)	16
10	EFFECT OF CONDITION OF THE EXISTING PAVEMENT ON THE OVERLAY THICKNESS (NAVY DESIGN – EDGE LOADING)	17
11	EFFECT OF DISTANCE OF THE FWD PLATE FROM THE CRACK ON E-RATIO	19
12	EFFECT OF DISTANCE OF THE FWD PLATE FROM THE CRACK IN THE EXISTING PAVEMENT ON BACKCALCULATED E-RATIO	19
13	LAYOUT OF A TEST STRIP TESTED AT THE NAPTF IN MARCH IN 2002 (MCQUEEN ET AL. 2002)	33
14	CRACK PATTERN IN TEST STRIP (MCQUEEN ET AL. 2002)	33
15	NUMBER OF SUSTAINED GEAR PASSES	34
16	ISLAB2000 FINITE ELEMENT MODEL OF CRACKS IN THE UNDERLYING PAVEMENT	42
17	EFFECT OF A CRACK IN THE UNDERLYING PAVEMENT ON PREDICTED STRESSES IN AT THE BOTTOM OF THE PCC OVERLAY	43
18	EFFECT OF THE OVERLAY THICKNESS ON THE MAXIMUM OVERLAY STRESSES AT THE BOTTOM SURFACE FROM B-777 GEAR LOADING	44
19	PREDICTED TEMPERATURE DISTRIBUTION THOUGHT PCC OVERLAY THICKNESS AT NAPTF FOR A TYPICAL DAY IN SEPTEMBER	45
20	FREQUENCIES OF EQUIVALENT DIFFERENCE BETWEEN PCC OVERLAY TOP AND BOTTOM SURFACES PREDICTED BY EICM	46
21	FREQUENCIES OF EQUIVALENT DIFFERENCES BETWEEN PCC OVERLAY TOP AND BOTTOM SURFACES PREDICTED BY EICM FOR DAYTIME AND ADJUSTED FOR BUILT-IN CURLING AND SHRINKAGE WARPING	47
22	COMPARISON OF FREQUENCIES OF EQUIVALENT DIFFERENCE BETWEEN TOP AND BOTTOM SURFACES TEMPERATURES OF THE PCC OVERLAY AND TEST STRIP PAVEMENTS AS PREDICTED BY EICM	48

23	APPROXIMATE GEAR POSITION FOR CRITICAL BOTTOM SURFACE OF THE TOP LAYER STRESSES	49
24	APPROXIMATE GEAR POSITION FOR CRITICAL TOP SURFACE STRESSES	49
25	COMPARISON OF BOTTOM SURFACE STRESSES FOR THE UNBONDED OVERLAYS AND TEST STRIPS	50
26	COMPARISON OF TOP SURFACE STRESSES FOR THE UNBONDED OVERLAYS AND TEST STRIPS	51
27	GRADATION PLOT USED FOR CONCRETE MIX DESIGN (MCQUEEN ET AL. 2002)	55
28	PLAN VIEW OF THE UNDERLYING PAVEMENT AND THE OVERLAY	61
29	JOINT DETAIL, J1	63
30	JOINT DETAIL, J2	63
31	SAWING PATTERN TO CREATE SHATTERED SLABS IN THE EXISTING PAVEMENT	64
32	POWER BUGGY USED AT THE NAPTF TO TRANSPORT FRESH CONCRETE FROM MIXER	73
33	SETTING FORMWORK FOR THE CONSTRUCTION OF TEST STRIPS AT THE NAPTF	74
34	STRAIGHTEDGE STRIKE-OFF OF CONCRETE IN TEST STRIPS AT THE NAPTF	75
35	VIBRATING CONCRETE DURING PLACEMENT OF TEST STRIPS AT THE NAPTF	76
36	PLACEMENT OF BURLAP OVER CONCRETE TEST STRIPS FOR 28-DAY WET CURE	77
37	WET SAW CUTTING JOINTS IN CONCRETE TEST STRIPS AT THE NAPTF	78
38	PROPOSED HUMIDITY SENSOR, G-CAP™ 2	81
39	THERMOCOUPLE STACK	83
40	JOINT WIDTH MEASUREMENT	84
41	CHAIRS FOR STRAIN GAGES	85
42	STRAIN GAGE INSTALLATION	86
43	STRAIN GAGE PLACEMENT IN THE SLAB	86
44	MDD LAYOUT IN THE PCC TEST SECTION	87
45	MDD INSTALLATION AT THE NAPTF	88
46	PORTABLE SURFACE DEFLECTION MEASURING DEVICE	89
47	SENSOR PLACEMENT IN THE LOW STRENGTH SUBGRADE SECTION.	91
48	SENSOR PLACEMENT IN THE MEDIUM STRENGTH SUBGRADE SECTION	92
49	SENSOR PLACEMENT IN THE MEDIUM STRENGTH SUBGRADE SECTION	93
50	SLAB LIFT-OFF GAGES IN THE L-SECTIONS	115
51	SLAB LIFT-OFF GAGES IN THE M-SECTIONS	115
52	SLAB LIFT-OFF GAGES IN THE H-SECTIONS	116
53	THERMOCOUPLES IN THE L-SECTION	116
54	THERMOCOUPLES IN THE M-SECTION	116
55	THERMOCOUPLES IN THE H-SECTION	117
56	HUMIDITY GAGES IN THE L-SECTION	117
57	HUMIDITY GAGES IN THE M-SECTION	117
58	HUMIDITY GAGES IN THE H-SECTION	118

59	JOINT GAGES IN THE L-SECTION	118
60	JOINT GAGES IN THE M-SECTION	118
61	JOINT GAGES IN THE H-SECTION	119
62	MDD IN THE L-SECTION	119
63	MDD IN THE M-SECTION	119
64	MDD IN THE H-SECTION	120
65	SINGLE STRAIN GAGE IN THE L-SECTION	120
66	SINGLE STRAIN GAGE IN THE M-SECTION	120
67	SINGLE STRAIN GAGE IN THE H-SECTION	121
68	STRAIN GAGE ARRANGEMENT TO DETECT STRESS CONCENTRATION IN OVERLAY ABOVE A CRACK IN THE UNDERLYING PAVEMENT	121
69	RS LOCATIONS IN THE UNDERLYING SLABS OF THE L-SECTION	122
70	RS LOCATIONS IN THE UNDERLYING SLABS OF THE M-SECTION	122
71	RS LOCATIONS IN THE UNDERLYING SLABS OF THE H-SECTION	123
72	RS IN THE L-SECTION OVERLAYS	123
73	RS IN THE M-SECTION OVERLAYS	123
74	RS IN THE H-SECTION OVERLAYS	124
75	RS GAGE PATTERN IN PCC SLABS OVER UNDERLYING PAVEMENT WITH MISMATCHED TRANSVERSE AND LONGITUDINAL JOINTS	124
76	FAA HWD SENSOR CONFIGURATION	148
77	PROPOSED SENSOR CONFIGURATION AT NAPTF	148
78	TYPICAL TRAFFIC WANDER PATTERN USED AT NAPTF	151
79	RECOMMENDED POSITIONS OF LOADING TRACKS	151
80	TESTING PATTERN FOR GENERAL OVERLAY HWD TESTING	154
81	LOAD FREQUENCY IN EACH TRACK DUE TO THE LOADING PATTERN USED AT NAPTF	158
82	CRITICAL LOAD POSITIONS AND DAMAGE LOCATIONS	159
83	RECOMMENDED LOAD PATHS	159
84	TESTING PATTERN FOR MONTHLY HWD TESTING ON THE OVERLAY	160
85	BASIC RELATIONSHIPS AFFECTING PAVEMENT BEHAVIOR AND PERFORMANCE	178
86	TRANSVERSE CRACKING (BOTTOM-UP) VERSUS COMPUTED FATIGUE DAMAGE ILLUSTRATION	186
87	EFFECT OF INTERFACE CONDITION ON STRAIN DISTRIBUTION	189
88	STRAIN GAGE ARRANGEMENT TO DETECT STRESS CONCENTRATION IN OVERLAY ABOVE A CRACK IN THE UNDERLYING PAVEMENT	190

LIST OF TABLES

Table	Page
1 REQUIRED OVERLAY THICKNESS FROM LEDFAA	37
2 OVERLAY PERFORMANCE LIFE FROM LEDFAA	37
3 COMPARISON OF LEDFAA AND NAVY DESIGN PROCEDURES	38
4 REQUIRED PCC OVERLAY DESIGN THICKNESS FROM NAVY DESIGN PROCEDURE. CENTER SLAB LOAD POSITION DESIGN	40
5 REQUIRED PCC OVERLAY DESIGN THICKNESS FROM NAVY DESIGN PROCEDURE. EDGE SLAB LOAD POSITION DESIGN	40
6 CONCRETE MIX DESIGN USED IN TEST STRIPS AT THE NAPTF (MCQUEEN ET AL. 2002)	52
7 SUMMARY OF KEY DESIGN FEATURES IN EACH EXPERIMENT CELL	66
8 COORDINATES FOR SENSORS IN THE LOW STRENGTH SUBGRADE SECTION	94
9 COORDINATES FOR SENSORS IN THE MEDIUM STRENGTH SUBGRADE SECTION	102
10 COORDINATES FOR SENSORS IN THE HIGH STRENGTH SUBGRADE SECTION	109
11 NUMBER OF STATIC SENSORS IN THE TEST PLAN.	125
12 NUMBER OF DYNAMIC SENSORS IN THE TEST PLAN	126
13 COST ESTIMATE FOR INSTRUMENTATION	126
14 COST SUMMARY FOR NEW CONSTRUCTION AT THE NAPTF	128
15 TOP-LEVEL TASKS IN CONSTRUCTION PLAN FOR NAPTF	129
16 CONSTRUCTION MATERIALS PLAN	136
17 SUBGRADE CHARACTERIZATION: RECOMMENDED LOCATIONS FOR CBR AND DCP TESTING	138
18. QUALITY CONTROL TESTING PLAN, ITEM P-154, SUBBASE COURSE	139
19 QUALITY CONTROL TESTING PLAN, NJ DOT SECTION 903, PLANT-MIXED BITUMINOUS PAVEMENT FOR INTERLAYER	140
20 QUALITY CONTROL TESTING PLAN, ITEM P-501, PORTLAND CEMENT CONCRETE PAVEMENT	141
21 RECOMMENDED LOCATIONS FOR CBR AND DCP TESTING	146
22 CONFIGURATION OF “CARRIAGE 2” DURING ACCELERATED LOAD TESTING	157
23 RECOMMENDED LOCATIONS FOR HWD TESTING	163
24 EFFECT OF GEAR CONFIGURATION	175
25 EFFECT OF LONGITUDINAL CRACKING IN THE EXISTING PAVEMENT	175
26 EFFECT OF SHATTERED SLABS IN THE EXISTING PAVEMENT	176
27 EFFECT OF MISMATCHING JOINTS IN THE OVERLAY AND THE EXISTING PAVEMENT	176
28 EFFECT OF DOWELS IN OVERLAY JOINTS MISMATCHED WITH JOINTS IN THE EXISTING PAVEMENT	176
29 EFFECT OF HIGH-SEVERITY TRANSVERSE CRACKING IN THE EXISTING PAVEMENT	177
30 EFFECT OF SEVERITY LEVEL OF TRANSVERSE CRACKING IN THE EXISTING PAVEMENT	177
31 EFFECT OF SPALLING OF CRACKS AND JOINTS IN THE EXISTING PAVEMENT	177

32 POSSIBLE DIVISIONS OF EACH SITE CONDITION CELLS INTO TWO
SUBGROUPS

179

EXECUTIVE SUMMARY

Current trends in pavement design philosophy rely on increasingly sophisticated analytical modeling coupled with correlations with laboratory, accelerated trafficking, and in-service tests. Overlay design philosophy has tended to lag behind this trend, and much of today's airfield overlay design still relies on empirical relations developed in the 1950s. The FAA has developed an improved rigid pavement overlay design methodology based on layered elastic theory, but its performance correlations are based on accelerated traffic tests largely conducted in the 1940s and 1950s, before analytical models such as layered elastic theory were easily solvable in practice. Consequently, material characterization and data collection from these old tests do not necessarily provide the desired information for use with more modern analytical models. The FAA is now in the process of developing an advanced pavement design procedure based on finite element modeling, which requires modeling data far more detailed than ever envisioned in these older tests.

This reports documents the development of an experimental design for a large-scale, accelerated testing program at the FAA National Airfield Pavement Test Facility (NAPTF) to obtain performance data on concrete overlays to support modern analysis based on layered elastic theory and finite element analysis methods. The overlays to be considered will be rigid overlays over rigid and flexible pavements that carry aircraft with single wheel loads greater than 30,000 lb.

The proposed series of testing at the NAPTF will be an important step toward improving the current mechanistic-empirical design procedures for unbonded PCC overlays of airport pavements. The data collected from this testing will help develop more reliable and cost-effective design solutions for unbonded PCC overlays

1. INTRODUCTION

The Federal Aviation Administration (FAA) is developing an advanced pavement design procedure based on sound theoretical principles and full-scale validation tests. The new design procedure will take advantage of today's enhanced computational abilities that offer the ability to analyze complex pavement structures and flexibility to evaluate the effects of complex gear configurations under both traffic and environmental loads. To achieve this goal, the activities illustrated in figure 1 have been initiated.

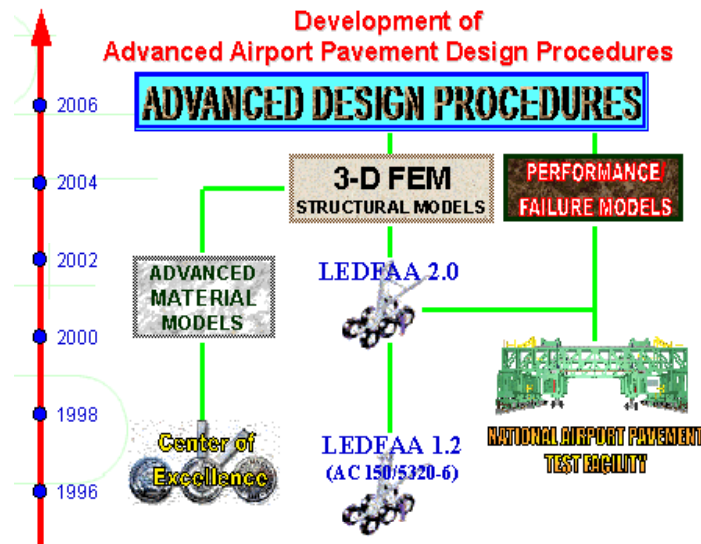


FIGURE 1. "ROADMAP" FOR THE DEVELOPMENT OF FAA PAVEMENT DESIGN PROCEDURE (FAA WEBSITE)

- Development of structural models for airport pavements (layered elastic and finite element based).
- Development of advanced material models, such as stress-dependent moduli for unbound layers.
- Development of failure models in the form of regression functions relating the pavement structural responses (stresses, strains, or deflections) to the number of coverages to failure.

To obtain the data needed to develop reliable failure models, the National Airport Pavement Test Facility (NAPTF) was built. The testing vehicle at this facility can simulate repeated loading by aircraft weighing up to 1.2 million pounds. Data from the NAPTF will be used to develop advanced failure models of new pavements and overlays that are applicable to the new generation of aircraft, including the six-wheel B-777, and future models. A testing program for performance evaluation of portland cement concrete (PCC) and asphalt concrete (AC) pavements

is currently underway. The next stage will be accelerated testing of overlays, including PCC overlays.

1.1 RESEARCH OBJECTIVES

The objective of the work being reported is to develop an experimental plan for a large-scale, accelerated testing program for PCC overlays at the NAPTF. The testing program will provide performance data to develop design criteria for PCC overlays utilizing modern analysis methods such as layered elastic theory and finite element analysis methods.

1.2 SCOPE OF WORK

The scope of this project includes the following:

- Conduct a brief literature review focused on specific issues related to critical airfield pavement design parameters.
- Identify and rank design parameters in order of importance.
- Design test factorial.
- Identify critical responses and develop instrumentation plan.
- Develop testing program (both destructive and nondestructive).
- Prepare final budget, construction documentation, and test plan.
- Prepare quality assurance/quality control (QA/QC) plans for data collection and data analysis.

1.3 ASSUMPTIONS

The experimental plan described herein was developed with the following assumptions:

- The test plan for measurement of the first-priority parameters should be a one-time test, but the entire NAPTF will be available for the testing program.
- The NAPTF will have three subgrade sections of low, medium, and high strength, each approximately 300 ft long.
- The “existing pavement” (the pavement to be overlaid) will be constructed as a part of experimental program.
- Further research will be needed beyond the testing program described in this report; however, the data from this series of testing will clarify numerous issues and the results may be used to update the overlay design procedure.

1.4 REPORT ORGANIZATION

This report documents the development of the experimental plan for full-scale accelerated testing of PCC overlays. The chapters in this report are organized as follows:

Chapter 1—introduction

Chapter 2—background information and factors affecting performance of PCC overlays

Chapter 3—overview of the proposed testing program and background on key design parameters (layer thicknesses, joint spacing, and PCC mix selection)

Chapter 4—details of experimental design and key aspects test pavement construction

Chapter 5—instrumentation plan

Chapter 6—cost estimate

Chapter 7—construction schedule

Chapter 8—construction and material specifications

Chapter 9—testing procedure

Chapter 10—data analysis roadmap

Chapter 11—summary and recommendations

Additional information related to the test plan and profile, itemized cost estimate, detailed construction schedule, materials, and QA/QC specifications is provided in appendixes.

THIS PAGE INTENTIONALLY LEFT BLANK

2. CRITICAL FACTORS FOR PERFORMANCE OF PCC OVERLAY

This chapter summarizes the factors affecting the performance of PCC overlays. The factors were grouped into the following categories:

- Site condition
- Existing pavement parameters and condition
- Overlay design and construction features

Discussion of each of these groups of factors is presented below. Included in these discussions is a description of how these factors are accounted for in the LEDFAA (Hayhoe et al. 2002) and Navy design (Navy's Military Handbook 1021/4) procedures. These procedures were selected because LEDFAA is the latest FAA design procedure for airfield pavements and the Navy design procedure is an alternative mechanistic design procedure.

2.1 SITE CONDITIONS

The following site condition factors affect the PCC overlay performance:

- Traffic loading
- Environmental loading
- Subgrade support

The effect of each of these factors will be discussed below. Although existing pavement structure and condition may also be classified as site condition factors, due to their importance they will be discussed in a separated section.

2.1.1 Traffic Loading

Traffic loading plays a key role in the performance of concrete overlays. All available overlay design procedures use a traffic loading parameter for design. Repeated heavy aircraft gear loads on JPCP overlays can result in the following major types of damage:

- Top-down cracking of the overlay slab
- Corner cracking of the overlay slab
- Bottom-up cracking of the overlay slab
- Progressive deterioration of the underlying pavement

The negative influence of traffic loading on the performance of concrete overlays will be exacerbated if certain design features, such as overlay thickness and proper joint spacing, are not adequate. The main loading parameters affecting PCC overlay performance are:

- Gear load
- Gear geometry
 - number of wheels in a gear
 - distances between wheels in a gear

- tire area and shape
- Number of passes
- Load position
 - center slab
 - slab edge
 - slab corner
- Load distribution (traffic wander)
- Tire pressure

These parameters affect PCC overlay performance in the same way they affect the behavior of new pavements.

The NAPTF rail-based test vehicle has two loading carriages that can be configured for up to six wheels per carriage with loads up to 75,000 lb per wheel. The test vehicle is programmed for a controlled aircraft wander simulation. The NAPTF test vehicle simulates realistic aircraft wander by varying the lateral position of the carriages. The wander pattern used during traffic testing consists of a fixed sequence of 66 vehicle passes arranged in 9 wander positions (or tracks). The wander positions and sequences were chosen to simulate a normal distribution of aircraft traffic with a standard deviation of 30.5 inches (representing the current design condition for airport taxiways).

In the current NAPTF testing program of new PCC and AC pavements, the effect of gear geometry is studied through side-by-side comparison of pavement responses and pavement performance under the B-777 and B-747 loading. Such comparisons should be also conducted for the PCC overlays, although it they are not necessary for the entire experimental design factorial.

Loading position (slab center, slab edge, and slab corner) dramatically affects magnitude and location of critical responses new PCC pavements and PCC overlays. In addition, load position with respect to cracks and joints in the existing pavement should also be investigated. This will be done by measuring of the corresponding pavement responses in static and dynamic (moving gear) tests.

Although up to 500 passes per day can be performed at the NAPTF, it is desirable to design a test program aimed at total of 10,000 to 20,000 passes. Even if performance prediction of the current model is accurate, any difference in as-constructed versus as-designed parameters (e.g., PCC strength, PCC thickness, subgrade strength) may cause significant over or underprediction of the overlay life. This creates a risk for very early failure or that no significant level of distresses will be achieved in a reasonable timeframe.

Gear load is an extremely important parameter affecting the number of gear passes the overlay can survive. The research team, however, does not see it would be feasible to vary gear load in the overlay experiment at the NAPTF. The main reason is that the number of design load repetitions should be in a fairly narrow range that will not allow for significant change in load level. The research team foresees testing at a level of 45,000 lb per wheel for first 10,000

repetitions. If no significant distress is observed for most sections at that time (indicating conservatism current design models), the load will be increased up to 55,000 lb per wheel.

Although tire pressure has a moderate effect on PCC stresses at the bottom of the PCC overlay, it does not vary in a wide range for commercial aircrafts. Since airplane tires are designed to operate at a particular tire deflection, currently at the NAPTF tire deflection is kept constant providing a constant tire contact area and prolonging tire life. The research group recommends keeping this procedure during the overlay test.

2.1.2 Climate

Daily temperature and moisture variations have a significant influence on the performance of concrete pavements and contribute to the mechanisms that cause certain distresses. Temperature and moisture effects during construction can also have a significant effect on the performance of a concrete pavement. The resulting temperature or moisture gradients cause restrained curling and warping deflections and stresses that, although by themselves are usually not critical, can lead to critical stresses when traffic loads are imposed. These stresses can have a major effect on the performance of a concrete overlay placed on a stiff slab if they are not considered directly in design and construction.

2.1.2.1 Temperature For a PCC overlay, a positive temperature gradient (PCC top surface is warmer than PCC bottom surface) during the day will cause the overlay slab to curl downward at the corners. During warm temperatures and under repeated heavy loads, this can cause plastic flow and permanent deformation of the AC interlayer at the corner, causing permanent loss of support. It is common for a much greater temperature gradient to exist in the overlay slab than in the interlayer and underlying pavement. As shown in figure 2, when the top surface of the 13-in-thick PCC overlay temperature reaches 120 °F, the PCC overlay bottom temperature stays about 80 °F. This can lead to curling in the overlay that may cause the separation of the overlay from the existing slab, as illustrated in figure 3. The resulting restrained curling stresses can significantly increase edge bending stresses at the bottom of the slab when traffic loads are applied. Similarly, during the night, a negative temperature gradient can cause the top slab to curl upward at the corners and lead to loss of support at the corners, as shown in figure 4. Combined corner stresses on the top of the slab from traffic loads and restrained curling (temperature and moisture gradient) can be excessive and lead to corner breaks and transverse cracks for non-doweled joints.

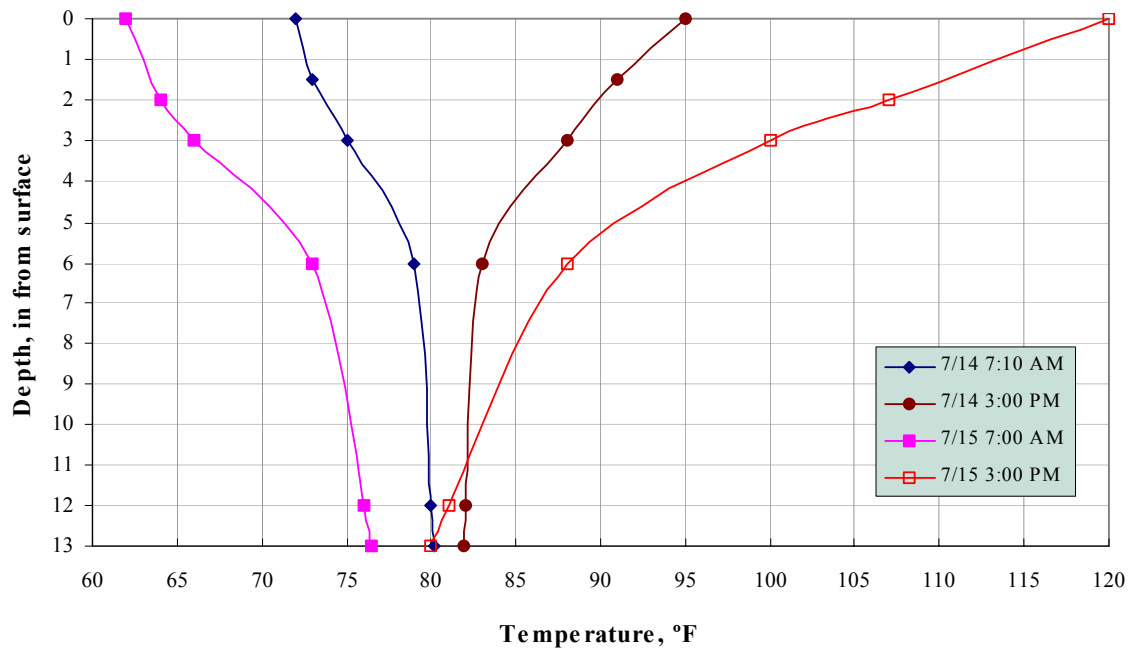


FIGURE 2. TEMPERATURE PROFILE IN A PCC SLAB

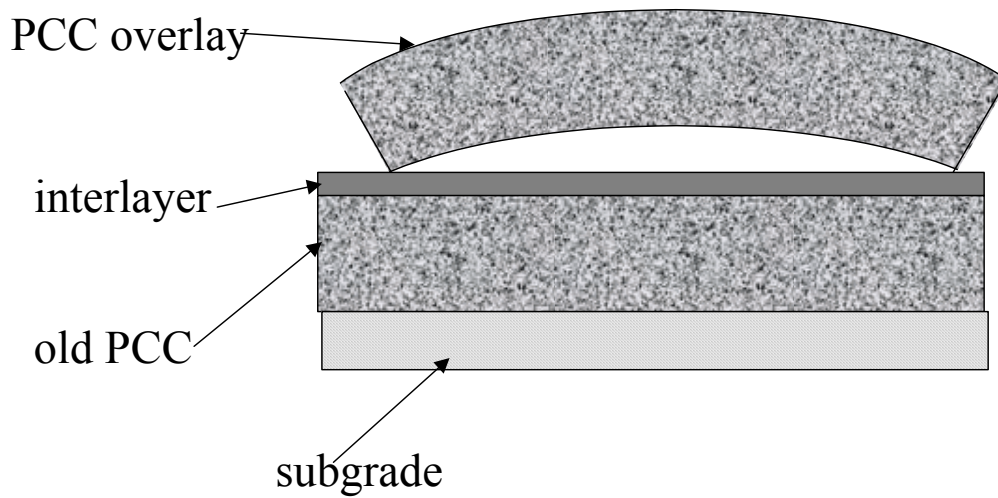


FIGURE 3. DEVELOPMENT OF VOID UNDER UNBONDED CONCRETE OVERLAY DUE TO DAY TIME CURLING

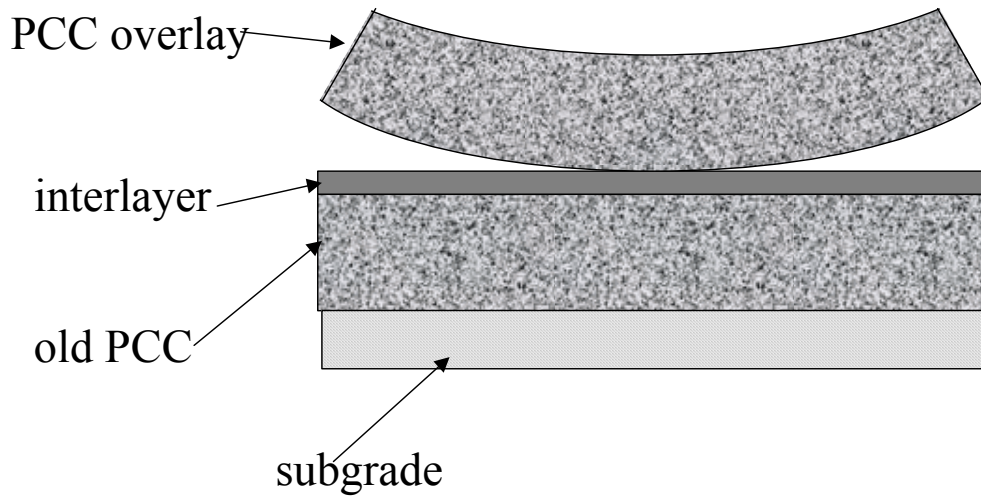


FIGURE 4. DEVELOPMENT OF VOID UNDER UNBONDED CONCRETE OVERLAY DUE TO NIGHT TIME CURLING

2.1.2.2 Moisture Climatic conditions also have a significant influence on the distribution of moisture and free water in pavements, and the volume changes that accompany the loss or gain of moisture in an overlay slab can influence performance in several ways. In hardened concrete, loss of water from within leads to irreversible drying shrinkage. Non-uniform or differential drying shrinkage can lead to warping and cause restrained warping stresses to develop in a concrete pavement. The warping also results in upward movement at corners and edges, causing loss of support along the slab edges that will lead to high stresses at the top of the slab when traffic loads are applied. The effect of warping is especially significant in dry climates. Such warping effects can often be characterized by an equivalent temperature gradient that causes the same deterioration.

2.1.2.3 Seasonal Temperatures Seasonal temperature variations can also lead to restrained horizontal strains and stresses as a result of expansion and contraction of the pavement layers in an overlay. For a concrete overlay, since the overlay, interlayer, and existing slab can have different coefficients of thermal expansion, differential movements between the layers can cause stresses due to friction between the layers. These restrained stresses usually are not significant in mature concrete pavements with adequate joint spacing. However, the presence of cracks and joints in the underlying pavement may cause reflective cracking if an adequate interlayer is not provided or if the overlay thickness is not sufficient.

2.1.2.4 Combined Effects In the cases of curling and warping of a concrete overlay due to temperature and moisture variations, because the underlying pavement acts as a very stiff base,

the stresses developed in the overlay can be much higher than those experienced by a pavement on a less stiff base. The results from a study of a pavement that was built over a relatively stiff cement-treated base showed significant curling and warping of the pavement. The results from a study in Chile also point to a high occurrence of transverse cracking and corner breaks of non-doweled jointed plain concrete pavement (JPCP) overlays having a cement-treated aggregate interlayer over old asphalt concrete and PCC pavements. These sections had an average of 23 percent cracked slabs (Poblete et al. 1989). Similar designs that were constructed on the natural subgrade showed an average of only 6 percent slab cracking. It was observed that all the pavement sections remained in a permanently upward warped/curled position that resulted in measurable rocking of the non-doweled pavement slabs when loaded at the corner. This situation leads to top-down cracking from loads located at the non-doweled joints.

The NAPTF does not have the capability to control temperature and moisture loading. Nevertheless, the pavements at the NAPTF are subjected to daily and seasonal temperature cycles. Although the absence of direct sunshine and changes in humidity make these cycles different from field conditions, careful recording of temperature profiles will provide valuable information for future mechanistic interpretation of the test results.

2.1.3 Subgrade

The structural support provided by the subgrade is an important factor that affects the long-term performance of concrete pavements, particularly in terms of uniformity. For concrete overlays, the influence of the subgrade appears to be less than with a conventional pavement, since the influence of the existing pavement will be very strong. However, the subgrade support is important to the design of an overlay, and most of the existing design procedures require a subgrade support parameter, such as the subgrade k-value or subgrade modulus of elasticity, as input. It should also be noted that a stiff subgrade (high k-value) would lead to increased slab stresses from curling, unless joint spacing is reduced.

Elastic properties of the subgrade are important input parameters into the current airfield pavement design procedures for PCC overlays. Figures 5 shows the effect of subgrade type on the required overlay thickness required by LEDFAA. Figures 6 and 7 show the effect of subgrade type on the required overlay thickness required by two options of the Navy Design procedure: design based on the interior loading stresses and PCA beam fatigue model and design based on the edge loading stresses and the slab fatigue model (Darter and Roman 1989). In the example considered, a 10-in-thick PCC pavement with a structural condition index (SCI) of 60 is strengthened to carry up to 30,000 load applications of the B777-200A. One can see that both procedures required a thicker overlay for a softer subgrade to achieve the same overlay life. Correspondingly, the same overlay thickness leads to different overlay lives for different subgrade types.

NAPTF has three different strengths of subgrades (low CBR 3-4, medium CBR 7-9, and high CBR 30-40). Therefore, the effect of subgrade on overlay performance can be investigated directly (i.e., the test should evaluate whether the subgrade plays as important role on the overlay performance as it is predicted by the current design procedures).

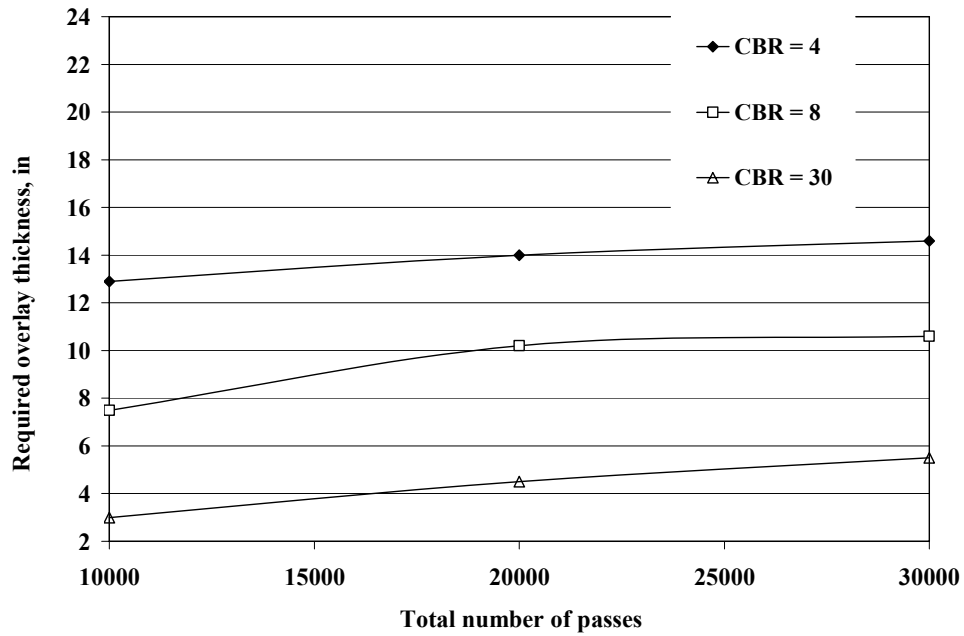


FIGURE 5. EFFECT OF SUBGRADE TYPE ON UNBONDED PCC OVERLAY THICKNESS REQUIRED BY LEDFAA

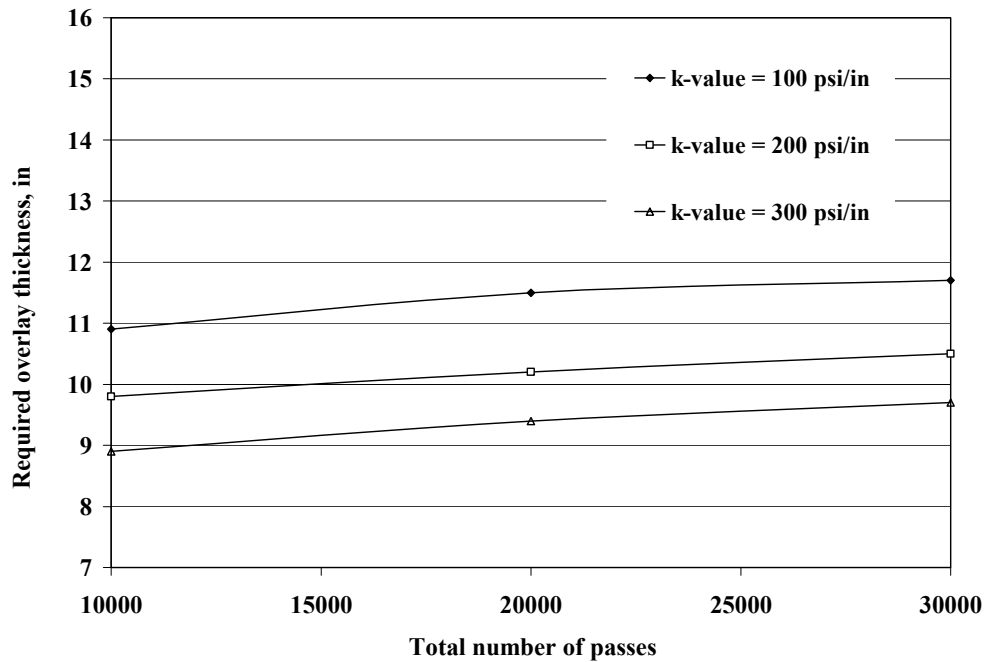


FIGURE 6. EFFECT OF SUBGRADE TYPE ON UNBONDED PCC OVERLAY THICKNESS REQUIRED BY NAVY DESIGN PROGRAM (CENTER LOADING)

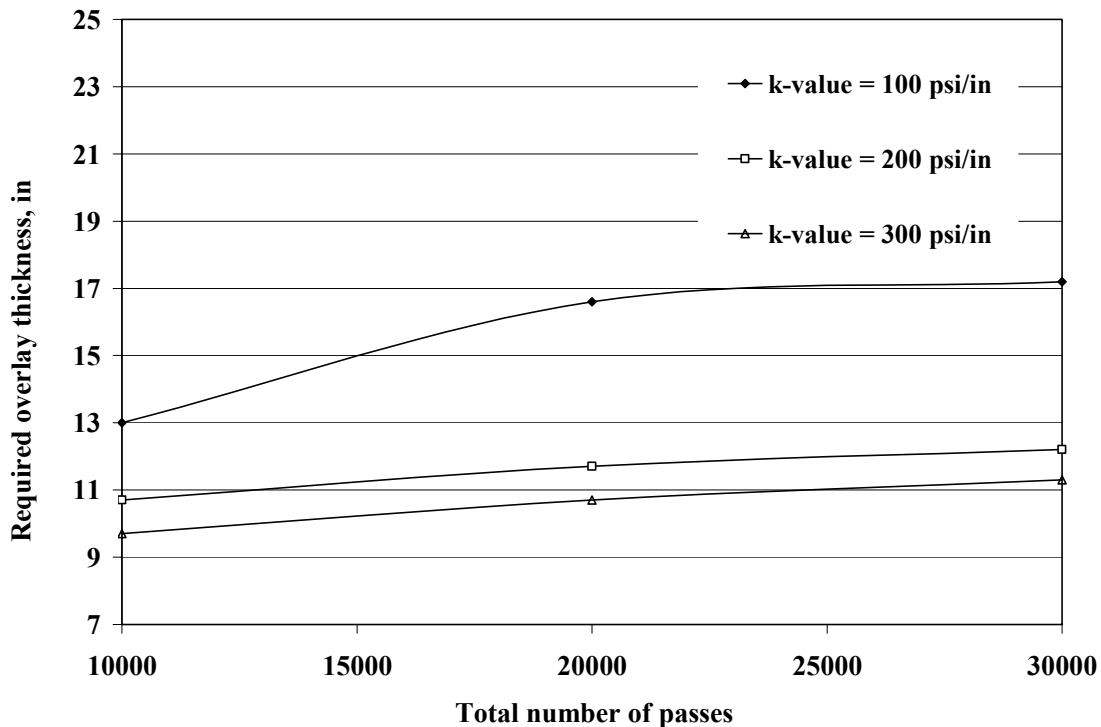


FIGURE 7. EFFECT OF SUBGRADE TYPE ON UNBONDED PCC OVERLAY THICKNESS REQUIRED BY NAVY DESIGN PROGRAM (EDGE LOADING)

2.2 EXISTING PCC PAVEMENT

Two aspects of the existing pavement influence the long-term performance of an unbonded or partially bonded concrete overlay. First, the structural characteristics of the underlying PCC slab are essential to design, and most of the existing design procedures (for both airport and highway pavements) require inputs that include the thickness, material properties, cracking of the underlying slab, and joint/crack load transfer for the determination of the overlay thickness (Rollings 1988, Tayabji and Ocamoto 1985). Second, the condition of the existing pavement (uniformity of support) determines the amount and type of preoverlay repair necessary to avoid reflection cracking. In addition, the information obtained from an evaluation of the existing pavement is needed to determine the feasibility of constructing an overlay and is an essential input in the selection of the overlay type.

2.2.1 Existing Pavement Design Parameters

The following elements of the existing pavement's design affect overlay performance:

- PCC thickness
- PCC strength
- PCC modulus of elasticity
- PCC Poisson's ratio
- PCC coefficient of thermal expansion
- Presence and properties of stabilized layers below the existing pavement
- Joint spacing
- Pavement type (JPCP/JRCP)

The structural contribution of the existing pavement can be characterized by an effective radius of relative stiffness, which combines the bending stiffness of the existing pavement and the bending stiffness of the stabilized layers below. An effective radius of relative stiffness can be determined from FWD deflection measurements (if available) or analytically from the thicknesses and moduli of elasticity of the PCC and stabilized layers.

The coefficient of thermal expansion of PCC affects curling of the underlying pavement. For unbonded overlays it is not an important parameter because the overlay acts as a thermal blanket and isolates the existing pavement from daily changes in temperature. Seasonal temperature changes also are not very important because an interlayer isolates horizontal movements of the overlay and existing pavement. At the same time, the coefficient of thermal expansion of the existing pavement may have a greater effect on performance of partially bonded overlays. If an existing pavement has cracks, the cracks tend to propagate through the overlay. Since this parameter controls the amount of movement in the existing pavement due to temperature change, it affects the crack-driving force. Therefore, an increase in the coefficient of thermal expansion makes reflective cracking more likely.

Although the existing pavement material properties affect performance of the PCC overlay, it is not economically feasible to test those effects in full-scale tests. Therefore, only one PCC mix will be used in the design experiment.

2.2.2 Existing Pavement Conditions

In all major overlay design procedures for airport and highway pavements, existing pavement condition is a factor affecting both overlay type and overlay design parameters (thickness, joint spacing, etc.). Therefore, the effect of the existing pavement condition on overlay performance should be evaluated carefully in this experiment.

Typically, the evaluation of the existing pavement involves a visual distress survey, material quality testing (coring, boring, and laboratory testing), and deflection testing and an analysis of the collected data to determine the physical condition and structural capacity of the existing pavement.

The following distresses of existing PCC pavements affecting PCC overlay performance were identified in this study:

- Corner break
- Transverse, longitudinal, and diagonal cracking
- Shattered slabs
- Shrinkage cracks
- Spalling along joints
- D-cracking
- Reactive aggregate reaction
- Popouts
- Scaling
- Blowups
- Pumping and loss of support
- Joint faulting

Although differences exist in the definition and methods of accounting for the existing pavement's condition, in most design procedures a subjective adjustment factor is used to reduce the thickness of the existing pavement to obtain an equivalent structural capacity.

FAA Advisory Circular AC 150/5320-6D accounts for the existing pavement condition through the condition factor, C_r . The condition factor may vary from 1.0 to 0.35. A condition factor equal to 1 means that the existing PCC pavement is in good structural condition with little or no structural cracking. If the existing pavement has some initial structural cracking but little progressive distress (such as spalling and multiple cracks), then C_r should be equal to 0.75. C_r equal to 0.35 should be assigned if the existing pavement is badly cracked and may show multiple cracking, shattered slabs, and faulting.

The layered elastic design procedure adopted by the FAA, LEDFAA, uses structural condition index, SCI, to characterize the condition of the existing pavement. The SCI is a truncated pavement condition index (PCI) that accounts only for distresses that can be reflected in the layered elastic analytical model. Like the PCI, SCI is varied from 0 to 100, where a value of 100 corresponds to an excellent structural condition and 0 corresponds to complete loss of structural capacity. The following distresses are included in the SCI calculation:

- Corner break
- Transverse, longitudinal, and diagonal cracking
- Shattered slabs
- Shrinkage cracks
- Spalling along joints
- Spalling corners

The following relationship between SCI and C_r was identified by Rollings (1988):

$$SCI = 93.2 C_r + 7.1$$

In the LEDFAA, SCI affects both selection of the PCC overlay type and thickness. Bonded PCC overlay is recommended if the SCI is close to 100. A partially bonded overlay is recommended

if the SCI is greater than 77. If the SCI is less than 77, only an unbonded PCC overlay is recommended.

The modulus of elasticity of the existing pavement is a function of the pavement condition and is defined as follows:

$$E_{SL} = E_0 \left[0.02 + 0.0064 SCI + (0.00584 SCI)^2 \right]$$

where

E_{SL} – design modulus of elasticity of the existing slab

E_0 – initial modulus of elasticity of the existing slab

SCI – structural condition index of the existing slab

Reduction in the modulus of elasticity of the existing slab leads to an increase in predicted PCC overlay stresses, reduces predicted design life, and requires an increased overlay thickness to achieve the same level of performance as if the existing slab modulus were equal to the initial value.

In addition to accounting for distresses at the time of overlay, LEDFAA assumes that the existing pavement continues to deteriorate after being overlaid. The existing pavement's SCI continues to decrease during design life.

To illustrate the effect of pavement condition on required unbonded overlay thickness, a series of LEDFAA and Navy design program runs were performed. For the LEDFAA analysis, the subgrade's CBR was assumed to be equal to 8. For Navy runs, the coefficient of subgrade reaction was assumed to be equal to 200 psi/in. The following structure was assumed for the existing pavement:

- 10-in thick PCC layer
- 12-in thick crushed stone aggregate base

Figures 8 through 10 present required design thicknesses for different numbers of projected B-777 passes obtained from LEDFAA and Navy Design program. A higher SCI value of the existing pavement at the time of rehabilitation leads to a decrease in required overlay thickness.

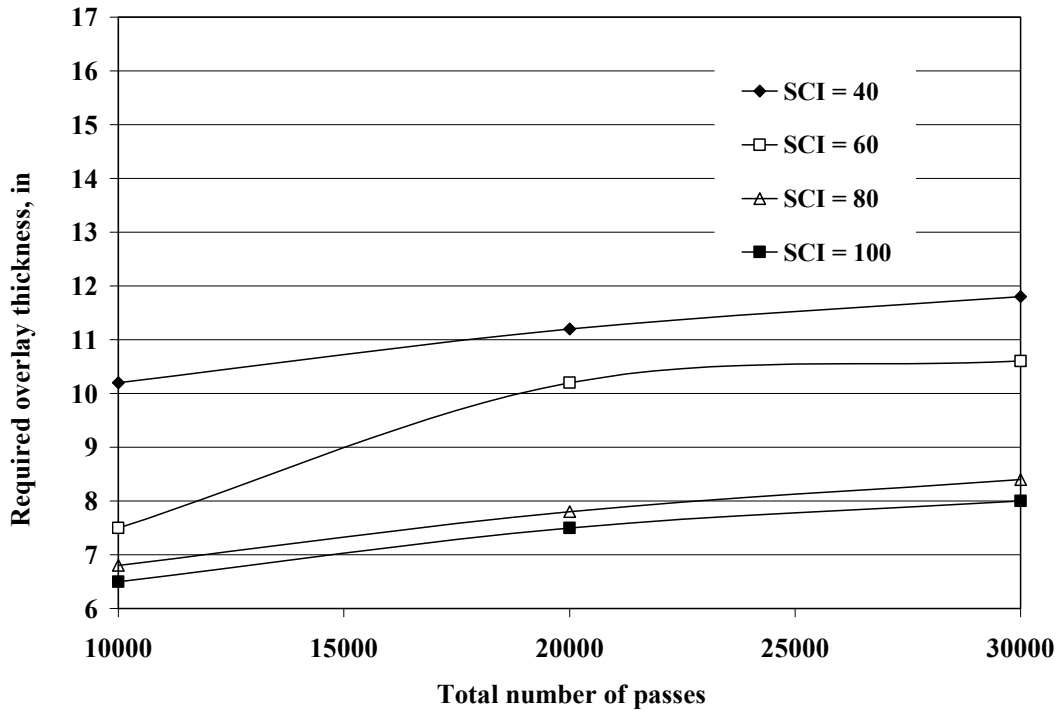


FIGURE 8. EFFECT OF CONDITION OF THE EXISTING PAVEMENT ON THE OVERLAY THICKNESS (LEDFAA)

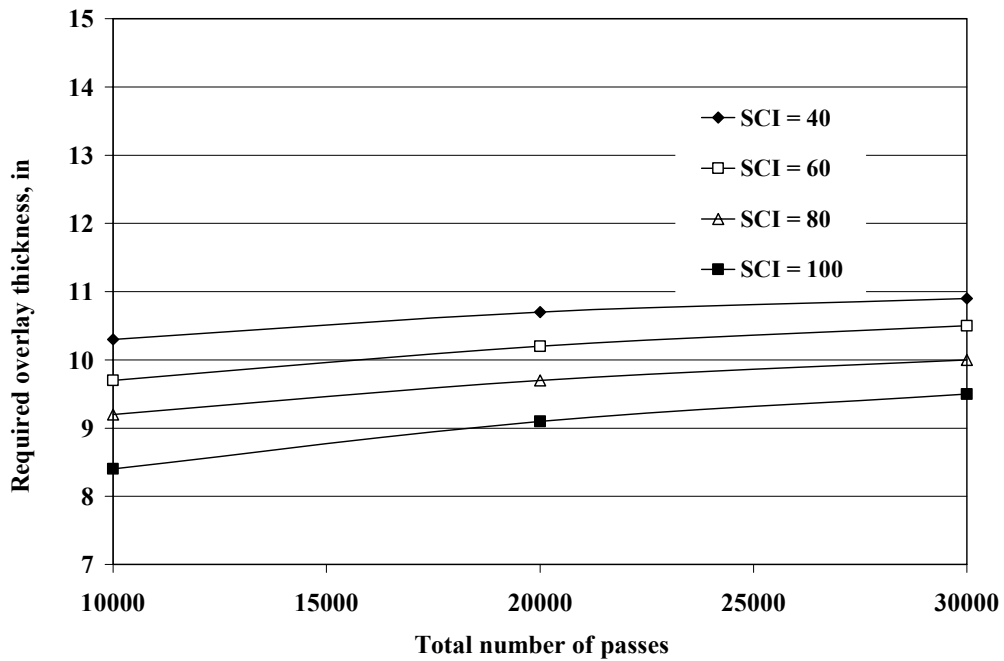


FIGURE 9. EFFECT OF CONDITION OF THE EXISTING PAVEMENT ON THE OVERLAY THICKNESS (NAVY DESIGN – CENTER LOADING)

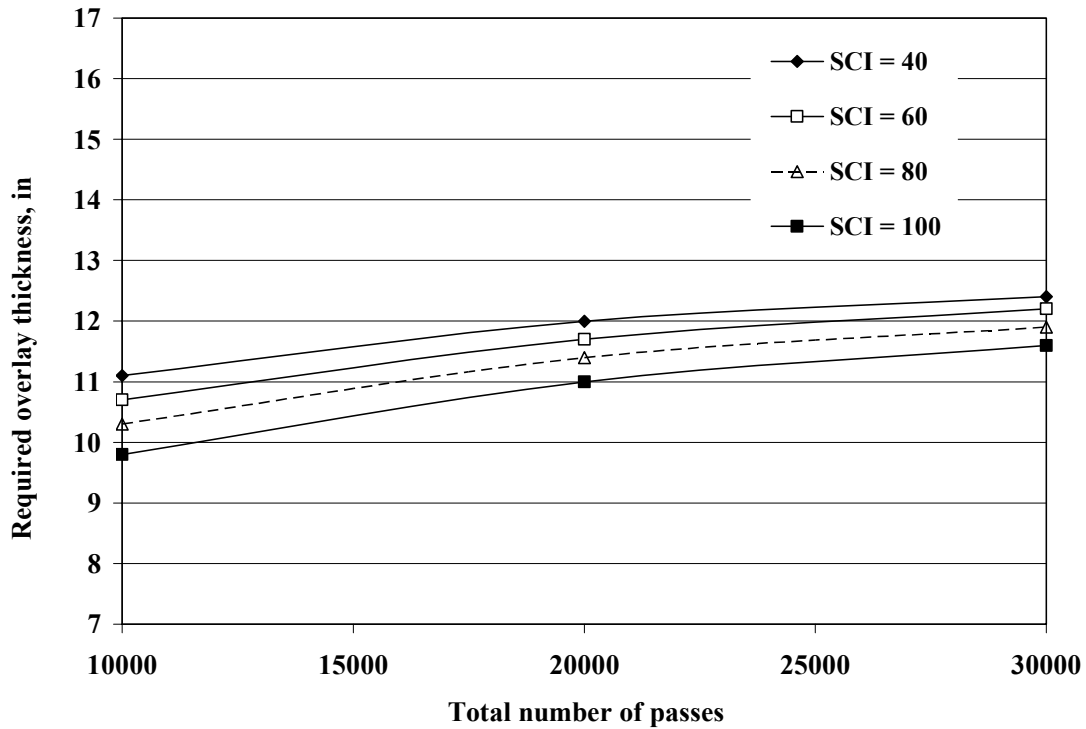


FIGURE 10. EFFECT OF CONDITION OF THE EXISTING PAVEMENT ON THE OVERLAY THICKNESS (NAVY DESIGN – EDGE LOADING)

Although the introduction of the SCI was a very important step toward quantifying the effect of structural condition of the existing pavement in an objective, rational manner, certain aspects of the SCI should be evaluated in this study:

- SCI is based on the relationship between the extent of an individual distress and the corresponding deduct value (DV) used in PCI. Therefore, SCI calculation is based purely on expert opinion and does not have any theoretical justification. Moreover, the combined effect of multiple distresses accounts for the interaction of these distresses in a very crude way. In some cases, the presence of an additional distress may even slightly increase SCI.
- The SCI is based purely on the results of visual survey. Joint deterioration is considered through visual assessment of joint spalling. It is true high spalling can indicate poor load transfer efficiency, which significantly increases PCC bending stresses and may cause cracking. However, in some cases, spalling is a serviceability distress and does not significantly affect pavement structural capacity.
- LEDFAA models the existing pavement behavior only as a function of the SCI. This means that it is assumed that the influence of an individual distress is the same for all types and designs of overlays. This may not be the case. For example, an asphalt

interlayer between the overlay and the existing pavement may eliminate any negative effect of spalling in the existing pavement; therefore, spalling should not be included in the SCI calculation. At the same time, for bonded and partially bonded overlays, the effect of spalling may be pronounced. Also, joint mismatching in the unbonded overlay may significantly mitigate the effect of load transfer (as indicated by low faulting on highway unbonded overlay constructed with mismatched joints).

- The relationship between the SCI and E-ratio (reduction factor in PCC modulus of elasticity) was developed from the data obtained by progressively cracking the test slabs and measuring the FWD deflections at each stage (Rollings 1988). Backcalculated PCC moduli of elasticity were then correlated to the SCI. This approach has significant limitations:
 - The backcalculated values may depend significantly on the position of the FWD with respect to crack location.
 - The presence of the overlay on top of the existing pavement may significantly alter deflection response of a cracked pavement.

To illustrate these effects, several ISLAB2000 finite element runs were performed. A 16-in-thick PCC pavement with 25- by 25-ft slab spacing was modeled to have a transverse crack in the middle of the slab. The deflection load transfer efficiency of the crack was assumed to be 60 percent. An FWD load was simulated at different distances from the crack. The deflections from those loads were calculated and the PCC moduli of elasticity were backcalculated as if the slab had no crack. Figure 11 presents E-ratios obtained by normalizing the backcalculated moduli to the actual slab modulus.

The E-ratio is affected strongly by the distance of the Falling Weight Deflectometer (FWD) plate from the crack. If the load plate is located near the crack, the backcalculated slab elastic modulus is much lower than elastic modulus value used as ISLAB2000 input. This agrees with Rollings' interpretation of the field deflection data. However, to investigate behavior of a cracked slab after being overlaid, another series of ISLAB2000 runs was performed. A 9-in-thick PCC overlay with a cracked existing slab was loaded by an FWD-type loading at several distances from a crack in the existing pavement. The crack was modeled using very soft elements so no load transfer through the crack was assumed. Figure 12 presents the E-ratio for the slab as a function of the distance from the crack.

A conclusion from these examples is that the E-ratio of the existing slab is much higher and much less dependent on crack location if a PCC overlay is present. Although such analysis should be considered cautiously (a real overlay may behave differently from the model behavior), it shows a need for further investigation of this issue.

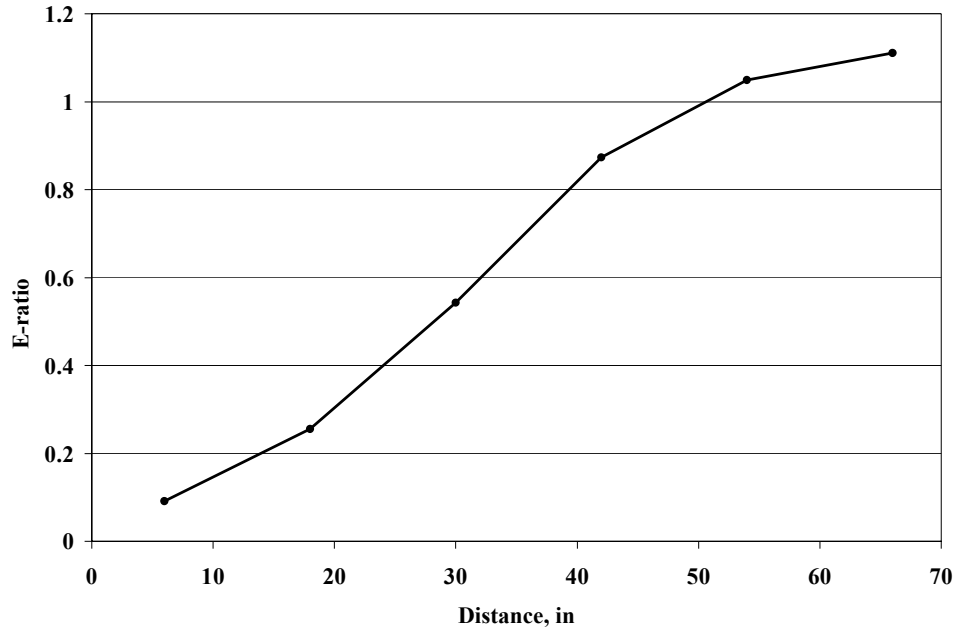


FIGURE 11. EFFECT OF DISTANCE OF THE FWD PLATE FROM THE CRACK ON E-RATIO

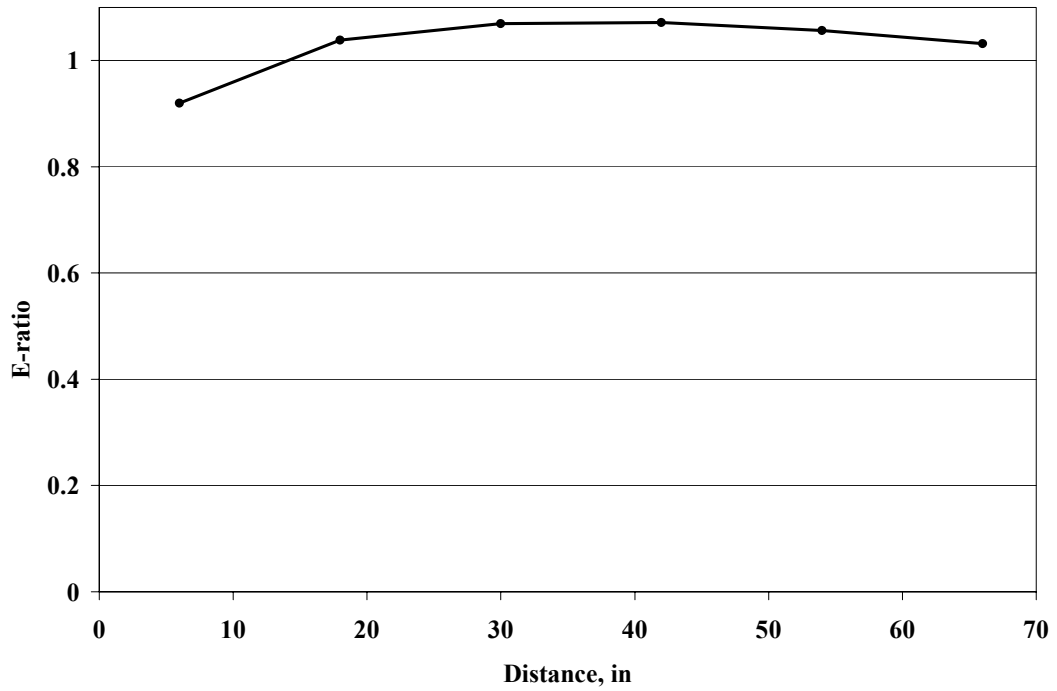


FIGURE 12. EFFECT OF DISTANCE OF THE FWD PLATE FROM THE CRACK IN THE EXISTING PAVEMENT ON BACKCALCULATED E-RATIO

- Other distresses excluded from SCI calculation may affect structural behavior of the existing pavements. For example, a recent study showed that the ratio between interior and corner slab deflections of airport pavements is much higher for pavements that exhibit significant D-cracking. Currently those distresses are not considered in the LEDFAA procedure.
- There is still much unknown about the effects of specific conditions in existing pavements on the performance of the overlays. Testing at the NAPTF may provide valuable information to help us better understand this issue.

Among others, the following questions will be answered by this factorial:

- Do sections with the same SCI but different types of distresses on the existing pavement behave similarly? (The research group expects that sections with lower SCI and cracking will behave worse than those with spalling).
- What is the effect of different distresses on composite overlay/slab behavior?

2.3 EXISTING AC PAVEMENTS

Although structural contribution of an existing AC pavement toward PCC overlay structural capacity is less than the contribution of an existing PCC pavement, the existing AC pavement also affects the performance of PCC overlay. Like for the existing PCC pavements, two aspects of the existing pavement influence the long-term performance of a PCC overlay: the structural characteristics of the underlying pavement and the condition of the existing pavement.

2.3.1 Existing Pavement Design Parameters

The following design elements of the existing AC pavement affect the overlay performance:

- AC thickness
- AC modulus of elasticity
- Thicknesses of the underlying layers (base, subbase, etc.)
- Moduli of elasticity of underlying layers

The structural contribution of the existing pavement can be characterized by an effective slab thickness, which combines the bending stiffness of the existing pavement and the bending stiffness of the stabilized layers below. An effective slab thickness can be determined from FWD deflection measurements (if available) or analytically from the thicknesses and moduli of elasticity of the AC and stabilized layers.

Although material properties affect overlay performance, the research team does not envision to test different AC mixes for the underlying pavements at NAPTF. It might be of interest,

however, to test the effect of different pavement types (conventional and full depth AC) on the overlay behavior.

2.3.2 Existing Pavement Conditions

AC pavement distresses may be divided into three groups:

- Rutting
- Cracking
- Material deterioration

Rutting dramatically affects serviceability of an AC pavement. At the same time, if rutting is the only major AC distress, such a pavement would be an ideal foundation for a PCC overlay. An absence of cracking and material deterioration would indicate that such a pavement is structurally sound. Milling of the top surface of AC pavement may provide more uniform PCC thickness and ensure better bond between the overlay and the AC layer. Therefore, relatively thinner PCC overlay may be used to rehabilitate such a pavement.

The presence of cracking or material deterioration significantly reduces the structural capacity of the AC pavement and, subsequently, the structural contribution of the existing AC layer to the PCC overlay structural capacity.

At least two levels of AC cracking are proposed for tests at the NAPTF. This will help assess the extent of reduction of structural contribution of AC pavement due to cracking.

Also, the effect of milling of AC surface on ensuring of a good bond between the PCC overlay and AC layer should be tested by comparison with performance of a PCC overlay over a non-milled AC pavement.

2.4 DESIGN FEATURES THAT AFFECT PERFORMANCE OF PCC OVERLAYS

The design features that influence the performance of PCC overlays include preoverlay repair, overlay thickness, type of overlay, overlay materials, interlayer, joint spacing and design, mismatching of joints, subdrainage, and reinforcement content.

2.4.1 Preoverlay Repair

One of the advantages of concrete overlays is that they require very little preoverlay repair, and the less preoverlay repair that is required, the more cost-effective the overlay. However, certain distresses in advanced stages, such as shattered slabs, settlements, poor joint/crack load transfer, and punchouts, may need to be repaired prior to overlay construction because they influence overlay performance. Very little documentation exists on PCC overlay failures due to underlying pavement deterioration.

Some preoverlay repairs (such as level-up of settlement) are necessary to provide an adequate surface for the construction of the overlay. Also, in some instances, without preoverlay repairs

the thickness of the interlayer and overlay that will be required to provide the desired performance would be cost prohibitive. A critical issue for overlays, therefore, is the determination of the type and extent of preoverlay repair that is economical over the design period and provides the expected overlay performance.

Examples of the distresses that normally need to be addressed prior to placing an unbonded overlay include the following:

- Joint deterioration - High-severity spalls at existing pavement joints are filled and compacted with asphalt concrete patching mix.
- Broken slabs - Badly shattered slabs with working cracks are replaced full-depth.
- Unstable slabs - Slabs with large deflections or pumping problems are replaced full-depth or undersealed.
- Joint or crack faulting - Faulting is not a problem when a thick AC interlayer (≥ 1 in) is used.

The type and thickness of the interlayer influences the preoverlay repair that is required. The use of a thicker interlayer (preferably an AC layer) may reduce the amount of preoverlay repair. Also, if the pavement to be overlaid has a history of durability problems, it may be necessary to reduce further deterioration of the pavement after it is overlaid. Potential remedies include the provision of better subdrainage.

Although preoverlay repair affects the performance of a PCC overlay, the research team does not think it is feasible to include the amount of preoverlay repair in the experimental factorial.

2.4.2 Overlay Thickness

The thickness of the overlay design is a function of the structural capacity required to meet the demands of the site conditions: traffic loading, climate, subgrade, and the condition of the existing pavement. However, the required thickness is also a function of other design features such as joint spacing and concrete strength.

2.4.3 Overlay Type

Designing a jointed reinforced concrete pavement (JRCP) overlay is not dramatically different from designing a JPCP overlay. If an overlay joint spacing is greater than 20 ft, then reinforcement is recommended. Reinforcement in JRCP is designed not to prevent cracks from forming but to keep them tight, provide high load transfer efficiency, and prevent cracks from deterioration. However, since the rate of deterioration depends not only on traffic loading but also on environmental loading, the research team does not recommend testing JRCP overlays at the NAPTF.

Other PCC overlay types, such as CRCP and prestressed PCC are not commonly used in rehabilitation of airport pavements and, therefore, are not recommended for testing at the NAPTF.

2.4.4 Overlay Materials

The materials used for PCC overlays are no different from those used for concrete pavements on grade. Conventional concrete mixes that will provide high-quality concrete are adequate, and a majority of concrete overlays have been built with standard concrete mixes. Because overlays sometimes have to be built while traffic is maintained, fast-track mixes that allow high early strength gain and make it possible for a pavement to be opened to traffic within 6 to 24 hours are particularly attractive.

Specialty concretes, such as fiber reinforced concrete, have also been used for PCC overlays of airport and highway pavements (Betterton and Knutson 1978, McGhee 1994). Regardless of the type of concrete mix used, the usual characteristics of conventional mixes that influence pavement performance will also influence the performance of a concrete overlay:

- PCC bending strength
- PCC modulus of elasticity
- PCC Poisson's ratio
- PCC coefficient of thermal expansion
- PCC shrinkage coefficient

An increase in PCC strength increases pavement life (assuming all other conditions are the same), whereas an increase in PCC modulus of elasticity, coefficient of thermal expansion, and shrinkage coefficient increases PCC stresses and, therefore, may reduce pavement life.

It is commonly believed that an increase in PCC bending strength should increase overlay design life dramatically. However, this is not necessarily the case. An increase in PCC strength is usually followed by an increase in PCC elastic modulus, which mitigates the positive effect of stress increase. For highway pavements, this effect can be demonstrated using the PRS 3.0 model (Khazanovich and Yu 2001). Moreover, higher strength concrete usually has a higher coefficient of thermal expansion (which increases the magnitude of temperature curling) and shrinkage coefficient (which increases slab warping).

Although the effect of material properties is significant, only one mix is recommended for NAPTF overlay study.

2.4.5 Interlayer

The interlayer has a major influence on the performance of unbonded concrete overlays. The primary purpose of the interlayer is to isolate the overlay from the existing slab. However, it must provide adequate friction so that joints will form uniformly in the overlay. Therefore, a certain amount of bonding and friction is required between the overlay slab, the interlayer, and the existing slab. Thus, the term "unbonded" is not technically correct. The interlayer can also act as a leveling course and reduce the variation in support along the project.

Numerous materials have been used as interlayers. These include hot-mix AC, bituminous surface treatments, lean concrete, cement-treated aggregate, polyethylene sheeting, geotextiles, unbound aggregate layer, heavy roofing paper, and curing compounds (Spellman et al. 1971, Hutchinson 1982). The thickness of the layers ranges from 6 mils for polyethylene sheeting to 6 in for an AC leveling course.

An adequate interlayer can have a tremendous influence on the performance of an unbonded concrete overlay. A good interlayer can retard or arrest reflection cracking. However, when a material incapable of isolating the movements of the existing slab from the overlay is used as a separation material, or the thickness of the interlayer is not adequate, it can lead to poor performance of the unbonded overlay. An inadequate thickness can bring about "keying" of the overlay into distress in the base slab. This can also happen when there is no interlayer and the two slabs somewhat bond together, as occurred on the Georgia sections which used only curing compound as a interlayer (Gulden and Brown 1984).

The best results have been obtained with a relatively thick AC interlayer as was shown in the NCHRP 10-41 study. An AC layer 1 to 2 in thick can effectively isolate the overlay from the base slabs and can also serve as a leveling course to smooth undulations and surface roughness.

Bituminous surface treatments, such as slurry seals and cutback or emulsified asphalt with a sand cover, have also been used successfully. Although they are thin, they can provide good performance when surface roughness is minimal in the existing pavement. However, the surface treatments can lead to performance problems under heavy traffic if they erode and cause faulting.

Stripping of AC interlayers can cause serious problems of erosion and faulting. All AC separation materials must be fully designed to prohibit stripping. In areas subject to significant fuel spillage the interlayer, and thus the performance of the overlay, may be at risk if the overlay joints are not properly sealed and scrupulously maintained.

Other thin interlayers, such as polyethylene sheeting, roofing paper, and curing compound, have not performed well as was found in the NCHRP 10-41 study. The poor performance of these materials was attributed to the inadequacy of the thin interlayer to isolate the concrete layers effectively. There have also been construction problems associated with polyethylene and waxed-based curing compounds.

2.4.6 Joint Design (JPCP/JRCP)

In general, the factors related to joints that influence the performance of conventional concrete pavements also affect concrete overlay performance.

2.4.6.1 Joint Spacing Joint spacing of the overlay is particularly important to the performance of JPCP overlays. For unbonded JPCP overlays and whitetoppings, a shorter transverse joint spacing is recommended than that used for a conventional pavement on an aggregate base. However, it may be similar to that for a conventional pavement on a very stiff lean concrete base course. The rule of thumb is that the transverse joint spacing in feet should not exceed 1.75 times the overlay thickness in inches. This compares reasonably well with the FAA recommendation that limits transverse joint spacing to 20 ft for JPCP unbonded overlays. Longer transverse joint spacing can be used for JRCP unbonded overlays as long as adequate reinforcement is provided to prevent movement of cracks in the overlay tight. For partially bonded PCC overlays, matching of joints in the existing pavements and the overlay is required.

FAA joint spacing recommendations have been used successfully worldwide by the military. In the early 1980s, the Air Force mandated 20 ft spacing based on observation of more cracked slabs in 25 ft slabs than in 20 ft – this jibes with a recent FAA study. The military does not adjust joint spacing based on the underlying material.

2.4.6.2 Load Transfer Devices For heavy design loads and highly trafficked overlays, it is desirable to use dowels to provide sufficient load transfer and reduce the potential for corner cracking. Design of joints in the unbonded overlays and whitetopping is similar to design of joints in new PCC pavements. There has always been a question, however, as to where to put load transfer devices in partially bonded overlays. The location of the neutral axis (logical location for LT device) is difficult to determine in the partially bonded condition. It is recommended to test at least two positions of dowels to compare joint performance. The load transfer will be evaluated using FWD deflection data as well as ratios of strains in the loaded and unloaded slabs induced by a moving gear loading.

2.5 RECOMMENDATIONS

As discussed herein, performance of PCC overlays is affected by many factors. The NAPTF offers an excellent opportunity for accelerated testing of unbonded, partially bonded, and whitetopping overlays for heavy airfield pavements. To be recommended for testing at the NAPTF, a factor should satisfy the following conditions:

- Identified as important by the available pavement design procedures, by the research team evaluation, or both.
- Identified to be possible and economically feasible

The research team also evaluated the overall relative importance of testing of different types of PCC overlays at the NAPTF and recommends the following ranking:

- Unbonded PCC overlay – very important
- Whitetopping for heavy airfield pavements – important

- Partially bonded PCC overlays – important

It was decided that in the first round of testing at the NAPTF only unbonded overlays will be tested. The effect of the following critical factors will be included in the experimental design for overlay study at the NAPTF:

- Underlying pavement structure and condition: different levels and/or combination of distresses.
- Effect of joint mismatching (for unbonded overlays)
- PCC joint design (doweled versus undoweled)
- Effect of subgrade type
- Effect of gear geometry
- Effect of traffic wander

These factors will be evaluated by their effects on structural responses obtained from FWD testing and strain, deflection, and pressure gages installed in the overlay, interlayer, and existing pavement as well as overlay performance.

If a possibility to perform another round of testing at the NAPTF or another facility comes up, the following factors should be tested:

- Whitetopping for heavy airfield pavements (thickness design and effect of milling)
- Partially bonded PCC overlay
- Effect of an AC interlayer on overlay performance (compare performance of unbonded overlays with different interlayer thicknesses with performance of a partially bonded overlays)

3. EXPERIMENTAL PROGRAM – OVERVIEW

This chapter discusses an overall approach to the experimental design and selection of the main parameters (e.g., layer thicknesses, joint spacing, and PCC mix design). The details of the experimental design are presented in chapter 4.

3.1 EXPERIMENTAL PLAN OVERVIEW

As discussed in chapter 2, the performance of PCC overlays is affected by many factors. The NAPTF offers an excellent opportunity for accelerated testing of unbonded, partially bonded, and whitetopping overlays. Unbonded overlays were selected as the first priority of the testing program, and the testing at the NAPTF will be an important step toward improving the current mechanistic-empirical design procedures for unbonded PCC overlays of airport pavements. To achieve this goal, various activities are required, including the following:

- Verification of the structural models of unbonded overlays
- Development of understanding of the mechanism of deterioration of unbonded overlays
- Improved characterization of structural contribution of the underlying pavement, including the effect of the existing pavement condition
- Calibration of the performance prediction model
- Development of recommendations for joint matching and for use of dowels

The proposed testing program is designed to provide crucial information for accomplishing the above tasks. The requirements of the experimental program are discussed below, including the proposed methods for meeting these requirements.

3.1.1 Structural Model Verification

Validation of structural models is important to ensure that the overlay designs are based on realistic estimates of key pavement responses (stresses and deflections). Of interest are the pavement responses under critical combinations of load configuration, slab configuration, and underlying pavement condition. The combinations that cause critical stresses or deflections in unbonded overlays have been identified and, based on this information, a test pavement layout was developed for testing the crucial cases. The data collected from this series of testing will enable validation of the structural responses predicted by various tools. The testing will also provide valuable information for developing improved structural models that will facilitate future analyses of unbonded overlays.

Currently, mechanistic-empirical design procedures are based on either Westergaard or layered elastic theory. The latest FAA overlay design program, LEDFAA, uses a layered elastic analysis program to predict pavement responses. Although the program cannot account for discontinuities in pavement layers, the design procedure addresses this limitation by progressive reduction of the existing slab modulus to account for deterioration of cracks in the existing pavement and by correcting interior stresses to account for the presence of joints in the overlay. Full-scale testing will help validate these corrections.

An alternative to layered elastic programs is the use of finite element programs. These programs can explicitly analyze the effect of edge loading; thus, they require no correction factors. However, the explicit modeling of the edge loading condition alone does not address all problems associated with analyzing unbonded overlays. Other complicating factors include the cracks or other deterioration in the underlying pavement and interaction between pavement layers. Often, the stresses predicted over cracks in the underlying pavement are exceedingly high, and they are not likely to reflect the actual stresses experienced by PCC overlays. Full-scale testing is needed to obtain crucial information for quantifying the true state of stress in unbonded overlays. This information will be valuable for improving the structural models, which will facilitate future design analysis.

The scope of this series of testing includes the investigation of several key factors that affect the structural response of unbonded overlays, including the effects of cracks in the underlying pavement, layer interaction, subgrade stiffness, and gear configuration.

3.1.1.1 Effect of cracks in the underlying pavement The effects of cracks in the underlying pavement on stresses in the overlay are very difficult to analyze. Although modeling of such problems is possible using existing finite element analysis programs, the validity of the analysis results cannot be assured without experimental verification. The proposed program calls for testing a full set of possible slab configurations, including fully match joints (no cracks), a crack in one direction, cracks in two directions, and shattered slabs. The pavement responses obtained from this series of testing will be invaluable in validating analytical predictions and for developing structural models that facilitate analyses of such problems.

3.1.1.2 Effect of friction between the layers It is a generally accepted practice to ignore friction between the unbonded PCC overlay and the existing pavement. It is highly possible, however, that an AC interlayer provides significant composite action between the PCC layers. By measuring PCC strains in the overlay and existing pavement, one can obtain a degree of composite action under a heavy gear load. Properly accounting for the layer interaction may lead to better prediction of pavement life.

3.1.1.3 Effect of subgrade stiffness The PCC overlay thickness required by the existing design procedures depends greatly on subgrade stiffness. However, the properties and conditions of the existing PCC layer may have even greater effect on the overlay responses than subgrade stiffness. Comparing the structural responses of PCC overlay measured on sections with different subgrade properties but the same existing pavement condition and design should provide valuable information for verification and future development of structural models. NAPTF provides an opportunity to conduct testing on three different levels of subgrade stiffness.

3.1.1.4 Effect of gear configuration Comparison of responses from a 6-wheel gear loading and 4-wheel gear loading will provide information regarding how accurately structural models handle different gear configurations and if any improvements in this respect are required. The following structural responses under heavy gear load will be measured in this study:

- Subgrade deflections
- PCC overlay and existing pavement deflections (overlay corner and center slab location)

- Strains at the bottom and top surface of the underlying pavement (center slab and longitudinal edge locations)
- Strains at the bottom and top surface of the overlay (center slab and longitudinal edge, as well as above cracks in the existing slab)
- Relative displacement of the overlay with respect to existing pavement (overlay edges and corners)
- Horizontal movements of joints in the existing PCC slab

In addition, the following Heavy Weight Deflectometer (HWD) measurements will be performed:

- Existing pavement center slab, slab edge, and slab corner deflections
- Across joints and cracks in the existing pavement for different distances of the HWD load plate from the joints/cracks
- PCC overlay center slab, slab edge, and slab corner deflections
- PCC deflection across the slab centerline at 1-ft intervals

HWD deflections will permit backcalculation of pavement system elastic parameters, evaluation of joint load transfer efficiency, and evaluation of the effect of cracks in the existing pavement on the overlay deflections.

PCC temperature curling and moisture warping are not considered directly in the available airport pavement design procedures, but measurements of PCC temperature and moisture will provide important data for future development of structural models.

3.1.2 Verification of Pavement Deterioration Mechanism

Different design procedures address deterioration of the existing PCC pavement after overlaying differently. Many design procedures ignore deterioration in the underlying pavement that occurs after overlaying. LEDFAA considers the effects of continued deterioration in underlying pavement. The deterioration is represented in terms of continued reduction in the modulus of elasticity of the underlying pavement, which causes an increase in the overlay stresses and deflections. However, whether the underlying pavement actually continues to deteriorate after overlaying and how the continued deterioration in the underlying pavement affects the structural response of the overlay are not well known. Through measurement of structural responses from strain and deflection gages and HWD deflection data, valuable information regarding the effects of any changes in the structural condition of the underlying pavement will be obtained.

Joint gages in the underlying pavement will provide information about changes in joint opening over time, which can also affect the structural contribution of the underlying pavement. The testing program also calls for a visual survey of the underlying slabs after the completion of testing on the overlay on selected sections. The overlay slabs and the interlayer can be removed after the completion of load testing to enable this survey. The presence of additional distresses in the existing pavement and the extent of additional deterioration (amount and severity) will provide valuable information regarding the need to consider such deterioration in the design.

3.1.3 Existing Pavement Condition Characterization and Structural Contribution

Overlay thicknesses required by both LEDFAA (layered elastic based) and Navy (Westergaard theory based) design procedures depend on the assigned structural condition of the existing pavement. Currently, the condition is considered through a subjective condition index (C_r) or the structural condition index (SCI). Although the SCI provides a rational and objective estimate of the pavement condition, the adequacy of the SCI needs to be verified. In particular, the following questions should be answered:

- What is the relative contribution toward the reduction of structural contribution of the existing pavement of the following distresses, which affect SCI:
 - Transverse cracking?
 - Longitudinal cracking?
 - Corner cracking
 - Shattered cracking
 - Joint spalling

Currently, the SCI treats these distresses equally. However, as was discussed in chapter 2, joint spalling may not affect the overlay behavior at all.

- Does the level of crack deterioration affect the structural contribution of the existing pavement? Currently, different severities of cracking affect SCI significantly.
- How much of the structural contribution of the existing pavement is affected by severity of cracking and spalling?

To evaluate the effects of different distresses on the overlay structural responses and performance, the following structural conditions of the existing pavement will be simulated for each subgrade type:

- No distresses, matched transverse and longitudinal joints
- Mismatched transverse and longitudinal joints
- High-severity longitudinal cracks in the existing pavement
- High-severity transverse cracks in the existing pavement
- High-severity shattered slabs
- High-severity spalled transverse cracks in the existing pavement (low strength subgrade only)
- Low-severity transverse cracks in the existing pavement

In addition to relative comparison of the effect of different distresses for the same loading and subgrade support conditions, the experiment will allow researchers to investigate the effect of subgrade support and gear geometry on such ranking. If required, information obtained from this experiment will permit modification of the SCI.

3.1.4 Performance Model Calibration

The data from the testing will permit calibration of the performance prediction models that relate overlay structural responses (PCC tensile stresses) predicted by a structural model to observed distresses (bottom-up or top-down cracking). Cracking initiated at the bottom of the PCC overlay and propagated to the top PCC surface (bottom-up cracking) will be related to the critical tensile stresses at the bottom of the overlay. Cracking initiated at the top surface of the PCC overlay and propagated through overlay thickness (top-down cracking) will be related to the critical tensile stresses at the bottom of the overlay.

Calibration of the performance prediction model is the most important step in the development of mechanistic-empirical design procedures. The testing program should provide information for calibration of unbonded PCC overlay cracking models. Although only one overlay thickness is proposed for the testing, it is expected that variability in support conditions (both subgrade and existing pavement) will provide a wide spectrum of PCC responses and observed pavement life. That information, in addition to information obtained from full-scale tests of new pavements (if available), should provide a wealth of information for performance model calibration.

3.1.5 Development of Design Recommendations

Currently, the overlay design procedures mainly deal with the overlay thickness design. The effects of joint matching and the use of dowels may have a significant impact on overlay performance, but insufficient data are currently available to draw any conclusions. A common practice for unbonded PCC overlays of highway pavements is to mismatch joints. FAA circular AC 5320-6D states that overlay contraction joints can be over or within 1 ft of existing expansion, construction, or contraction joints. It also states that if a concrete overlay with a leveling course is used, the joint pattern in the overlay does not have to match the joint pattern in the existing pavement. If joint mismatching results in measurable benefit, the practice should be recommended. If the effects are negligible, no special efforts need to be made to mismatch joints.

In this study, the benefit of joint mismatching will be investigated. The behavior of test sections with matched joints will be compared directly to the behavior of joints mismatched in one or both directions. This comparison will be conducted for three subgrade types and two gear configurations. Therefore, the test will enable the development of specific recommendations regarding joint mismatching.

In terms of doweling, the FAA circular states that dowels should be used in expansion joints and butt-type construction joints. They also must be used in the last three transverse contraction joints from a free edge. Contraction joints in the interior of a slab may be dummy joints (aggregate interlock only). In this study, the behavior of overlay sections with doweled contraction joints will be compared with the behavior of undoweled contraction joints. The information obtained can be used for verifying/updating FAA recommendations.

3.2 EXPERIMENTAL PAVEMENT STRUCTURE

This section presents design of the key parameters of the overlay structure to be tested at the NAPTF. This will include selection of the existing pavement parameters (thickness and joint spacing), interlayer thickness, and unbonded overlay parameters, as well as PCC mix and curing procedure selection.

3.2.1 Existing Pavement Parameters

The underlying pavement thickness is an important consideration for evaluating the effects of the existing pavement condition on structural response and performance of unbonded overlays. To ensure that the interaction between the pavement layers in the test pavement represents the field conditions, the underlying pavement thickness must be selected proportionally to the overlay thickness, such that the relative thickness of the underlying pavement with respect to the overlay in the test pavement is similar to that of in-service pavements. One way of achieving this balance is to select the underlying pavement thickness that will provide the service life that is in line with the target service life of the overlay. Of course, the actual structural capacity of the underlying pavement will be reduced by the saw cuts introduced in the slabs to simulate the cracks in the underlying pavement.

In general, the design lives of unbonded concrete overlays are similar to those of new pavements. Therefore, the target design life of the intact underlying slab should be similar to that of the overlay. The target design life for the control sections in the testing program is on the order of 10,000 to 50,000 load repetitions (passes). Thus, the basic approach to thickness selection for the underlying pavement is to provide a structure that would crack in the same range of load repetitions, if the tests were conducted directly on the underlying pavement (i.e., without the overlay).

The concrete pavement thickness design is complicated by the effects of differential shrinkage, creep, and the temperature gradient built into the slabs. The slab curling and warping due to these effects can introduce very high stresses, but the actual amount of built-in curling and warping is difficult to determine. The best available information that could be used to estimate the magnitude of built-in curling and warping that is likely to develop in the test pavement is the performance data from the past tests conducted at NAPTF in March 2002. A test strip constructed in 2001 and tested in 2002 had eight 15 by 15 ft slabs and four 20 by 20 ft slabs, as shown in figure 13. Two different mixes and curing methods were used. The northern slabs were constructed using the same mix design and curing method as the original rigid pavement sections constructed in 1999, whereas southern slabs were constructed using an optimized mix design and curing method to reduce built-in curling and shrinkage warping.

Figure 14 presents the crack pattern in the test strip after it was subjected to traffic, and figure 15 presents the number of gear passes each slab in the test strip sustained until failure. The 20-ft slabs failed after a relatively small number of load applications for both mix designs. The main mode of failure was top-down cracking caused by corner loading. At the same time, the 15-ft slabs sustained many more load applications, and their cracking pattern is more representative of

failures of airfield pavements. Therefore, the 15-ft joint spacing is more appropriate for test pavements at the NAPTF.

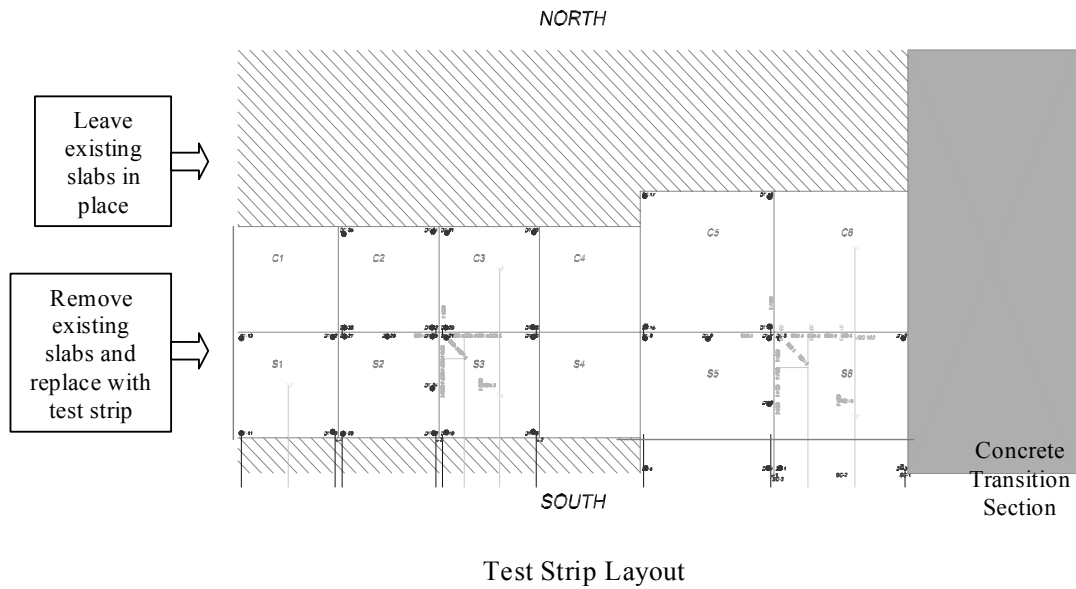


FIGURE 13. LAYOUT OF A TEST STRIP TESTED AT THE NAPTF IN MARCH IN 2002 (MCQUEEN ET AL. 2002)

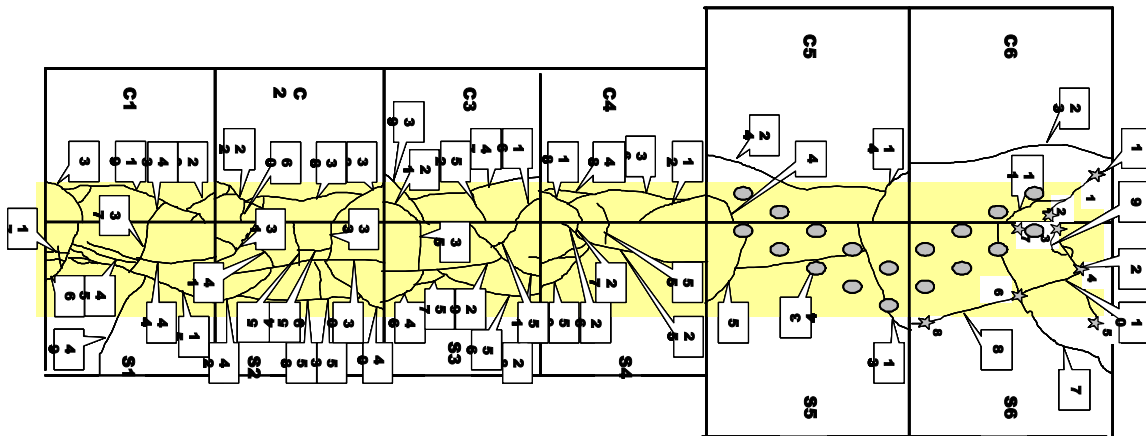


FIGURE 14. CRACK PATTERN IN TEST STRIP (MCQUEEN ET AL. 2002)

Denotes # of Passes	500	3000	2300	1700	800	50	◀ C-slabs, old mix
	800	<i>Edge Cracks Formed Before Corner After 4000 - 5000 Passes</i>			800	50	◀ S-slabs, optimized mix

FIGURE 15. NUMBER OF SUSTAINED GEAR PASSES
(MCQUEEN ET AL. 2002)

The series of tests conducted on 11-in JPCP with 15-ft joint spacing showed extensive cracking after 4,000 load repetitions if a modified mix design and curing were used. The desirable load capacity for the underlying pavement is about 10 times this level (about 40,000 load passes). Under similar conditions (similar concrete mix, similar curing, and the same joint spacing), 12-in slabs should provide the desired level of load repetitions. Thus, the recommended slab thickness and joint spacing for the underlying pavement are 12 in and 15 ft, respectively.

The test strip referenced above was built on a medium strength subgrade. As was stated in the previous chapters, the PCC overlay thickness required by the existing design procedures depends significantly on subgrade stiffness. The research team’s opinion, however, is that the properties of the underlying pavement and its condition affect unbonded overlay behavior for a greater extent than the subgrade properties. To verify this assumption, the research team decided to use the same underlying pavement thickness and joint spacing for all three subgrade types (low strength, medium strength, and high strength).

3.2.2 AC Interlayer Parameters

Currently, there are no guidelines available for selection of the interlayer thickness and properties. At this time, however, testing of different interlayer thicknesses and properties it is not appropriate for the full-scale testing. Significant analytical work and lab testing should be conducted to design the experiment properly. For this project, the interlayer thickness of 2 in was selected. This thickness was recommended by the NCHRP 10-41 study, which investigated the performance of unbonded concrete overlays for highway pavements.

3.2.3 Overlay Parameters

Selection of the overlay parameters for full-scale testing is a challenging problem. On the one hand, too thin an overlay may fail after a few load applications and not provide sufficient information to achieve goals of the experimental program. On the other hand, too thick an overlay may not fail after a very larger number of load applications, which also will not provide information about overlay failure.

Since current design procedures do not consider joint spacing directly, joint spacing was selected based on the results of tests conducted at the NAPTF in March–April 2000 and test strip sections conducted in March 2002.

The rigid pavement sections tested in March 2000 had 20-ft joint spacing and sustained only approximately 900 gear passes. A predominant mode of failure was top-down corner cracking caused by a combination of corner loading, slab curling, and warping.

The test strip tested in 2002 also indicated that 20- by 20-ft slabs are susceptible to top-down cracking, whereas 15- by 15-ft slabs sustained many more load repetitions and failed in longitudinal cracking, which is more typical mode of failure in the field. Therefore, a 15-ft joint spacing was selected for the unbonded overlay.

This selection was compared to the current FAA recommendations. FAA Circular AC 5320-6D does not provide specific recommendations for selection of joint spacing for unbonded PCC overlays. For a new 9-in-thick rigid pavement with a granular base, the recommended maximum joint spacing is 20 ft, which is greater than the selected thickness. For a new pavement with a stabilized base, the ratio of joint spacing to the radius of relative stiffness should not exceed 6. Assuming the coefficient of subgrade reaction on top of the existing PCC slab is 500 psi/in and the PCC modulus of elasticity is equal to 6 million psi (backcalculated values from the previous tests), the radius of relative stiffness would be equal to 29.28 in, and the maximum joint spacing would be equal to 14.7 ft. Considering that too short joint spacing may be not representative of field conditions, a 15-ft joint spacing was selected.

The required overlay thickness was determined using the FAA design procedure, LEDFAA, the Navy design procedure, and mechanistic checks. The results of the analysis using each of these procedures are discussed below.

3.2.4 Overlay Design Using LEDFAA

To determine the required unbonded overlay thickness, a series of LEDFAA runs was performed. The following structure was assumed for the existing pavement:

- Existing PCC layer is 12 in thick
- Crushed stone base is 12 in thick
- PCC modulus of rupture is equal to 750 psi for both the PCC overlay and existing pavement
- CBR is equal to 4, 8, and 30 for low strength, medium strength, and high strength subgrades, respectively
- Aircraft type is a B-777-200C with gross load equal to 568,400 lb, which corresponds to a wheel load in the main gear equal to 45,000 lb
- Target number of load repetitions is 10,000
- The structural condition index (SCI) of the existing pavement was varied from 40 (poor condition) to 100 (excellent condition)

Table 1 presents the required unbonded overlay PCC thickness obtained from LEDFAA analysis for different combinations of subgrade strength and existing pavement conditions. For a soft subgrade (CBR = 4), LEDFAA requires an overlay thickness between 7.3 and 11.4 in, depending on condition of the existing pavement. For other subgrade types, an unrealistically low overlay thickness of 3 in was obtained.

Analysis of the B747 gear led to very similar results. The overlay thickness varied from 6.9 to 11.0 in for the soft subgrade, but the minimum allowed thickness of 3 in was obtained for medium and high strength subgrades regardless of the existing pavement condition.

Using LEDFAA, the performance life of 9-in PCC overlays was checked for B-777 and B-747 gears. For each gear type, wheel loads of 45,000 and 65,000 lb per wheel were considered. Table 2 presents the results of this analysis. The expected design life of a 9-in overlay under a B-747 gear with a wheel load of 45,000 lb varies from 2,200 (soft subgrade, poor pavement condition) to several million repetitions (strong subgrade, good pavement conditions). A similar performance life is predicted for a B-777 gear. However, according to LEDFAA, for each subgrade type there will be at least one existing pavement condition that will survive at least 20,000 passes and fail not later than after 50,000 passes.

It can be also observed that an increase in gear load from 45,000 lb to 65,000 lb per wheel load significantly reduces the predicted overlay life, but even for this loading, sections subjected to B-777 gear loading are not expected to fail if the underlying pavement is in good condition. However, as was discussed above, the research team does not expect so huge a difference in design life for the sections with the same overlay parameters and existing pavement conditions but different subgrades. Considering that LEDFAA predictions for soft subgrade appear to be more realistic, one can conclude that sections with a stiff subgrade will fail after a reasonable number of load applications.

Based on these results, one can conclude that, according to LEDFAA, a 9-in thickness is appropriate for test sections at the NAPTF.

3.2.5 Overlay Design Using Navy Design

The Navy overlay design procedure was used as an additional check to verify overlay thickness selection. Standard NAVFAC policy requires that Navy design be based on a center (interior) loading Westergaard solution and PCA fatigue beam model (Packard 1973). However, the edge stress option is included in the Navy design software to allow the designer to evaluate how a thickness design is impacted by an edge loading condition as compared to an interior loading condition. Table 3 provides comparison of LEDFAA and the two options of the Navy design program. The effects of various design factors are considered in different ways in different design procedures; therefore, the use of the Navy design program provides an independent appraisal of the overlay design thickness.

TABLE 1. REQUIRED OVERLAY THICKNESS FROM LEDFAA.

Subgrade CBR	SCI	Overlay thickness, in	
		B747-400	B777-200C
4	40	11.0	11.5
4	60	8.2	8.6
4	80	7.3	7.8
4	100	6.9	7.4
8	40	9.0	3
8	60	4.9	3
8	80	3	3
8	100	3	3
30	40	3	3
30	60	3	3
30	80	3	3
30	100	3	3

TABLE 2. OVERLAY PERFORMANCE LIFE FROM LEDFAA.

Subgrade CBR	SCI	Number of passes until failure			
		B747-400		B777-200C	
		45000 lb/wheel	65000 lb/wheel	45000 lb/wheel	65000 lb/wheel
4	40	2200	300	3000	400
4	60	14200	700	12200	600
4	80	29300	1000	19900	700
4	100	39200	1200	26100	10000
8	40	10100	700	24900	1600
8	60	53100	2300	146000	4500
8	80	151400	3500	369000	6900
8	100	228500	4600	518000	8500
30	40	35200	2200	196000	9000
30	60	209000	8700	1364000	37700
30	80	1018000	29400	7341000	150200
30	100	3559000	45900	37182000	272000

TABLE 3. COMPARISON OF LEDFAA AND NAVY DESIGN PROCEDURES

Design Factors	LEDFAA	Navy Design – Interior Loading	Navy Design – Edge Loading
Analytical model	Layered elastic theory	Plate on Winkler foundation, interior loading. Empirical equation for effective thickness, $(h_e^n = h_{OL}^n + C h_{SL}^n)$	Plate on Winkler foundation, edge loading. Empirical equation for effective thickness, $(h_e^n = h_{OL}^n + C h_{SL}^n)$
Analytical model	JULEA	Westergaard's solution	H51 (Kreger 1967)
Failure criteria	Deterioration in terms of a structural condition index	Failure of a simply supported beam with the same stress history	50 percent cracked slabs
Fatigue Model	Rolling (1988) model based on full scale testing.	PCA beam fatigue model (Packard 1973).	Corp of Engineers fatigue model based on full scale testing (Darter 1990).
Cracking in existing pavement before overlay	Modulus of elasticity of existing pavement is reduced	Effective thickness of existing pavement is reduced	Effective thickness of existing pavement is reduced
Interface condition	Varies between full bonding and completely unbonded	Power in design equation is adjusted to account for level of bonding	Power in design equation is adjusted to account for level of bonding
Material properties	Modulus of elasticity and Poisson's ratio for all materials, and flexural strength of overlay concrete	Equivalent required thickness, "h," as input to empirical equation loading Empirical equation, $(h^n = h^n - h_e^n)$	Equivalent required thickness, "h," as input to empirical equation
Difference in strength/modulus of overlay and base pavement concrete	Included directly in calculation of stresses and design factors	Thickness of base pavement is adjusted	Thickness of base pavement is adjusted
Cracking in base pavement before overlay	Modulus of elasticity of base pavement is reduced	Effective thickness of base pavement is reduced	Effective thickness of base pavement is reduced
Cracking of underlying pavement after overlay	Modulus of elasticity of base is reduced to compensate for cracking under traffic	Not directly considered	Not directly considered
Temperature curling or moisture warping	Not considered	Not considered	Not considered

The following structure was assumed for the existing pavement:

- Existing PCC layer is 12 in thick
- Crushed stone base is 12 in thick
- PCC modulus of rupture is equal to 750 psi for both the PCC overlay and existing pavement
- Subgrade k-value was assumed to be equal to 100, 200, and 300 psi/in for low strength, medium strength, and high strength subgrade sections, respectively. Those values were assumed based on the results of backcalculation performed by Guo and Marsey (2001) for new PCC pavement sections. According to Guo and Marsey, backcalculation for low strength, medium strength, and high strength subgrade sections resulted in dynamic k-values equal to 200, 400, and 600 psi/in, respectively. Since the Navy design procedure requires static k-value, the dynamic k-values for each section were divided by 2 to obtain static k-values, as recommended by Darter et al. (1995).
- Aircraft type is a B-777-200-C with 6-wheel gear load equal to 270,000 lb and aircraft B-747-400 with 4-wheel gear load of 180,000 lb
- Target number of load repetitions is 10,000
- The structural condition index (SCI) of the existing pavement is varied from 40 (poor condition) to 100 (excellent condition)
- Joint transfer efficiency is selected equal to 70 percent for edge loading design

Tables 4 and 5 present the required PCC thicknesses for center load and edge load designs, respectively. According to the Navy design procedure (center slab load location design), all subgrade sections will sustain at least 10,000 gear passes. Only a section with a very poor existing pavement condition (SCI = 40, which corresponds to shattered slabs) will fail earlier. A design check based on the edge loading condition predicts early failures for the B-777 gear on a soft subgrade if the existing pavement is not in excellent condition, but for other subgrades, it predicts a design life greater than 10,000 gear passes. It should be also noted that k-values selected for this analysis are lower than those recommended in the Navy Design Manual (200 psi/in for soft subgrade and 500 psi/in for strong subgrade). If those values were used, the required overlay thicknesses would be much lower.

Based on these results, one can conclude that, according to the Navy design procedure, a 9-in thickness is appropriate for test sections at the NAPTF.

TABLE 4. REQUIRED PCC OVERLAY DESIGN THICKNESS FROM NAVY DESIGN PROCEDURE. CENTER SLAB LOAD POSITION DESIGN

k – value, pci	SCI	Overlay thickness, in	
		B747-400	B777-200C
100	40	9.43	8
100	60	8.0	8.
100	80	8	8
100	100	8	8
200	40	8	8
200	60	8	8
200	80	8	8
200	100	8	8
300	40	8	8
300	60	8	8
300	80	8	8
300	100	8	8

Note: 8-in thickness represents the minimum thickness recommended by the Navy design procedure.

TABLE 5. REQUIRED PCC OVERLAY DESIGN THICKNESS FROM NAVY DESIGN PROCEDURE. EDGE SLAB LOAD POSITION DESIGN

k – value, pci	SCI	Overlay thickness, in	
		B747-400	B777-200C
100	40	10.99	10.29
100	60	10.11	9.17
100	80	8.91	8
100	100	8.00	8
200	40	8.72	8
200	60	8	8
200	80	8	8
200	100	8	8
300	40	8	8
300	60	8	8
300	80	8	8
300	100	8	8

Note: 8-in thickness represents the minimum thickness recommended by the Navy design procedure.

3.2.6 Mechanistic Analysis of Unbonded PCC Overlay

Mechanistic modeling of unbonded PCC overlays is a challenging engineering problem. The complex interaction between the pavement layers and effects of cracks and joints in the existing pavement on the overlay behavior makes prediction of the structural responses (stresses, strains, and deflections) very complex. Prediction of the overlay failure is another challenge. A mathematical model may predict concentration of high stresses in the overlay, but those stresses may be not critical due to the highly localized nature of those stresses. Moreover, uncertainty with concrete strength level and expected amount of built-in curling and moisture warping makes the prediction of the overlay life even more difficult. Nevertheless, an attempt was made to predict behavior and possible mechanism of failure of unbonded PCC overlays using mechanistic analysis. Two structural finite element models describing the behavior of unbonded PCC overlays (one without cracking in existing pavement and another with cracking in existing pavement) were developed. Using those models, critical PCC overlay stresses were calculated and recommendations were made regarding the overlay system's ability to sustain the desired range of load repetitions. The results of this analysis are presented below.

3.2.6.1 Structural Model Development

The finite element program ISLAB2000 (Khazanovich et al. 2000) was used for the development of unbonded overlay models. ISLAB2000 is a completely re-written version of the finite element program ILLI-SLAB (Tabatabae and Barenberg 1980) that retains all the positive features of ILLI-SLAB and has also several other positive features, including the following:

- Ability to analyze separation between the pavement layers (Totski interface). This feature makes ILSL2 and ISLAB2000 more like 3D models than like 2D models (sometimes they are referred to as “2.5D” models)
- Ability to analyze mismatched joints and cracks

Two finite element models were developed in this study. The first model utilizes a feature specific for ISLAB2000—the Totski model. This model was used to evaluate the effect of cracks in the underlying pavement on PCC overlay responses. The existing pavement and the overlays were modeled as two independent plate layers separated by a spring layer that models an AC interlayer. The overlay is loaded by a dual tridem gear loading loaded symmetrically with respect to the crack in the existing pavement. Figure 16 shows a fragment of this finite element model. One can see that the existing pavement has a crack with low load transfer efficiency, which is bridged by the overlay.

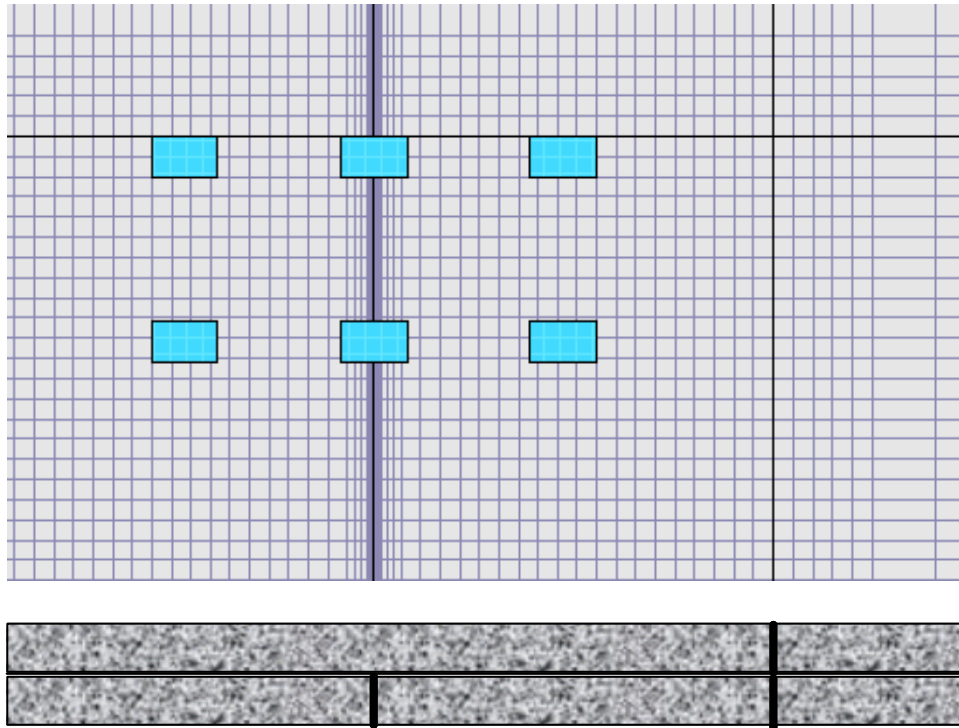


FIGURE 16. ISLAB2000 FINITE ELEMENT MODEL OF CRACKS IN THE UNDERLYING PAVEMENT

Figure 17 presents a typical unbonded stress distribution at the bottom of the PCC overlay along the overlay edge under a heavy gear load for non-cracked and cracked underlying pavements. Both corresponding stress distributions increase until they reach a maximum under the center of applied load. As could be expected, the presence of a crack in the underlying pavement increases overlay stresses. However, if the underlying pavement is not cracked, then stresses in the overlay increase gradually, whereas the presence of a crack causes a significant jump in stresses under the maximum stresses.

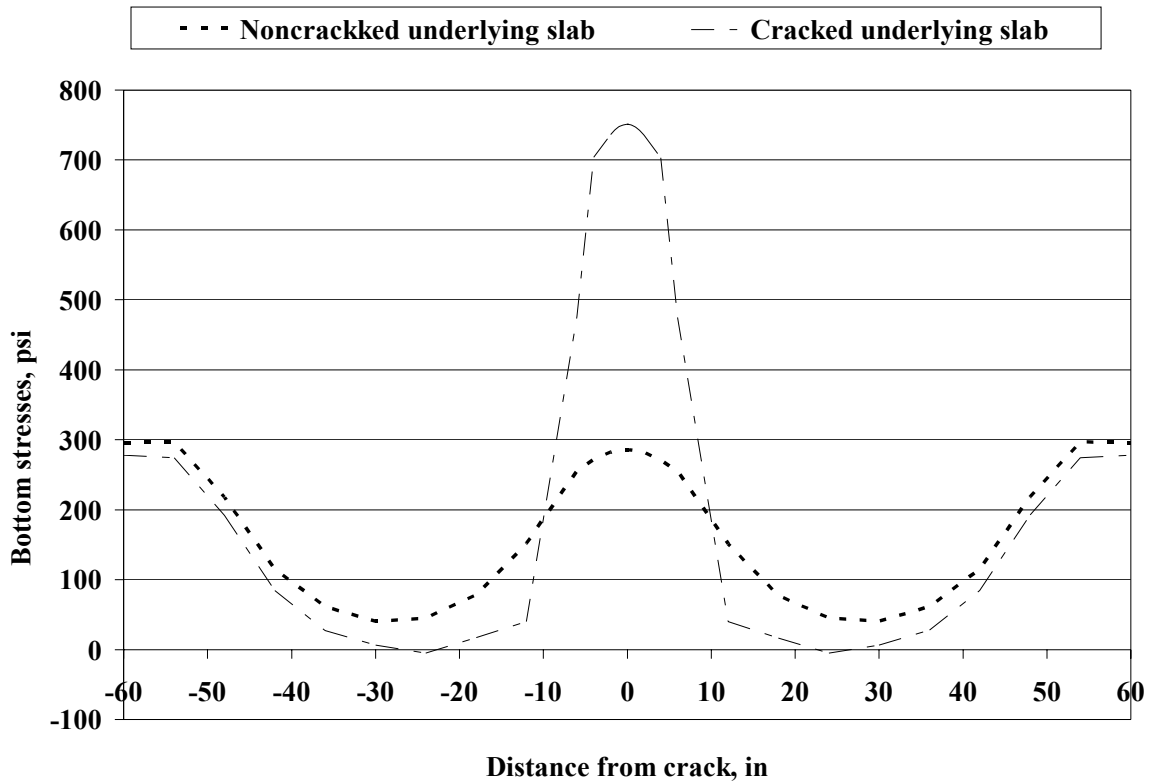


FIGURE 17. EFFECT OF A CRACK IN THE UNDERLYING PAVEMENT ON PREDICTED STRESSES IN AT THE BOTTOM OF THE PCC OVERLAY

The effect of the apparent dramatic increase in overlay stresses above cracks in the underlying pavement deserves special discussion. Although these stresses are mathematically high, they do not necessarily cause significant damage in the overlay because they affect only a small area. The presence of an adequate crack-arresting layer may significantly mitigate the effect of these stresses. Moreover, it is quite possible that significant stress redistribution takes place in the pavement system, such that these high stresses exist only in a mathematical model and do not actually exist within the overlay. Currently, this uncertainty creates a significant challenge in performing a mechanistic check of PCC overlay design; however, full-scale testing at the NAPTF provides an excellent opportunity to shed light on this problem.

A factorial of finite element runs was performed to evaluate the effect of the overlay thickness on maximum overlay stresses at the bottom of the overlay for cracked and uncracked existing pavements for different overlay thicknesses. The overlay was loaded by a B-777 gear load (270,000 lb); no temperature loading was considered. The overlay thickness was varied from 6 to 10 in.

Figure 18 presents the results of this analysis. An increase in the overlay thickness leads to a slight increase in overlay stresses if the existing pavement is not cracked and a decrease in the overlay stresses if the existing pavement is cracked. Although a relatively high level of stresses

is observed for overlay thicknesses of 9 in, considering the localized character of those stresses, it is reasonable to assume that a 9-in-thick overlay should be able to sustain a substantial number of load applications even if a crack is present in the existing pavement.

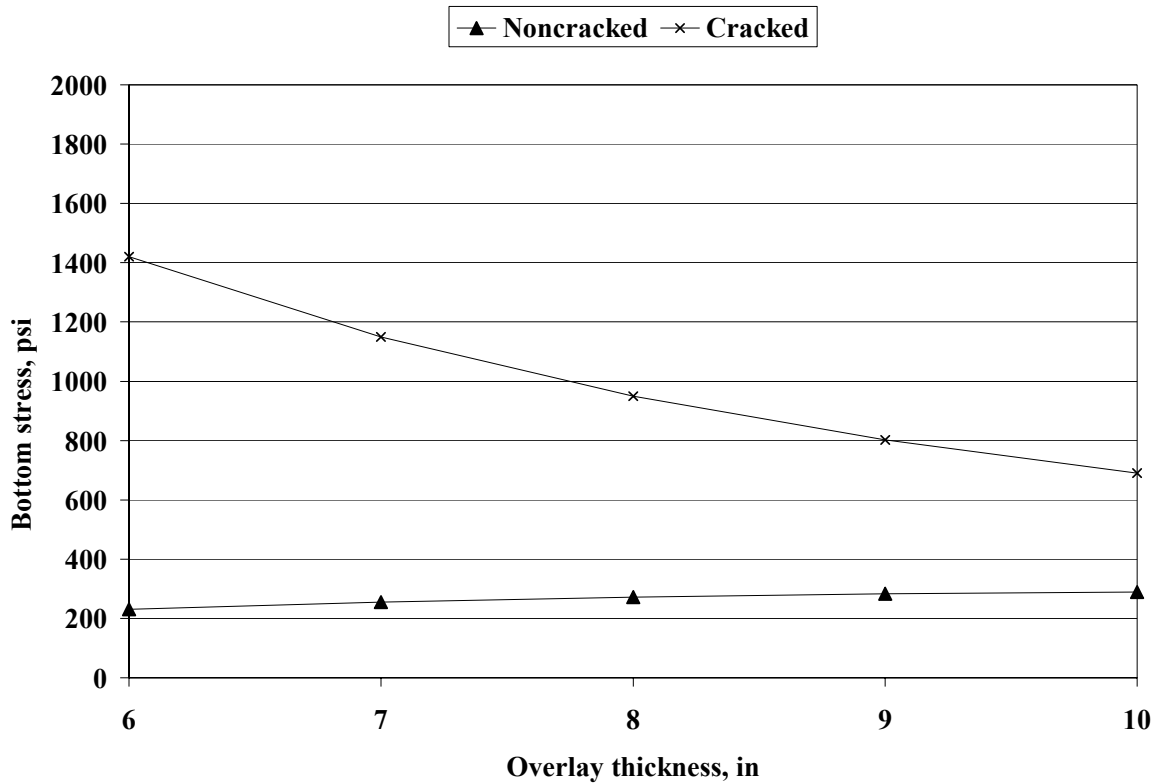


FIGURE 18. EFFECT OF THE OVERLAY THICKNESS ON THE MAXIMUM OVERLAY STRESSES AT THE BOTTOM SURFACE FROM B-777 GEAR LOADING

3.2.6.2 Analysis of PCC Overlay Curling and Warping

Although NAPTF is an indoor facility, the PCC pavement sections still experience curling due to variation of the PCC temperature throughout the pavement thickness. In this study, the Enhanced Integrated Climatic Model (EICM) was used to predict temperature distribution throughout unbonded overlay PCC thickness. The EICM was originally developed at the University of Illinois (Dempsey 1986) and was expanded under the NCHRP 1-37A study. The following system was considered:

- PCC overlay thickness – 9 in
- Existing pavement thickness – 12 in
- AC interlayer thickness – 2 in
- PCC thermal conductivity - 1.25 BTU/hr-ft-F°
- PCC heat capacity – 0.28 BTU/lb-F°

- AC thermal conductivity - 1.0 BTU/hr-ft-F°
- AC heat capacity – 0.23 BTU/lb-F°
- Aggregate base
- Subgrade A-6

To account for indoor conditions, surface shortwave absorptivity was assumed equal to 0 (which corresponds to the absence of direct solar radiation). Figure 19 present typical temperature distributions throughout the PCC slab obtained for September. Comparison of these distributions with distributions obtained for outdoor pavement section showed similar daily variations, but there is a time shift (PCC surface warms up later in the day than it would outdoors), and the temperature gradient at the top surface is not as dramatic as it would be predicted for the outdoor conditions.

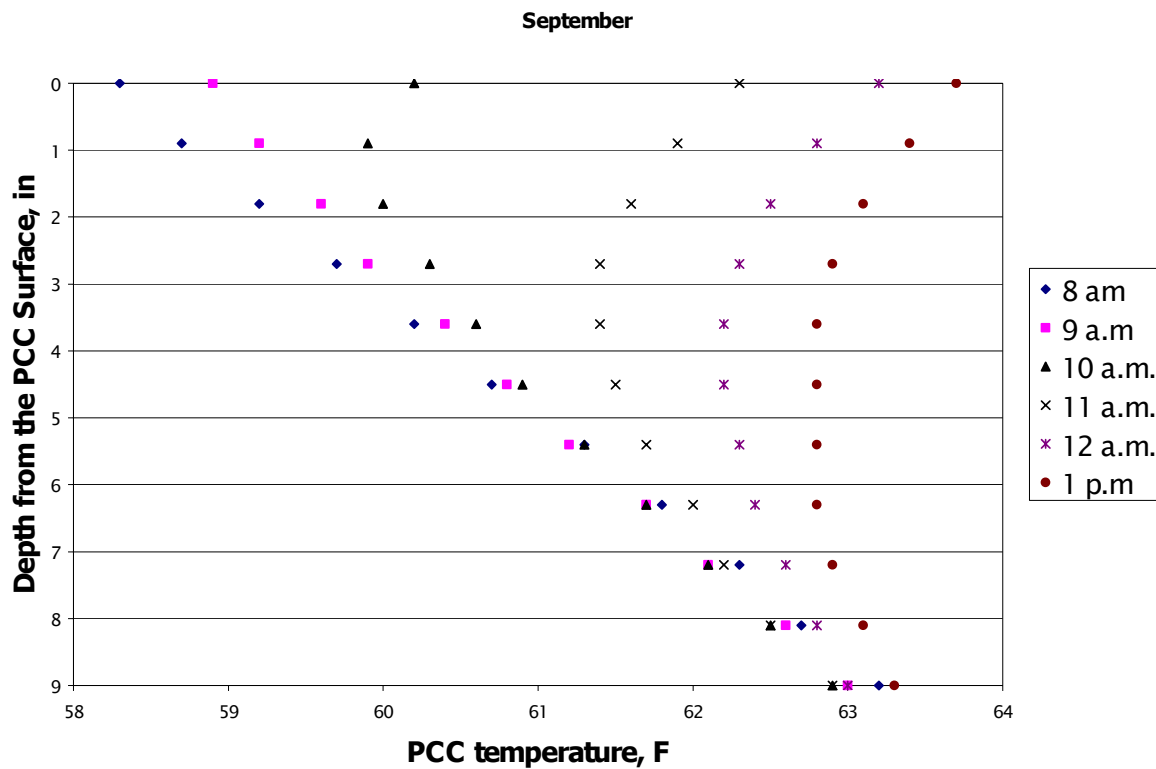


FIGURE 19. PREDICTED TEMPERATURE DISTRIBUTION THROUGHOUT PCC OVERLAY THICKNESS AT NAPTF FOR A TYPICAL DAY IN SEPTEMBER

For each temperature profile, an equivalent temperature distribution (linear distribution through the depth which causes the same deflection profile in the unbonded overlay as an original non-linear distribution) was calculated using a methodology proposed by Khazanovich (1994). Figure 20 presents frequency distributions of the equivalent temperature differences between the top and bottom PCC overlay surfaces obtained for the entire year and for daytime (8 am to 4 pm)

only. One can observe that, even during the daytime, the PCC overlay is subjected to negative temperature gradients for a substantial portion of the day.

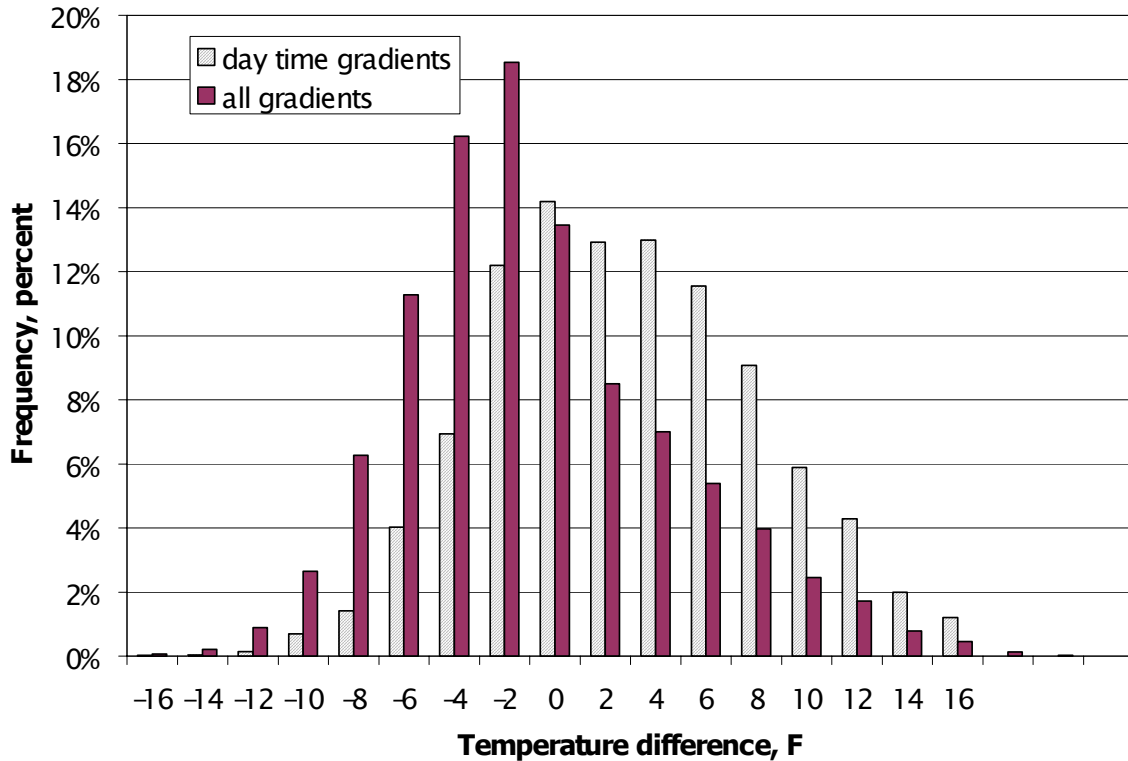


FIGURE 20. FREQUENCIES OF EQUIVALENT DIFFERENCE BETWEEN PCC OVERLAY TOP AND BOTTOM SURFACES PREDICTED BY EICM

The calculated temperature differences do not account for moisture warping and built-in temperature gradients. The latter accounts for non-uniformity in temperature distribution during PCC hardening, which results in PCC slab warping if no temperature or moisture gradients exist. Therefore, these temperature distributions should be shifted to account for built-in curling and moisture warping. The magnitude of this shifting factor depends on many factors (temperature during PCC placement, PCC properties, and air humidity) and currently cannot be predicted exactly. However, according to the FHWA-sponsored Rigid Pavement Performance (RPPR) study, for outdoor pavements this parameter typically varies from -8 to -12 °F, but might be as low as -16 °F. The shift factor for indoor pavements can be higher than for outdoor pavements, but figure 21 shows that even if only a -12 °F shift is applied, during the majority of the daytime the overlay should experience a negative temperature gradient.

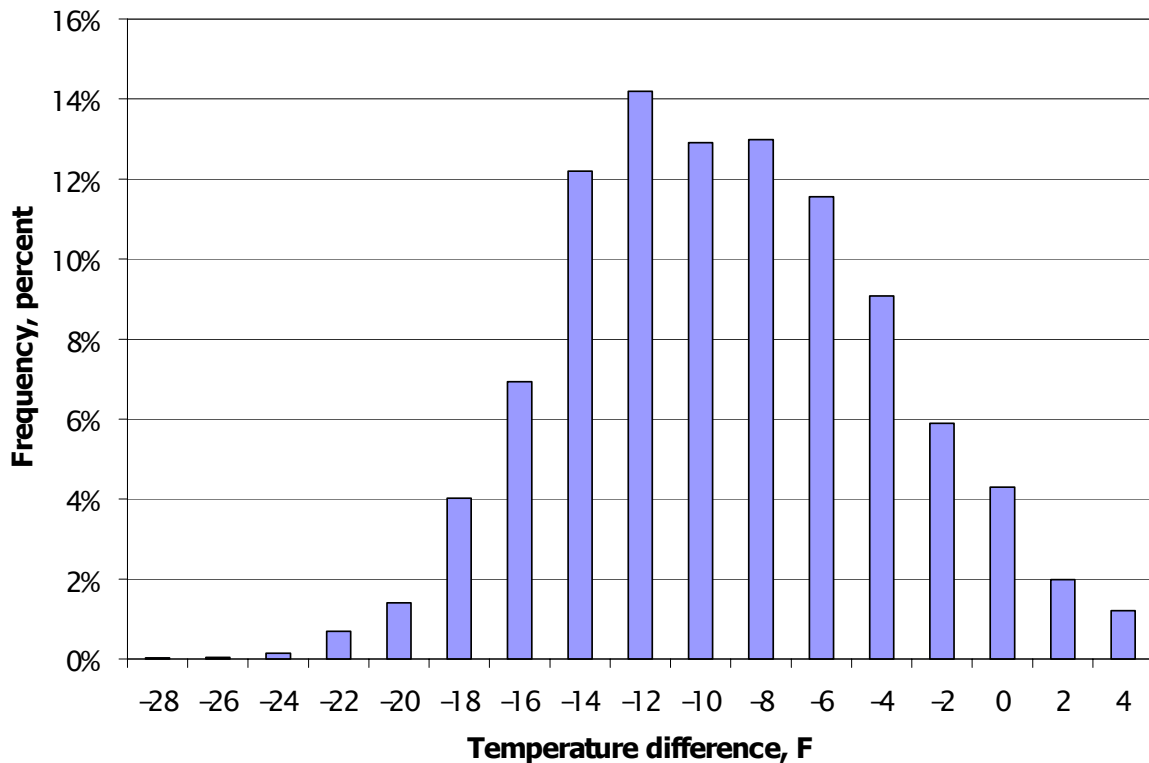


FIGURE 21. FREQUENCIES OF EQUIVALENT DIFFERENCES BETWEEN PCC OVERLAY TOP AND BOTTOM SURFACES PREDICTED BY EICM FOR DAYTIME AND ADJUSTED FOR BUILT-IN CURLING AND SHRINKAGE WARPING

These temperature distributions were compared with the temperature distributions predicted for the test strip slabs constructed at the NAPTF in September 2001. The following parameters were assumed:

- PCC slab thickness – 11 in
- Lean concrete base (LCB) thickness – 6 in
- PCC thermal conductivity - 1.25 BTU/hr-ft-F°
- PCC heat capacity – 0.28 BTU/lb-F°
- LCB thermal conductivity - 1.0 BTU/hr-ft-F°
- LCB heat capacity – 0.23 BTU/lb-F°
- Aggregate base
- Subgrade A-7-6

Figure 22 presents the frequencies of equivalent difference between top and bottom surfaces temperatures of the PCC overlay and test strip pavements as predicted by EICM for the entire year. The overlay experiences more high negative temperature gradients than the new pavement. This does not mean that the resulting negative gradient will be more severe for the overlay, necessarily, since the presence of the AC interlayer may reduce the amount of built-in curling.

Nevertheless, it is fair to assume that the overlay will experience at least similar warping conditions as were experienced by the test strip slabs.

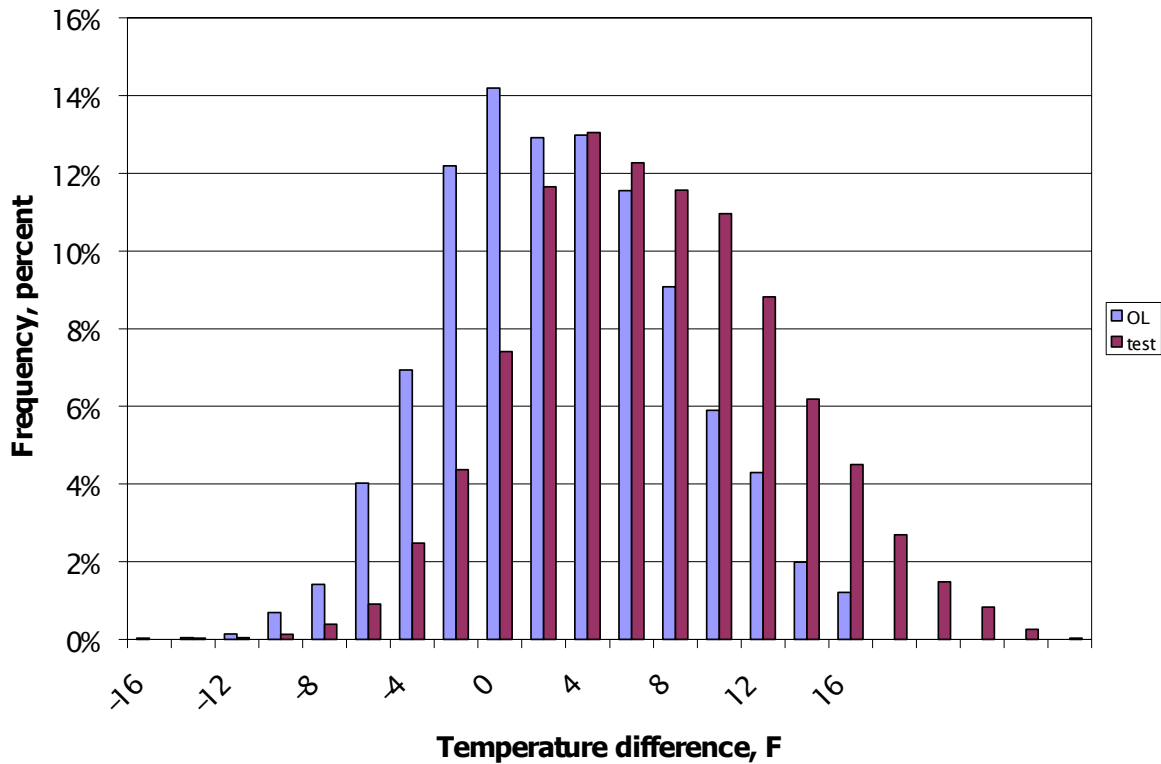


FIGURE 22. COMPARISON OF FREQUENCIES OF EQUIVALENT DIFFERENCE BETWEEN TOP AND BOTTOM SURFACES TEMPERATURES OF THE PCC OVERLAY AND TEST STRIP PAVEMENTS AS PREDICTED BY EICM

To investigate the effect of the slab warping on the overlay behavior, finite element models for the test strips slabs and the unbonded overlay were developed. It was assumed that the existing pavement has no cracks and the unbonded interface was used to model the interface condition between the overlay and the existing pavement, as well as the test strips and the lean concrete base.

Both pavement systems were subjected to different negative temperature gradients and a B747 gear load. The gear load was moved along the longitudinal edge to capture the most critical load positions for bottom and top PCC overlay and test slab stresses (see figures 23 and 24, respectively). The total gear load was assigned to be equal to 220,000 lb (55,000 lb per wheel) for the test strip slabs and 180,000 lb (45,000 lb per wheel) for the overlay. The coefficients of subgrade reaction were assumed to be equal to 200, 400, and 600 psi/in for soft, medium, and strong subgrades, respectively.

Figure 25 presents a comparison of the bottom surface stresses predicted by ISLAB2000 for the PCC overlays and test strips. For the entire range of negative temperature gradients, stresses in the overlay were much lower than those predicted for the test strip. Therefore, significantly longer resistance to bottom-up cracking can be expected for unbonded overlays than was observed for the test strip slabs.

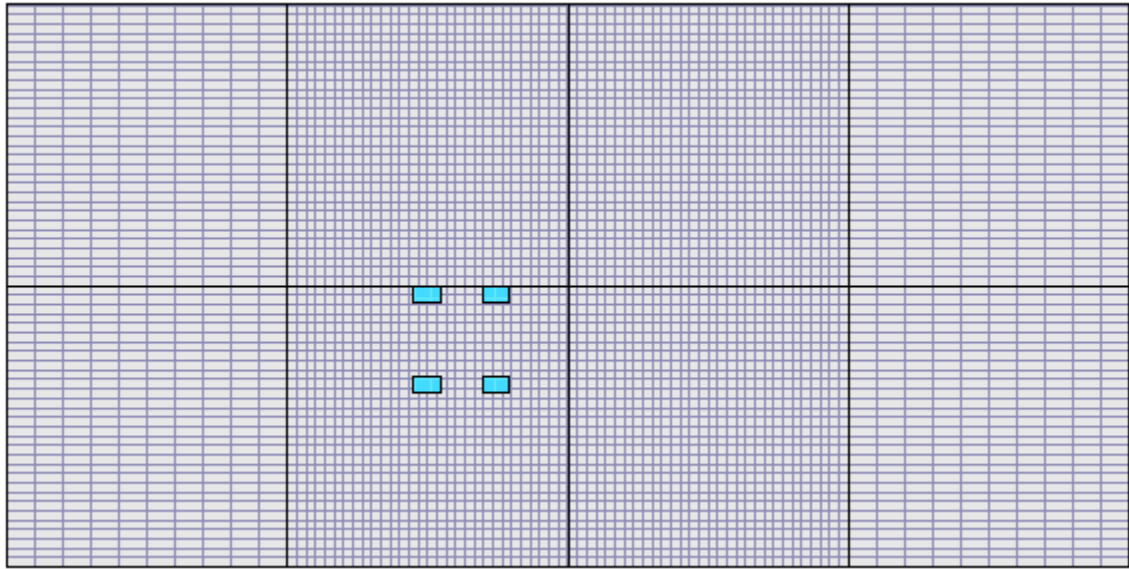


FIGURE 23. APPROXIMATE GEAR POSITION FOR CRITICAL BOTTOM SURFACE OF THE TOP LAYER STRESSES

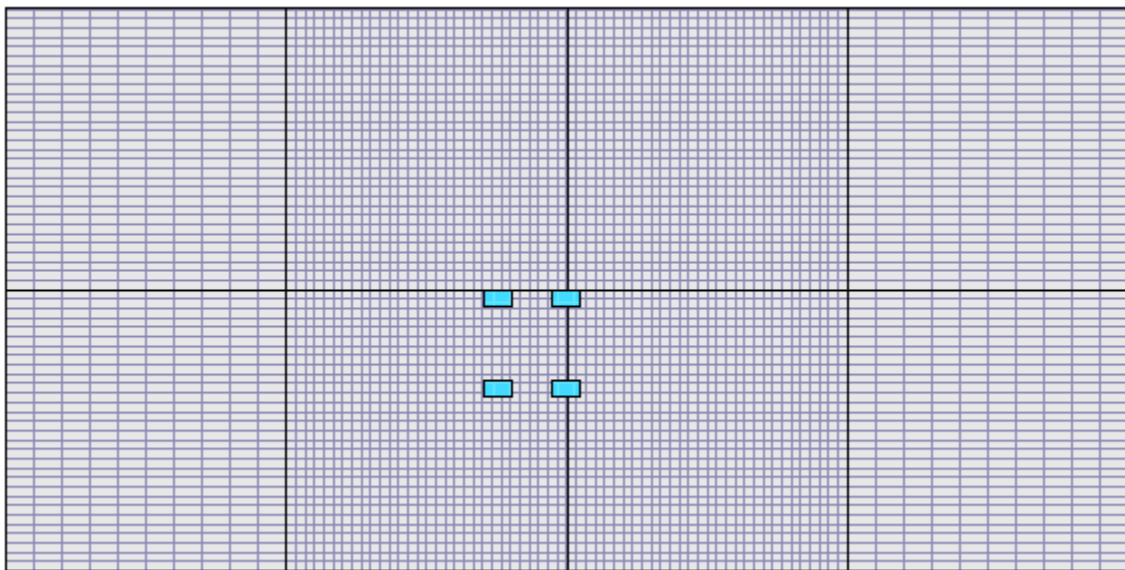


FIGURE 24. APPROXIMATE GEAR POSITION FOR CRITICAL TOP SURFACE STRESSES

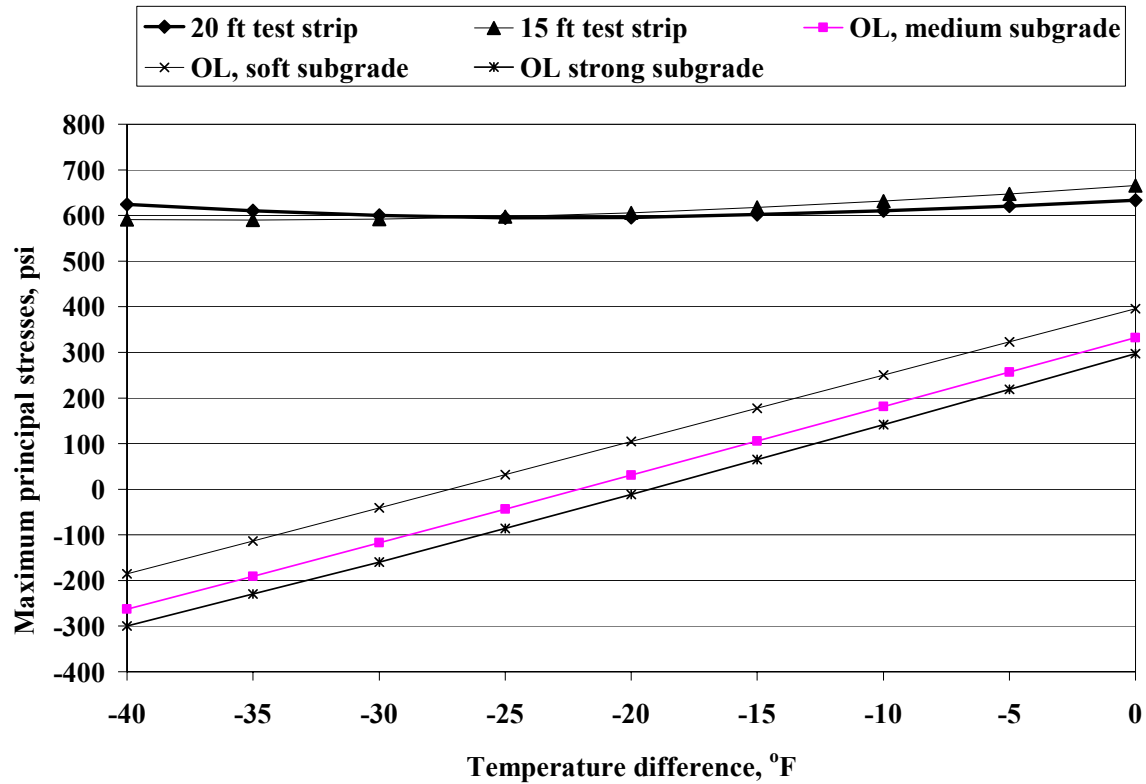


FIGURE 25. COMPARISON OF BOTTOM SURFACE STRESSES FOR THE UNBONDED OVERLAYS AND TEST STRIPS

A different picture was observed for the critical top surface stresses (see figure 26). For high equivalent temperature differences, the overlay stresses are predicted to be somewhere between the stresses predicted for the 15- and 20-ft test strip sections. Therefore, it is reasonable to assume that if the warping conditions and the PCC material properties for the overlay are the same as they were for test strip slabs, then the expected number of load repetitions is between 800 and 5,000. To increase the number of load passes, the built-in curling and moisture warping should be reduced. Therefore, it is important to pay special attention to PCC overlay curing during construction.

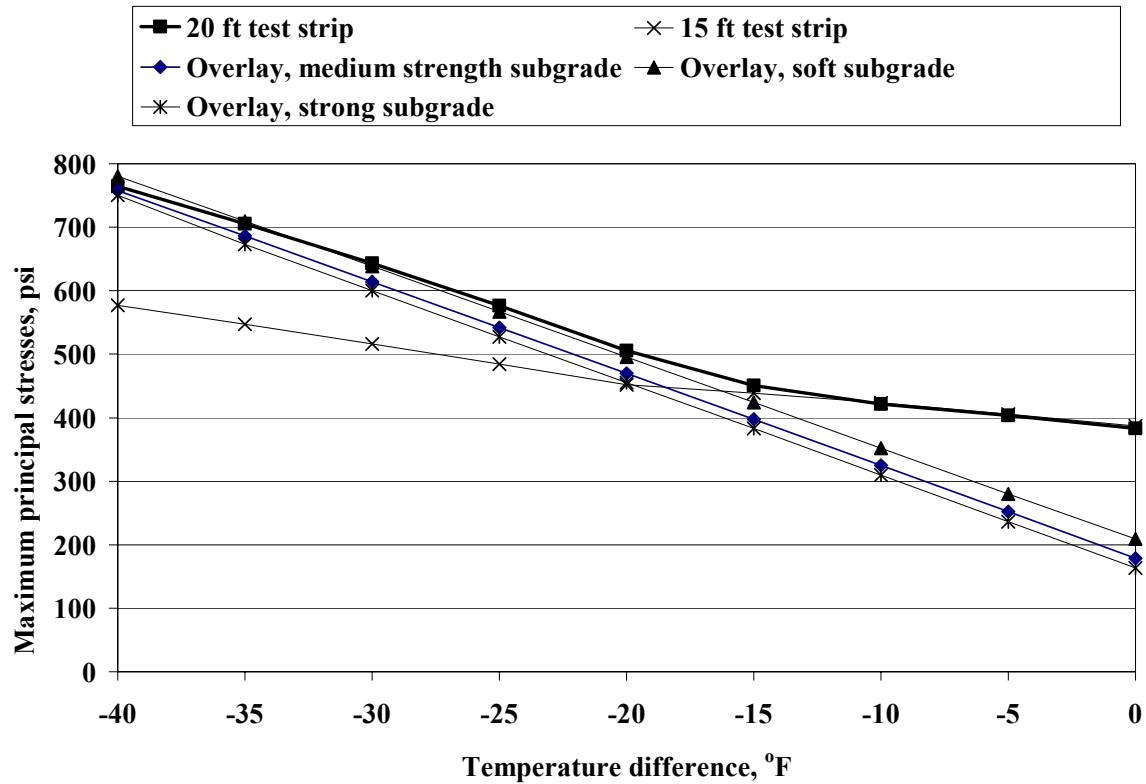


FIGURE 26. COMPARISON OF TOP SURFACE STRESSES FOR THE UNBONDED OVERLAYS AND TEST STRIPS

3.2.7 Final Pavement Structure

Based on this analysis and the results of the LEDFAA, Navy design procedure, and mechanistic checks, the following pavement parameters were selected:

- Overlay thickness – 9 in
- Overlay joint spacing – 15 ft
- Existing pavement thickness – 12 in
- Existing pavement joint spacing (uncracked sections) – 15 ft

The overlay longitudinal joints near the wheel path and transverse joints were assigned to be doweled, with a dowel diameter equal to 1.25 in and dowel spacing equal to 12 in. Several transverse joints in the overlay were selected to be undoweled to compare the performance of doweled and undoweled overlays.

3.3 PCC MIX PROPERTIES

Although PCC mix design will not be done under this project, the properties of the mix have a major impact on the performance of PCC overlays. Therefore, the mix properties design

deserves some discussion. It is assumed that the properties of the PCC layers will be similar to those used in the latest NAPTF test strip experiment. This section provides some background information related to the past NAPTF PCC mix designs and discusses factors that may affect PCC mix properties at the NAPTF.

Original (1999) construction of the rigid test pavements at the NAPTF was based on field design and general construction practices, even though the pavements at the NAPTF are constructed indoors. The various trial mixes made for the original PCC slabs had relatively high flexural strength (in excess of 850 psi) due to the good quality of available aggregates. Because of the indoor construction, the behavior of the rigid test pavements was different from the behavior typically observed in the field. Due to excessive upward curling, these sections failed in top-down corner cracking.

In 2001, the FAA built instrumented concrete test strips to monitor the amount of shrinkage occurring in the slabs. The effects of concrete mix design, curing techniques, and slab dimensions on performance were studied. One strip of test slabs (C-slabs) was produced by duplicating the concrete mix design originally used in the first construction of the test pavements at the NAPTF. These slabs were designated as the control slabs. The other strip of test slabs (S-slabs) was placed using a new concrete mix design based on an extensive laboratory investigation. All slabs were instrumented so that a relative comparison of performance and response of the two mixes could be studied. Since S-slabs exhibited better performance and their failure better reflected typical (bottom-up) fatigue failure, the concrete mix design for the test strips S-slabs at the NAPTF (see table 6) is recommended as the mix design for both existing pavements and unbonded overlay in the proposed tests. Laboratory testing done on the range of mixes for the test strips at the NAPTF resulted in flexural strength ranging from 870 psi to 1,150 psi.

TABLE 6. CONCRETE MIX DESIGN USED IN TEST STRIPS AT THE NAPTF
(MCQUEEN ET AL. 2002)

Mix Constituent	Amount
No. 57 Coarse Aggregate	1,450 lbs
No. 9 Intermediate Aggregate	790 lbs
Concrete Sand	1,120 lbs
Water	231 lbs
Type I Cement	525 lbs
Air	4.9%
HRWR Additive	10 oz per 100 lbs
Slump	3 inches
Water/Cement Ratio	0.44
Yield	27.1 cy
Workability	34.1%
Coarseness	58.4%
Mortar	53%

The following sections discuss the effects of different parameters on PCC mix properties.

3.3.1 Water-Cement Ratio

A key factor affecting strength and quality of concrete is the water to cement ratio (w:c). It affects both the durability and shrinkage of a concrete mixture, as well as the workability. Stiff mixes using low w:c ratios (0.3 to 0.4) are difficult to place in fixed forms, as used in the NAPTF. Therefore, the original concrete mix design was selected with a w:c ratio of 0.5. However, the resulting shrinkage in the concrete was measured to be 0.08%. To minimize differential shrinkage in the NAPTF concrete pavements, a reduced w:c ratio appeared appropriate, and the test strips placed in 2001 were constructed to have a w:c ratio of 0.44. Because the strength of concrete is inversely related to the w:c ratio in that as w:c increases, the strength decreases, the mix with 0.44 w:c ratio gives higher strength slabs, which may require more time and loading to failure. Lower cement content may be necessary to maintain reasonable strength.

3.3.2 Moisture Content

The moisture content of concrete is very influential on workability. High moisture results in curling/warping of slabs and can induce stresses that make slabs more vulnerable to loading. Maintaining a low moisture content can decrease air content in the mix by approximately ½ to 1 percentage point per gallon of water. However, high fluid mixes can cause a loss of air (*PCA "Design and Control of Concrete Mixes"*). The moisture content is reduced by increased air content, aggregate size and shape, addition of water-reducing admixtures, and reduced w:c ratio. Air content may not be important if the PCC slabs are not subject to freeze-thaw.

The water/cement ratio of 0.44 used in the test strips at the NAPTF was a result of 231 lbs of water in the mix. This moisture content then resulted in a workability of 34.1%.

3.3.3 Cement Type and Amount

Type I cement is typically used for airfield pavement construction and was used in the NAPTF pavements, both in the original mix and in the test strips. McQueen et al. (2002) reported that the Type I cement found locally to the NAPTF resulted in high flexural strengths (greater than 800 psi). Some expansive cements (Types K, M, and S in ASTM C 845) are currently under investigation for pavement applications that can be effective when minimization of concrete shrinkage is required.

The amount of cement in a concrete mix is the most important factor affecting durability. Typically, the quantity of cement paste is based on the strength requirements, minimum cement factor, or exposure conditions, as well as the void content of the combined fine and coarse aggregates. Increasing the cement content will decrease the air content of the concrete mix. The PCA design manual states that minimizing cement (and water) contents includes employing the stiffest practical mixture, using the largest practical maximum aggregate size, and optimizing the fine-to-coarse aggregate ratio.

Because the Type I cement used in the NAPTF resulted in high strength concrete, a lower cement content was required in the mix design. Laboratory tests were conducted on mixes containing cement contents of 400 lbs and 500 lb. However, results of the laboratory testing indicated that workability was harsh and made hand-placement difficult. This discovery prompted the use of a higher cement content (525 lb) to increase workability in the test slabs.

3.3.4 Aggregate Properties

The properties of different aggregates typically affect the performance and workability of concrete, as well as the amount of water required in the mix. Properties of interest in the selection of aggregates for the NAPTF pavements include:

- Specific gravity
- Absorption
- Natural moisture
- Fineness modulus
- Maximum aggregate size
- Dry-rodded unit weight
- Aggregate type

In a laboratory investigation reported by McQueen et al. (2002), the coarse aggregate used in the original mix (No. 57) was compared to a mix containing a No. 467 coarse aggregate. The investigation showed that there were no differences in the resulting shrinkage of the concrete. However, since the concrete mix must be placed carefully around instrumentation, the smaller aggregate (No. 57) was selected for the new optimal mix design.

The No. 9 intermediate aggregate was found to be better suited for the new mixture for the NAPTF slabs. This aggregate was used in the concrete test strips placed in November 2001 and exhibited adequate performance. Sand (“sewer sand”) that is local to the NAPTF was used for finer aggregates. For coarse aggregates, the optimal mix design required good quality aggregates from Pennsylvania quarries. The aggregate properties also influence the proportioning of the mixture (i.e., water content, slumps). Some aggregate types, such as cherts and siliceous components, have been found to cause excessive volume change in the hardened concrete. Therefore, the mixes for the test slabs at the NAPTF used traprock and dolomite coarse aggregates.

In general, both crushed and uncrushed aggregates can achieve similar strength for the same cement factor, given a satisfactory gradation. However, crushed aggregates typically form a stronger bond with cement paste than the uncrushed smoother aggregates. Tests indicate that crushed-stone aggregates generate higher compressive strengths than uncrushed aggregates of the same size and cement content. A crushed fine aggregate (meeting NJ DOT No. 9 specification) was used in the mix at the NAPTF to increase workability.

Aggregates typically must meet the requirements of the ASTM C 33 specification to be considered for use in a concrete mix. Some of the qualities important for aggregates include soundness, frost resistance, and resistance to degradation by traffic and weathering. If recycled concrete is reused as aggregate, it is critical that it meets the same gradation and quality requirements as normal aggregates. If the crushed concrete is to be used as fine aggregate, natural sand should be added to the new mixture to improve workability.

3.3.5 Aggregate Gradation

The gradation of aggregates will affect the amount of concrete made with a given amount of cement and water. Using larger sizes of coarse aggregate will reduce the amount of water required for the mixture, and consequently reduces the resulting cement content. A No. 57 coarse aggregate grading with a 50% coarse aggregate/50% sand blend was used in the original mix design, and recommended in the new mix design, of slabs at the NAPTF. Original concrete pavements yielded shrinkage of 0.08%, while the new mix considered for the test strips, which introduced an intermediate No. 9 aggregate, was designed for a targeted 0.05% shrinkage. The gradation plot used by McQueen et al. for the test strip concrete mixes at the NAPTF is presented in figure 27.

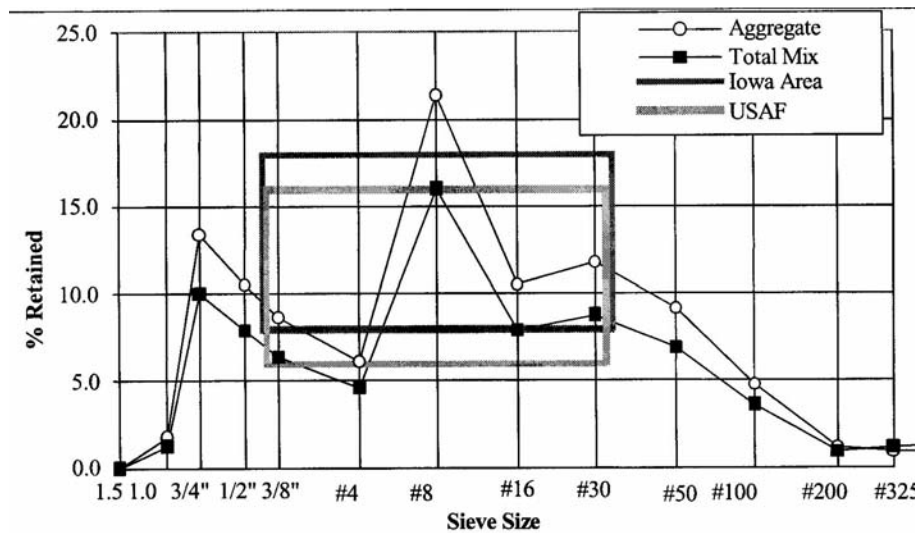


FIGURE 27. GRADATION PLOT USED FOR CONCRETE MIX DESIGN (MCQUEEN ET AL. 2002)

Removal of fines such as clay and dust from coarse aggregates is a necessary step in the gradation part of a mix design. Dust should be removed since it affects the quantity of fines and will alter the water demand. The aggregate-paste bond will be affected by the presence of clay fines. The mortar used in the test strips at the NAPTF was measured at 53% and yielded a slump of 3 inches, after the addition of a water reducer.

3.3.6 Water-reducing Admixtures

Water-reducing admixtures reduce the w:c ratio and typically improve the workability of concrete. Laboratory testing for the NAPTF test strips showed that the mix design resulted in a harsh mix with a maximum slump of 1 inch. This type of mix would make it extremely difficult to place concrete efficiently around the numerous instrumentation in the slabs. A high-range water reducer (HRWR) was added and a more workable mix (3-inch slump) was achieved for the test strips. However, the results from laboratory testing indicated that the addition of HRWR actually increased the amount of shrinkage (greater than 0.04%) in concrete slabs.

The addition of water-reducing admixtures can lower water requirements from 5 to 10 percent and may result in a mix more prone to shrinkage. Superplasticizers reduce the water requirements even further (from 12 to 30 percent). It is important to consider the water portion of admixtures as part of the water content (if admixture's water content affects w:c ratio by more than 0.01). Use of HRWR and superplasticizer must be used with caution so that the properties of the hardened concrete are not affected by their use.

3.3.7 Fly Ash Admixture

Fly ash is defined as fine residue resulting from combustion of pulverized coal and is typically collected as a byproduct of thermal-power-generating stations. Fly ash has been shown to improve workability in conventional mixes, while also decreasing the potential for bleeding and segregation. Using fly ash in a concrete mix will reduce the heat of hydration and retard the setting time. It is crucial that proper curing (i.e., time, temperature, and moisture) of concrete be assured when fly ash is present in the mix to prevent excessive strength gain or other undesirable effects.

Fly ash has not been recommended for the concrete mixes to be used at the NAPTF.

3.3.8 Air Entrainment Admixtures

Air-entrained concrete was developed mostly to improve resistance to freeze/thaw and deicing chemicals. These problems are not anticipated to occur in the NAPTF; however, it is of interest to state the effects of entrained air on concrete properties. Some of the effects of adding entrained air include:

- Increased slump
- Increased sulfate resistance
- Reduced bleeding
- Reduced compressive strength (~ 2 to 6%)
- Improved freeze/thaw resistance
- Reduced flexural strength (~ 2 to 4%)
- Decreased modulus of elasticity
- Increased workability
- Decreased water demand of wet concrete for equal slump

An air-entraining admixture is added to the concrete mix at the mixer. The admixtures are typically liquids and consist of some form of wood resin, fatty and resinous acids, synthetic materials, and sulphonated hydrocarbons. If too much air is added into a concrete mix, a small amount of defoaming agent can be added to counteract excessive air.

3.3.9 Shrinkage Reducing Agents

Set-retarding and water-reducing admixtures can help to control the shrinkage in concrete. Water-reducing agents include sulphonated condensates, lignosulphonates, hydroxylated acids, carbohydrates, and superplasticizers. Consideration should be taken in terms of proportioning when adding shrinkage reducing agents. For example, the addition of a water reducer can result in a decreased compressive strength and increased slump loss, as well as produce higher air contents (1 to 2% from lignin admixtures) than a conventional mix. The side effects from using any shrinkage reducing agent should be noted prior to addition into the concrete mixture, in order to proportion mix parameters accordingly.

THIS PAGE INTENTIONALLY LEFT BLANK

4. EXPERIMENTAL DESIGN

4.1 INTRODUCTION

Test sections have been designed of unbonded concrete overlays over a concrete base pavement over three subgrade strengths. The test sections will have a range of joint locations and spacing, and simulated distress conditions. The test site is the NAPTF, and the experimental design assumes that the pavement structure test bed will be 900 ft long by 66 ft wide placed on the underlying subgrade (approximately 10 ft deep). The test site will consist of the prepared test bed with three different subgrade strengths—low, medium, and high strengths (also referred to as L, M, and H herein). After removing the previous test structure, the top surface of the subgrade will be reworked, recompacted, and regraded to meet the following design requirements in terms of CBR:

Section	CBR
Low strength	4
Medium strength	8
High strength	30

The test sections on each subgrade type will be 300 ft long, as shown in figure 28, with the low strength subgrade being at the west end of the test track. The medium and high strength subgrades follow towards the east. Appropriate locations have been identified to provide transition slabs (i.e., slabs from which no data will be collected or analyzed) from one design condition to another. These conditions include changing from:

- One subgrade type to another
- One gear configuration to another (i.e., a dual tandem to a dual tridem gear, or vice versa)
- One underlying pavement condition to another

The existing PCC pavement in this experiment will be built first and will eventually be overlaid. Therefore, throughout this chapter, the existing pavement may be also referred to as “underlying pavement” or “underlying slabs” in the experimental design section.

The test section is 60 feet wide and will consist of 4 test slabs in the transverse direction. The typical size for a test slab is 15 feet x 15 feet. The typical thicknesses of the underlying slab, the interface layer, and the overlay are 12 in, 2 in, and 9 in, respectively.

4.1.1 Coordinates

A 3-D coordinate system will be adopted to identify specific test locations and sensor positions along the length, width, and depth of the test track. As indicated in figure 28, the origin will coincide with the top surface of the overlay at the west end of the test track centerline. The length of the test track will span along the positive X-axis, i.e. X-axis values increase from west to east. While the slabs to the north of the centerline will span along the positive Y-axis, the

slabs to the south will span along the negative Y-axis, i.e. Y-axis values increase from south to north. Z-axis values increase downward, i.e. increase with depth.

In addition, all rows and column of slabs in the overlays are assigned letters a, b, c, or d and numbers 1 through 60, respectively (Figure 28) and provide a unique identity to each slab. For example, slab c4 is located, based on its position, in the row c and column 4.

4.2 TEST PLAN DETAILS

The experimental design consists of several different conditions of the underlying slabs and the overlay. Each test section is divided into test cells, each of which has a unique combination of test parameters (gear type, underlying slab, overlay condition and joint type). The cell identification, such as L1-N, M2-S, H4, and so on, identifies each test cell. For example, L1-N refers to test cell 1, on a low strength subgrade to the north of the centerline. Similarly, H4 refers to test cell 4 on a high strength subgrade, regardless of which side of the centerline the test cell may be located. Further, all slabs in the overlay have an assigned number in the longitudinal and transverse direction. A brief discussion of all the parameters included in the experimental design is presented in the following paragraphs of this section.

4.2.1 Joint/Crack Alignment

Transverse and longitudinal joint locations in the underlying slabs have been chosen so that all possible combinations of matched and mismatched transverse and longitudinal joints/cracks are simulated in the experimental matrix. The joints in both directions match and align themselves perfectly on some test cells, namely, L2-N, L2-S, M2-N, M2-S, H2-N, and H2-S. Cells L1-N, L1-S, M1-N, M1-S, H1-N, and H1-S have matched transverse joints but mismatched longitudinal joints. Similarly cells L6, L7, and M7 have mismatched transverse joints and matched longitudinal joints. Finally, cells L4, L5, M4, M5, H4, and H5 have mismatched transverse and longitudinal joints.

4.2.2 Transverse Joints

The PCC overlay consists of regular contraction transverse joints and several joints connecting test cells with transition slabs. All regular contraction joints are doweled except those in cells L4, M4, and H4. The contraction joints are created by 3-in-deep and 3/16-in-wide saw cuts. In doweled joints, dowel diameter and dowel spacing are 1.25 in and 12 in, respectively. Dowels should not be placed closer than 6 in to the longitudinal edges of the overlay slabs.

Special transverse joints are designed to prevent propagation of a longitudinal crack across a transverse joint from one test cell to another. These joints are either construction joints or created by a full-depth 1/4-in-wide saw cut. The transverse joints in the overlay, identified as type J1, are supported by staggering the joint in the underlying pavement by 2 feet, as shown in figure 29. Joints LJ1, MJ1, and HJ1 are of type J1. Transverse joints identified as type J2 are full-depth joints (see figure 30). Joints LJ2, LJ3, LJ4, MJ2, MJ3, MJ4, HJ2, and HJ3 are of type J2.

Saw cuts in the underlying slabs model joints and cracks of different degree of deterioration of cracks and joints in the existing pavement. Transverse joints matched with the transverse joint in the overlay assumed to be of moderate level of deterioration and created by saw cuts 6 in deep and 3/16 in wide. Transverse joints mismatched with the transverse joints in the overlay are assumed to be badly deteriorated and created by a full-depth 1/4-in-wide saw cut. Cell L6 has underlying slabs with doweled transverse joints to model low severity cracks. These joints are created by 3-in-deep and 3/16-in-wide saw cuts.

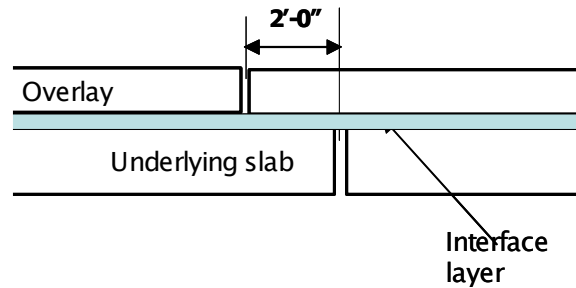


FIGURE 29. JOINT DETAIL, J1

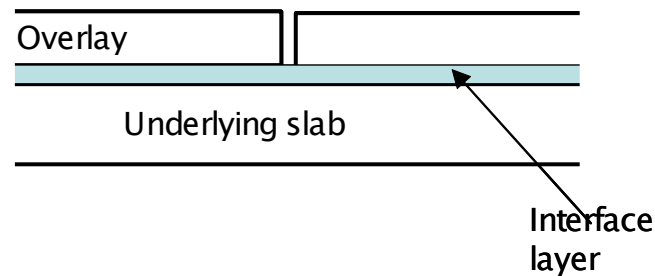


FIGURE 30. JOINT DETAIL, J2

4.2.3 Longitudinal Joints

The centerline longitudinal joint in the overlay is an undoweled construction joint that should isolate northern and southern test cells from propagation of transverse cracks. Longitudinal joints to the north and south of the centerline joint on the overlay will be created by 3-in-deep and 3/16-in-wide saw cuts and will be doweled with 1.25-in dowels with dowel spacing equal to 12 in.

The longitudinal joints in the underlying slabs model joints and cracks of different degrees of deterioration of cracks and joints in the existing pavement. All joints are non-doweled and do not have tie bars. Longitudinal joints identified as JC in the underlying slab simulate high-

severity cracking and, hence, are either construction joints or created by full-depth saw cuts. All other longitudinal joints are half-depth joints.

4.2.4 Shattered Slabs

Test cells L3-N, L3-S, M3-N, M3-S, H3-N, and H3-S will have shattered slabs created with full-depth longitudinal and diagonal saw cuts that divide the slabs into six pieces.

To achieve this, each slab in the underlying pavement will be sawed full-depth in a pattern as represented by the dashed lines in figure 31 below. The sawing will be done at 45-degree angles and initiated from the mid-length locations of longitudinal and transverse edges. In addition, the slabs will also be sawed in the longitudinal direction at the slab centerline.

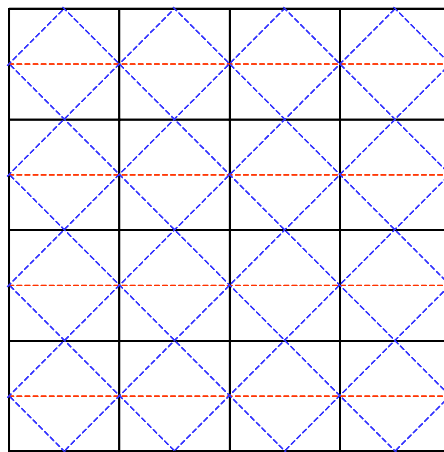


FIGURE 31. SAWING PATTERN TO CREATE SHATTERED SLABS IN THE EXISTING PAVEMENT

4.2.5 Joint Sealing

Since joints at the NAPTF are not subjected to severe environmental conditions, and joint filling with incompressibles is not an issue, all joints in the existing and underlying pavement will be unsealed.

4.2.6 Spalling

Slabs a18, b18, c18, and d18 in test cell L8 will have a spalled transverse joint in the underlying slab created by jackhammer. All loose materials will be removed prior to AC interlayer placement.

4.2.7 Transition Slabs

Transition slabs will be provided as marked on figure 28. These transition slabs will not provide response data for analysis. The main purpose of these slabs is to provide sufficient distance for

the slabs to develop stress and deformation responses typical of the conditions they are designed for while transitioning from one subgrade type to another or one gear configuration to another.

4.2.8 Wheel Load and Configuration

The capability of the NAPTF load frame to simulate dual tandem and dual tridem gear configurations will be utilized fully in this test program. In the low strength subgrade sections, for the transverse joint in cells L1, L2, and L3, the slabs to the north of the centerline, L1-N, L2-N, and L3-N, will be loaded with a dual tandem gear, while the slabs to the south of the centerline, L1-S, L2-S, and L3-S will be loaded with a dual tridem gear configuration. As the axle approaches the slab to the east of joint LJ3, the fore dual wheels of the tridem gear to the south of the centerline are lifted off the ground and will exert no tire pressure on the slabs. Therefore, the cells to the east of LJ3 (i.e., cells L5, L7, L8) will be loaded by a tandem gear configuration.

Similarly, while cells M7, M5, and H5 will be loaded with a tandem gear, cells M3-S, M2-S, M1-S, H1-S, H2-S, and H3-S will be loaded with a tridem gear configuration. It is important to note that all cells to the north of the centerline will be loaded with a tandem gear configuration.

4.2.9 Shoulders

Shoulders will be placed along the entire test track to both the south and north of the test cells. These shoulders are 3 feet wide and will be constructed of 2 inches of AC over a 12-in granular layer (P-154) over 22 inches of sand.

Table 7 gives a summary of the test matrix and identifies the parameters chosen in each test cell

TABLE 7. SUMMARY OF KEY DESIGN FEATURES IN EACH EXPERIMENT CELL

Subgrade Type	Joints	Dual Tandem					Dual Tridem				
		Doweled Overlay				Undoweled Overlay	Doweled Overlay				Undoweled Overlay
		SL – Doweled Joint	SL – Undoweled joint	SL – Spalled Joint	SL – Shattered Slab	SL – Undoweled Joint	SL – Doweled Joint	SL – Undoweled joint	SL – Spalled Joint	SL – Shattered Slab	SL – Undoweled Joint
Low	M-T, M-L		L2-N		L3-N			L2-S		L3-S	
	MM-T, M-L	L6	L7	L8							
	M-T, MM-L		L1-N					L1-S			
	MM-T, MM-L		L5			L4					
Medium	M-T, M-L		M2-N		M3-N			M2-S		M3-S	
	MM-T, M-L		M7								
	M-T, MM-L		M1-N					M1-S			
	M-T, MM-L		M5			M4					
High	M-T, M-L		H2-N		H3-N			H2-S		H3-S	
	MM-T, M-L										
	M-T, MM-L		H-1N					H1-S			
	M-T, MM-L		H5			H4					

4.3 DESCRIPTION OF TEST CELLS

The unique combination of parameters in each test cell is described in the following paragraphs.

Cell L1-N (Slabs a1, a2, a3, b1, b2, b3): This test cell is on a **low** strength subgrade, has **matched transverse** joints, **mismatched longitudinal** joints, and is loaded by a **dual tandem** gear. The overlay is **doweled** and the underlying slab is **undoweled**.

Cell L1-S (Slabs c1, c2, c3, d1, d2, d3): This test cell is on a **low** strength subgrade, has **matched transverse** joints, **mismatched longitudinal** joints, and is loaded by a **dual tridem** gear. The overlay is **doweled** and the underlying slab is **undoweled**.

The transverse joint to the east of L1 cells, LJ1, is of type J1. Slab 4 is a transition slab.

Cell L2-N (Slabs a5, a6, a7, b5, b6, b7): This test cell is on a **low** strength subgrade, has **matched transverse** joints, **matched longitudinal** joints, and is loaded by a **dual tandem** gear. The overlay is **doweled** and the underlying slab is **undoweled**.

Cell L2-S (Slabs c5, c6, c7, d5, d6, d7): This test cell is on a **low** strength subgrade, has **matched transverse** joints, **matched longitudinal** joints, and is loaded by a **dual tridem** gear. The overlay is **doweled** and the underlying slab is **undoweled**.

The transverse joint LJ1 and LJ2 are full-depth joints of type J1. Slabs a8, b8, c8, and d8 are transition slabs.

Cell L3-N (Slabs a9, a10, a11, b9, b10, b11): This test cell is on a **low** strength subgrade, has **shattered underlying slabs**, and is loaded by a **dual tandem** gear. The overlay is **doweled** and the underlying slab is **undoweled**.

Cell L3-S (Slabs c9, c10, c11, d9, d10, d11): This test cell is on a **low** strength subgrade, has **shattered underlying slabs**, and is loaded by a **dual tridem** gear. The overlay is **doweled** and the underlying slab is **undoweled**.

Slabs a8, b8, c8, d8, and a12, b12, c12, and d12 are transition slabs, and joint LJ2 and LJ3 are of type J1 and J2, respectively.

Cell L4 (Slabs a14, a15, b14, b15, a16, b16): This test cell is on a **low** strength subgrade, has **mismatched transverse** joints, **mismatched longitudinal** joints, and is loaded by a **dual tandem** gear. The overlay is **undoweled** and the underlying slab is **undoweled**.

Cell L5 (Slabs c14, c15, d14, d15, c16, d17): This test cell is on a **low** strength subgrade, has **mismatched transverse** joints, **mismatched longitudinal** joints, and is loaded by a **dual tandem** gear. The overlay is **doweled** and the underlying slab is **undoweled**.

Joints LJ3 and LJ4 are full-depth joints of type J2.

Cell L6 (Slabs a17, a18, a19, b17, b18, b19): This test cell is on a **low** strength subgrade, has **mismatched transverse** joints, **matched longitudinal** joints, and is loaded by a **dual tandem** gear. The overlay is **doweled** and the underlying slab is **doweled**.

Cell L7 (Slabs a17, c18, c19, d17, d18, d19): This test cell is on a **low** strength subgrade, has **mismatched transverse** joints, **matched longitudinal** joints, and is loaded by a **dual tandem** gear. The overlay is **doweled** and the underlying slab is **undoweled**.

Cell L8 (Slab a20, b20, c20, d20): This test cell is on a **low** strength subgrade, has **matched longitudinal** joints and is loaded by a **dual tandem** gear. The overlay is **doweled** and the underlying slab has a **spalled joint**.

The M-section is to the east of cell L8. Slabs 21 and 22 are transition slabs.

Cell M1-N (Slabs a38, a39, a40, b38, b39, b40): This test cell is on a **medium** strength subgrade, has **matched transverse** joints, **mismatched longitudinal** joints, and is loaded by a **dual tandem** gear. The overlay is **doweled** and the underlying slab is **undoweled**.

Cell M1-S (Slabs c38, c39, c40, d38, d39, d40): This test cell is on a **medium** strength subgrade, has **matched transverse** joints, **mismatched longitudinal** joints, and is loaded by a **dual tridem** gear. The overlay is **doweled** and the underlying slab is **undoweled**.

The H-section begins to the east of this cell, and joint MJ1 is of type J1. Slabs a41, b41, c41, d41, a42, b42, c42, and d42 east of the M1 cells are transition slabs and transition to high strength subgrade sections.

Cell M2-N (Slabs a34, a35, a36, b34, b35, b36): This test cell is on a **medium** strength subgrade, has **matched transverse** joints, **matched longitudinal** joints, and is loaded by a **dual tandem** gear. The overlay is **doweled** and the underlying slab is **undoweled**.

Cell M2-S (Slabs c34, c35, c36, d34, d35, d36): This test cell is on a **medium** strength subgrade, has **matched transverse** joints, **matched longitudinal** joints, and is loaded by a **dual tridem** gear. The overlay is **doweled** and the underlying slab is **undoweled**.

Slabs a37, b37, c37, d37 are transition slabs, and joints MJ1 and MJ2 are full-depth joints of type J1.

Cell M3-N (Slabs a30, a31, a32, b30, b31, b32): This test cell is on a **medium** strength subgrade, has **shattered underlying**, and is loaded by a **dual tandem** gear. The overlay is **doweled** and the underlying slab is **undoweled**.

Cell M3-S (Slabs c30, c31, c32, d30, d31, d32): This test cell is on a **medium** strength subgrade, has **shattered underlying**, and is loaded by a **dual tridem** gear. The overlay is **doweled** and the underlying slab is **undoweled**.

Slabs a29, b29, c29, d29, a33, b33, c33, and d33 are transition slabs and joints MJ2 and MJ3 are full depth joints of type J1 and J2, respectively.

Cell M4 (Slabs a26, a27, b26, b27): This test cell is on a **medium** strength subgrade, has **mismatched transverse** joints, **mismatched longitudinal** joints, and is loaded by a **dual tandem** gear. The overlay is **undoweled** and the underlying slab is **undoweled**.

Cell M5 (Slabs c26, c27, d26, d27): This test cell is on a **medium** strength subgrade, has **mismatched transverse** joints, **mismatched longitudinal** joints, and is loaded by a **dual tandem** gear. The overlay is **doweled** and the underlying slab is **undoweled**.

Slabs a25, b25, c25, d25, a28, b28, d28, and d28 are transition slabs. Joints MJ3 and MJ4 are of type J2.

Cell M7 (Slabs a23 b23, c23, d23, a24, b24, c24, d24): This test cell is on a **medium** strength subgrade, has **mismatched transverse** joints, **matched longitudinal** joints, and is loaded by a **dual tandem** gear. The overlay is **doweled** and the underlying slab is **undoweled**.

Slabs a21, b21, c21, d21, a22, b22, c22, and d22 are transition slabs. Joint MJ4, to the east of cell M7, is of type J2.

Cell H1-N (Slabs a43, a44, a45, b43, b44, b45): This test cell is on a **high** strength subgrade, has **matched transverse** joints, **mismatched longitudinal** joints, and is loaded by a **dual tandem** gear. The overlay is **doweled** and the underlying slab is **undoweled**.

Cell H1-S (Slabs c43, c44, c45, d43, d44, d45): This test cell is on a **high** strength subgrade, has **matched transverse** joints, **mismatched longitudinal** joints, and is loaded by a **dual tridem** gear. The overlay is **doweled** and the underlying slab is **undoweled**.

Slabs a41, b41, c41, d41, a42, b42, c42, d42, a46, b46, c46, and d46 are transition slabs. Joint HJ1 to the east of cells H1 is of type J1.

Cell H2-N (Slabs a47, a48, a49, b47, b48, b49): This test cell is on a **high** strength subgrade, has **matched transverse** joints, **matched longitudinal** joints, and is loaded by a **dual tandem** gear. The overlay is **doweled** and the underlying slab is **undoweled**.

Cell H2-S (Slabs c47, c48, c49, d47, d48, d49): This test cell is on a **high** strength subgrade, has **matched transverse** joints, **matched longitudinal** joints, and is loaded by a **dual tridem** gear. The overlay is **doweled** and the underlying slab is **undoweled**.

Slabs a46, b46, c46, d46, a50, b50, c50, and d50 are transition slabs, and joint HJ1 is of type J1.

Cell H3-N (Slabs a52, a53, a54, b52, b53, b54): This test cell is on a **high** strength subgrade, has **shattered underlying**, and is loaded by a **dual tandem** gear. The overlay is **doweled** and the underlying slab is **undoweled**.

Cell H3-S (Slabs c52, c53, c54, d52, d53, d54): This test cell is on a **high** strength subgrade, has **shattered underlying**, and is loaded by a **dual tridem** gear. The overlay is **doweled** and the underlying slab is **undoweled**.

Slabs a51, b51, c51, d51, a55, b55, c55, and d55 are transition slabs, and joints HJ2 and HJ3 are of type J1 and J2, respectively.

Cell H4 (Slabs a57, a58, a59, b57, b58, b59): This test cell is on a **high** strength subgrade, has **mismatched transverse** joints, **mismatched longitudinal** joints, and is loaded by a **dual tandem** gear. The overlay is **undoweled** and the underlying slab is **undoweled**.

Cell H5 (Slabs c57, c58, c59, d57, d58, d59): This test cell is on a **high** strength subgrade, has **mismatched transverse** joints, **mismatched longitudinal** joints, and is loaded by a **dual tandem** gear. The overlay is **doweled** and the underlying slab is **undoweled**.

Slabs a56, b56, c56, d56, a60, b60, c60, and d60 are transition slabs. Joint HJ3 is of type J2.

4.4 CONSTRUCTION OF TEST SECTIONS

This section describes the following “good concreting” aspects involving construction of the test sections:

- PCC mixing
- Mix handling
- Preparation of underlying pavement surface
- Transporting and handling
- PCC placement
- Weather at time of placement
- PCC surface finishing
- Consolidation
- Curing
- Sawing joints

4.4.1 PCC Mixing

All concrete should be mixed thoroughly until it is uniform in appearance to ensure it is combined into a homogeneous mix. If the concrete has been mixed adequately, samples taken from different portions of a batch will have virtually the same properties. All concrete pavement placed at the NAPTF is required to be produced from batch plants and equipment that is in accordance with ASTM C 94.

Construction at the NAPTF requires mixing to be done in a central plant mixer that complies with ASTM C 94 requirements. Up to 10 percent of mixing water should be added in the drum before the solid parts of the mix are added. During addition of the cementitious portion of the mix, water should be added uniformly, leaving approximately another 10 percent water to be added after all other materials are already in the drum. If water-reducing or retarding admixtures are planned, they must be added within 1 minute after the addition of water to the cementitious material.

Ready mixing of concrete is typically done off-site and transported to the project site in a fresh and unset form. Ready-mixed concrete is delivered to the construction area by either a truck agitator or truck mixer. However, shrink-mixed concrete is manufactured partially in a stationary mixer and then finished in a truck mixer. Truck-mixed concrete is mixed entirely in a truck mixer. It is indicated in ASTM C 94 that 70 to 100 revolutions of the drum, at the rotational rate deemed by the manufacturer as mixing speed, are needed to produce the specified uniformity of concrete. Mixing speed is approximately 6 to 18 rpm. Concrete must be discharged at the job site within 90 minutes or prior to the drum revolving 300 times after the introduction of water to solids or cement to aggregates.

Truck mixers and agitator or non-agitator trucks should all conform to ASTM C 94 specifications to be acceptable for carrying concrete mix to the construction site at the NAPTF.

4.4.2 Method of Mixture Handling

Good planning can help to select the appropriate method of mix handling before a crisis occurs. Three aspects are normally taken into account:

- Delays - a plan to combine personnel, machinery, and equipment efficiently to reduce the delay time during concrete placement is required.
- Early stiffening and drying out - although concrete begins to stiffen as soon as the cement and water are mixed, normally the stiffening within the first 30 minutes is not a major problem. Advanced planning should minimize the number of variables that would prevent the concrete from a full consolidation.
- Segregation – the tendency of coarser aggregate to separate from the sand-cement mortar should be prevented. Careful thought must be given to the selection of the method and equipment to transport and handle the concrete.

Concrete volume, time, distance, and climatic conditions must be considered before choosing a transporting and handling method. In addition, end-discharge, bucket capacity, chute slopes, cross sections, drop heights, pump power, discharge rate, and worker skills are some of the considerations for ensuring an adequate concrete mix.

Specifications written for the construction of concrete pavements at the NAPTF indicate that stockpiles should be constructed in such a way that segregation and intermixing of deleterious materials does not occur. Also, batch plants are required to proportion aggregates and bulk cement by weight, and assure that loss of cement does not occur in the transporting of material from the holding container to the mixer. These specifications are presented in detail in appendix D.

4.4.3 Preparation of Existing (Underlying) Pavement Surface

The contract specifications presented in appendix D indicate the details for preparing and treating the existing pavement surface prior to overlay placement. The surface of the underlying

pavement must be cleaned thoroughly, and the actual condition of the existing rigid pavement will dictate the amount and type of cleaning treatment required. Any oil or grease must be scrubbed with detergent and a wire brush, although these elements are not likely to be found in abundance on the NAPTF rigid pavements.

4.4.4 Transporting and Handling

Specifications concerning the transporting and handling of concrete to be placed in the NAPTF are presented in appendix D. The type of equipment selected for the transportation and handling of concrete depends greatly on concrete mix properties, job site location and conditions, and type of existing pavement and pavement structure to be paved. Mix segregation typifies the damage that can occur during transportation and handling, and is apt to occur during the discharging of handling equipment (unless the mix is discharged vertically). If segregation is anticipated due to the type of handling equipment used, changes must be made beforehand to the mix design that will ensure a more cohesive concrete. In this case, some corrections to the mix design include good aggregate gradation, sufficient air and cement contents, lower slumps, or proper proportioning of fine to coarse aggregate. Loss of mortar, due to equipment malfunctioning, will result in decreased strength, density, and durability of the concrete. Tempering the concrete mix with water at the job site is required when slump loss occurs due to long truck waiting times or haul distances; however, this procedure is not recommended since it can affect the w:c ratio.

Because of the limits on machinery type and size associated with constructing at the NAPTF, a power-driven cart (power buggy) is likely to be the equipment used for handling concrete, once at the job site. Power buggies retain the advantages provided by a handcart, but also handle greater quantities of concrete at one time and can operate for longer distances. Riding-type buggies are cited for a maximum distance of 1000 feet and have increased hourly capacity. These units can handle grades as steep as 35% (not considered an issue at the NAPTF) and require at least a 5-ft width maneuvering space. The discharging of concrete from the power buggy should be performed in a manner that minimizes potential for mix segregation. Likewise, using a system as described will protect the low and medium strength subgrades from settling under the heavy loading induced by a fully-loaded concrete mixer truck. A typical power buggy is shown in figure 32.



FIGURE 32. POWER BUGGY USED AT THE NAPTF TO TRANSPORT FRESH CONCRETE FROM MIXER

4.4.5 PCC Placement

All loose material and debris must be removed before placement of the concrete. Equipment used to place concrete must be in good working condition, and some replacement equipment must be available in the event of a breakdown. Because of the machinery size limits and extensive instrumentation included in the overlay placement at the NAPTF, a combination of machine and hand spreading, finishing, and floating is recommended.

In slab construction, placing should start along the perimeter at one end of the work with each batch discharged against previously placed concrete. In general, concrete should be placed in horizontal layers of uniform thickness, each layer being thoroughly consolidated before the next is placed. Timing between placements of layers is important and should be rapid enough so that the concrete has not yet set when a new layer is placed upon it. Guidelines for placing concrete pavements at the NAPTF are included in appendix D.

Forms should be accurately set, clean, tight, and well constructed. Wood forms must be cleaned and oiled before the concrete is placed, to avoid absorption of water from the concrete. The use of extra large nails, or a great number of nails, should be avoided to facilitate form removal. All forms should be designed for quick removal with minimum damage to the concrete. They also should be designed to have sufficient strength for resisting the pressure caused by the concrete and be strong enough to support any mechanical placing and finishing equipment used. The specifications for form setting at the NAPTF are outlined in appendix D. Figure 33 shows forms being placed for the construction of test strips at the NAPTF.



FIGURE 33. SETTING FORMWORK FOR THE CONSTRUCTION OF TEST STRIPS AT THE NAPTF

4.4.6 Weather at Time of Placement

The requirements for temperature at the time of placement of concrete in the NAPTF are described in appendix D. The temperature at which concrete is placed can have varying effects on different properties and requirements. For example, in hot weather the concrete is warm and may result in a decrease in air content. This decrease could be deferred by adding more air-entraining admixture. The occurrence of plastic-shrinkage cracks is another concern related to paving in hot weather. Plastic-shrinkage cracks are caused by excessive moisture loss from concrete before curing has begun. Fog spray equipment can be used to apply a very fine water mist to the concrete to replace concrete moisture lost by evaporation. Placement of concrete pavement in extremely high temperatures or temperatures less than 40 degrees Fahrenheit is not recommended. If paving in winter weather is necessary, an accelerator admixture may be approved to quicken the setting time.

4.4.7 PCC Surface Finishing

Since the surface receives the greatest exposure to weathering and traffic, a high-quality concrete is required at the surface. Finishing operations must be conducted to obtain a dense, smooth surface at the proper grade. Excessive finishing must be minimized because it tends to attract a surplus of mortar, water, and undesirable soft materials to the surface, leading to scaling and surface deterioration. Normally, if mechanical operations are properly conducted, very little hand finishing is required. However, hand finishing will be necessary in this particular NAPTF project due to the installed instrumentation and measuring devices.

After concrete is placed, a method with which to strike-off the concrete is necessary. In the original construction of concrete pavements at the NAPTF, a vibratory screed was used to strike-off the concrete. However, in the construction of the test strips, a straightedge was used successfully for strike-off, as shown in figure 34.

The final texture of the surface must be provided with a burlap drag, broom, artificial turf, wire comb, or grooving. These methods result in different skid-resistance textures and should be used carefully. For instance, the wire comb provides the most skid-resistance texture, but if the spacing is too close or too wide it may cause raveling or noise. If a pavement surface texture is inadequate in terms of texturing, grinding or grooving may be utilized to restore skid resistance to the surface. A combination of roller bug and bull float was used for finishing the concrete test strips at the NAPTF.



FIGURE 34. STRAIGHTEDGE STRIKE-OFF OF CONCRETE IN TEST STRIPS AT THE NAPTF

The specifications required for finishing and surface texturing in new concrete pavements at the NAPTF are included in appendix D.

4.4.8 Consolidation

The main objective of the consolidating process is to mold the concrete within the forms and around embedded items to eliminate stone pockets, honeycomb, and entrapped air. The selection of the consolidation method depends on the consistency of the mixture and the placing conditions, such as complexity of the formwork and amount and spacing of reinforcement if it exists.

Vibration, either external or internal, is the most widely used method for consolidating concrete. Hand-operated internal vibrators were used, and are recommended, for use at the NAPTF, in order to avoid damaging the imbedded instrumentation. The vibrator used in the construction of the test strips at the NAPTF is shown in figure 35.



FIGURE 35. VIBRATING CONCRETE DURING PLACEMENT OF TEST STRIPS AT THE NAPTF

4.4.9 Curing

It is critical that concrete be protected against the loss of moisture and rapid temperature change in the early stages of construction. If loss of water occurs, shrinkage causes tensile stresses that may develop into cracks if the concrete has not attained adequate tensile strength. Curing has a strong influence on the properties of hardened concrete, such as durability, strength, abrasion resistance, and volume stability.

Saturated cover curing is recommended for PCC construction at the NAPTF. The saturated cover to be used can be burlap. Curing shall begin as soon as concrete has hardened. Special types of burlap are typically used as wet coverings and must be kept damp continuously by covering with a film of polyethylene film or periodic water spraying. Fabric coverings saturated with water, such as burlap, cotton, or other moisture-retaining fabrics, are commonly used for curing. The requirements for burlap are included in AASHTO M182 and ASTM C 171. Wet, moisture-retaining fabric coverings should be placed as soon as the concrete has hardened sufficiently to prevent surface damage. Wet soils, hay, straw and other materials are also proposed as less expensive alternatives, but are also potentially less effective due to environmental conditions. A wet cure period of 28-days using burlap to cover concrete slabs was used as the curing method for the concrete test strips at the NAPTF. Figure 36 shows the placement of burlap on concrete test strips. A liquid sealing membrane was applied on concrete test strips after curing was completed. The requirements for curing of concrete pavements at the NAPTF are outlined in appendix D.



FIGURE 36. PLACEMENT OF BURLAP OVER CONCRETE TEST STRIPS FOR 28-DAY WET CURE

Curing times depends on the type of cement, mixture proportion, required strength, size and shape of the concrete member, and ambient weather. Since all desirable properties of concrete are enhanced by curing, the curing period should be as long as practical.

4.4.10 Sawing Joints

Contraction joints should be saw-cut in the concrete to conform to the details and dimensions specified. The proper time for sawing the joints is based on the particular conditions on the job site during each concrete placement. This is normally 4 to 12 hours after the concrete hardens. A slight raveling of the sawed edges is acceptable and indicates proper timing for the sawing operation. If sawing is delayed too long, the concrete may crack before it is sawed, or ahead of the saw blade cutting the contraction joint. Contraction joints should extend into the slab to a depth of at least one-fourth the slab thickness. The joint depths required in the new concrete overlays will be presented in the plan drawings.

Wet saw cutting of joints was employed on the concrete test strips placed at the NAPTF. Joints were cut approximately 8 hours after placement. A view of the joint cutting procedure at the NAPTF is shown in figure 37.



FIGURE 37. WET SAW CUTTING JOINTS IN CONCRETE TEST STRIPS AT THE NAPTF

Sawing of the joints should be performed consecutively in the same sequence as the concrete is placed in the lane. Before sawing a joint, the concrete should be examined closely for cracks, and the joints should not be sawed if a crack has occurred near the joint.

5. INSTRUMENTATION AND DATA ACQUISITION FOR THE NAPTF TEST

This section describes the instrumentation included in the test plan. First, the proposed sensors to record the following are outlined:

- Moisture and temperature conditions through the test period
- Pavement responses to temperature and moisture conditions
- Pavement responses to applied wheel loads

This includes a short description of the sensor, its purpose, specifications, principles of operation, and installation. Next, a brief discussion is presented on the proposed placement of sensors. The horizontal and vertical position of sensors along the test track is described.

The adequacy of the existing data acquisition system in the test center is also explained in brief.

5.1 SENSORS

The sensors to be utilized in the NAPTF test sections can be classified under two broad categories—a) those that measure the temperature and moisture in the slab, and slab deformations as a result of changes in temperature and moisture, and b) those that measure slab response as a result of applied loads. Sensors in the former category are referred to as static sensors, and those in the latter category are called dynamic sensors.

Data from static sensors are collected at regular (and desired) time intervals. However, data from dynamic sensors are collected only when the applied wheel loads are active on the pavement system in the vicinity of the gages. The timing of the data collection is facilitated by a series of triggers placed in the transition sections just prior to the test section. These triggers activate the signal-processing unit (SPU) connected to the dynamic sensors as the test vehicle is approaching the test section, which allows the data acquisition system to collect data only from the section that is loaded and makes the data acquisition and data analysis process more efficient. As the test vehicle goes past the test sections, the data collection process stops.

It is proposed that static sensor data will be collected at intervals of 15 minutes in the first month after placing the concrete for both the existing pavement and the overlay. Thereafter, data can be collected every hour during the course of the experiments. This rate of data collection will provide an insight into the early age and long-term behavior of existing PCC pavements and overlays. The dynamic sensor data will be collected when the sensor is triggered by the approach of the wheel in each pass.

The preliminary list of sensors to be utilized in the test is as follows:

- 1) Humidity sensors to measure PCC shrinkage and moisture gradients
Sensor type: Static
- 2) Thermocouples (type T) to measure temperature gradients at regular intervals
Sensor type: Static

- 3) Linear Variable Differential Transformer (LVDT) - Joint displacement gages to measure joint opening in the existing slab
Sensor type: Static
- 4) Linear potentiometers to measure slab lift-off
Sensor type: Static
- 5) Concrete Strain Gages (CSG) to measure strain in PCC overlay and existing slab
Sensor type: Dynamic
- 6) Thermocouples (type T) to measure temperature gradients during each dynamic measurement
Sensor type: Dynamic
- 7) Multi Depth Deflectometer (MDD) to measure the deflection at multiple vertical locations at a single point, i.e. at different z-values for a given (x, y) point.
Sensor type: Dynamic
- 8) LVDT to measure the surface deflection adjacent to the wheel path (portable device)
Sensor type: Dynamic

Items 1 through 4 are static sensors and items 5 through 8 are dynamic sensors. Data from thermocouples will be collected not only at regular intervals (along with all static sensors), but also when data from dynamic sensors will be collected (along with other dynamic sensors). This will provide the true temperature conditions at the instant when each set of data is collected for the dynamic gages. In addition, it allows a direct temperature measurement in the immediate vicinity of the strain measurements and provides another data source to define temperature gradients.

The sensors proposed in this report reflect the experimental plan of the research team. The precise names, brands, and models of the sensors are not necessarily finalized for all sensors. However the research team merely outlines the specifications required at a minimum for each sensor.

5.1.1 Humidity Gages

The proposed humidity gage is the commercially available G-CAP™ 2 Relative Humidity Sensor, a polymer capacitive based sensor, factory calibrated to within 1 picofarad (pf), +/- 3% RH accuracy. The result is an RH sensing element with uniform calibration and interchangeability.

The G-CAP sensor offers low drift performance of less than 1% per year, reducing calibration problems, and features a negligible temperature coefficient of less than 0.05% RH/°C, thus ensuring accurate and reliable operation in applications where the final product will be exposed to wide temperature ranges. A picture of the proposed humidity sensor is shown in figure 38.

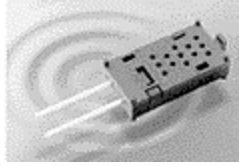


FIGURE 38. PROPOSED HUMIDITY SENSOR, G-CAP™ 2

Features

- Interchangeability better than 3%
- Survives 100% RH
- Temperature coefficient less than 0.05% RH/°F
- Linearity better than +/-2%
- Simple support circuitry requirements
- Innovative packaging for improved performance
- Economical
- Alternative mounting configurations
- Calibrated or uncalibrated versions

Specifications

Performance:

- Operating Ranges:
 - Humidity: 0% to 100% RH
 - Temperature: -40 to 85°C (-40° to 185°F)
 - Capacitance: 148 pf +/- 1 pf at 25°C (77°F)
 - 0% RH, 10 KHz, 1 VRMS
 - Frequency Range: D.C. to 1 MHz
 - Temperature effect: Less than 0.05% RH /°F
 - Long-Term Stability: Less than 1% drift per year, typical
 - Hysteresis: Less than 2% RH at 25°C
 - Sensor interchangeability: Better than +/- 3% RH (calibrated version only)
- Time Response:
 - 63% change for a 25%-75% step change
 - 150 LFM air flow
 - 75 seconds typical
 - 120 seconds maximum.

Power:

Maximum Voltage: 5 Volts (across sensor leads) 1 VRMS recommended

Mechanical:

Assembly: Sensor can be soldered onto PCB.

Lead Strength: 2 lb. pull test with no damage.

Material:

Case: PBT plastic, 15% glass fill.

Pins: Copper with .00001" min. tin plate.

Humidity sensors will be embedded at different depths of the slab. They will be placed 1 inch from the top of the slab, at one-third depth, at mid-depth, and 1 inch from the bottom of the slab. The following section on sensor placement will discuss the location of the humidity sensors at different locations of the test section. A total of 54 humidity sensors will be used in the test.

5.1.2 Thermocouples – Type T (static)

Thermocouples of type T, embedded in the PCC existing slab and overlay, are suggested for this experiment. A thermocouple is the preferred temperature-measuring device in experiments of this nature because they can be embedded in the material, allowing measurement of temperature at any desired depth and automatic data collection.

A thermocouple is a temperature-measuring sensor and consists of two dissimilar metals, joined together at one end, which produce a small unique voltage at a given temperature. The temperature difference is measured by measuring the voltage across the junction. This temperature is interpreted based on the calibration of the system. A picture of a thermocouple stack, identical to the one proposed for this experiment, is shown in figure 39.

Thermocouples are available in different combinations of metals or calibrations. The four most common calibrations are J, K, T, and E. Each calibration has a different temperature range and environment, although the maximum temperature varies with the diameter of the wire used in the thermocouple. The proposed thermocouple calibration is a copper-constantan calibration or Type T.

At a minimum, the thermocouples to be used in the tests will have an accuracy of ± 0.2 deg C and a range of -40 to 150 deg C.



FIGURE 39. THERMOCOUPLE STACK

Thermocouples will be embedded at different depths of the PCC slab in both the existing pavement and the overlay. In both PCC layers, the chosen temperature sensors will be placed at 0.5 in and 2 in from the top, at mid-depth, and at 2 in and 0.5 in from the bottom. A total of 11,700 feet will be used in all sections for static measurements.

Thermistors were used in the earlier experiments conducted at NAPTF. If the data logging system is more compatible with thermistors, the proposed test can be conducted with thermistors.

5.1.3 LVDT – Joint Gages

The LVDT is the most commonly used variable-inductance transducer for measuring displacements as accurate as ± 0.001 inch. It is an electro-mechanical device designed to produce an AC voltage output proportional to the relative displacement of the transformer and the armature. The LVDT works on the principle that the output voltage is proportional to the number of coil windings in a transformer. When an LVDT is placed on a specimen, the core around which the coil is wound slides through the transformer by an amount equal to the displacement of the specimen. When the iron core slides through the transformer, a certain number of coil windings are affected by the proximity of the sliding core and thus generate a unique voltage output. The displacement can be determined using the measured voltage and a calibration factor.

In installing the LVDT, the core must contact directly or indirectly with the measured surface, which is not always possible or desirable. However, a non-contact thickness gage can be achieved by including a pneumatic servo to maintain the air gap between the nozzle and the work piece.

The LVDTs to be used for measuring joint openings in the existing slabs will, at a minimum, have a range of ± 0.25 inch with an accuracy of 0.01 inch. The sensor placement for joint width measurement is shown in figure 40. The LVDT will be placed at the mid-depth of the slab, and a total of 26 joint gages will be used in the tests.



FIGURE 40. JOINT WIDTH MEASUREMENT

5.1.4 Linear Potentiometers (Slab lift-off measurement)

The current test setup at NAPTF has linear potentiometers to measure vertical movements of the slabs at its corners. Gages similar to those currently being used at the NAPTF will be employed in this experimental setup. The selection of an appropriate potentiometer is based on the length of the stroke to be measured, which entails choosing the power rating and the resistance value for the sensor. The sensor should have a range of at least ± 0.5 inch and an accuracy of 0.001 inch. A total of 96 slab lift-off gages will be used in the test.

5.1.5 Concrete Strain Gages

Strain gages will be used to measure the strain in the PCC overlay and existing slabs. The proposed strain gage layout makes optimal use of the data acquisition capabilities at the NAPTF. Strain measurements will be mostly made at the top and bottom of the slab. Strain gages will be placed at 1.5 in from the top and bottom of the slab in both the overlay and the existing slab. Strain gage chairs will be used to position these strain gage sensors 1.5 in from the top and bottom layers of the slab. A schematic of the strain gage sensor is shown in figure 41.

When strain is measured at an edge location, a single strain gage, unidirectionally oriented, will be used to measure the strain in the critical stress direction. This strain gage will be connected to a wheatstone bridge circuit in a quarter bridge configuration. Bridge completion units will be used for this purpose. Single strain gages are referred to as “S-gages” in this report.

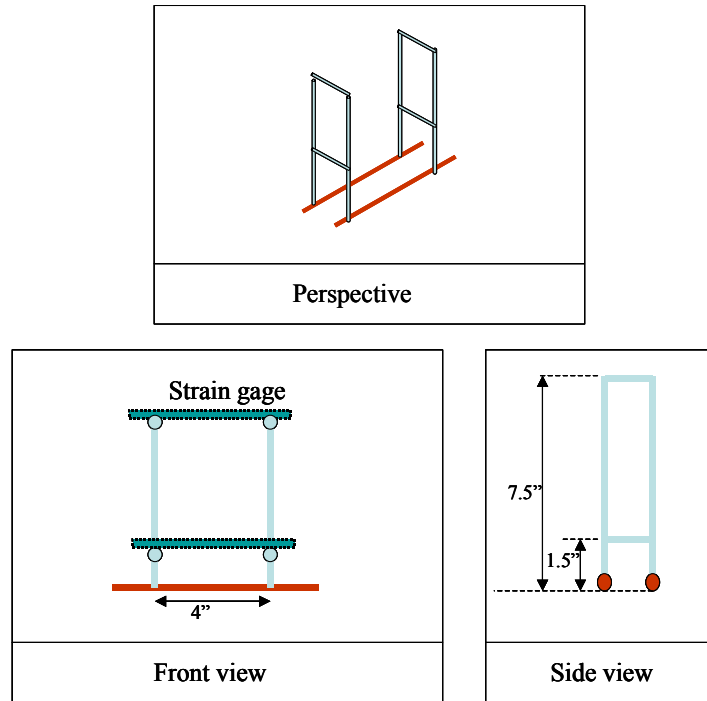


FIGURE 41. CHAIRS FOR STRAIN GAGES

When strain measurements are made in the interior of a slab, a strain gage rosette will be employed to define the strain field at the location. A strain gage rosette is an arrangement of two or more (typically three) closely positioned gage grids, separately oriented to measure the normal strains along each of their directions. By obtaining three independent strain measures in a known orientation, the Cartesian components of strain can be determined. Suitable coordinate transformation equations based on basic principles of engineering mechanics can be used to achieve this. The proposed strain rosette, as shown in figure 42, is a three element rectangular rosette and gages will be oriented at 0-45-90 deg positions. The rosette units will be referred to as “RS” in this report. Each strain gage in the rosette will be connected to a wheatstone bridge circuit in a quarter bridge configuration using bridge completion units similar to the S-gages.

The single strain gage will be either the PML-60-2L gage manufactured by Texas Measurements or an equivalent gage. The 3-element rosette will be the PMR-60-2L sensor also manufactured by Texas Measurements. The strain gages will be 120-ohm resistance gages, with a gage length of 60 mm, a width of 1 mm and have a gage factor of 2.0.

The gages, at a minimum, have a range of 1500 microstrain, and an accuracy of 1 microstrain operating in a temperature range of -20 to 60 deg C. They will also be temperature compensated. Each strain gage assembly will be physically protected and a typical installation is shown in figure 43. A total of 400 single strain gages and 132 rosettes will be used in the entire test program.



FIGURE 42. STRAIN GAGE INSTALLATION



FIGURE 43. STRAIN GAGE PLACEMENT IN THE SLAB

5.1.6 Thermocouples –Type T (dynamic)

These sensors are same as the static thermocouples but will differ in the manner in which data are collected. These sensors will be connected to the dynamic data acquisition system that records data only when triggered by the approach of the loading gear on the test section.

Thermocouples for dynamic measurements will be embedded at different depths of the PCC slab in existing pavement and the overlay. In both PCC layers, the chosen temperature sensors will

be placed at 0.5 in, 2 in, from the top, at mid-depth, and at 2 in and 0.5 in from the bottom. A total of 11,700 feet will be used in all sections for dynamic measurements.

5.1.7 Multi-depth Deflectometer

An MDD is an instrument that, as the name suggests, measures the deflection of the system at the surface and at various depths. The MDDs proposed for this experiment are same as the CTL-manufactured MDDs that have been used in earlier experiments at the NAPTF. Each MDD consists of five displacement transducers positioned in the head assembly of the MDD at the pavement surface. The head assembly is positioned above a lined borehole with a depth of 10 feet. At the bottom of the bore hole an expandable hydraulic anchor is placed as a stable reference point. Six snap ring anchors are placed at various depths in the lined bore hole, and the displacement transducers are connected to the anchors with carbon-graphite fiberglass composite rods. This material provides rigidity but is flexible to bending. The displacement transducers in the MDD will be Data Instruments MLT-1,2.

Figure 44 shows the layout of the MDD in the pavement system. Transducers are located in all layers, enabling the measurement of vertical displacement in each layer. Figure 45 shows the installation of an MDD in one of the previous experiments at NAPTF. The installation procedure followed at NAPTF for the previous experiments will be used for the current test plan.

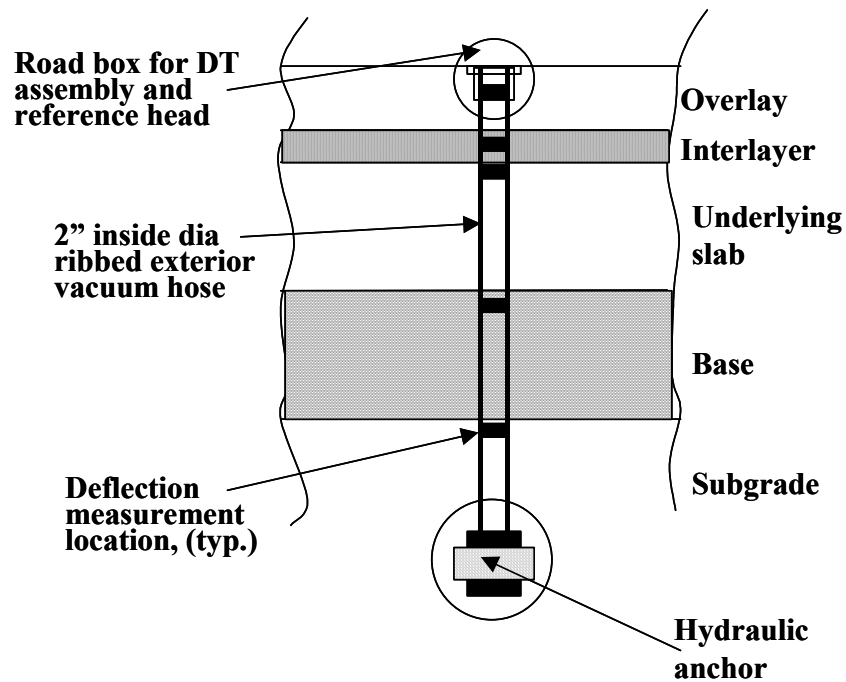


FIGURE 44. MDD LAYOUT IN THE PCC TEST SECTION

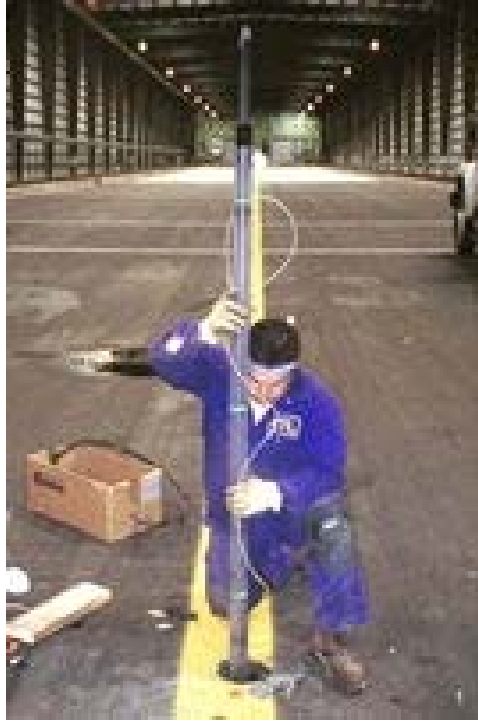


FIGURE 45. MDD INSTALLATION AT THE NAPTF

The measurement range of the MDD will be 1 to 2 inches, and it can be operated in a temperature range of -40 to 80 deg C. This is a dynamic sensor and will have a frequency greater than 100 hertz. A total of 12 MDDs, each with 5 transducers, will be used in the proposed experimental plan.

5.1.8 LVDT – Surface Deflections

Surface deflections of the PCC slab will be measured using LVDTs. The principle behind the operation of an LVDT is explained in item 3. These sensors will be portable gages that can measure deflection adjacent to the wheel as it traverses along the pavement. The portable device is mounted to the wheel and can traverse along the entire test track. This will allow for a better understanding of the response of the pavement sections under rolling wheel conditions and under the effects of the underlying pavement structure. Figure 46 shows a type of surface deflection measuring device.

The range for the sensor to measure surface deflection is ± 0.50 inch with an accuracy of 0.001 inch. This is a portable device and will comprise of 6 gages in total.

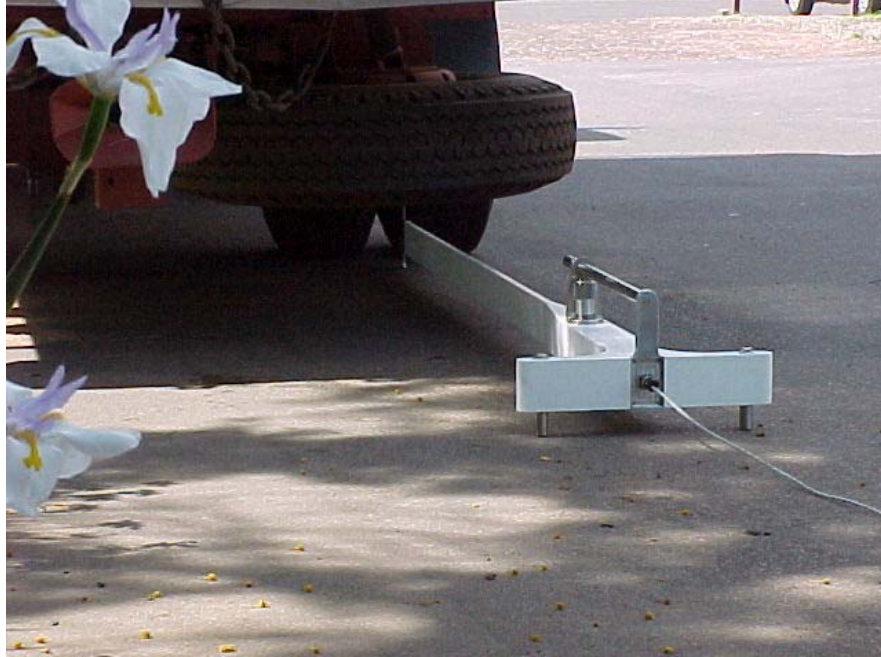


FIGURE 46. PORTABLE SURFACE DEFLECTION MEASURING DEVICE

5.1.9 Accessories

Appropriate accessories will be required to complete the instrumentation in the test sections. Accessories include shielded sensor cables and lead wires, depending on the gage type being wired.

During the installation process, care will be taken to avoid tension in the lead wires, and sufficient planning will be required in the routing of the lead wires. When sensors are placed in different layers of the pavement system, care will also be taken to protect the cables from construction activities continuing for subsequent layers. A detailed lead wire routing plan will be developed prior to sensor installation.

Accessories also include the sensor chairs for positioning the concrete strain gages at the required depths. These steel chairs can be affixed in the ground to spatially orient it perfectly to the required x, y, z coordinates. Steel chairs will be spot welded together with 1/8-in steel stock.

5.2 SENSOR PLACEMENT

Sensors will be placed suitably in the test sections to record critical pavement responses, as well as pavement temperature and moisture levels. Figures 47, 48, and 49 show a summary of sensor placement in the low, medium, and high strength subgrade sections.

Static sensors that record pavement temperature and moisture levels, as well as pavement responses to climatic changes, will be placed in select locations of the test section to provide data that can be applied to the entire test section. In other words, these sensors need not be placed in each test cell. However, dynamic sensors will be placed in each test cell, and pavement response data collected from the dynamic sensors will reflect performance of the overlay on the specific distress conditions of the underlying slab in each test cell.

Tables 8, 9, and 10 list the x, y, z coordinates of the sensor locations in the low strength, medium strength, and high strength-sections. They also indicate the sensor type (static or dynamic) and the slab ID.

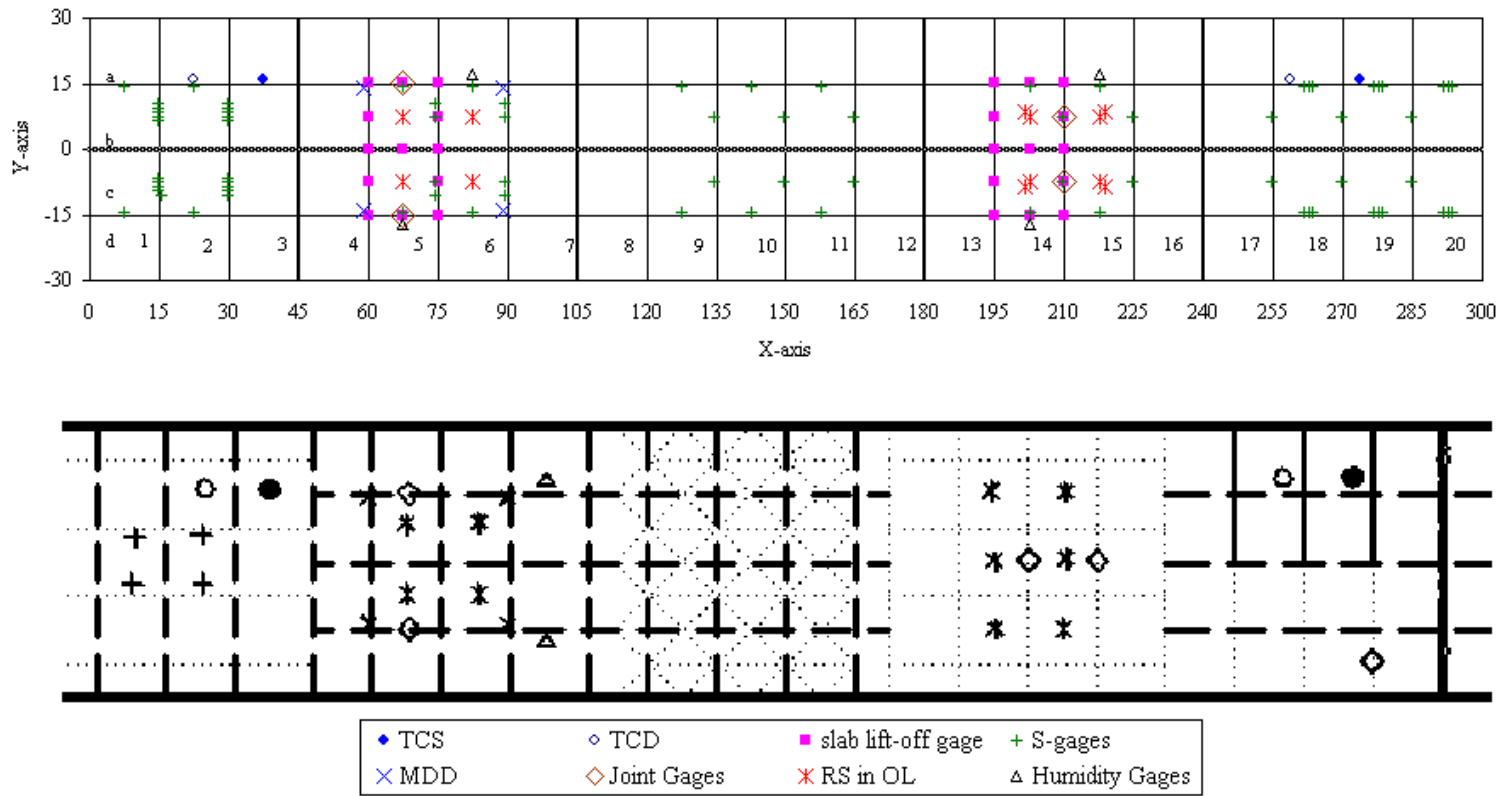


FIGURE 47. SENSOR PLACEMENT IN THE LOW STRENGTH SUBGRADE SECTION

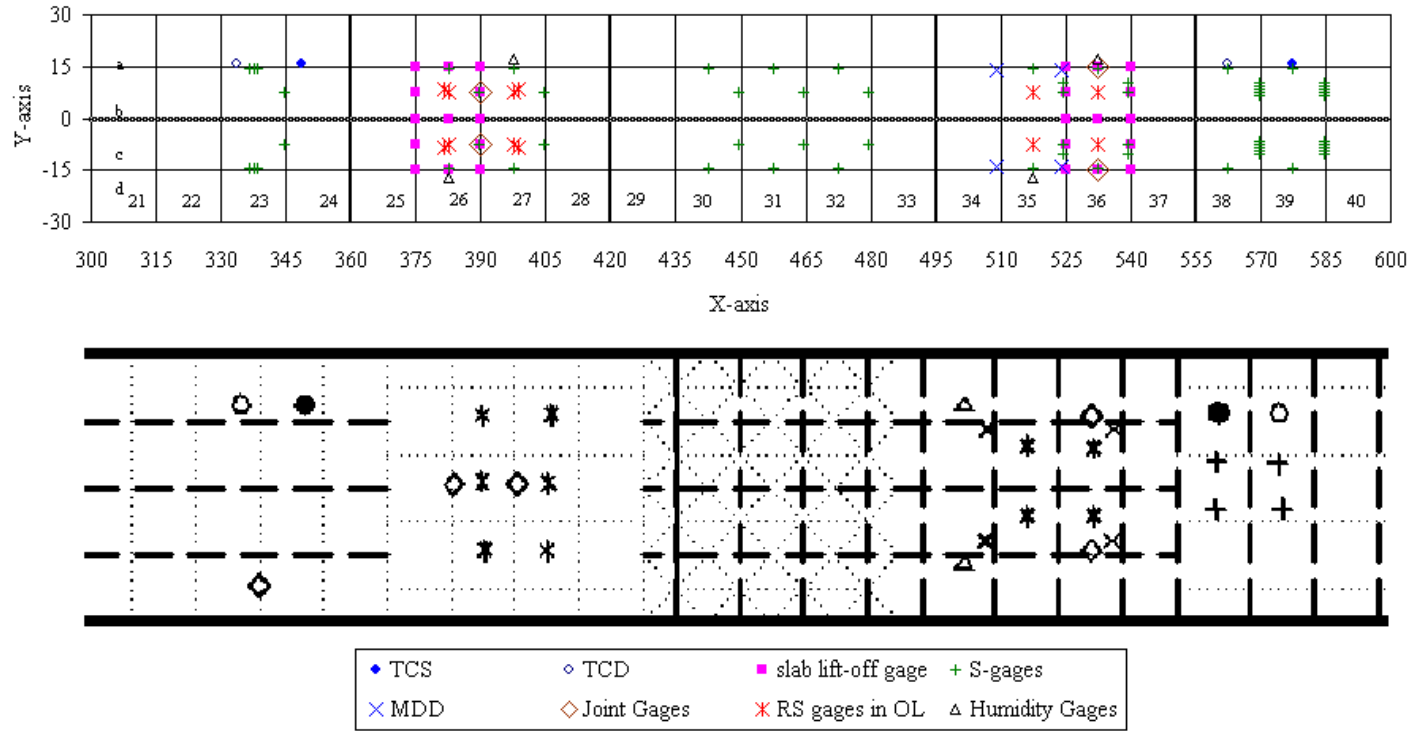


FIGURE 48. SENSOR PLACEMENT IN THE MEDIUM STRENGTH SUBGRADE SECTION

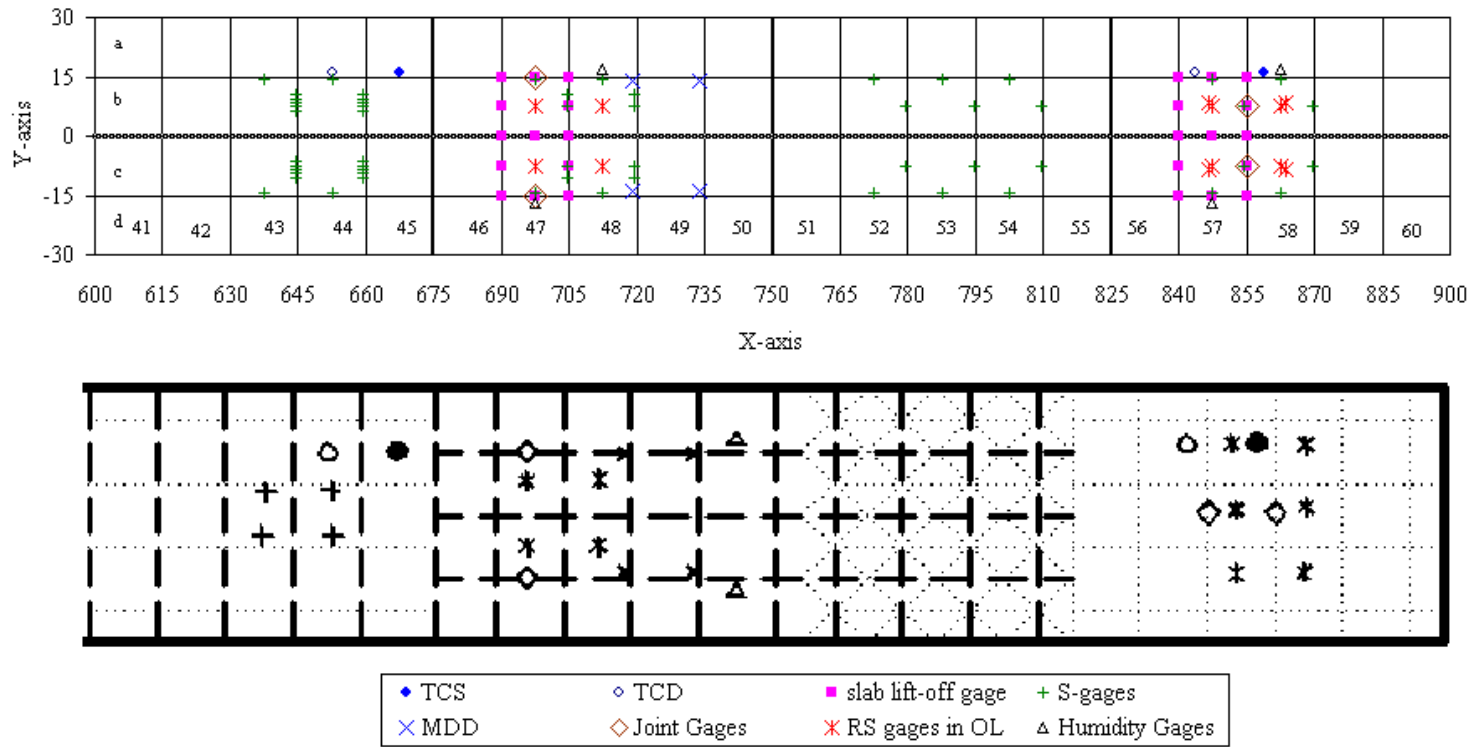


FIGURE 49. SENSOR PLACEMENT IN THE MEDIUM STRENGTH SUBGRADE SECTION

TABLE 8. COORDINATES FOR SENSORS IN THE LOW STRENGTH SUBGRADE SECTION

Sensor	Sensor type	Cell	Layer	slab # - x	slab # - y	Coordinates, ft												Total
						x	y	z1	z2	z3	z4	z5	z6	z7	z8	z9	z10	
Humid-G	static	L2-N	OL	6	a	82.5	17	1	3	8								3
Humid-G	static	L2-N	SL	7	a	97.5	17	12	14	19								3
Humid-G	static	L2-S	OL	5	d	67.5	-17	1	3	8								3
Humid-G	static	L2-S	SL	7	d	97.5	-17	12	14	19								3
Humid-G	static	L4	OL	15	a	217.5	17	1	3	8								3
Humid-G	static	L5	OL	14	d	202.5	-17	1	3	8								3
JG	static	L2-N	OL	5	a	67.5	15	4.5										1
JG	static	L2-N	SL	5	a	67.5	15	17										1
JG	static	L2-S	OL	5	d	67.5	-15	4.5										1
JG	static	L2-S	SL	5	d	67.5	-15	17										1
JG	static	L4	SL	14	b	202.5	0	17										1
JG	static	L4	OL	15	b	210	7.5	4.5										1
JG	static	L4	SL	15	b	217.5	0	17										1
JG	static	L5	OL	15	c	210	-7.5	4.5										1
JG	static	L7	SL	19	d	277.5	-22.5	17										1
slab-lift-G	static	L2-N	OL	5	b	60	15	9										1
slab-lift-G	static	L2-N	OL	5	b	60	7.5	9										1
slab-lift-G	static	L2-N	OL	5	b	60	0	9										1
slab-lift-G	static	L2-N	OL	5	b	67.5	15	9										1
slab-lift-G	static	L2-N	OL	5	b	67.5	0	9										1

TABLE 8. COORDINATES FOR SENSORS IN THE LOW STRENGTH SUBGRADE SECTION (CONT.)

Sensor	Sensor type	Cell	Layer	slab # - x	slab # - y	Coordinates, ft											Total	
						x	y	z1	z2	z3	z4	z5	z6	z7	z8	z9		z10
slab-lift-G	static	L2-N	OL	5	b	75	15	9										1
slab-lift-G	static	L2-N	OL	5	b	75	7.5	9										1
slab-lift-G	static	L2-N	OL	5	b	75	0	9										1
slab-lift-G	static	L2-S	OL	5	c	60	0	9										1
slab-lift-G	static	L2-S	OL	5	c	60	-7.5	9										1
slab-lift-G	static	L2-S	OL	5	c	60	-15	9										1
slab-lift-G	static	L2-S	OL	5	c	67.5	0	9										1
slab-lift-G	static	L2-S	OL	5	c	67.5	-15	9										1
slab-lift-G	static	L2-S	OL	5	c	75	0	9										1
slab-lift-G	static	L2-S	OL	5	c	75	-7.5	9										1
slab-lift-G	static	L2-S	OL	5	c	75	-15	9										1
slab-lift-G	static	L4	OL	14	b	195	15	9										1
slab-lift-G	static	L4	OL	14	b	195	7.5	9										1
slab-lift-G	static	L4	OL	14	b	195	0	9										1
slab-lift-G	static	L4	OL	14	b	202.5	15	9										1
slab-lift-G	static	L4	OL	14	b	202.5	0	9										1
slab-lift-G	static	L4	OL	14	b	210	15	9										1
slab-lift-G	static	L4	OL	14	b	210	7.5	9										1
slab-lift-G	static	L4	OL	14	b	210	0	9										1
slab-lift-G	static	L5	OL	14	c	195	0	9										1
slab-lift-G	static	L5	OL	14	c	195	-7.5	9										1
slab-lift-G	static	L5	OL	14	c	195	-15	9										1

95

TABLE 8. COORDINATES FOR SENSORS IN THE LOW STRENGTH SUBGRADE SECTION (CONT.)

Sensor	Sensor type	Cell	Layer	slab # - x	slab # - y	Coordinates, ft												Total
						x	y	z1	z2	z3	z4	z5	z6	z7	z8	z9	z10	
slab-lift-G	static	L5	OL	14	c	202.5	0	9										1
slab-lift-G	static	L5	OL	14	c	202.5	-15	9										1
slab-lift-G	static	L5	OL	14	c	210	0	9										1
slab-lift-G	static	L5	OL	14	c	210	-7.5	9										1
slab-lift-G	static	L5	OL	14	c	210	-15	9										1
TCS	static	L1-N	OL + SL	3	a	37.5	16	0.5	2	4.5	7	8.5	11.5	13.5	17	21	22.5	10
TCS	static	L6	OL + SL	19	a	273.75	16	0.5	2	4.5	7	8.5	11.5	13.5	17	21	22.5	10
MDD	dynamic	L2-N	all layers	4	b	59	14	0.5	9.5	11.5	24	29.5						5
MDD	dynamic	L2-N	all layers	6	b	89	14	0.5	9.5	11.5	24	29.5						5
MDD	dynamic	L2-S	all layers	4	c	59	-14	0.5	9.5	11.5	24	29.5						5
MDD	dynamic	L2-S	all layers	6	c	89	-14	0.5	9.5	11.5	24	29.5						5
RS-OL	dynamic	L2-N	OL	5	b	67.5	7.5	1.5	7.5									6
RS-OL	dynamic	L2-N	OL	6	b	82.5	7.5	1.5	7.5									6
RS-OL	dynamic	L2-S	OL	5	c	67.5	-7.5	1.5	7.5									6
RS-OL	dynamic	L2-S	OL	6	c	82.5	-7.5	1.5	7.5									6
RS-OL	dynamic	L4	OL	14	b	202.5	7.5	1.5	7.5									6
RS-OL	dynamic	L4	OL	14	b	201.5	8.5	1.5	7.5									6
RS-OL	dynamic	L4	OL	15	b	217.5	7.5	1.5	7.5									6
RS-OL	dynamic	L4	OL	15	b	218.5	8.5	1.5	7.5									6
RS-OL	dynamic	L5	OL	14	c	202.5	-7.5	1.5	7.5									6

TABLE 8. COORDINATES FOR SENSORS IN THE LOW STRENGTH SUBGRADE SECTION (CONT.)

Sensor	Sensor type	Cell	Layer	slab # - x	slab # - y	Coordinates, ft												Total
						x	y	z1	z2	z3	z4	z5	z6	z7	z8	z9	z10	
RS-OL	dynamic	L5	OL	14	c	201.5	-8.5	1.5	7.5									6
RS-OL	dynamic	L5	OL	15	c	217.5	-7.5	1.5	7.5									6
RS-OL	dynamic	L5	OL	15	c	218.5	-8.5	1.5	7.5									6
RS-SL	dynamic	L2-N	SL	5	b	67.5	7.5	12.5	21.5									6
RS-SL	dynamic	L2-N	SL	6	b	82.5	7.5	12.5	21.5									6
RS-SL	dynamic	L2-S	SL	5	c	67.5	-7.5	12.5	21.5									6
RS-SL	dynamic	L2-S	SL	6	c	82.5	-7.5	12.5	21.5									6
RS-SL	dynamic	L4	SL	14	a	195	15	12.5	21.5									6
RS-SL	dynamic	L4	SL	15	a	210	15	12.5	21.5									6
RS-SL	dynamic	L5	SL	14	c	195	-15	12.5	21.5									6
RS-SL	dynamic	L5	SL	15	c	210	-15	12.5	21.5									6
RS-SL	dynamic	L4	SL	14	c	195	0	12.5	21.5									6
RS-SL	dynamic	L5	SL	15	c	210	0	12.5	21.5									6
S-OL	dynamic	L1-N	OL	1	b	7.5	14.5	1.5	7.5									2
S-OL	dynamic	L1-N	OL	1	b	14.5	6.5	1.5	7.5									2
S-OL	dynamic	L1-N	OL	1	b	14.5	7.5	1.5	7.5									2
S-OL	dynamic	L1-N	OL	1	b	14.5	8.5	1.5	7.5									2
S-OL	dynamic	L1-N	OL	1	b	14.5	9.5	1.5	7.5									2
S-OL	dynamic	L1-N	OL	1	b	14.5	10.5	1.5	7.5									2
S-OL	dynamic	L1-N	OL	2	b	22.5	14.5	1.5	7.5									2
S-OL	dynamic	L1-N	OL	2	b	29.5	6.5	1.5	7.5									2

TABLE 8. COORDINATES FOR SENSORS IN THE LOW STRENGTH SUBGRADE SECTION (CONT.)

Sensor	Sensor type	Cell	Layer	slab # - x	slab # - y	Coordinates, ft												Total
						x	y	z1	z2	z3	z4	z5	z6	z7	z8	z9	z10	
S-OL	dynamic	L1-N	OL	2	b	29.5	7.5	1.5	7.5									2
S-OL	dynamic	L1-N	OL	2	b	29.5	8.5	1.5	7.5									2
S-OL	dynamic	L1-N	OL	2	b	29.5	9.5	1.5	7.5									2
S-OL	dynamic	L1-N	OL	2	b	29.5	10.5	1.5	7.5									2
S-OL	dynamic	L1-S	OL	1	c	7.5	-14.5	1.5	7.5									2
S-OL	dynamic	L1-S	OL	1	c	14.5	-8.5	1.5	7.5									2
S-OL	dynamic	L1-S	OL	1	c	14.5	-7.5	1.5	7.5									2
S-OL	dynamic	L1-S	OL	1	c	14.5	-6.5	1.5	7.5									2
S-OL	dynamic	L1-S	OL	1	c	14.5	-9.5	1.5	7.5									2
S-OL	dynamic	L1-S	OL	1	c	15.5	-10.5	1.5	7.5									2
S-OL	dynamic	L1-S	OL	2	c	22.5	-14.5	1.5	7.5									2
S-OL	dynamic	L1-S	OL	2	c	29.5	-8.5	1.5	7.5									2
S-OL	dynamic	L1-S	OL	2	c	29.5	-7.5	1.5	7.5									2
S-OL	dynamic	L1-S	OL	2	c	29.5	-6.5	1.5	7.5									2
S-OL	dynamic	L1-S	OL	2	c	29.5	-9.5	1.5	7.5									2
S-OL	dynamic	L1-S	OL	2	c	29.5	-10.5	1.5	7.5									2
S-OL	dynamic	L2-N	OL	5	b	74.5	7.5	1.5	7.5									2
S-OL	dynamic	L2-N	OL	5	b	67.5	14.5	1.5	7.5									2
S-OL	dynamic	L2-N	OL	5	b	74.5	10.5	1.5	7.5									2
S-OL	dynamic	L2-N	OL	6	b	89.5	7.5	1.5	7.5									2
S-OL	dynamic	L2-N	OL	6	b	82.5	14.5	1.5	7.5									2
S-OL	dynamic	L2-N	OL	6	b	89.5	10.5	1.5	7.5									2
S-OL	dynamic	L2-S	OL	5	c	67.5	-14.5	1.5	7.5									2

TABLE 8. COORDINATES FOR SENSORS IN THE LOW STRENGTH SUBGRADE SECTION (CONT.)

Sensor	Sensor type	Cell	Layer	slab # - x	slab # - y	Coordinates, ft												Total
						x	y	z1	z2	z3	z4	z5	z6	z7	z8	z9	z10	
S-OL	dynamic	L2-S	OL	5	c	74.5	-7.5	1.5	7.5									2
S-OL	dynamic	L2-S	OL	5	c	74.5	-10.5	1.5	7.5									2
S-OL	dynamic	L2-S	OL	6	c	82.5	-14.5	1.5	7.5									2
S-OL	dynamic	L2-S	OL	6	c	89.5	-7.5	1.5	7.5									2
S-OL	dynamic	L2-S	OL	6	c	89.5	-10.5	1.5	7.5									2
S-OL	dynamic	L3-N	OL	9	b	134.5	7.5	1.5	7.5									2
S-OL	dynamic	L3-N	OL	9	b	127.5	14.5	1.5	7.5									2
S-OL	dynamic	L3-N	OL	10	b	149.5	7.5	1.5	7.5									2
S-OL	dynamic	L3-N	OL	10	b	142.5	14.5	1.5	7.5									2
S-OL	dynamic	L3-N	OL	11	b	164.5	7.5	1.5	7.5									2
S-OL	dynamic	L3-N	OL	11	b	157.5	14.5	1.5	7.5									2
S-OL	dynamic	L3-S	OL	9	c	127.5	-14.5	1.5	7.5									2
S-OL	dynamic	L3-S	OL	9	c	134.5	-7.5	1.5	7.5									2
S-OL	dynamic	L3-S	OL	10	c	142.5	-14.5	1.5	7.5									2
S-OL	dynamic	L3-S	OL	10	c	149.5	-7.5	1.5	7.5									2
S-OL	dynamic	L3-S	OL	11	c	157.5	-14.5	1.5	7.5									2
S-OL	dynamic	L3-S	OL	11	c	164.5	-7.5	1.5	7.5									2
S-OL	dynamic	L4	OL	14	b	209.5	7.5	1.5	7.5									2
S-OL	dynamic	L4	OL	14	b	202.5	14.5	1.5	7.5									2
S-OL	dynamic	L4	OL	15	b	224.5	7.5	1.5	7.5									2
S-OL	dynamic	L4	OL	15	b	217.5	14.5	1.5	7.5									2
S-OL	dynamic	L5	OL	14	c	202.5	-14.5	1.5	7.5									2
S-OL	dynamic	L5	OL	14	c	209.5	-7.5	1.5	7.5									2

TABLE 8. COORDINATES FOR SENSORS IN THE LOW STRENGTH SUBGRADE SECTION (CONT.)

Sensor	Sensor type	Cell	Layer	slab # - x	slab # - y	Coordinates, ft												Total
						x	y	z1	z2	z3	z4	z5	z6	z7	z8	z9	z10	
S-OL	dynamic	L5	OL	15	c	217.5	-14.5	1.5	7.5									2
S-OL	dynamic	L5	OL	15	c	224.5	-7.5	1.5	7.5									2
S-OL	dynamic	L6	OL	17	b	254.5	7.5	1.5	7.5									2
S-OL	dynamic	L6	OL	18	b	269.5	7.5	1.5	7.5									2
S-OL	dynamic	L6	OL	18	b	263.5	14.5	1.5	7.5									2
S-OL	dynamic	L6	OL	18	b	262.5	14.5	1.5	7.5									2
S-OL	dynamic	L6	OL	18	b	261.5	14.5	1.5	7.5									2
S-OL	dynamic	L6	OL	19	b	284.5	7.5	1.5	7.5									2
S-OL	dynamic	L6	OL	19	b	278.5	14.5	1.5	7.5									2
S-OL	dynamic	L6	OL	19	b	277.5	14.5	1.5	7.5									2
S-OL	dynamic	L6	OL	19	b	276.5	14.5	1.5	7.5									2
S-OL	dynamic	L7	OL	17	c	254.5	-7.5	1.5	7.5									2
S-OL	dynamic	L7	OL	18	c	263.5	-14.5	1.5	7.5									2
S-OL	dynamic	L7	OL	18	c	262.5	-14.5	1.5	7.5									2
S-OL	dynamic	L7	OL	18	c	261.5	-14.5	1.5	7.5									2
S-OL	dynamic	L7	OL	18	c	269.5	-7.5	1.5	7.5									2
S-OL	dynamic	L7	OL	19	c	278.5	-14.5	1.5	7.5									2
S-OL	dynamic	L7	OL	19	c	277.5	-14.5	1.5	7.5									2
S-OL	dynamic	L7	OL	19	c	276.5	-14.5	1.5	7.5									2
S-OL	dynamic	L7	OL	19	c	284.5	-7.5	1.5	7.5									2
S-OL	dynamic	L8	OL	20	b	293.5	14.5	1.5	7.5									2
S-OL	dynamic	L8	OL	20	b	292.5	14.5	1.5	7.5									2
S-OL	dynamic	L8	OL	20	b	291.5	14.5	1.5	7.5									2

TABLE 8. COORDINATES FOR SENSORS IN THE LOW STRENGTH SUBGRADE SECTION (CONT.)

Sensor	Sensor type	Cell	Layer	slab # - x	slab # - y	Coordinates, ft												Total
						x	y	z1	z2	z3	z4	z5	z6	z7	z8	z9	z10	
S-OL	dynamic	L8	OL	20	c	293.5	-14.5	1.5	7.5									2
S-OL	dynamic	L8	OL	20	c	292.5	-14.5	1.5	7.5									2
S-OL	dynamic	L8	OL	20	c	291.5	-14.5	1.5	7.5									2
S-SL	dynamic	L1-N	SL	1	b	7.5	7.5	12.5	21.5									2
S-SL	dynamic	L1-N	SL	2	b	22.5	7.5	12.5	21.5									2
S-SL	dynamic	L1-S	SL	1	c	7.5	-7.5	12.5	21.5									2
S-SL	dynamic	L1-S	SL	2	c	22.5	-7.5	12.5	21.5									2
TCD	dynamic	L1-N	OL + SL	2	a	22.5	16	0.5	2	4.5	7	8.5	11.5	13.5	17	21	22.5	10
TCD	dynamic	L6	OL + SL	18	a	258.75	16	0.5	2	4.5	7	8.5	11.5	13.5	17	21	22.5	10

101

TABLE 9. COORDINATES FOR SENSORS IN THE MEDIUM STRENGTH SUBGRADE SECTION

Sensor	Sensor type	Cell	Layer	slab # - x	slab # - y	Coordinates, ft												Total
						x	y	z1	z2	z3	z4	z5	z6	z7	z8	z9	z10	
Humid-G	static	M2-N	SL	34	a	502.5	17	12	14	19								3
Humid-G	static	M2-N	OL	36	a	532.5	17	1	3	8								3
Humid-G	static	M2-S	SL	34	d	502.5	-17	12	14	19								3
Humid-G	static	M2-S	OL	35	d	517.5	-17	1	3	8								3
Humid-G	static	M4	OL	27	a	397.5	17	1	3	8								3
Humid-G	static	M5	OL	26	d	382.5	-17	1	3	8								3
JG	static	M2-N	OL	36	a	532.5	15	4.5										1
JG	static	M2-N	SL	36	a	532.5	15	17										1
JG	static	M2-S	OL	36	d	532.5	-15	4.5										1
JG	static	M2-S	SL	36	d	532.5	-15	17										1
JG	static	M4	SL	26	b	382.5	0	17										1
JG	static	M4	OL	27	b	390	7.5	4.5										1
JG	static	M4	SL	27	b	397.5	0	17										1
JG	static	M5	OL	27	c	390	-7.5	4.5										1
JG	static	M7	SL	23	d	337.5	-22.5	17										1
slab-lift-G	static	M2-N	OL	36	b	525	15	9										1
slab-lift-G	static	M2-N	OL	36	b	525	7.5	9										1
slab-lift-G	static	M2-N	OL	36	b	525	0	9										1
slab-lift-G	static	M2-N	OL	36	b	532.5	15	9										1
slab-lift-G	static	M2-N	OL	36	b	532.5	0	9										1

TABLE 9. COORDINATES FOR SENSORS IN THE MEDIUM STRENGTH SUBGRADE SECTION (CONT.)

Sensor	Sensor type	Cell	Layer	slab # - x	slab # - y	Coordinates, ft												Total
						X	y	z1	z2	z3	z4	z5	z6	z7	z8	z9	z10	
slab-lift-G	static	M2-N	OL	36	b	540	15	9										1
slab-lift-G	static	M2-N	OL	36	b	540	7.5	9										1
slab-lift-G	static	M2-N	OL	36	b	540	0	9										1
slab-lift-G	static	M2-S	OL	36	c	525	0	9										1
slab-lift-G	static	M2-S	OL	36	c	525	-7.5	9										1
slab-lift-G	static	M2-S	OL	36	c	525	-15	9										1
slab-lift-G	static	M2-S	OL	36	c	532.5	0	9										1
slab-lift-G	static	M2-S	OL	36	c	532.5	-15	9										1
slab-lift-G	static	M2-S	OL	36	c	540	0	9										1
slab-lift-G	static	M2-S	OL	36	c	540	-7.5	9										1
slab-lift-G	static	M2-S	OL	36	c	540	-15	9										1
slab-lift-G	static	M4	OL	26	b	375	15	9										1
slab-lift-G	static	M4	OL	26	b	375	7.5	9										1
slab-lift-G	static	M4	OL	26	b	375	0	9										1
slab-lift-G	static	M4	OL	26	b	382.5	15	9										1
slab-lift-G	static	M4	OL	26	b	382.5	0	9										1
slab-lift-G	static	M4	OL	26	b	390	15	9										1
slab-lift-G	static	M4	OL	26	b	390	7.5	9										1
slab-lift-G	static	M4	OL	26	b	390	0	9										1
slab-lift-G	static	M5	OL	26	c	375	0	9										1
slab-lift-G	static	M5	OL	26	c	375	-7.5	9										1
slab-lift-G	static	M5	OL	26	c	375	-15	9										1

TABLE 9. COORDINATES FOR SENSORS IN THE MEDIUM STRENGTH SUBGRADE SECTION (CONT.)

Sensor	Sensor type	Cell	Layer	slab # - x	slab # - y	Coordinates, ft											Total	
						X	y	z1	z2	z3	z4	z5	z6	z7	z8	z9		z10
slab-lift-G	static	M5	OL	26	c	382.5	0	9										1
slab-lift-G	static	M5	OL	26	c	382.5	-15	9										1
slab-lift-G	static	M5	OL	26	c	390	0	9										1
slab-lift-G	static	M5	OL	26	c	390	-7.5	9										1
slab-lift-G	static	M5	OL	26	c	390	-15	9										1
TCS	static	M1-N	OL + SL	39	a	577.5	16	0.5	2	4.5	7	8.5	11.5	13.5	17	21	22.5	10
TCS	static	M7	OL + SL	24	a	348.75	16	0.5	2	4.5	7	8.5	11.5	13.5	17	21	22.5	10
MDD	dynamic	M2-N	all layers	34	b	509	14	0.5	9.5	11.5	24	29.5						5
MDD	dynamic	M2-N	all layers	35	b	524	14	0.5	9.5	11.5	24	29.5						5
MDD	dynamic	M2-S	all layers	34	c	509	-14	0.5	9.5	11.5	24	29.5						5
MDD	dynamic	M2-S	all layers	35	c	524	-14	0.5	9.5	11.5	24	29.5						5
RS-OL	dynamic	M2-N	OL	35	b	517.5	7.5	1.5	7.5									6
RS-OL	dynamic	M2-N	OL	36	b	532.5	7.5	1.5	7.5									6
RS-OL	dynamic	M2-S	OL	35	c	517.5	-7.5	1.5	7.5									6
RS-OL	dynamic	M2-S	OL	36	c	532.5	-7.5	1.5	7.5									6
RS-OL	dynamic	M4	OL	26	b	382.5	7.5	1.5	7.5									6
RS-OL	dynamic	M4	OL	26	b	381.5	8.5	1.5	7.5									6
RS-OL	dynamic	M4	OL	27	b	397.5	7.5	1.5	7.5									6
RS-OL	dynamic	M4	OL	27	b	398.5	8.5	1.5	7.5									6
RS-OL	dynamic	M5	OL	26	c	382.5	-7.5	1.5	7.5									6

TABLE 9. COORDINATES FOR SENSORS IN THE MEDIUM STRENGTH SUBGRADE SECTION (CONT.)

Sensor	Sensor type	Cell	Layer	slab # - x	slab # - y	Coordinates, ft												Total
						X	y	z1	z2	z3	z4	z5	z6	z7	z8	z9	z10	
RS-OL	dynamic	M5	OL	26	c	381.5	-8.5	1.5	7.5									6
RS-OL	dynamic	M5	OL	27	c	397.5	-7.5	1.5	7.5									6
RS-OL	dynamic	M5	OL	27	c	398.5	-8.5	1.5	7.5									6
RS-SL	dynamic	M2-N	SL	35	b	517.5	7.5	12.5	21.5									6
RS-SL	dynamic	M2-N	SL	36	b	532.5	7.5	12.5	21.5									6
RS-SL	dynamic	M2-S	SL	35	c	517.5	-7.5	12.5	21.5									6
RS-SL	dynamic	M2-S	SL	36	c	532.5	-7.5	12.5	21.5									6
RS-SL	dynamic	M4	SL	27	a	390	15	12.5	21.5									6
RS-SL	dynamic	M4	SL	27	b	390	0	12.5	21.5									6
RS-SL	dynamic	M4	SL	28	a	405	15	12.5	21.5									6
RS-SL	dynamic	M4	SL	28	b	405	0	12.5	21.5									6
RS-SL	dynamic	M5	SL	27	c	390	-15	12.5	21.5									6
RS-SL	dynamic	M5	SL	28	c	405	-15	12.5	21.5									6
S-OL	dynamic	M1-N	OL	38	b	562.5	14.5	1.5	7.5									2
S-OL	dynamic	M1-N	OL	38	b	569.5	6.5	1.5	7.5									2
S-OL	dynamic	M1-N	OL	38	b	569.5	7.5	1.5	7.5									2
S-OL	dynamic	M1-N	OL	38	b	569.5	8.5	1.5	7.5									2
S-OL	dynamic	M1-N	OL	38	b	569.5	9.5	1.5	7.5									2
S-OL	dynamic	M1-N	OL	38	b	569.5	10.5	1.5	7.5									2
S-OL	dynamic	M1-N	OL	39	b	577.5	14.5	1.5	7.5									2
S-OL	dynamic	M1-N	OL	39	b	584.5	6.5	1.5	7.5									2

TABLE 9. COORDINATES FOR SENSORS IN THE MEDIUM STRENGTH SUBGRADE SECTION (CONT.)

Sensor	Sensor type	Cell	Layer	slab # - x	slab # - y	Coordinates, ft												Total
						X	y	z1	z2	z3	z4	z5	z6	z7	z8	z9	z10	
S-OL	dynamic	M1-N	OL	39	b	584.5	7.5	1.5	7.5									2
S-OL	dynamic	M1-N	OL	39	b	584.5	8.5	1.5	7.5									2
S-OL	dynamic	M1-N	OL	39	b	584.5	9.5	1.5	7.5									2
S-OL	dynamic	M1-N	OL	39	b	584.5	10.5	1.5	7.5									2
S-OL	dynamic	M1-S	OL	38	c	562.5	-14.5	1.5	7.5									2
S-OL	dynamic	M1-S	OL	38	c	569.5	-8.5	1.5	7.5									2
S-OL	dynamic	M1-S	OL	38	c	569.5	-7.5	1.5	7.5									2
S-OL	dynamic	M1-S	OL	38	c	569.5	-6.5	1.5	7.5									2
S-OL	dynamic	M1-S	OL	38	c	569.5	-9.5	1.5	7.5									2
S-OL	dynamic	M1-S	OL	38	c	569.5	-10.5	1.5	7.5									2
S-OL	dynamic	M1-S	OL	39	c	577.5	-14.5	1.5	7.5									2
S-OL	dynamic	M1-S	OL	39	c	584.5	-8.5	1.5	7.5									2
S-OL	dynamic	M1-S	OL	39	c	584.5	-7.5	1.5	7.5									2
S-OL	dynamic	M1-S	OL	39	c	584.5	-6.5	1.5	7.5									2
S-OL	dynamic	M1-S	OL	39	c	584.5	-9.5	1.5	7.5									2
S-OL	dynamic	M1-S	OL	39	c	584.5	-10.5	1.5	7.5									2
S-OL	dynamic	M2-N	OL	35	b	524.5	10.5	1.5	7.5									2
S-OL	dynamic	M2-N	OL	35	b	524.5	7.5	1.5	7.5									2
S-OL	dynamic	M2-N	OL	35	b	517.5	14.5	1.5	7.5									2
S-OL	dynamic	M2-N	OL	36	b	539.5	7.5	1.5	7.5									2
S-OL	dynamic	M2-N	OL	36	b	532.5	14.5	1.5	7.5									2
S-OL	dynamic	M2-N	OL	36	b	539.5	10.5	1.5	7.5									2
S-OL	dynamic	M2-S	OL	35	c	524.5	-10.5	1.5	7.5									2

TABLE 9. COORDINATES FOR SENSORS IN THE MEDIUM STRENGTH SUBGRADE SECTION (CONT.)

Sensor	Sensor type	Cell	Layer	slab # - x	slab # - y	Coordinates, ft												Total
						X	y	z1	z2	z3	z4	z5	z6	z7	z8	z9	z10	
S-OL	dynamic	M2-S	OL	35	c	517.5	-14.5	1.5	7.5									2
S-OL	dynamic	M2-S	OL	35	c	524.5	-7.5	1.5	7.5									2
S-OL	dynamic	M2-S	OL	36	c	532.5	-14.5	1.5	7.5									2
S-OL	dynamic	M2-S	OL	36	c	539.5	-7.5	1.5	7.5									2
S-OL	dynamic	M2-S	OL	36	c	539.5	-10.5	1.5	7.5									2
S-OL	dynamic	M3-N	OL	30	b	449.5	7.5	1.5	7.5									2
S-OL	dynamic	M3-N	OL	30	b	442.5	14.5	1.5	7.5									2
S-OL	dynamic	M3-N	OL	31	b	464.5	7.5	1.5	7.5									2
S-OL	dynamic	M3-N	OL	31	b	457.5	14.5	1.5	7.5									2
S-OL	dynamic	M3-N	OL	32	b	479.5	7.5	1.5	7.5									2
S-OL	dynamic	M3-N	OL	32	b	472.5	14.5	1.5	7.5									2
S-OL	dynamic	M3-S	OL	30	c	442.5	-14.5	1.5	7.5									2
S-OL	dynamic	M3-S	OL	30	c	449.5	-7.5	1.5	7.5									2
S-OL	dynamic	M3-S	OL	31	c	457.5	-14.5	1.5	7.5									2
S-OL	dynamic	M3-S	OL	31	c	464.5	-7.5	1.5	7.5									2
S-OL	dynamic	M3-S	OL	32	c	472.5	-14.5	1.5	7.5									2
S-OL	dynamic	M3-S	OL	32	c	479.5	-7.5	1.5	7.5									2
S-OL	dynamic	M4	OL	26	b	389.5	7.5	1.5	7.5									2
S-OL	dynamic	M4	OL	26	b	382.5	14.5	1.5	7.5									2
S-OL	dynamic	M4	OL	27	b	404.5	7.5	1.5	7.5									2
S-OL	dynamic	M4	OL	27	b	397.5	14.5	1.5	7.5									2
S-OL	dynamic	M5	OL	26	c	382.5	-14.5	1.5	7.5									2
S-OL	dynamic	M5	OL	26	c	389.5	-7.5	1.5	7.5									2

TABLE 9. COORDINATES FOR SENSORS IN THE MEDIUM STRENGTH SUBGRADE SECTION (CONT.)

Sensor	Sensor type	Cell	Layer	slab # - x	slab # - y	Coordinates, ft												Total
						X	y	z1	z2	z3	z4	z5	z6	z7	z8	z9	z10	
S-OL	dynamic	M5	OL	27	c	397.5	-14.5	1.5	7.5									2
S-OL	dynamic	M5	OL	27	c	404.5	-7.5	1.5	7.5									2
S-OL	dynamic	M7	OL	23	b	344.5	7.5	1.5	7.5									2
S-OL	dynamic	M7	OL	23	b	338.5	14.5	1.5	7.5									2
S-OL	dynamic	M7	OL	23	b	337.5	14.5	1.5	7.5									2
S-OL	dynamic	M7	OL	23	b	336.5	14.5	1.5	7.5									2
S-OL	dynamic	M7	OL	23	c	338.5	-14.5	1.5	7.5									2
S-OL	dynamic	M7	OL	23	c	337.5	-14.5	1.5	7.5									2
S-OL	dynamic	M7	OL	23	c	336.5	-14.5	1.5	7.5									2
S-OL	dynamic	M7	OL	23	c	344.5	-7.5	1.5	7.5									2
S-SL	dynamic	M1-N	SL	38	b	562.5	7.5	12.5	21.5									2
S-SL	dynamic	M1-N	SL	39	b	577.5	7.5	12.5	21.5									2
S-SL	dynamic	M1-S	SL	38	c	562.5	-7.5	12.5	21.5									2
S-SL	dynamic	M1-S	SL	39	c	577.5	-7.5	12.5	21.5									2
TCD	dynamic	M1-N	OL + SL	38	a	562.5	16	0.5	2	4.5	7	8.5	11.5	13.5	17	21	22.5	10
TCD	dynamic	M7	OL + SL	23	a	333.75	16	0.5	2	4.5	7	8.5	11.5	13.5	17	21	22.5	10

TABLE 10. COORDINATES FOR SENSORS IN THE HIGH STRENGTH SUBGRADE SECTION

Sensor	Sensor type	Cell	Layer	slab # - x	slab # - y	Coordinates, ft												Total
						x	y	z1	z2	z3	z4	z5	z6	z7	z8	z9	z10	
Humid-G	static	H2-N	OL	48	a	712.5	17	1	3	8								3
Humid-G	static	H2-N	SL	50	a	742.5	17	12	14	19								3
Humid-G	static	H2-S	OL	47	d	697.5	-17	1	3	8								3
Humid-G	static	H2-S	SL	50	d	742.5	-17	12	14	19								3
Humid-G	static	H4	OL	58	a	862.5	17	1	3	8								3
Humid-G	static	H5	OL	57	d	847.5	-17	1	3	8								3
JG	static	H2-N	OL	47	a	697.5	15	4.5										1
JG	static	H2-N	SL	47	a	697.5	15	17										1
JG	static	H2-S	OL	47	d	697.5	-15	4.5										1
JG	static	H2-S	SL	47	d	697.5	-15	17										1
JG	static	H4	SL	57	b	847.5	0	17										1
JG	static	H4	OL	58	b	855	7.5	4.5										1
JG	static	H4	SL	58	b	862.5	0	17										1
JG	static	H5	OL	58	c	855	-7.5	4.5										1
slab-lift-G	static	H2-N	OL	47	b	690	15	9										1
slab-lift-G	static	H2-N	OL	47	b	690	7.5	9										1
slab-lift-G	static	H2-N	OL	47	b	690	0	9										1
slab-lift-G	static	H2-N	OL	47	b	697.5	15	9										1
slab-lift-G	static	H2-N	OL	47	b	697.5	0	9										1

TABLE 10. COORDINATES FOR SENSORS IN THE HIGH STRENGTH SUBGRADE SECTION (CONT.)

Sensor	Sensor type	Cell	Layer	slab # - x	slab # - y	Coordinates, ft												Total
						x	y	z1	z2	z3	z4	z5	z6	z7	z8	z9	z10	
slab-lift-G	static	H2-N	OL	47	b	705	15	9										1
slab-lift-G	static	H2-N	OL	47	b	705	7.5	9										1
slab-lift-G	static	H2-N	OL	47	b	705	0	9										1
slab-lift-G	static	H2-S	OL	47	c	690	0	9										1
slab-lift-G	static	H2-S	OL	47	c	690	-7.5	9										1
slab-lift-G	static	H2-S	OL	47	c	690	-15	9										1
slab-lift-G	static	H2-S	OL	47	c	697.5	0	9										1
slab-lift-G	static	H2-S	OL	47	c	697.5	-15	9										1
slab-lift-G	static	H2-S	OL	47	c	705	0	9										1
slab-lift-G	static	H2-S	OL	47	c	705	-7.5	9										1
slab-lift-G	static	H2-S	OL	47	c	705	-15	9										1
slab-lift-G	static	H4	OL	57	b	840	15	9										1
slab-lift-G	static	H4	OL	57	b	840	7.5	9										1
slab-lift-G	static	H4	OL	57	b	840	0	9										1
slab-lift-G	static	H4	OL	57	b	847.5	15	9										1
slab-lift-G	static	H4	OL	57	b	847.5	0	9										1
slab-lift-G	static	H4	OL	57	b	855	15	9										1
slab-lift-G	static	H4	OL	57	b	855	7.5	9										1
slab-lift-G	static	H4	OL	57	b	855	0	9										1
slab-lift-G	static	H5	OL	57	c	840	0	9										1
slab-lift-G	static	H5	OL	57	c	840	-7.5	9										1
slab-lift-G	static	H5	OL	57	c	840	-15	9										1
slab-lift-G	static	H5	OL	57	c	847.5	0	9										1
slab-lift-G	static	H5	OL	57	c	847.5	-15	9										1
slab-lift-G	static	H5	OL	57	c	855	0	9										1

TABLE 10. COORDINATES FOR SENSORS IN THE HIGH STRENGTH SUBGRADE SECTION (CONT.)

Sensor	Sensor type	Cell	Layer	slab # - x	slab # - y	Coordinates, ft												Total
						x	y	z1	z2	z3	z4	z5	z6	z7	z8	z9	z10	
slab-lift-G	static	H5	OL	57	c	855	-7.5	9										1
slab-lift-G	static	H5	OL	57	c	855	-15	9										1
TCS	static	H1-N	OL + SL	45	a	667.5	16	0.5	2	4.5	7	8.5	11.5	13.5	17	21	22.5	10
TCS	static	H4	OL + SL	58	a	858.75	16	0.5	2	4.5	7	8.5	11.5	13.5	17	21	22.5	10
MDD	dynamic	H2-N	all layers	48	b	719	14	0.5	9.5	11.5	24	29.5						5
MDD	dynamic	H2-N	all layers	49	b	734	14	0.5	9.5	11.5	24	29.5						5
MDD	dynamic	H2-S	all layers	48	c	719	-14	0.5	9.5	11.5	24	29.5						5
MDD	dynamic	H2-S	all layers	49	c	734	-14	0.5	9.5	11.5	24	29.5						5
RS-OL	dynamic	H2-N	OL	47	b	697.5	7.5	1.5	7.5									6
RS-OL	dynamic	H2-N	OL	48	b	712.5	7.5	1.5	7.5									6
RS-OL	dynamic	H2-S	OL	47	c	697.5	-7.5	1.5	7.5									6
RS-OL	dynamic	H2-S	OL	48	c	712.5	-7.5	1.5	7.5									6
RS-OL	dynamic	H4	OL	57	b	847.5	7.5	1.5	7.5									6
RS-OL	dynamic	H4	OL	57	b	846.5	8.5	1.5	7.5									6
RS-OL	dynamic	H4	OL	58	b	862.5	7.5	1.5	7.5									6
RS-OL	dynamic	H4	OL	58	b	863.5	8.5	1.5	7.5									6
RS-OL	dynamic	H5	OL	57	c	847.5	-7.5	1.5	7.5									6
RS-OL	dynamic	H5	OL	57	c	846.5	-8.5	1.5	7.5									6
RS-OL	dynamic	H5	OL	58	c	862.5	-7.5	1.5	7.5									6
RS-OL	dynamic	H5	OL	58	c	863.5	-8.5	1.5	7.5									6
RS-SL	dynamic	H2-N	SL	47	b	697.5	7.5	12.5	21.5									6
RS-SL	dynamic	H2-N	SL	48	b	712.5	7.5	12.5	21.5									6

TABLE 10. COORDINATES FOR SENSORS IN THE HIGH STRENGTH SUBGRADE SECTION (CONT.)

Sensor	Sensor type	Cell	Layer	slab # - x	slab # - y	Coordinates, ft											Total	
						x	y	z1	z2	z3	z4	z5	z6	z7	z8	z9		z10
RS-SL	dynamic	H2-S	SL	47	c	697.5	-7.5	12.5	21.5									6
RS-SL	dynamic	H2-S	SL	48	c	712.5	-7.5	12.5	21.5									6
RS-SL	dynamic	H4	SL	58	a	855	15	12.5	21.5									6
RS-SL	dynamic	H4	SL	58	b	855	0	12.5	21.5									6
RS-SL	dynamic	H4	SL	59	a	870	15	12.5	21.5									6
RS-SL	dynamic	H4	SL	59	b	870	0	12.5	21.5									6
RS-SL	dynamic	H5	SL	58	c	855	-15	12.5	21.5									6
RS-SL	dynamic	H5	SL	59	c	870	-15	12.5	21.5									6
S OL	dynamic	H1-N	OL	43	b	637.5	14.5	1.5	7.5									2
S OL	dynamic	H1-N	OL	43	b	644.5	6.5	1.5	7.5									2
S OL	dynamic	H1-N	OL	43	b	644.5	7.5	1.5	7.5									2
S OL	dynamic	H1-N	OL	43	b	644.5	8.5	1.5	7.5									2
S-OL	dynamic	H1-N	OL	43	b	644.5	9.5	1.5	7.5									2
S-OL	dynamic	H1-N	OL	43	b	644.5	10.5	1.5	7.5									2
S OL	dynamic	H1-N	OL	44	b	652.5	14.5	1.5	7.5									2
S OL	dynamic	H1-N	OL	44	b	659.5	6.5	1.5	7.5									2
S OL	dynamic	H1-N	OL	44	b	659.5	7.5	1.5	7.5									2
S OL	dynamic	H1-N	OL	44	b	659.5	8.5	1.5	7.5									2
S-OL	dynamic	H1-N	OL	44	b	659.5	9.5	1.5	7.5									2
S-OL	dynamic	H1-N	OL	44	b	659.5	10.5	1.5	7.5									2
S OL	dynamic	H1-S	OL	43	c	637.5	-14.5	1.5	7.5									2
S-OL	dynamic	H1-S	OL	43	c	644.5	-10.5	1.5	7.5									2
S-OL	dynamic	H1-S	OL	43	c	644.5	-9.5	1.5	7.5									2
S OL	dynamic	H1-S	OL	43	c	644.5	-8.5	1.5	7.5									2
S OL	dynamic	H1-S	OL	43	c	644.5	-7.5	1.5	7.5									2
S OL	dynamic	H1-S	OL	43	c	644.5	-6.5	1.5	7.5									2

TABLE 10. COORDINATES FOR SENSORS IN THE HIGH STRENGTH SUBGRADE SECTION (CONT.)

Sensor	Sensor type	Cell	Layer	slab # - x	slab # - y	Coordinates, ft												Total
						x	y	z1	z2	z3	z4	z5	z6	z7	z8	z9	z10	
S_OL	dynamic	H1-S	OL	44	c	652.5	-14.5	1.5	7.5									2
S-OL	dynamic	H1-S	OL	44	c	659.5	-10.5	1.5	7.5									2
S-OL	dynamic	H1-S	OL	44	c	659.5	-9.5	1.5	7.5									2
S_OL	dynamic	H1-S	OL	44	c	659.5	-8.5	1.5	7.5									2
S_OL	dynamic	H1-S	OL	44	c	659.5	-7.5	1.5	7.5									2
S_OL	dynamic	H1-S	OL	44	c	659.5	-6.5	1.5	7.5									2
S_OL	dynamic	H2-N	OL	47	b	697.5	14.5	1.5	7.5									2
S_OL	dynamic	H2-N	OL	47	b	704.5	7.5	1.5	7.5									2
S-OL	dynamic	H2-N	OL	47	b	704.5	10.5	1.5	7.5									2
S_OL	dynamic	H2-N	OL	48	b	712.5	14.5	1.5	7.5									2
S_OL	dynamic	H2-N	OL	48	b	719.5	7.5	1.5	7.5									2
S-OL	dynamic	H2-N	OL	48	b	719.5	10.5	1.5	7.5									2
S_OL	dynamic	H2-S	OL	47	c	697.5	-14.5	1.5	7.5									2
S-OL	dynamic	H2-S	OL	47	c	704.5	-10.5	1.5	7.5									2
S_OL	dynamic	H2-S	OL	47	c	704.5	-7.5	1.5	7.5									2
S_OL	dynamic	H2-S	OL	48	c	712.5	-14.5	1.5	7.5									2
S-OL	dynamic	H2-S	OL	48	c	719.5	-10.5	1.5	7.5									2
S_OL	dynamic	H2-S	OL	48	c	719.5	-7.5	1.5	7.5									2
S_OL	dynamic	H3-N	OL	52	b	772.5	14.5	1.5	7.5									2
S_OL	dynamic	H3-N	OL	52	b	779.5	7.5	1.5	7.5									2
S_OL	dynamic	H3-N	OL	53	b	787.5	14.5	1.5	7.5									2
S_OL	dynamic	H3-N	OL	53	b	794.5	7.5	1.5	7.5									2
S_OL	dynamic	H3-N	OL	54	b	802.5	14.5	1.5	7.5									2
S_OL	dynamic	H3-N																2
S_OL	dynamic	H3-S																2
S_OL	dynamic	H3-S																2

113

TABLE 10. COORDINATES FOR SENSORS IN THE HIGH STRENGTH SUBGRADE SECTION (CONT.)

Sensor	Sensor type	Cell	Layer	slab # - x	slab # - y	Coordinates, ft												Total
						x	y	z1	z2	z3	z4	z5	z6	z7	z8	z9	z10	
S_OL	dynamic	H3-S	OL	53	c	787.5	-14.5	1.5	7.5									2
S_OL	dynamic	H3-S	OL	53	c	794.5	-7.5	1.5	7.5									2
S_OL	dynamic	H3-S	OL	54	c	802.5	-14.5	1.5	7.5									2
S_OL	dynamic	H3-S	OL	54	c	809.5	-7.5	1.5	7.5									2
S_OL	dynamic	H4	OL	57	b	847.5	14.5	1.5	7.5									2
S_OL	dynamic	H4	OL	57	b	854.5	7.5	1.5	7.5									2
S_OL	dynamic	H4	OL	58	b	862.5	14.5	1.5	7.5									2
S_OL	dynamic	H4	OL	58	b	869.5	7.5	1.5	7.5									2
S_OL	dynamic	H5	OL	57	c	847.5	-14.5	1.5	7.5									2
S_OL	dynamic	H5	OL	57	c	854.5	-7.5	1.5	7.5									2
S_OL	dynamic	H5	OL	58	c	862.5	-14.5	1.5	7.5									2
S_OL	dynamic	H5	OL	58	c	869.5	-7.5	1.5	7.5									2
S-SL	dynamic	H1-N	SL	43	b	637.5	7.5	12.5	21.5									2
S-SL	dynamic	H1-N	SL	44	b	652.5	7.5	12.5	21.5									2
S-SL	dynamic	H1-S	SL	43	c	637.5	-7.5	12.5	21.5									2
S-SL	dynamic	H1-S	SL	44	c	652.5	-7.5	12.5	21.5									2
TCD	dynamic	H1-N	OL + SL	44	a	652.5	16	0.5	2	4.5	7	8.5	11.5	13.5	17	21	22.5	10
TCD	dynamic	H4	OL + SL	57	a	843.75	16	0.5	2	4.5	7	8.5	11.5	13.5	17	21	22.5	10

5.2.1 Slab Lift-off Gages

Slab lift-off gages, identified as squares in the figures below, will be placed at the four corners of a chosen slab so that the vertical movements at the slab corners can be measured. In addition, these sensors will also be placed at the mid-length and mid-width of the longitudinal and transverse edges, respectively. This will enable the measurement of slab corner lift-off, as well as the estimation of slab curvature along both the transverse and longitudinal edges. Figures 50, 51, and 52 show the locations of slab lift-off gage instrumentation in the L-, M-, and H-sections. Slab lift-off gages will be placed in slabs b5, c5, b14, and c14 in the L-section, b26, c26, b36, and c36 in the M-section, and b47, c47, b57, and c57 in the H-section.

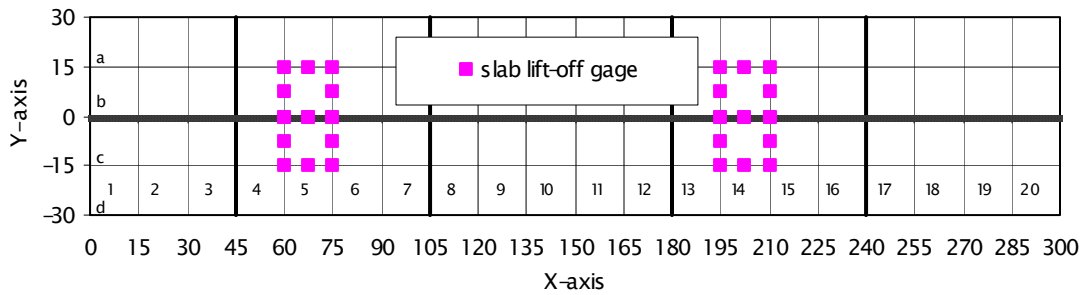


FIGURE 50. SLAB LIFT-OFF GAGES IN THE L-SECTIONS

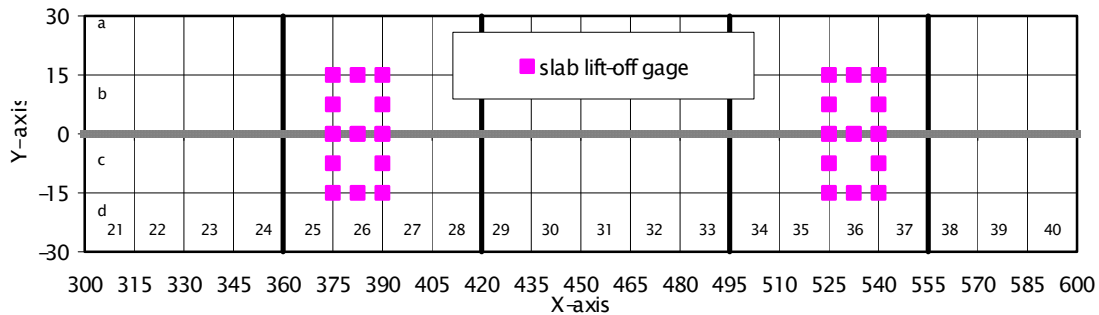


FIGURE 51. SLAB LIFT-OFF GAGES IN THE M-SECTIONS

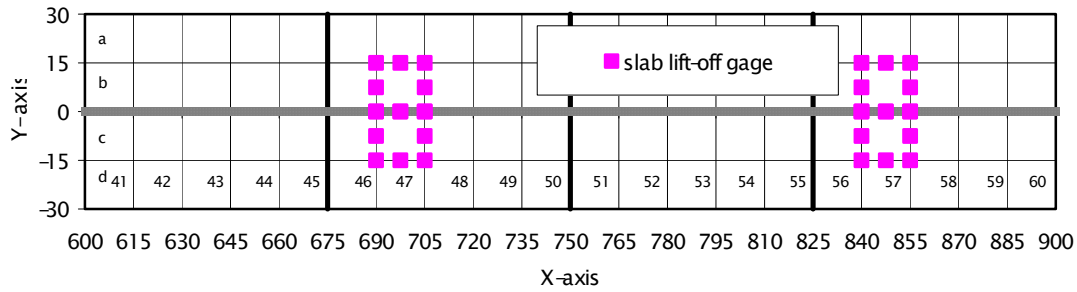


FIGURE 52. SLAB LIFT-OFF GAGES IN THE H-SECTIONS

5.2.2 Thermocouples

Figures 53, 54, and 55 show the layout for the thermocouples in the L-, M-, and H-sections. The thermocouples that will be connected to the static data logger are identified as TCS, and those that take dynamic measurements are identified as TCD. Since the temperature of the pavements is almost the same along the entire test section, these measurements will be applicable all test cells. As stated in the previous section, the TCS and TCD gages will measure the pavement temperature at several depths of the slab.

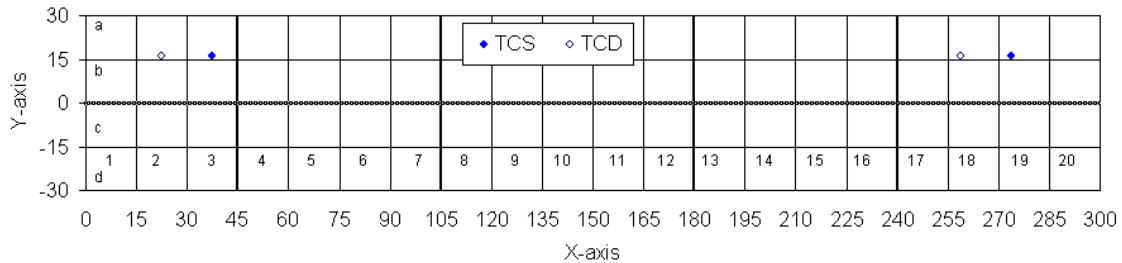


FIGURE 53. THERMOCOUPLES IN THE L-SECTION

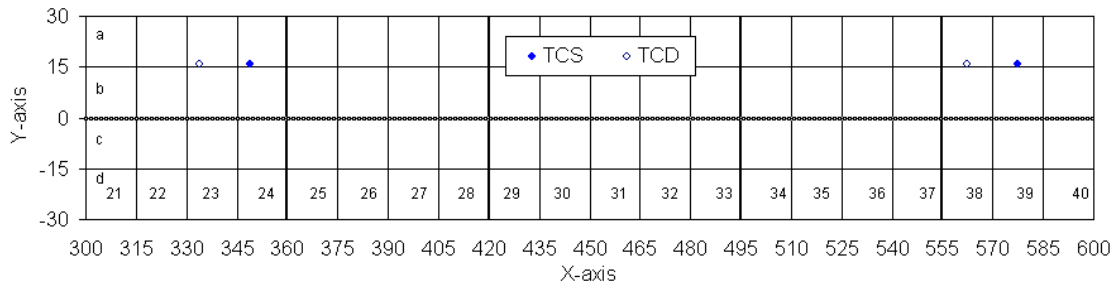


FIGURE 54. THERMOCOUPLES IN THE M-SECTION

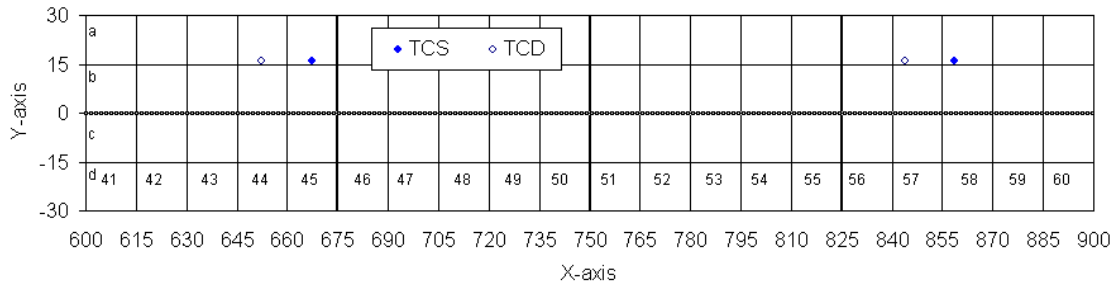


FIGURE 55. THERMOCOUPLES IN THE H-SECTION

5.2.3 Humidity Gages

Humidity gages will be placed in both the underlying slab and the overlay at different depths. Similar to the thermocouples, the moisture levels in the slab recorded at a few locations are applicable to all test cells within the test section. Figures 56, 57, and 58 show the locations of the humidity gages in the overlay and underlying slab for the L-, M-, and H-sections.

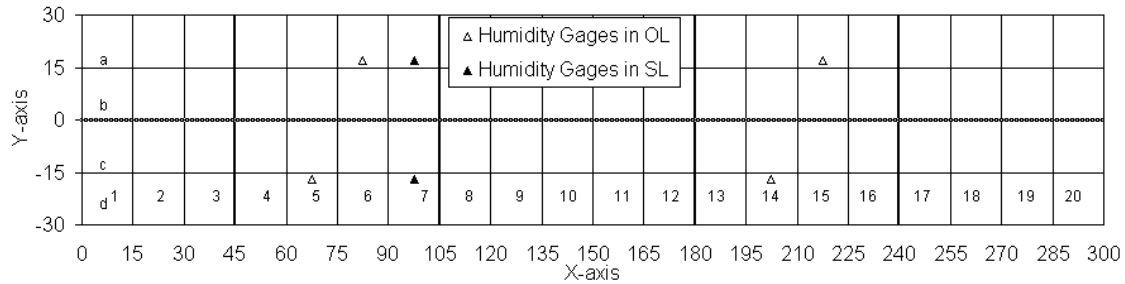


FIGURE 56. HUMIDITY GAGES IN THE L-SECTION

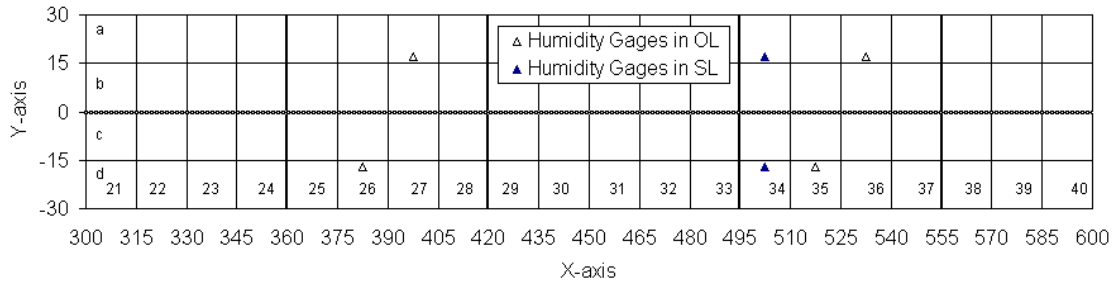


FIGURE 57. HUMIDITY GAGES IN THE M-SECTION

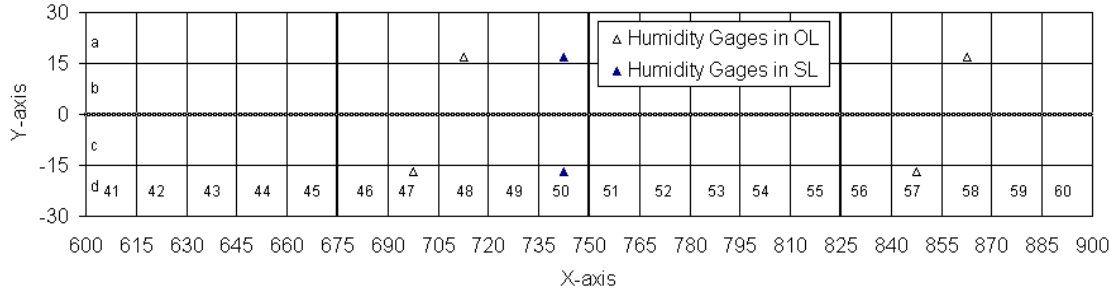


FIGURE 58. HUMIDITY GAGES IN THE H-SECTION

5.2.4 Joint Gages

Joint gages will be placed in the overlay and underlying slabs to record joint movements with changes in temperature and moisture conditions in the PCC through out the test period. These gages will be placed across both the longitudinal and transverse joints. Figures 59, 60, and 61 show the joint gage locations in the L-, M-, and H-sections. Joint gages will be placed at the mid-depth of the slab.

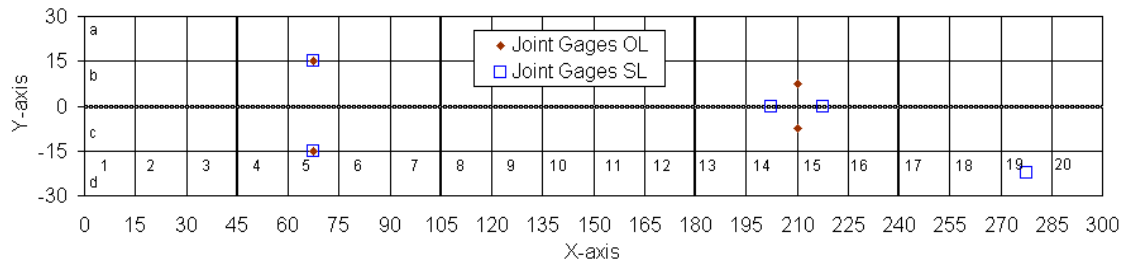


FIGURE 59. JOINT GAGES IN THE L-SECTION

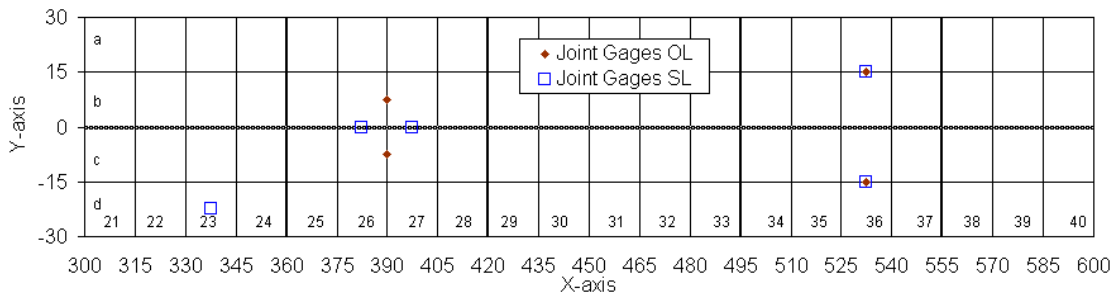


FIGURE 60. JOINT GAGES IN THE M-SECTION

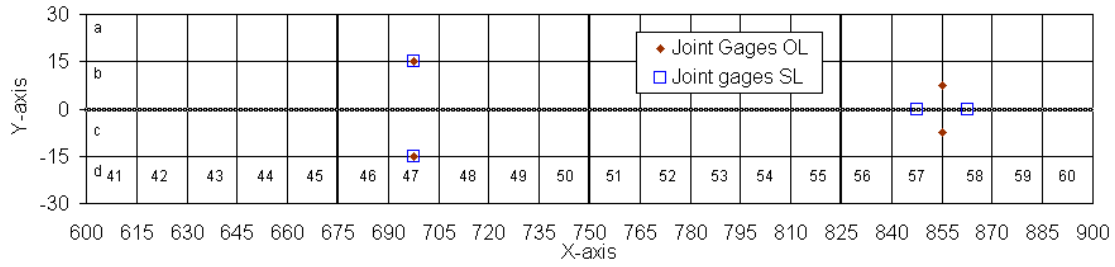


FIGURE 61. JOINT GAGES IN THE H-SECTION

5.2.5 MDD

Figures 62, 63, and 64 show the locations of the MDDs in the L-, M-, and H-sections. The MDDs are located in slab corners—the critical locations for slab deflection. The locations chosen for MDDs allow the measurement of the corner deflection on the approach side and the leave side of the joint.

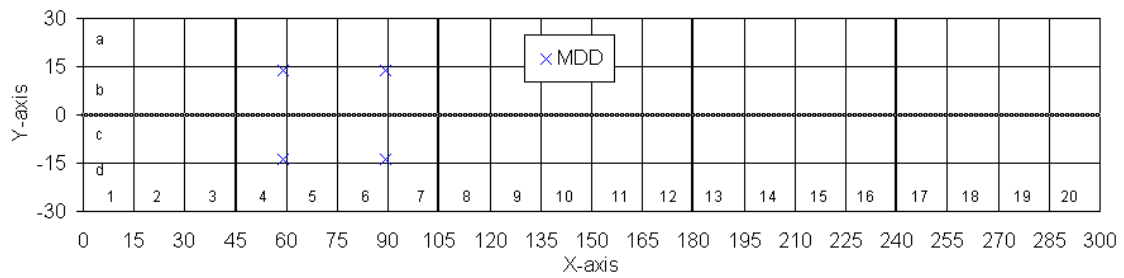


FIGURE 62. MDD IN THE L-SECTION

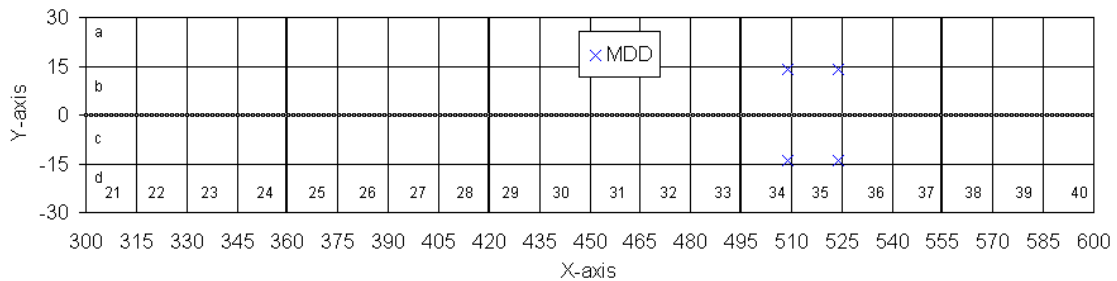


FIGURE 63. MDD IN THE M-SECTION

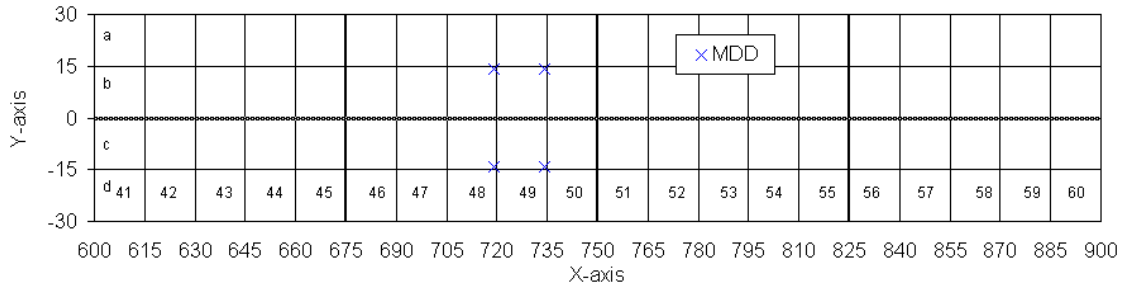


FIGURE 64. MDD IN THE H-SECTION

5.2.6 Strain Gage – S-gages

Single strain gages used to measure unidirectional strain are referred to as S-gages. These gages are placed 1.5 inches from the top and bottom of the overlay.

5.2.7 S-gages in the Underlying Slab

Figures 65, 66, and 67 show the locations for the single strain gages placed in the underlying slabs of the L-, M-, and H-sections. These gages have been placed at the longitudinal edge of the underlying slabs in test cells L1-N, L1-S, M1-N, M1-S, H1-N, and H1-S. Because these cells have mismatched longitudinal joints, the interior of the overlay slab is right above the S-gages in the underlying slab. (Please note that figures 65, 66 and 67 show the plan view of the overlay slab.)

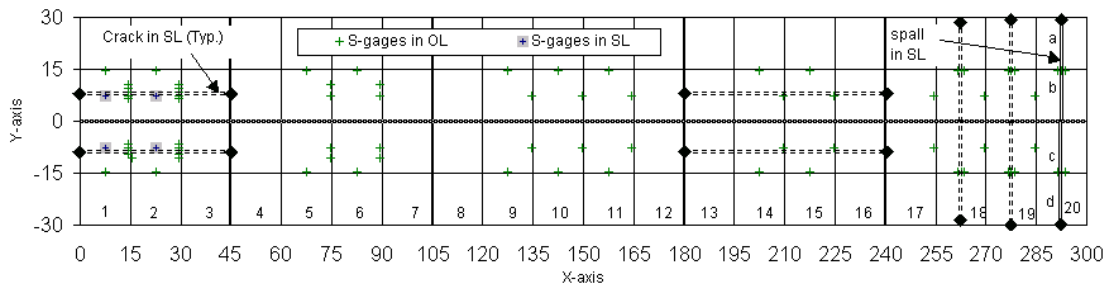


FIGURE 65. SINGLE STRAIN GAGE IN THE L-SECTION

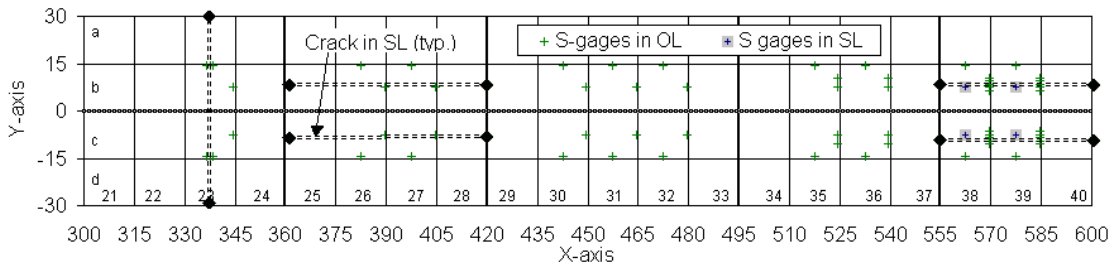


FIGURE 66. SINGLE STRAIN GAGE IN THE M-SECTION

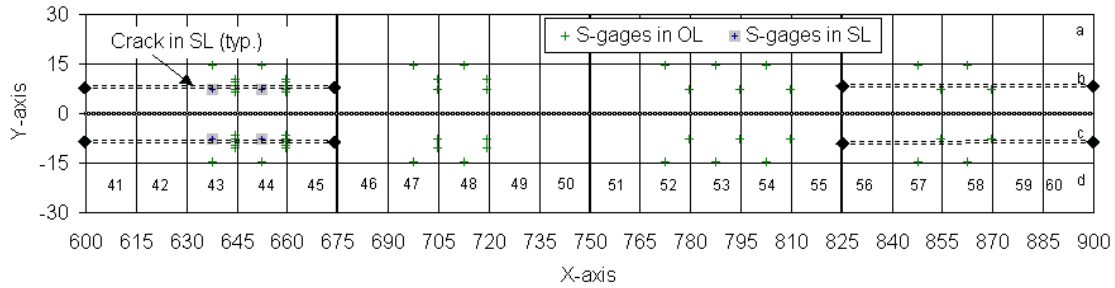


FIGURE 67. SINGLE STRAIN GAGE IN THE H-SECTION

5.2.8 S-gages in the Overlay

Figures 65, 66, and 67 also show the locations for the single strain gages placed in the L-, M-, and H-sections. The S-gages are placed in critical stress locations—along either the transverse edge or the longitudinal edge. Note that the gages at the longitudinal edge are oriented along the longitudinal direction, and those at the transverse edge are oriented along the transverse direction.

Slabs b1, b2, c1, and c1 (test cells L1-N and L1-S) of the L-sections have misaligned longitudinal joints with the underlying slab, creating critical stresses at the mid-width location of the transverse joint. Therefore, three strain gages are placed 12 inches apart along the transverse edge giving an opportunity to detect stress concentration at the edge right above the crack in the underlying slab, as shown in figure 68.

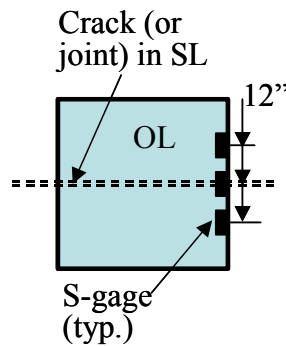


FIGURE 68. STRAIN GAGE ARRANGEMENT TO DETECT STRESS CONCENTRATION IN OVERLAY ABOVE A CRACK IN THE UNDERLYING PAVEMENT

Similarly, in slabs b18, b19, b20, c18, c19, and c20 (test cells L6, L7, L8), which have underlying slabs with misaligned transverse joints, a series of three gages are placed along the longitudinal edge of the slabs. This will allow strain measurements above the underlying crack and aid in detecting stress concentrations along the longitudinal joint. Corresponding cells with mismatched transverse and longitudinal joints in the M- and H-sections have slabs instrumented with similar series of gages, as shown in figures 66 and 67.

5.2.9 Strain Gage Rosettes – RS

Strain gage rosettes, identified as RS, will be placed in the interior locations of the underlying slabs and the overlay. These sensors will be placed at two depths in the slab—1.5 inches from the top and bottom layers.

5.2.10 RS in the Underlying Slabs

In the underlying slabs, the research team proposes to place the RS in test cells L2-N, M2-N, H2-N, L2-S, M2-S, and H2-S with matched transverse and longitudinal joints, and in cells L4, L5, M4, M5, H4, and H5 with mismatched transverse and longitudinal joints. Figures 69, 70, and 71 show the locations of the rosettes in the L-, M-, and H-sections. These figures show the locations on the plan view of the overlay slabs; in reality, the gages will be placed in the underlying slabs.

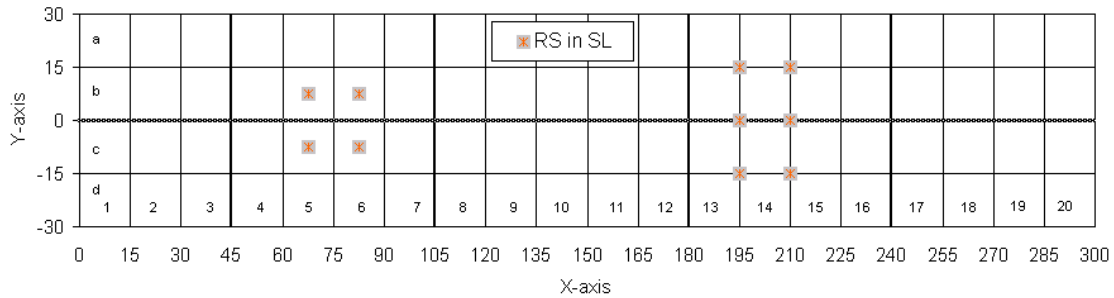


FIGURE 69. RS LOCATIONS IN THE UNDERLYING SLABS OF THE L-SECTION

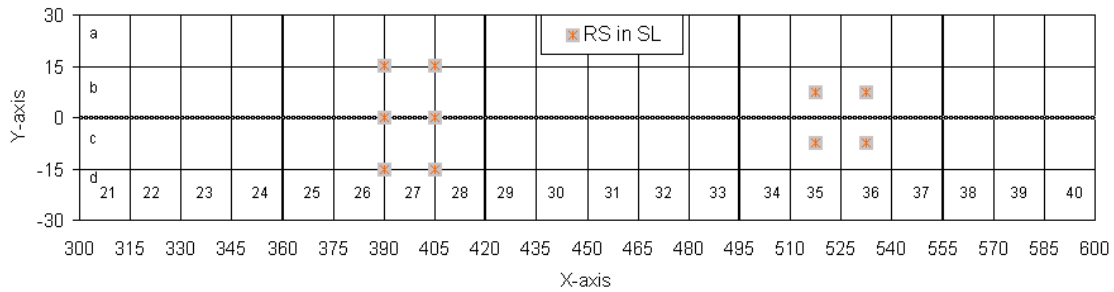


FIGURE 70. RS LOCATIONS IN THE UNDERLYING SLABS OF THE M-SECTION

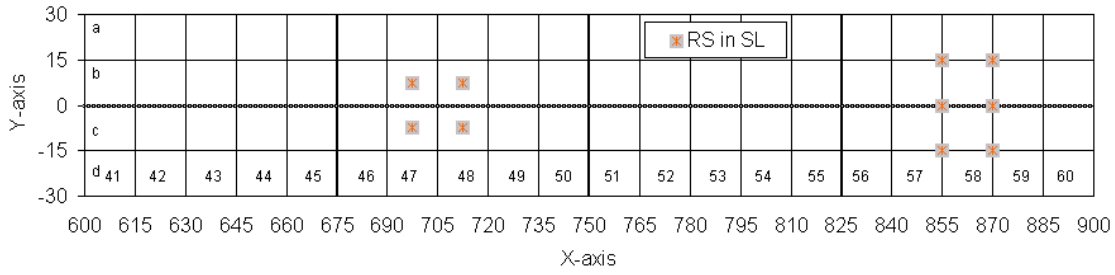


FIGURE 71 RS LOCATIONS IN THE UNDERLYING SLABS OF THE H-SECTION

5.2.11 RS in the Overlay

Strain gage rosettes will also be placed in the interior locations of the PCC overlay slabs. Figures 72, 73, and 74 show the locations for the RS gages in the L-, M-, and H-sections.

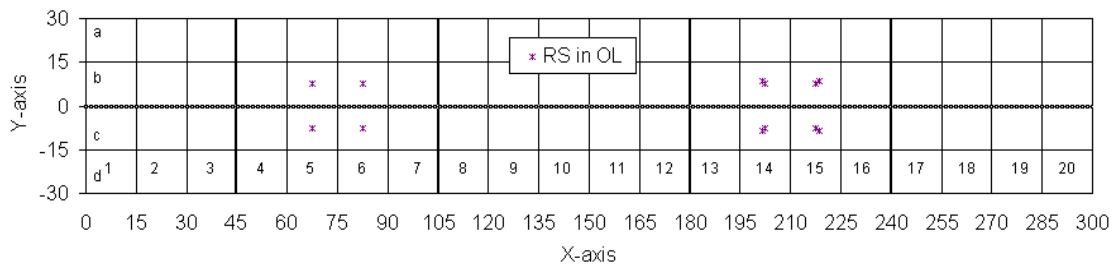


FIGURE 72. RS IN THE L-SECTION OVERLAYS

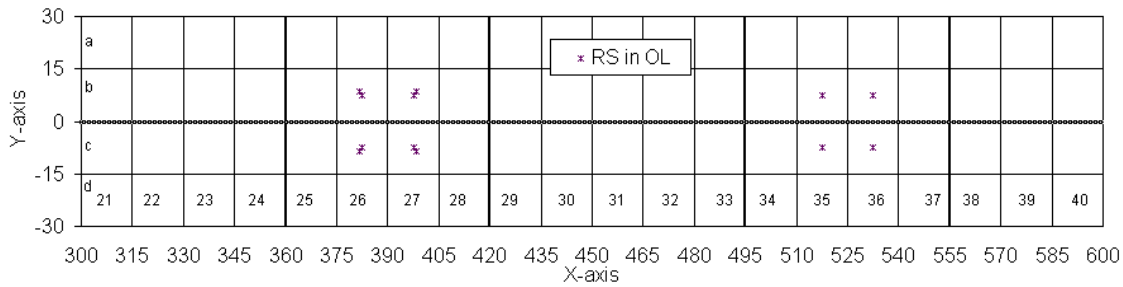


FIGURE 73. RS IN THE M-SECTION OVERLAYS

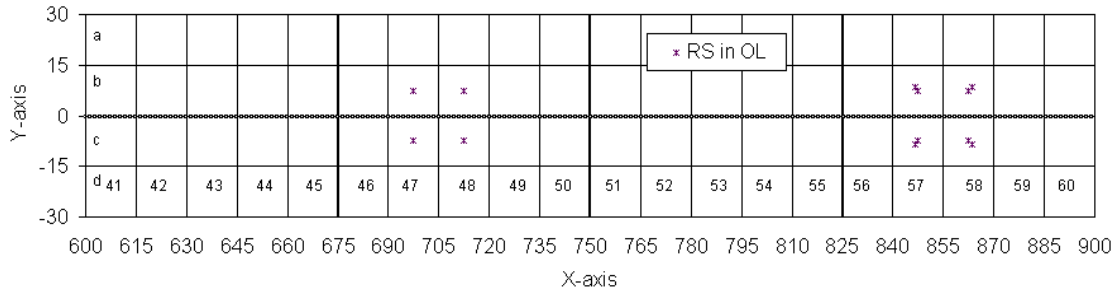


FIGURE 74. RS IN THE H-SECTION OVERLAYS

In slabs b17, c17, b18, and c18 of test cells L4 and L5 of the L-sections, two RS sensors are placed in the interior of the slab—one in the midpanel and the other at an offset of 12 inches in both the longitudinal and transverse directions, as shown in figure 75. This is proposed by the research team because the underlying slabs in these test cells have mismatched transverse and longitudinal joints. Therefore, the gage at the midpanel is above a slab corner in the underlying pavement, allowing strain measurement at this critical location. The sensor placed at an offset from the midpanel will allow an investigation of stress the field in the overlay over this distress condition. Similar patterns are used in the corresponding test cells of the M- and H-sections.

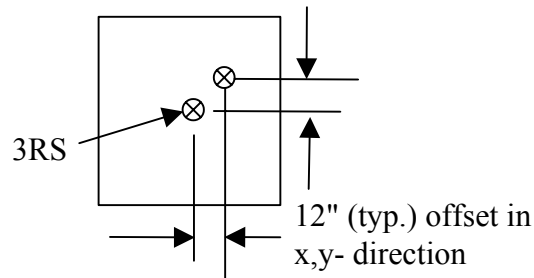


FIGURE 75. RS GAGE PATTERN IN PCC SLABS OVER UNDERLYING PAVEMENT WITH MISMATCHED TRANSVERSE AND LONGITUDINAL JOINTS

It is to be noted that the L-, M-, and H-sections have 11, 9, and 8 test cells, respectively. In general, identical sensors and sensor placements are used in corresponding cells of the L-, M-, and H-sections.

5.3 ADEQUACY OF DATA ACQUISITION SYSTEM

In making the choice of the sensor type and quantities in the proposed test plan, the research team has accounted for the data acquisition capabilities of the currently existing system at the NAPTF. Appendix F has the section describing the currently existing data acquisition system at the NAPTF.

5.3.1 Static Data Logger

The current system has a static data logger with 5 multiplexers comprising of 32 channels each. The current system would therefore allow the use of 160 static sensors (5*32). The current test plan includes the following static gages, as shown in table 11. The research team proposes the use of three additional boards having a total capacity of 96 additional channels to accommodate the use of all proposed sensors. The total number of available channels will now be increased to 256.

TABLE 11. NUMBER OF STATIC SENSORS IN THE TEST PLAN

Sensor type	L-section	M-section	H-section	Total
Thermocouple	20	20	20	60
Slab lift-off	32	32	32	96
Joint gages	9	9	8	26
Humidity gages	18	18	18	54
Total	79	79	78	236

5.3.2 High-Speed Data Acquisition System for Dynamic Sensor

The current data acquisition system consists of six signal-processing units (SPU). It is proposed that SPU 1 and 2 be used for the L-section, SPU 3 and 4 for the M-section, and SPU 5 and 6 for the H-sections. A total of 345 channels are now available for each subgrade type. Therefore, it will be necessary to activate two SPUs each time the trigger sensors activate the data acquisition process to collect data. A summary of the number sensors used in each test section is shown below in table 12. Note that each RS gage has three strain gages, thereby requiring three channels. Similarly, each MDD has five transducers requiring five channels to collect data from the different layers. It is evident from table 12 that the existing data collection equipment will suffice for this experiment.

5.4 COST ESTIMATE

The estimated cost for the instrumentation proposed in the test plan is presented in table 13. The total cost is estimated to be \$419, 213.

TABLE 12. NUMBER OF DYNAMIC SENSORS IN THE TEST PLAN

Sensor type	L-section	M-section	H-section	Total channels
Thermocouple	20	20	20	60
MDD*	4*5 = 20	4*5 = 20	4*5 = 20	60
S-gages in OL	160	128	112	400
S-gages in SL	8	8	8	24
RS in SL**	24*3 = 72	24*3 = 72	24*3 = 72	216
RS in OL**	20*3 = 60	20*3 = 60	20*3 = 60	180
Portable LVDT	3	3	3	9
Total Channels	343 (<345)	311 (<345)	295 (<345)	982

*Each MDD has 5 transducers and hence requires 5 channels

** Each RS sensor has three strain gages and hence requires 3 channels

TABLE 13. COST ESTIMATE FOR INSTRUMENTATION

Sensor	Unit	Quantity	Cost per	Total
Joint gages (LVDT)	each	26	\$300	\$7,800
Strain Gages in single (S-gages)	each	396	\$23	\$9,108
Strain Gage Rosettes (RS)	each	128	\$60	\$7,680
MDD	each	12	\$5,000	\$60,000
Thermocouples (Static and Dynamic)	1000 foot	23.4	\$350	\$8,190
Humidity gage	each	54	\$100	\$5,400
Slab lift-off sensor - potentiometers	each	96	\$300	\$28,800
Portable surface deflection LVDT	each	4	\$1,000	\$4,000
Wire/cable	100 foot	562.5	\$50	\$28,125
Upgrades	each	3	\$15,000	\$45,000
Bridge completion units	each	829	\$30	\$24,870
chairs	each	262	\$20	\$5,240
Misc. Supplies				\$25,000
Sub-total				\$259,213
Labor	hours	2000	\$80	\$160,000
Total				\$419,213

6. COST ESTIMATE

6.1 INTRODUCTION

This chapter provides estimated costs for construction and testing of concrete overlay sections in the NAPTF, which can be used to assess the feasibility of building and testing such an experiment. The dollar amounts listed in the estimate are not exact; however, historical cost data were used as the basis on which to develop as accurate a cost estimate as possible. Various assumptions were made in the determination of construction and testing costs, as stated in the following sections.

6.2 CONSTRUCTION COST ESTIMATE

The construction cost estimate was calculated using data from two primary sources. Data were provided from the FAA that reflected the original 1996 bid costs for several construction items. For all items not included in the FAA estimate, costs were estimated from a second source, the R.S. Means Heavy Construction Cost Data manual (1997). In both cases, an inflation factor of 3.77% was applied to the base-year unit costs to convert them into 2002 dollars. It was also assumed that unit costs presented in the Means manual were derived for outdoor highway construction. However, the NAPTF requires the construction of airfield pavement, outfitted with a great deal of instrumentation, in an indoor environment. The delicate care required for constructing these instrumented pavements is difficult and often not cost-effective for construction contractors. For these reasons, a 300% escalation factor was applied to unit costs extracted from the Means manual for materials that require labor effort by the contractor, such as for placement of pavement layers, compaction, and curing. Costs derived from the FAA bid sheets already had an escalation factor applied, so additional escalation was not required. A contingencies estimate totaling 10% of the final project cost was applied to account for miscellaneous pavement repairs or other problems that may occur during construction.

A summary of the major items and the corresponding costs incurred is provided in table 14. The major portion of cost lies in the construction of the base pavement structure. Placement of the overlay and interlayer are the next most costly items. The total estimated cost for constructing the new overlay pavement sections at the NAPTF is \$1.47 million. Contingency money was allotted for any miscellaneous pavement repairs and/or changes. The total estimated cost for instrumentation is \$419,213 (see chapter 5 for details) and an estimated cost for data analysis is \$470,000, which brings the total program cost to \$2,307,509.

TABLE 14. COST SUMMARY FOR NEW CONSTRUCTION AT THE NAPTF.

Item		Total Cost
Pre-construction Planning		\$5,000
Base Construction	Granular Subbase Layer	\$715,151
	PCC Base Pavement	
Overlay Construction	HMA Interlayer	\$494,428
	PCC Overlay	
Shoulder Construction	HMA Shoulder	\$22,454
	Granular Subbase Support	
	Sand Backfill	
Other Construction Items		\$46,283
Quality Control Testing		\$50,000
Materials Characterization Testing		\$65,000
Contingencies		\$70,000
Instrumentation		\$419,213
Data Analysis		\$470,000
TOTAL COST		\$2,357,529

7. CONSTRUCTION SCHEDULE

7.1 INTRODUCTION

The schedule for the construction of concrete overlay sections in the NAPTF is presented in this chapter, along with guidelines for coordinating special testing, scheduling requirements, and submitting results, reports, and shop drawings. To ensure a timely sequence of construction and testing, the contractor should follow the schedule strictly. The guidelines for submittals and results are based on the FAA Special Provisions specifications (sections SP-6, SP-10, SP-11, and SP-15).

7.2 CONSTRUCTION SCHEDULE

The construction schedule was based on a combination of historical data from the original construction of the NAPTF and project management scheduling theory. The construction portion of the new overlay construction at the NAPTF is estimated to last approximately 6 months. Five months are allocated for the traffic testing, data collection, and observation of unbonded concrete overlays, resulting in a total project time of approximately 1 year.

The Microsoft Project 2000™ software was used to generate a schedule for construction of new concrete overlay sections. The schedule consists of primary construction tasks and a series of subtasks, as well as appropriate milestones indicating submittals and major project events. Some of the tasks can be completed simultaneously (e.g., preparations for laying bituminous interlayer conducted while curing of base concrete pavement is ongoing). Table 15 introduces the major tasks associated with the construction of the new overlay pavement sections.

TABLE 15. TOP-LEVEL TASKS IN CONSTRUCTION PLAN FOR NAPTF.

TASK ID NUMBER	TASK NAME	DURATION
1	Project Start	1 day
2	Contract Negotiations	1 day
3	Quality Control Schedule & Plan	1 day
4	Mobilization	5 days
5	Placement of Granular Subbase	23 days
13	Placement of PCC Base Pavement	51 days
22	Placement of Bituminous Interlayer	11 days
29	Placement of PCC Overlays	42 days
38	Shoulder: Placement of Backfill Sand	5 days
42	Shoulder: Placement of Granular Subbase	5 days
45	Shoulder: Bituminous Surface	7 days
52	Project End	1 day

A detailed construction schedule (including subtasks), milestone report, and listing of quality control tests is presented in appendix B.

7.3 COORDINATION REQUIREMENTS FOR SPECIAL TESTING

Coordination of special testing should be specified in accordance with FAA Special Provisions. Some specific requirements are presented below:

- a. **In-situ Testing.** Sampling and testing will be performed at various times during the construction to support research activities. This will require the contractor to cease work for a period to allow access to the site. Testing activities that will affect the construction schedule and require coordination shall consist primarily of CBR, moisture, and density testing on the surface of prepared subgrade and subbase layers. The contractor shall allow for a period of 7 non-consecutive days of inactivity during the construction period to allow for testing by the FAA.
- b. **Flexural Strength Tests.** In addition to the in-situ tests, samples of the fresh concrete (for both PCC base slabs and PCC overlay) will be taken, and beam specimens will be fabricated, cured and tested in flexure and compression, to support research activities. These tests will not be used for acceptance purposes. The contractor shall coordinate activities to allow FAA technicians to obtain samples of fresh concrete for specimen preparation.
- c. **Other Tests.** Other tests for material acceptance shall be performed in accordance with the applicable technical specifications.

7.4 CONTRACTOR'S SCHEDULE REQUIREMENTS

The contractor shall submit to the representative of the prime contractor, an A/E or consultant firm under contract to the IPRF with overall responsibility for the project, that will have responsibility for the day-to-day activities of the project (referred as the Engineer) and maintain a coordinated construction schedule for the work. Submission of the construction schedule will not relieve the contractor of overall responsibility for scheduling, sequencing, and coordinating the work to comply with the requirements of the contract.

The overall construction schedule for the project shall be a network diagram constructed in accordance with the Critical Path Method using Microsoft Project or other approved software or procedures. The schedule shall be submitted to the engineer at the pre-construction conference and shall provide the following information:

- Sequence of the work by staging milestones.
- Interdependent work activities and duration required to achieve milestones. The description and staging breakdown of the work activities for each milestone shall be complete and in accordance with the contract scope of work and subject to review by the engineer for conformance. An incomplete and/or deficient breakdown of the work activities shall be promptly corrected by the contractor.

- Work activity restraints - the contractor shall identify the work required during prior phases prior to commencement of the next phase (e.g., sensor installation, testing).
- Milestone dates and intermediate start and finish activity dates - Float shall be defined.
- Critical path (no float days) activities relevant to material procurement, delivery, and planned sequence of the work.
- Submittals (shop drawings, mix designs, and materials) and material delivery schedules. The contractor shall provide a description of submittal and submittal turnaround dates, and delivery dates for plant and construction equipment, essential construction components, and bulk construction materials that have been mutually coordinated with the milestones, and planned sequence of the work. The contractor shall use all data requirements and project control parameters in developing the schedule. The contractor shall provide for 2 weeks submittal turnaround time typically. Time for re-submittals shall be considered when providing time frame for submittals.

The construction schedule as assembled and organized shall be reviewed and approved jointly by the contractor and the engineer after any adjustments or amendments have been incorporated. **This document will, henceforth, become the schedule for the contractor's work and will be used to monitor progress, payment, and to forecast the work.**

The contractor will provide an update and analysis of the progress schedule on a monthly basis. The contractor submittals are as follows:

1. **Written Progress Report.** This report, submitted on the first of each month, shall address:
 - (a) Work in progress
 - (b) Percent of work activities complete
 - (c) Effects of actual completed work versus planned work; such as estimated time ahead or behind schedule
 - (d) Proposed action to bring a lagging schedule into line with the overall progress schedule
 - (e) Effects of changed material delivery dates on the overall progress schedule
 - (f) Work forecasts
 - (g) Natural and induced constraints
 - (h) Problems and work activities that require action by a contractor, engineer, and/or the owner
2. **Schedule Update.** This update shall be submitted on the first day of each month and supplement the written Progress Report.
3. **Materials Status Report Update.** Knowledge relevant to material status is essential for effective planning and execution of the work per the overall progress schedule and shall be provided via a periodically updated material status report. This report shall be submitted on the

first day of each month. This report shall include status of materials and equipment for all authorized work and changes in work.

7.5 SUBMITTALS AND SHOP DRAWINGS

Several requirements are cited for the preparation of submittals and shop drawings. It is pertinent that these documents are prepared according to the following guidelines:

1. Prior to fabrication and/or installation, the contractor shall submit in a timely fashion to the engineer for approval five copies of all applicable submittals or shop drawings as called for by the various Technical Specifications. The submittals shall be complete and detailed. If approved by the engineer, each of the submittals will be identified as having received such approval by being so stamped and dated.

The contractor shall make any corrections required by the engineer. Three copies of submittals will be retained by the engineer, and two will be returned to the contractor. The approval of the submittals by the engineer shall not be construed as a complete check, but will indicate only that the general method of construction and detailing is satisfactory. Approval of such submittals will not relieve the contractor of the responsibility for any error that may exist, as the contractor shall be ultimately responsible for the completed construction.

2. Submittals and shop drawings shall be submitted in a timely fashion, and in a logical sequence that is duly coordinated with the phasing of long lead time procurement and with fabrication and construction schedules.
3. Whenever the contractor's submittals or shop drawings contain any deviation from the Technical Requirements of the applicable contract drawings, maps, and specifications, the deviation shall be clearly identified on the drawing or submittal; and all submittals or drawings containing deviations must be accompanied by a Request for Deviation submitted in accordance with the provision in this division entitled "Deviations and Waivers."
4. The engineer will typically require a maximum of 2 weeks to review submittals and drawings for approval and return same to the contractor. Submittal marked "approved," "approved as noted," "returned for correction," "not approved," or "disapproved" shall be interpreted as follows:
 - a. Submittals or drawings marked "approved" authorize the contractor to proceed with work covered by such drawings.
 - b. Submittals or drawings marked "approved as noted" authorize the contractor to proceed with the work covered in accordance with the noted comments or corrections. The corrected submittals shall be resubmitted for approval.

- c. Submittals or drawings marked "returned for correction" require the contractor to make the necessary corrections and revisions and to resubmit corrected submittals for approval prior to proceeding with any work covered on the submittals. The engineer will examine and return such drawings normally within 1 week after receipt.
- d. Submittals or drawings marked "not approved" or "disapproved" indicate non-compliance with the contract requirements; resubmittal is required with the appropriate changes. No item of work requiring a submittal or shop drawing shall be accomplished until the drawings are "approved" or "approved as noted."

7.6 DRAWING INDEX

Two sets of Contract Drawings and Specifications will be furnished by the contractor without charge, except for any publications incorporated into the Technical Specifications by reference. Additional sets of Plans and Specifications will be available to the contractor at the cost of reproduction and assembly.

THIS PAGE INTENTIONALLY LEFT BLANK

8. CONSTRUCTION MATERIALS QC/QA PLAN AND SPECIFICATIONS

8.1 INTRODUCTION

As in any construction project, the most important factors are the types of materials used, control of these materials, and a sound construction plan to produce an acceptable end product. The construction plan and material specifications are introduced in this chapter, along with the QC/QA plan and specifications. The plans and specifications were prepared exclusively for the construction of unbonded concrete pavement overlays at the NAPTF indoor facility.

8.2 CONSTRUCTION MATERIALS SPECIFICATIONS

The specifications for construction materials are based on the FAA specifications in FAA Advisory Circular No. AC 150/5370-10A. However, some items were revised to accommodate special construction requirements and research-related issues for the construction of new PCC overlay pavement sections at the NAPTF. The materials to be included in the construction plan are shown in table 16. The base pavement consists of a 12-in crushed granular subbase overlaid by a 12-in-thick PCC slab. Slab dimensions will be 15 ft by 15 ft. Curing blankets will be used for curing the underlying concrete slabs, rather than a wet cure, to prevent the infiltration of water into the subbase layer. A bituminous filler will not be required to seal joints in the underlying concrete layer because a continuous bituminous interlayer will be placed on top of the base concrete. Different degrees of distress (i.e., cracking and spalling) will be simulated in these base pavement slabs. Joints will be saw cut to various depths in the underlying concrete pavement: partial (6-inch) and full (12-inch) depth, as indicated in the Plans.

The research will focus on the performance of unbonded concrete overlays. Therefore, a 2-in bituminous layer will first be placed on the base concrete pavement to serve as an interlayer between the base pavement and the concrete overlay. Finally, the concrete overlay will be placed on top of the bituminous interlayer. The overlay slabs will be 15 ft by 15 ft and 9 in thick. An aggressive 28-day wet cure will be required to cure the overlay to prevent shrinkage in the concrete slabs. The bituminous interlayer below the concrete overlay will serve to waterseal the underlying concrete. Joints will be saw cut to three different depths in the concrete overlay: regular (3-inch), partial (6-inch), and full (12-inch) depth, as indicated in the Plans. Bituminous shoulders will be constructed to 2.5 inches deep and 3 feet wide on either side of test pavement area. A 1-ft layer of crushed granular subbase and a 2-ft layer of local natural sand will be placed underneath the bituminous surface to provide support. Details on the pavement dimensions for both base pavement and the overlay slabs are shown in the Plans.

TABLE 16. CONSTRUCTION MATERIALS PLAN

PAVEMENT LAYER	MATERIAL DESIGNATION	DESCRIPTION	SPECIFICATION
Subbase	P-154	Granular, 100% crushed	FAA P-154M
Base Concrete	P-501	Unreinforced PCC	Revised FAA P-501M
Shoulder Surface	Bituminous Pavement	Typical highway HMA mix	NJ DOT Section 903/904
Shoulder Support	P-154	Granular, 100% crushed	FAA P-154M
Shoulder Backfill	Natural sand	Natural sand	NJ DOT Section 901.09
Interlayer	Bituminous Pavement	Typical highway HMA mix	NJ DOT Section 903/904
Concrete Overlay	P-501	Unreinforced PCC	Revised FAA P-501M

Most of the testing required on the construction materials includes standard quality control and materials tests. These tests are discussed in the next section and are detailed in appendix D for each material. However, some materials characterization testing will be conducted to provide additional descriptive data of the materials. These tests include the CBR and DCP tests on top of the subbase layer, sampling of subbase, subgrade, and PCC mixes, and FWD tests on the base concrete pavement and on concrete overlays.

Guidelines for construction techniques and activities relative to each pavement material are also outlined in appendix D. Activities such as forming joints, placing dowels, making saw cuts, and jack hammering of cracks to simulate spalling in the concrete pavements are outlined in the specifications. Because of the special nature of the NAPTF indoor construction site, joints may not form naturally within a desirable time period prior to placing the bituminous interlayer. Therefore, if half-cut joints in concrete pavement have not formed after 28 days, they should be induced by a seating trafficking. The seating trafficking should consist of two full wander cycles (i.e., 66 passes) at 20 kips per wheel and two full wander cycles at 30 kips per wheel.

To prepare the surface of the base concrete prior to placing the PCC overlay, special saw cuts and jack hammering will be performed on the base concrete slabs. For example, approximately 250 seating gear passes at a load of 20 kips per wheel (on a 4-wheel gear configuration) should be run on the underlying concrete pavement, prior to placement of the interlayer.

Dowels will be placed in the longitudinal joints, as indicated in the Plan drawings. A plan for curing, using a 28-day wet burlap cure and a curing compound, of the concrete pavements is also presented. Another activity in the construction plan is the painting of lines on the surface to delineate various test items, transitions, and centerlines on the pavement sections.

Using the materials as specified and following the proper construction plan will result in well-constructed pavements and yield successful pavement testing results.

8.3 QC/QA PLAN AND SPECIFICATIONS

To ensure proper construction, the contractor must perform QC testing both in the laboratory, at the material source (i.e., concrete plant), and on the project site at the NAPTF. Guidelines for quality control implementation are outlined in appendix E. The QC specifications are based on those developed by the FAA for the NAPTF with revisions to reflect special requirements for the new concrete overlay pavement construction.

Quality control testing constitutes most of the QC/QA plan and several tests are required for the various pavement layers. The QC testing plan developed for the FAA for construction of the original test pavements at the NAPTF can be applied to this project with some test additions and revisions. The QC/QA will be performed by a certified laboratory working as a subcontractor to the firm that has the overall responsibility for the entire project; it is assumed that this will be an A/E or consulting firm under contract to the IPRF.

Prior to construction of the base pavement, the subgrade materials should be characterized. The contractor will use the CBR and DCP tests for subgrade characterization and tests should be done in the 12 locations per subgrade, as shown in table 17. The CBR tests will be taken at four depth levels, every 6 inches down to a total of 2 ft, from the surface of the subgrade to obtain a CBR profile. The DCP tests should be performed down to a depth of 3 ft from the top into the subgrade.

The QC testing plan for the P-154M granular subbase is outlined in table 18. The test type, test standard, and test results are detailed along with sampling information, test location and frequency, and test control limits. Table 19 lists the QC tests necessary for the bituminous interlayer, and table 20 presents tests required for the P-501M materials (both base concrete and overlays). Most of the responsibility for QC lies on the QC program manager and the QC technicians, although some tests will be performed by the paving contractor or lab technicians.

TABLE 17. SUBGRADE CHARACTERIZATION: RECOMMENDED LOCATIONS FOR CBR AND DCP TESTING.

Location Number	Subgrade Type	Test Cell	x-coordinate (ft)	y-coordinate (ft)
1	Low Strength	L1N	30	15
2	Low Strength	L1S	30	-15
3	Low Strength	L2N	75	15
4	Low Strength	L2S	75	-15
5	Low Strength	L3N	135	15
6	Low Strength	L3S	135	-15
7	Low Strength	L4	210	15
8	Low Strength	L5	210	-15
9	Low Strength	L6	270	15
10	Low Strength	L7	270	-15
11	Medium Strength	M7N	345	15
12	Medium Strength	M7S	345	-15
13	Medium Strength	M4	375	15
14	Medium Strength	M5	375	-15
15	Medium Strength	M3N	450	15
16	Medium Strength	M3S	450	-15
17	Medium Strength	M2N	525	15
18	Medium Strength	M2S	525	-15
19	Medium Strength	M1N	585	15
20	Medium Strength	M1S	585	-15
21	High Strength	H1N	660	15
22	High Strength	H1S	660	-15
23	High Strength	H4	720	15
24	High Strength	H5	720	-15
25	High Strength	H3N	795	15
26	High Strength	H3S	795	-15
27	High Strength	H2N	870	15
28	High Strength	H2S	870	-15

TABLE 18. QUALITY CONTROL TESTING PLAN, ITEM P-154, SUBBASE COURSE

Test Type	Test Standard	Test Result	Sample Type	Sampling Location	Location of Test	Test Frequency	Responsibility	Control Requirements
Percent Fines and Sieve Analysis of Aggregate	ASTM C 117 and ASTM C 136	Particle size distribution	Bulk sample after compaction	Compacted lift	Laboratory	3 tests per 100 ft	QC Technician	3 in. (75.0 mm) JMF±4% No. 10 (2.0 mm) JMF±4% No. 40 (0.450 mm) JMF±4% No. 200 (0.075 mm) JMF±2%
Modified Compaction Effort	ASTM D 1557	Moisture-Density-Relationships	Stockpile Representative	Laboratory	Laboratory	1 set per subbase	Lab technician	Reference (target) moisture and density
Laboratory CBR	ASTM 1883	CBR – Unsoaked and Soaked	Stockpile Representative	Laboratory	Laboratory	1 set per subbase	Lab technician	Reference (target) CBR
Moisture Content and Density by Sand Cone or Nuclear Method	ASTM D 1556	In-situ moisture content and density	In-situ on compacted subbase	Top of compacted lift	On site	3 tests per 100ft	QC Technician	100% ±2% of max. density of lab compacted specimens; moisture content ±2% of optimum

TABLE 19. QUALITY CONTROL TESTING PLAN, NJ DOT SECTION 903, PLANT-MIXED BITUMINOUS PAVEMENT FOR INTERLAYER.

Test Type	Test Standard	Test Result	Sample Type	Sampling Location	Location of Test	Test Frequency	Responsibility	Control Requirements
Asphalt Content	NJ DOT Test Method B-5	Percent binder in bituminous paving mixture	Plant production from truck samples	From trucks at job site	Laboratory	Two random samples per 6000 sf	QC Technician	Consult specifications
Gradation of Extracted Aggregate	NJ DOT Test Method B-3 or AASHTO T 30	Particle size distribution of fine and coarse aggregates extracted from bituminous paving mixture	Plant production from truck samples	From trucks at job site	Laboratory	Two random samples per 6000 sf	QC Technician	Consult specifications
Laboratory Density	Asphalt Institute MS-2 Method 75-blow Marshall	Maximum Marshall density	Plant production from truck samples	From trucks at job site	Laboratory	Two random samples per 6000 sf	QC Technician	Not applicable
Maximum Specific Gravity of Mixture	AASHTO T 209	Specific gravity of bituminous mixture	Laboratory samples and plant production	From trucks at job site or laboratory prepared samples	Laboratory	Two samples per 6000 sf	QC Technician	Required for Marshall mixture analysis
Marshall Mixture Tests	Asphalt Institute MS-2 Method, 75-blow Marshall	Stability, flow, voids	Laboratory compacted specimens from plant production	From trucks at job site	Laboratory	Two samples per 6000 sf	QC Technician	Stability: JMF \pm 300 lbs Flow, JMF \pm 0.01 units Air voids total mix: JMF \pm 0.5%

TABLE 20. QUALITY CONTROL TESTING PLAN, ITEM P-501, PORTLAND CEMENT CONCRETE PAVEMENT

Test Type*	Test Standard	Test Result	Sample Type	Sampling Location	Location of Test	Test Frequency	Responsibility	Control Requirements
Sieve Analysis	ASTM C 117 and ASTM C 136	Particle size distribution	Bulk sample from stockpiles	Stockpiles	Laboratory	2 samples per 200 cu yd	QC Technician	Maximum Size JMF±4% No. 4 (4.75 mm) JMF±4% No. 10 (25.0 mm) JMF±3% No. 40 (0.450 mm) JMF±3% No. 80 (0.210 mm) JMF±2% No. 200 (0.075 mm) JMF±2%
Laboratory Determination of Moisture Content	ASTM D 2216, AASHTO T 265	Gravimetric moisture content of aggregate	Bulk sample from stockpiles	Stockpiles	Laboratory	2 samples per 200 cu yd	QC Technician	Per specifications
Slump of Hydraulic Cement Concrete	ASTM C 143	Slump of fresh concrete	Fresh concrete at job site	On site	Field	1 test per 75 cu yd	QC Technician	1 to 2 in. for side form concrete OR 1/2 to 1-1/2 in. for vibrated slip-formed concrete
Air Content of Freshly Mixed Concrete by the Pressure Method	ASTM C 231	Air content in freshly mixed concrete	Fresh concrete at job site	On site	Field	1 test per each 75 cu yd production	QC Technician	4.5 ± 1.2%
Water Content of Freshly Mixed Concrete	AASHTO TP-23	Water content in freshly mixed concrete	Fresh concrete at job site	On site	Laboratory	1 test per 75 cu yd	QC Technician	Per specifications
Flexural Strength	ASTM C 78	28-day flexural strength	Field cured for 28 days	On site	Laboratory	3 beams per 200 cu yd	QC Technician	All specimens must have strength within 10 percent of the design strength

TABLE 20. QUALITY CONTROL TESTING PLAN, ITEM P-501, PORTLAND CEMENT CONCRETE PAVEMENT (CONT.).

Test Type*	Test Standard	Test Result	Sample Type	Sampling Location	Location of Test	Test Frequency	Responsibility	Control Requirements
Pavement Thickness	ASTM C 174	Portland cement concrete pavement thickness	Field cores	On site	Field	5 random cores per cell	Concrete paving subcontractor	All cores must be within $\pm 1/4$ inch of design slab thickness
Shrinkage Test	ASTM C 157	Differential shrinkage in PCC	Fresh concrete at job site	On site	Laboratory	1 test per 200 cu yd	QC Technician	Limiting shrinkage of 0.04%

* Note: Tests apply for both underlying concrete pavement and concrete overlay

Because of the special indoor site conditions at the NAPTF, it is crucial to the success of the project that the contractor exercise careful quality control.

8.4 SPECIAL CONDITIONS FOR QC/QA

This section contains special conditions requirements for the reconstruction of concrete overlay test pavements at the NAPTF. The special conditions shall apply to each contract that is awarded for construction of various components of the new concrete overlay project.

The intent of these Special Conditions is to augment and/or supplement the contract's General Provisions, Technical Specifications, and Plans. Where any discrepancies exist between the Special Conditions and the General Provisions, Technical Specifications, or Plans, the Special Conditions shall take precedence.

8.4.1 Inspection and Testing

Inspection and testing are required both for contractor QC and acceptance of materials and construction by the Engineer (the representative of the prime contractor, an A/E or consultant firm under contract to the IPRF with overall responsibility for the project, that will have responsibility for the day-to-day activities of the project). Inspection and testing activities shall take place in accordance with the technical specifications and the QC Plan, and shall represent a particular lot of material or work period, as applicable. Work will not be allowed to proceed to the next lot or work period, as applicable, until quality control and acceptance tests, and/or inspection reports required by the QC Plan, have been recorded and approved.

In addition to the QC tests, the FAA will conduct tests on subgrade and pavement materials to support their research.

8.4.2 Protection of Existing Layers During Construction

The contractor shall prepare a plan for hauling, handling, and delivery of all materials to be placed in the NAPTF; no materials will be moved into the NAPTF until this plan has been approved by the engineer and the FAA. In addition, it is recommended that the contractor wait 7 days before driving concrete trucks over new slabs during construction.

8.4.3 Drawing Index

A complete set of Plans covering the contract shall be made available to each contractor. The drawing list with the particular project corresponding to each Plan is as follows:

<u>Sheet No.</u>	<u>Description</u>
1	As-built Plan and Profile
2	Underlying Pavement Joints
3	PCC Overlay Joints
4	Rigid Pavement Cross-Sections
<u>Sheet No.</u>	<u>Description</u>

8.4.4 Errors and Omissions

Should any tenderer find discrepancies, duplications, or omissions in the documents, or have doubt as to the meaning expressed by the documents, he/she shall make inquiries in writing at once to the engineer. Any changes, corrections, or clarifications to the documents deemed necessary by the engineer should be issued with a written addendum accordingly. Addenda thus issued will be a part of the contract documents. No oral, telephone, or letter instructions will be considered as having effect upon the contract documents; addenda only shall constitute a change to them. Tenderers are urged to make early examinations of contract documents and make inquiries about them, if necessary, to allow the engineer ample time to analyze such inquiries and to issue addenda when necessary, even though prices may not be determined until late in the tendering period.

The contractor shall notify the engineer in writing regarding any necessary items which may have been omitted from the Specifications or Plans or both, and any irregularities, discrepancies, or duplications between Plans and Specifications according to the evident intent. In case of such errors or omissions, the contractor shall not proceed with the work in uncertainty but shall consult the engineer regarding proper intent. The engineer will then issue clarification or make revisions accordingly.

8.4.5 QC/QA Testing

The contractor shall perform QC testing as indicated in appendix E. Quality control tests to be performed for characterizing the subgrade and for each material type (granular subbase, bituminous pavement, portland cement concrete) are presented in tables 17 through 20.

8.4.6 Auxiliary Sampling and Testing

The contractor shall take samples for special research tests as instructed by the engineer.

8.4.7 Final Acceptance

The contractor shall perform and complete all work according to the contract documents without fault or defect of any kind. When this condition of completion exists, the contractor shall request final inspection and the engineer will make the inspection promptly thereafter, recording any incomplete or defective work discovered on a punch list. The contractor shall then remedy each punch list item and make the work conform to the contract documents in every instance. The contractor shall then request inspection of all punch list items.

9. DATA COLLECTION PLAN

9.1 INTRODUCTION

This section presents plans for data collection before, during, and after accelerated load testing of unbonded PCC overlays at the NAPTF. This includes the following:

Data collection before accelerated load testing:

- Subgrade testing prior to construction of base layer
- Base testing after base placement
- Existing PCC layer testing
- Lab testing of material properties
- Nondestructive testing
- Separation layer material testing
- PCC overlay testing
- Nondestructive testing

Data collection during accelerated load testing:

- Accelerated load testing with aircraft gear
- Nondestructive testing
- Surface profile measurement

Data collection after accelerated load testing:

- Nondestructive testing
- Post-traffic evaluation of the interlayer and existing slab

These data will be collected in addition to the substantial data collection efforts that will be performed as part of construction QA/QC. The details for each test item are presented below.

9.2 DATA COLLECTION BEFORE FULL-SCALE TESTING

9.2.1 Subgrade Testing Prior to Construction of Base Layer

CBR and DCP testing will be conducted to obtain more accurate information about subgrade strength and to ensure uniformity of subgrade support within each test section.

These tests should be conducted at a minimum of 28 locations. Table 21 presents the recommended locations of CBR and DCP tests using the x-y coordinate system described in chapter 4.

TABLE 21. RECOMMENDED LOCATIONS FOR CBR AND DCP TESTING.

Location Number	Subgrade Type	Test Cell	x-coordinate, ft	y-coordinate, ft
1	Low Strength	L1N	30	15
2	Low Strength	L1S	30	-15
3	Low Strength	L2N	75	15
4	Low Strength	L2S	75	-15
5	Low Strength	L3N	135	15
6	Low Strength	L3S	135	-15
7	Low Strength	L4	210	15
8	Low Strength	L5	210	-15
9	Low Strength	L6	270	15
10	Low Strength	L7	270	-15
11	Medium Strength	M7N	345	15
12	Medium Strength	M7S	345	-15
13	Medium Strength	M4	375	15
14	Medium Strength	M5	375	-15
15	Medium Strength	M3N	450	15
16	Medium Strength	M3S	450	-15
17	Medium Strength	M2N	525	15
18	Medium Strength	M2S	525	-15
19	Medium Strength	M1N	585	15
20	Medium Strength	M1S	585	-15
21	High Strength	H1N	660	15
22	High Strength	H1S	660	-15
23	High Strength	M4	720	15
24	High Strength	M5	720	-15
25	High Strength	M3N	795	15
26	High Strength	M3S	795	-15
27	High Strength	M2N	870	15
28	High Strength	M2S	870	-15

9.2.2 Base Testing Prior to Construction of Base Layer

Chapter 8 and appendix D present information about QA/QC tests for the base layer. No additional testing is deemed necessary for the base layer.

9.2.3 Existing Pavement Testing

Extensive information about the existing PCC pavement properties, behavior, and performance under heavy gear loading should be collected at the NAPTF. The recommended tests include the following:

- PCC material properties
- HWD testing
- Static testing
- Slow rolling testing
- Low load traffic response testing

9.2.4 PCC Material Properties

Extensive information about the existing PCC pavement properties should be collected during and after layer placement, including the following:

- PCC overlay material properties
- Pavement response under HWD loading
- Pavement response under static loads
- Pavement response under slow rolling loads
- Pavement response under low load-level traffic

PCC material properties should be tested according to the corresponding ASTM tests. Data should be collected after 7 days, 14 days, 28 days, and 90 days. At least three specimens should be used for each test.

9.2.5 HWD Testing

During the testing periods in 1999 through 2002 at the NAPTF, heavy weight deflectometer (HWD) deflection testing was conducted routinely on asphalt and concrete pavement sections. The objectives of that testing were to determine uniformity of the test pavement structure and to measure pavement responses as traffic testing proceeds. These tests provide important information about structural characteristics of the subject pavements. Many airport authorities collect deflection data on their pavement systems for pavement management, rehabilitation evaluation, and forensic evaluation purposes, and they consider deflection data as important as pavement condition and distress data.

Extensive HWD testing is also recommended for the unbonded overlay testing program. One series of tests should be conducted after construction and initial trafficking of the existing PCC pavement but prior to placement of the asphalt interlayer and the PCC overlay to accomplish the following:

- Verify the uniformity of the existing pavement construction, particularly PCC thickness and subgrade strength.
- Determine the effective layer parameters and the joints/cracks transfer efficiency.
- Investigate the effect of temperature on the pavement responses.
- Enable comparison with the corresponding PCC overlay deflections after the overlay is placed.

A typical testing program is recommended for the HWD testing, which includes basin testing (center loading) and load-transfer testing across longitudinal and transverse joints.

The typical HWD configuration used at NAPTF consists of a 12-in diameter load plate and seven sensors placed as shown in figure 76. One sensor is placed at the center of the load plate, another is placed 12 inches in front of the load plate, and the remaining sensors are located behind the load plate at 12-in intervals. At each testing location, four HWD drops are made: a 36,000-lb seating loading and three drops at 12,000, 24,000, and 36,000 lb. Deflections from seating drops are not used in the analysis.

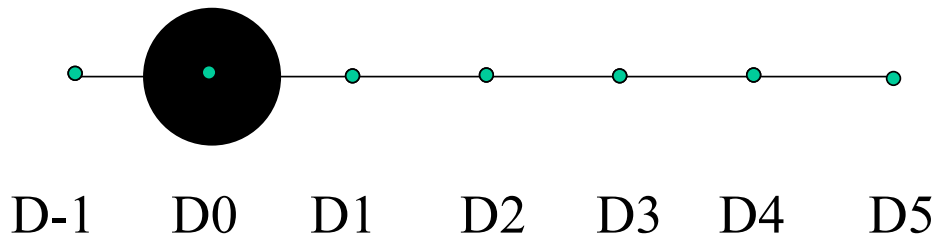


FIGURE 76. FAA HWD SENSOR CONFIGURATION

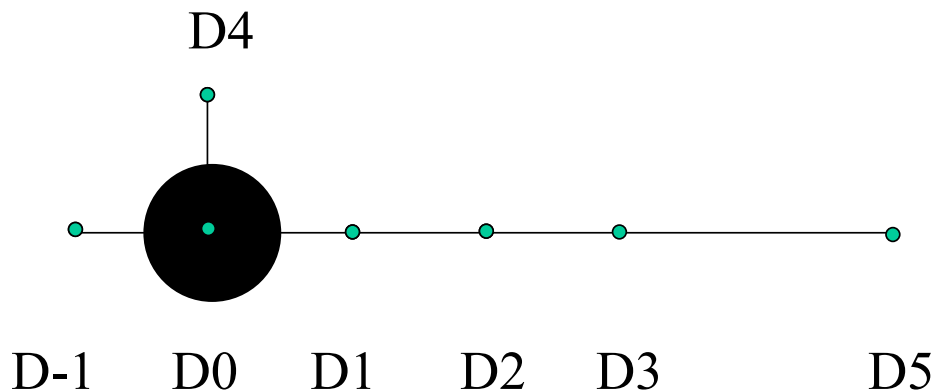


FIGURE 77. PROPOSED SENSOR CONFIGURATION AT NAPTF

A procedure similar to the FAA HWD data collection procedure is recommended for testing of the existing pavement. However, a slight modification in the sensor configuration is recommended to allow load transfer testing across longitudinal joints. This involves either adding the side sensor or moving the sensor located 48 in from the load plate to the side, as shown in figure 77. The side sensor should be placed 12 in away from the load plate center in a direction perpendicular to all other sensors. This sensor configuration will allow determination of the load transfer efficiency of longitudinal joints without requiring the HWD to move in a transverse direction.

The suggested locations for FWD testing are listed in table 23 at the end of this chapter. The testing program includes measurements in the following locations:

- Slab center
- Transverse joint/crack (for load transfer).
- Longitudinal joint/crack (for load transfer).

Some of the tests will be conducted directly above strain gauges in the existing pavement. At those locations, corresponding strain measurements will be also recorded.

9.2.6 Static Load Test

Static testing involves placing the gear loads directly over strain gauges and measuring the pavement response to accomplish the following:

- Measure existing pavement responses under precise control of load magnitude and position.
- Compare pavement responses under static and moving loads.
- Compare pavement responses under static and HWD loads.
- Compare the measured and computed responses.
- Compare the corresponding responses before and after the placement of the PCC overlay.
- Verify that the sensors installed in the existing pavement are functioning properly.

Static testing should be performed three times a day (in the morning, at noon, and in the afternoon). The tire pressure equal should be equal to 200 psi. The following magnitudes of the applied load should be used:

- 10,000 lb per wheel
- 20,000 lb per wheel
- 30,000 lb per wheel

However, the stresses generated by the load should not exceed 50 percent of the PCC modulus of rupture.

The following responses should be measured:

- PCC horizontal strain at the top surface
- PCC horizontal strain at the bottom surface

9.2.7 Slow Rolling Load Test

The slow rolling tests should be performed with the test vehicle moving at a speed of 0.5 feet/second over the slabs instrumented with strain gauges. Like static testing, the slow rolling testing should be performed three times a day (in the morning, at noon, and in the afternoon) and the following magnitudes of the applied load should be used:

- 10,000 lb per wheel

- 20,000 lb per wheel
- 30,000 lb per wheel

Also, the stresses generated by the load should not exceed 50 percent of the PCC modulus of rupture. Tire pressure equal to 200 psi will be used in all cases.

These tests have similar objectives as the static tests:

- Measure existing pavement response under precise control of load magnitude and position
- Compare pavement responses under static and moving loads.
- Compare slow-rolling load responses with the responses under HWD loads.
- Compare the measured and computed responses.
- Compare the corresponding responses before and after the placement of the PCC overlay
- Verify that the sensors installed in the existing pavement are functioning properly.

The following responses should be measured:

- PCC horizontal strain at the top surface
- PCC horizontal strain at the bottom surface

9.2.8 Traffic Load Test

At least four complete traffic wander cycles should be applied on the existing pavement prior to the placement of the separator layer, two complete cycles each at each of two load levels (20,000 lb and 30,000 lb load per wheel). The tire pressure will be equal to 200 psi. The purpose of this loading is to provide a “seating loading” (i.e., to provide some initial deformations in the existing pavement and wearing of the joint aggregate interlock). The traffic wander pattern used at NAPTF is shown in figure 78. A complete traffic wander cycle consists of 66 load passes distributed among 9 tracks. The loading tracks are typically spaced 10 in apart. For testing on both the existing pavement and the overlay, the carriage position that places the outer edge of the outer wheels directly on the outer edge of the test slabs should be selected as the mean wheel location (figure 79). Additional discussion on the positioning of the wheel tracks is given in the *Accelerated Load Testing* section.

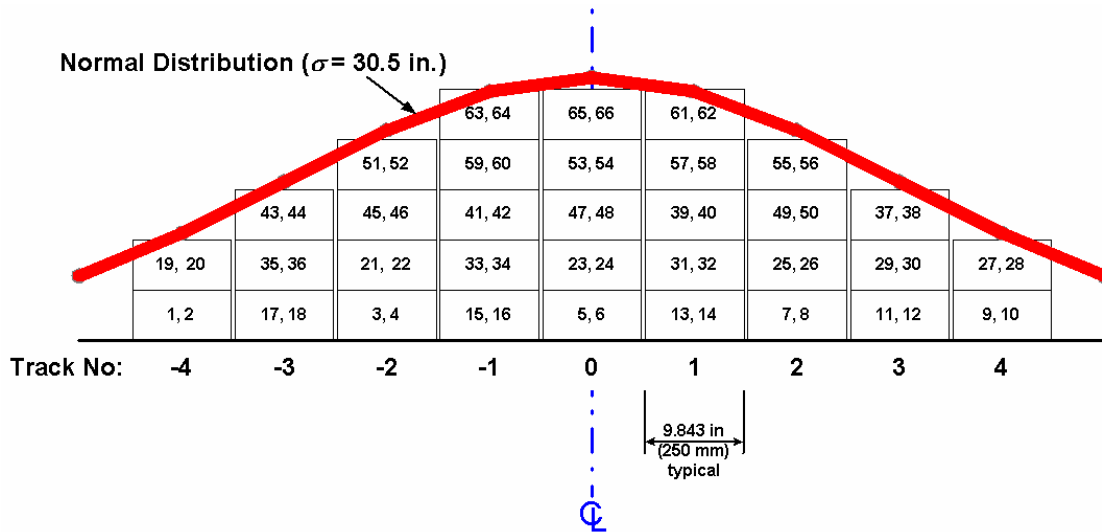


FIGURE 78. TYPICAL TRAFFIC WANDER PATTERN USED AT NAPTF

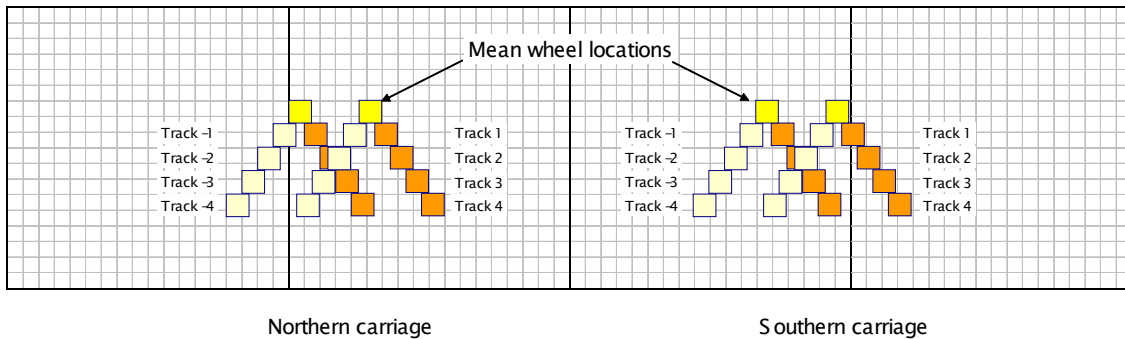


FIGURE 79. RECOMMENDED POSITIONS OF LOADING TRACKS

The suggested loading plan for the traffic testing on existing pavement consists of the following:

- Dual tandem gears (747 configuration) for both northern and southern gear carriages.
- Wheel loads of 20,000 lb per wheel and 30,000 lb per wheel.
- Tire pressures of 200 psi.
- Loading speed of 5 mph.
- Loading sequence as shown in figure 78 for two complete cycles for each of the two load levels.

Strains will be recorded during this testing for the following purposes:

- Compare the responses under static and moving loads.

- Compare the responses under moving gear loads with those under HWD loads.
- Compare the measured and computed responses
- Compare the corresponding responses before and after the placement of the PCC overlay.

9.2.9 Interlayer Properties

The AC interlayer properties will be tested as a part of construction QA/QC testing. No additional tests are recommended for the AC interlayer.

9.2.10 PCC Overlay Testing

Extensive information about the PCC overlay properties and responses needs to be collected prior to the initiation of accelerated load testing, including the following:

- PCC overlay material properties
- Pavement response under HWD loading
- Pavement response under static loads
- Pavement response under slow rolling loads
- Pavement response under low load-level traffic

Since PCC overlay curling and warping may significantly affect structural responses, the temperature and moisture profile through the overlay will be monitored continuously over the entire duration of full-scale testing.

9.2.11 PCC Overlay Material Properties Testing

The same material properties that were recommended for collection for the existing pavement should be collected for the PCC overlay. The information to be collected includes the following:

- PCC compressive strength (ASTM C39 test)
- PCC flexural strength (ASTM C78 test)
- PCC modulus of elasticity and Poisson's ratio (ASTM C469 test)
- PCC coefficient of thermal expansion (FHWA procedure)
- PCC ultimate shrinkage (ASTM STP 205)

The material testing for PCC properties should be conducted according to the corresponding ASTM tests. The PCC strength and modulus tests should be conducted at PCC age 7 days, 14 days, 28 days, and 90 days. At least three specimens should be used for each test.

9.2.12 Surface Profile Measurement

The surface profile of the PCC overlay should be measured using the Dipstick 28 days after construction to obtain reference data that can be used to determine any changes in the amount of permanent warping and curling of the overlay slabs over time. The exact time of measurement should be recorded so that the temperature and moisture conditions at that time can be determined. The measurement should be made under at least two different temperature conditions, preferably at the two temperature extremes that occur on the days of measurement (e.g., very early in the morning when the most negative temperature gradients occur in the slabs, and midday for the most positive temperature gradients). The range of curling deflections under the two temperature regimes will provide information about the actual support condition under the overlay slabs.

The profile measurements should be taken from the following locations:

- Along the longitudinal joint selected as the mean wheel path on each side.
- Across the approach and leave transverse joints of the middle slab in each test section.

9.2.13 HWD Testing

Extensive HWD testing of the PCC overlay should be performed after construction, during the trafficking, and after trafficking completion. The recommended testing prior to trafficking includes the following:

- General tests – the majority of the overlay slabs should be tested at the slab interior, edges, and corners.
- Specific tests – more comprehensive testing should be conducted on selected slabs.

9.2.13.1 General tests

General tests should be performed on all overlay slabs except transition slabs (slabs in rows 4, 8, 12, 13, 21, 22, 28,29, 33, 37, 41, 42, 46, 50, 51, 55, 56, and 60). For each slab, HWD deflections will be measured at slab center, transverse edge, longitudinal edge, and corner. These tests should be performed 28 days after construction and after completion of the accelerated load testing to accomplish the following:

- Verify the uniformity of the existing pavement construction, particularly PCC thickness and subgrade strength.
- Determine the effective overlay parameters and the joints/cracks transfer efficiency in the beginning and at the end of the overlay life.

Figure 80 presents the recommended testing pattern for slabs A1, B1, C1, and D1. The same testing pattern should be used for all other slabs in general testing. Figure 80 shows that the testing of 24 locations is recommended for the four slabs. The total number of locations for all

subgrades is 1,008. The anticipated duration of this testing is 5 days, based on typical production rates for HWD testing.

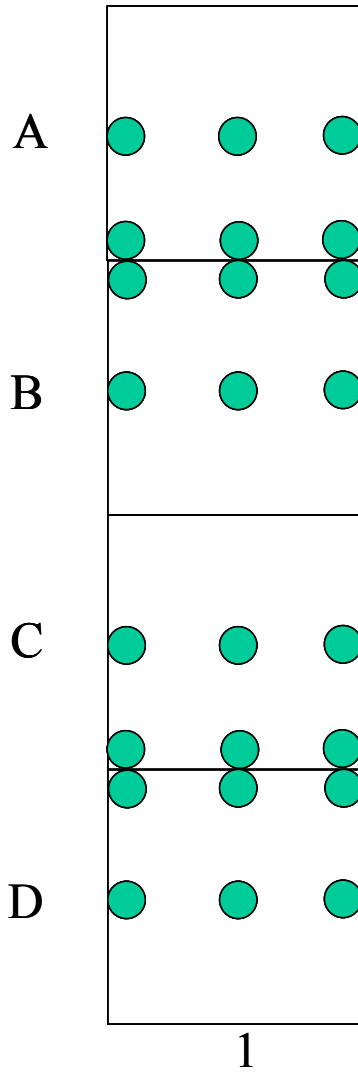


FIGURE 80. TESTING PATTERN FOR GENERAL OVERLAY HWD TESTING

9.2.13.2 Special Tests

Several slabs should be tested along and across a slab in small steps (1 ft) to check the uniformity of pavement responses and to investigate whether the proximity to underlying cracks affects the overlay deflections. The following slabs are recommended for special tests: B2, B5, B10, and B15. This testing should be performed after the completing the general HWD testing.

9.2.13.3 Static Load Test

Similar to the testing conducted over the existing pavement (prior to the overlay placement), static testing should be performed on the PCC overlay on top of strain gages for similar reasons:

- Measure existing pavement responses under precise control of load magnitude and position
- Compare pavement responses under static and moving loads.
- Compare pavement responses under static and HWD loads.
- Compare the measured and computed responses.
- Compare the corresponding responses before and after the placement of PCC overlay.
- Verify that the sensors installed in the existing pavement are functioning properly.
- Study the effect of wheel interaction on stresses from static gear loading by comparing dual tandem and dual tridem stresses.

Static testing should be performed three times a day (in the morning, at noon, and in the afternoon). The following magnitudes of the applied load should be used:

- 10,000 lb per wheel
- 20,000 lb per wheel
- 30,000 lb per wheel

However, the stresses generated by the load should not exceed 50 percent of the PCC modulus of rupture.

The following responses should be measured:

- PCC horizontal strain at the top surface
- PCC horizontal strain at the bottom surface
- Corner deflections

9.2.13.4 Slow Rolling Load Tests

The slow rolling load tests should be performed with the test vehicle moving at a speed of 0.5 feet/second. These tests have objectives similar to those of the static tests:

- Measure existing pavement responses under precise control of load magnitude and position.
- Compare pavement responses under static and moving loads.
- Compare pavement responses under slow rolling and HWD loads.
- Compare the measured and computed responses.
- Compare the corresponding responses before and after the placement of PCC overlay
- Verify that the sensors installed in the existing pavement are functioning properly.

Study the effect of wheel interaction on stresses from slow rolling gear loading by comparing dual tandem and dual tridem stresses.

The following responses should be measured:

- PCC horizontal strain at the top surface
- PCC horizontal strain at the mid-depth
- PCC horizontal strain at the bottom surface
- Corner deflections using MDD.

9.3 DATA COLLECTION DURING ACCELERATED LOAD TESTING

9.3.1 Traffic testing

Accelerated trafficking of the overlay should be conducted in three stages, as follows:

- Elastic response loading
- Main loading
- Overloading

During the first stage, four complete traffic wander cycles should be applied using the actual gears that will be used in the accelerated load testing, two complete cycles each at two different load levels. A complete wander cycle consists of 66 load passes distributed over 9 wheel tracks, as shown in figure 78. The recommended loads for this testing are gear loadings from 10,000 lb per wheel to 30,000 lb per wheel (tire pressures equal to 200 psi) moving at 5 mph. The main objective of this loading is to provide elastic response measurements. That information may be used to accomplish the following:

- Compare the responses under static and moving loads.
- Compare the responses under traffic loading with those under HWD loads.
- Compare the measured and computed responses.
- Compare the corresponding responses before and after the placement of PCC overlay.
- Study the effect of wheel interaction on stresses from high speed gear loading by comparing dual tandem and dual tridem stresses.

The main traffic loading consists of up to 750 complete traffic wander cycles (49,500 load passes) applied with aircraft gears at the load level of 45,000 lbs for each wheel. The sections that do not fail during these loading cycles will be trafficked by gear loading at 55,000 lbs per wheel.

The testing program developed in this study takes advantage of the ability of the NAPTF testing machine to simulate different gear loading and to change the gear configuration during testing. Two loading carriages designated as "Carriage 1" (north) and "Carriage 2" (south) will be used. "Carriage 1" will be configured as a dual tandem gear, and its configuration will not be changed during the testing. "Carriage 2" will change its configuration several times during a single pass

from a tridem gear to a dual tandem gear and back. Table 22 presents the configuration of "Carriage 1" for different slabs (test sections).

TABLE 22. CONFIGURATION OF "CARRIAGE 2" DURING ACCELERATED LOAD TESTING

Slabs	Configuration
1 –11	Dual tridem
12	Transition
13-28	Dual tandem
29	Transition
30- 55	Dual tridem
56	Transition
57-60	Dual tandem

Simulation of traffic wander in accelerated testing is important to ensure that the effects of traffic wander on pavement performance are reflected in the test results. Studies have shown that the traffic wander can be assumed normally distributed, and the loading scheme used at NAPTF was designed to approximate normal distribution. Figure 78 shows the typical wander pattern used at NAPTF. The gear loads are applied over nine discrete traffic paths (tracks), and the number of loads applied in each track is selected to approximate normal distribution with typical standard deviation for channelized traffic (30.5 in). The traffic paths are spaced 10 in apart, which provides partial overlapping of tire footprints that adequately simulates the continuous distribution experienced in the field. The load frequency in each track resulting from this loading scheme is shown in figure 81. Because stresses in concrete pavements are very sensitive to the load position, accurate load placement and accounting of the load positions is very important.

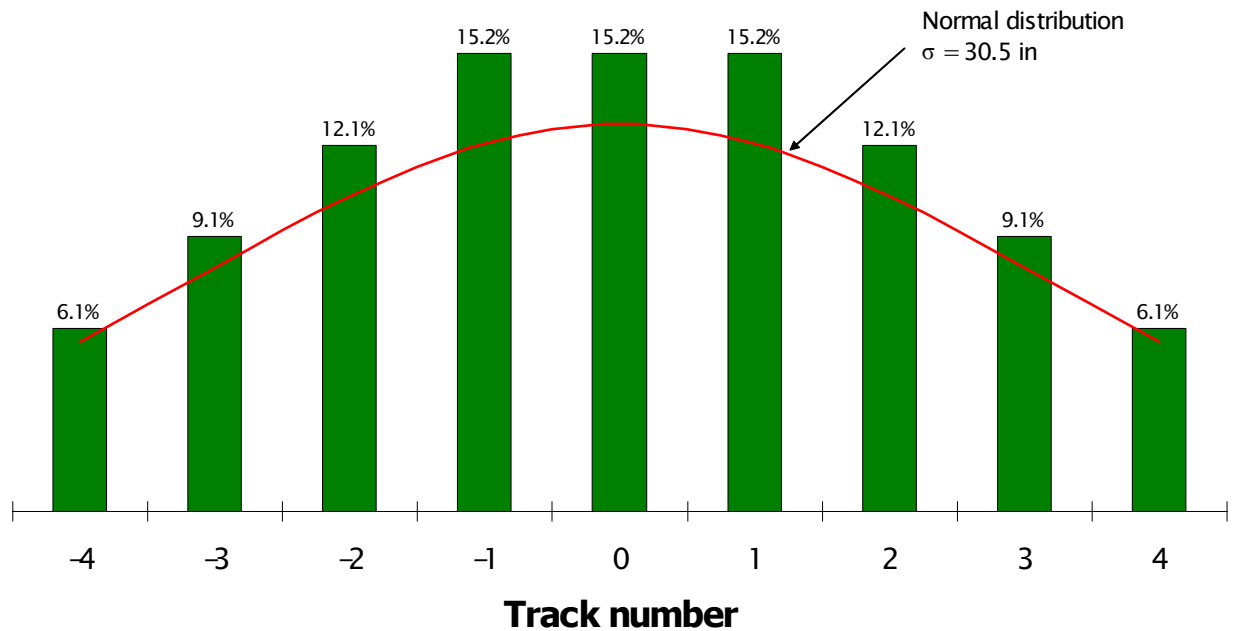


FIGURE 81. LOAD FREQUENCY IN EACH TRACK DUE TO THE LOADING PATTERN USED AT NAPTF

The critical stresses in concrete pavements are very sensitive to the load position. Maximum stresses occur when the loads are placed on or very close to a joint, and the stresses drop off rapidly as the load is moved away from the joint. The critical load positions and the damage locations for longitudinal and transverse cracking are shown in figure 82.

The recommended load placements for dual tandem (B747) and dual tridem (B777) aircraft gears are shown in figure 83. The mean wheel location is the loading condition that places the outside edge of the outer wheel on the doweled longitudinal joint on each side (as shown in figure 83). As in previous tests, 10-in steps are used for traffic paths. This is a highly efficient loading scheme in which about 80 percent of load passes produce a critical coverage for either longitudinal or transverse cracking. Loading in some tracks (e.g., Track -1 for B747 gear) produces a critical coverage for both transverse and longitudinal cracking. The pass to coverage ratio for the recommended loading scheme is about 2.7 for longitudinal-edge loading and about 2.0 for transverse-edge loading.

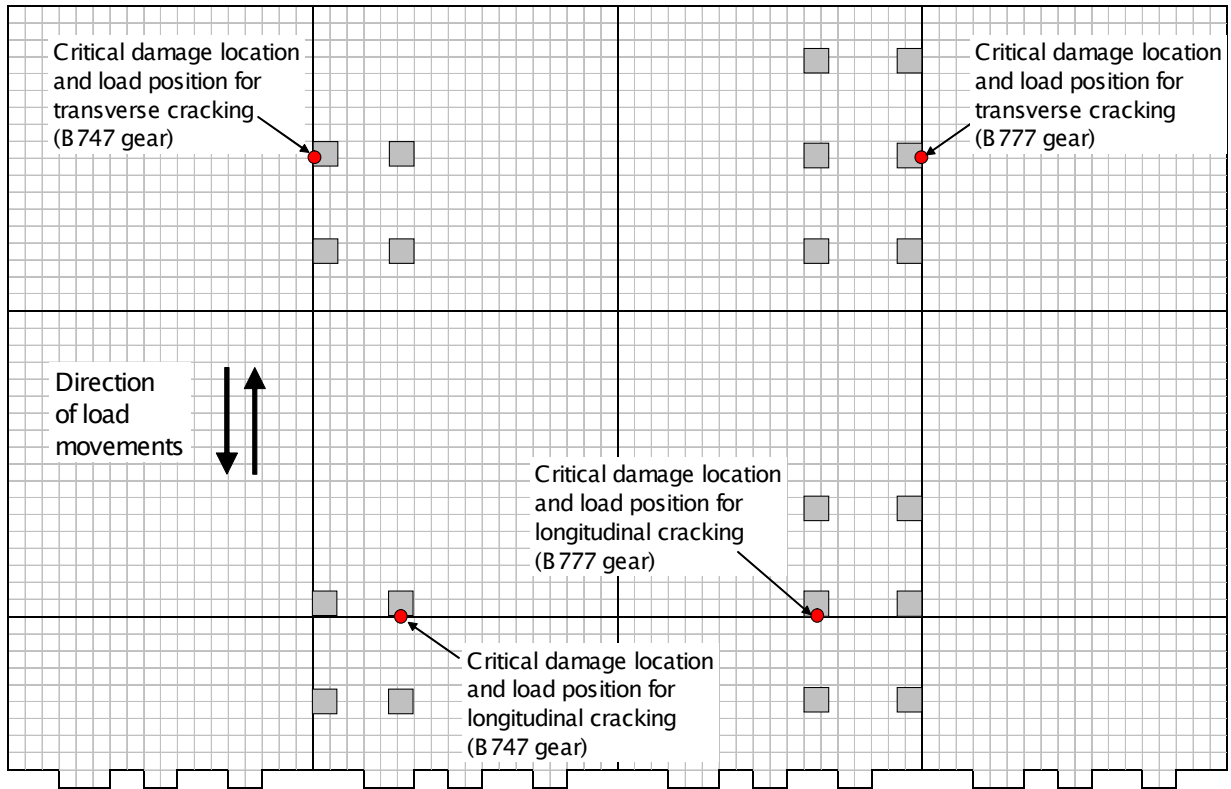


FIGURE 82. CRITICAL LOAD POSITIONS AND DAMAGE LOCATIONS

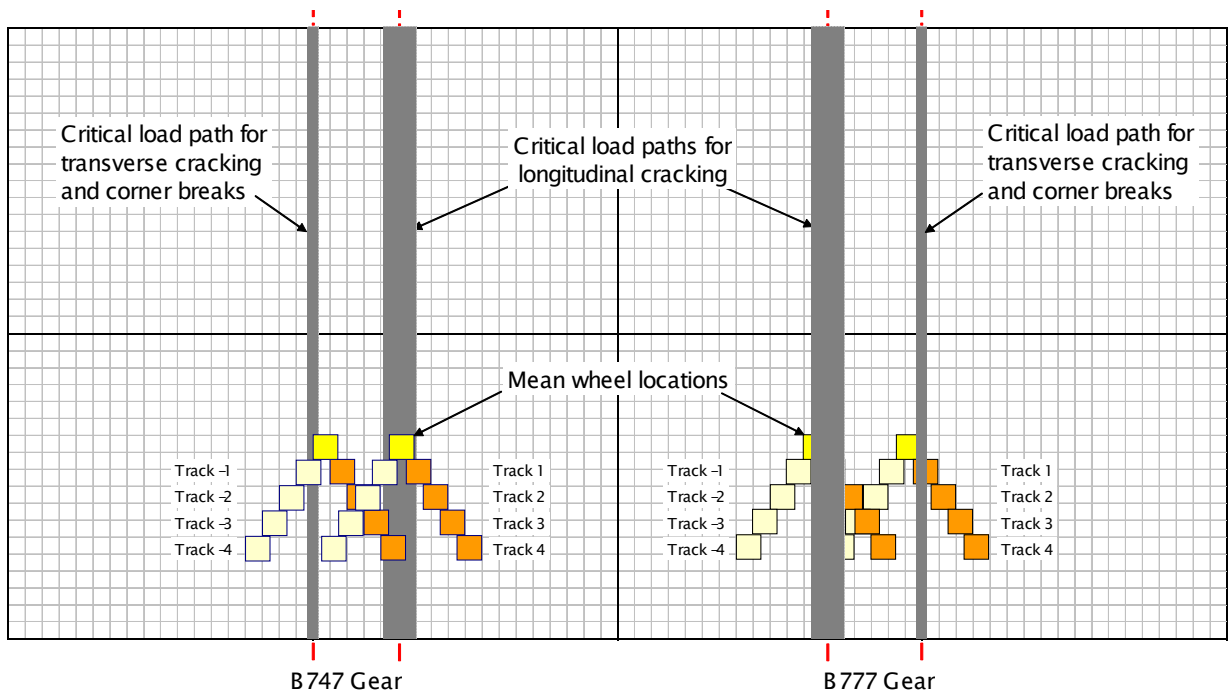


FIGURE 83. RECOMMENDED LOAD PATHS

After every 990 load passes, the overlay condition should be evaluated and all cracks and their condition recorded. The PCI should be calculated at this time also. It will provide useful data, cheap to collect and can be done quickly.

9.3.2 HWD Testing

Periodic HWD testing is recommended during accelerated load testing to detect any changes in the support condition over time and to obtain additional data that can be used to verify the data collected from the instrumentation. The periodic HWD testing should be conducted once a month or after every 10,000 load passes at the interior, edges, and corners of the selected slabs at two separate times of the day. The slabs recommended for periodic testing include the following: B2, B6, B10, B15, B18, B20, B23, B26, B31, B35, B39, B44, B48, B53, B58, C2, C6, C15, C18, C20, C23, C26, C31, C35, C39, C44, C48, C53, and C58. Figure 84 presents the testing pattern for slabs B2 and C2.

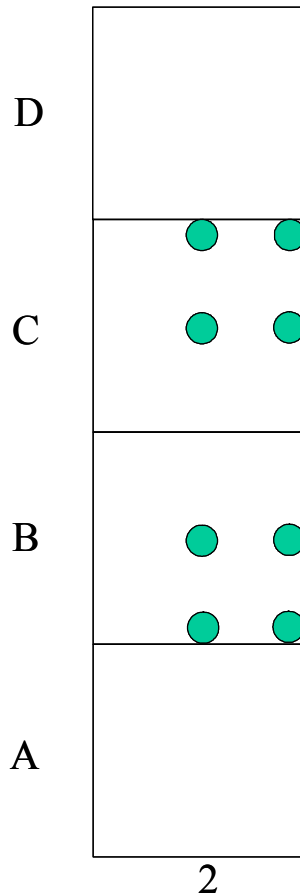


FIGURE 84. TESTING PATTERN FOR MONTHLY HWD TESTING ON THE OVERLAY

9.3.3 Profile Measurement

Profile measurements should be taken periodically using the Dipstick to monitor any changes in permanent warping and curling. The measurements should be taken at the exact same location as the reference measurements taken after the overlay construction:

- Along the longitudinal joint selected as the mean wheel path on each side.
- Along the longitudinal joint selected as the mean wheel path on each side.

The exact time of measurement should be recorded so that the temperature and moisture conditions at that time can be determined. The measurement should be made under at least two different temperature conditions, preferably at the two temperature extremes that occur on the days of measurement (e.g., very early in the morning when the most negative temperature gradients occur in the slabs, and midday for the most positive temperature gradients).

9.4 DATA COLLECTION AFTER ACCELERATED LOAD TESTING

9.4.1 HWD Testing

General tests should be performed on all overlay slabs except transition slabs (slabs in rows 4, 8, 12, 13, 21, 22, 28, 29, 33, 37, 41, 42, 46, 50, 51, 55, 56, and 60). For each slab, HWD deflections will be measured at slab center, transverse edge, longitudinal edge, and corner. These tests should be performed 28 days after construction and after completion of the accelerated load testing to accomplish the following:

- Verify the uniformity of the existing pavement construction, particularly PCC thickness and subgrade strength.
- Determine the effective overlay parameters and the joints/cracks transfer efficiency in the beginning and at the end of the overlay life.

Figure 80 presents the recommended testing pattern for slabs A1, B1, B3, and B4. The same testing pattern should be used for all other slabs in general testing. Figure 80 shows that the testing of 24 locations is recommended for the four slabs. The total number of locations for all subgrades is 1,008. The anticipated duration of this testing is 5 days, based on typical production rate for HWD testing.

9.4.2 Post-traffic testing evaluation

After the completion of the traffic testing, selected overlay slabs should be removed to evaluate the condition of the underlying pavement. It is preferable to remove the most damaged overlay slabs. At a minimum, at least one slab per test cell should be removed. The condition of the underlying AC interlayer beneath those slabs should also be evaluated. A visual survey should be sufficient to detect presence of cracks and/or non-uniform deformations, especially under cracks and joint in the overlay. After the visual evaluation, the interlayer should be removed for

the evaluation of the condition of the existing pavement. The underlying pavement should be surveyed visually to detect the presence of any new cracks in the underlying pavement.

TABLE 23. RECOMMENDED LOCATIONS FOR HWD TESTING

Test Cell	Load Position	x-coordinate, ft	y-coordinate, ft
L2N	Center	67.5	22.5
L2N	trans. Edge	74.5	22.5
L2N	trans. Edge	75.5	22.5
L2N	Center	82.5	22.5
L2N	trans. Edge	89.5	22.5
L2N	trans. Edge	90.5	22.5
L2N	Center	97.5	22.5
L2N	trans. Edge	104.5	22.5
L2N	trans. Edge	105.5	22.5
L6	Center	112.5	22.5
L6	trans. Edge	119.5	22.5
L6	trans. Edge	120.5	22.5
L6	Center	127.5	22.5
L6	trans. Edge	134.5	22.5
L6	trans. Edge	135.5	22.5
L6	Center	142.5	22.5
L6	trans. Edge	149.5	22.5
L6	trans. Edge	150.5	22.5
L6	Center	157.5	22.5
L6	trans. Edge	164.5	22.5
L6	trans. Edge	165.5	22.5
L6	Center	172.5	22.5
L8	trans. Edge	179.5	22.5
L6	trans. Edge	180.5	22.5
M6	Center	330	22.5
M6	trans. Edge	337	22.5
M6	trans. Edge	338	22.5
M6	Center	345	22.5
M6	trans. Edge	352	22.5
M6	trans. Edge	353	22.5
M6	Center	360	22.5
M6	trans. Edge	367	22.5
M6	trans. Edge	368	22.5
M6	Center	375	22.5
M2N	trans. Edge	494.5	22.5
M2N	trans. Edge	495.5	22.5
M2N	Center	502.5	22.5
M2N	trans. Edge	509.5	22.5
M2N	trans. Edge	510.5	22.5

TABLE 23. RECOMMENDED LOCATIONS FOR HWD TESTING (CONT.)

Test Cell	Load Position	x-coordinate, ft	y-coordinate, ft
M2N	center	517.5	22.5
M2N	trans. Edge	524.5	22.5
M2N	trans. Edge	525.5	22.5
M2N	Center	532.5	22.5
H2N	center	697.5	22.5
H2N	trans. edge	704.5	22.5
H2N	trans. edge	705.5	22.5
H2N	center	712.5	22.5
H2N	trans. edge	719.5	22.5
H2N	trans. edge	720.5	22.5
H2N	center	727.5	22.5
H2N	trans. edge	734.5	22.5
H2N	trans. edge	735.5	22.5
L3N	center	757.5	18.25
L3N	center	772.5	18.25
L3N	center	787.5	18.25
M3N	center	442.5	18.25
M3N	center	457.5	18.25
M3N	center	472.5	18.25
M3N	center	757.5	18.25
M3N	center	772.5	18.25
M3N	center	787.5	18.25
L2N	long. edge	82.5	15.5
L2N	long. edge	97.5	15.5
L6	long. edge	112.5	15.5
L6	long. edge	127.5	15.5
L6	long. edge	142.5	15.5
L6	long. edge	157.5	15.5
L6	long. edge	172.5	15.5
M6	long. edge	330	15.5
M6	long. edge	345	15.5
M6	long. edge	360	15.5
M6	long. edge	375	15.5
M2N	long. edge	502.5	15.5
M2N	long. edge	517.5	15.5
M2N	long. edge	532.5	15.5
H2N	long. edge	697.5	15.5
H2N	long. edge	712.5	15.5

TABLE 23. RECOMMENDED LOCATIONS FOR HWD TESTING (CONT.)

Test Cell	Load Position	x-coordinate, ft	y-coordinate, ft
H2N	long. edge	727.5	15.5
L1N	center	7.5	15
L1N	trans. edge	14.5	15
L1N	trans. edge	15.5	15
L1N	center	22.5	15
L1N	trans. edge	29.5	15
L1N	trans. edge	30.5	15
L1N	center	37.5	15
L4	trans. edge	187	15
L4	trans. edge	188	15
L4	center	195	15
L4	trans. edge	202	15
L4	trans. edge	203	15
L4	center	210	15
L4	trans. edge	217	15
L4	trans. edge	218	15
M4	trans. edge	382	15
M4	trans. edge	383	15
M4	center	390	15
M4	trans. edge	397	15
M4	trans. edge	398	15
M4	center	405	15
M4	trans. edge	412	15
M4	trans. edge	413	15
M1N	center	562.5	15
M1N	trans. edge	569.5	15
M1N	trans. edge	570.5	15
M1N	center	577.5	15
M1N	trans. edge	584.5	15
M1N	trans. edge	585.5	15
M1N	center	592.5	15
H1N	center	637.5	15
H1N	trans. edge	644.5	15
H1N	trans. edge	645.5	15
H1N	center	652.5	15
H1N	trans. edge	659.5	15
H1N	trans. edge	660.5	15
H1N	center	667.5	15
H4	trans. edge	817	15

TABLE 23. RECOMMENDED LOCATIONS FOR HWD TESTING (CONT.)

Test Cell	Load Position	x-coordinate, ft	y-coordinate, ft
H4	trans. edge	818	15
H4	center	825	15
H4	trans. edge	832	15
H4	trans. edge	833	15
H4	center	840	15
H4	trans. edge	847	15
H4	trans. edge	848	15
L2N	long. edge	82.5	14.5
L2N	long. edge	97.5	14.5
L6	long. edge	112.5	14.5
L6	long. edge	127.5	14.5
L6	long. edge	142.5	14.5
L6	long. edge	157.5	14.5
L6	long. edge	172.5	14.5
M6	long. edge	330	14.5
M6	long. edge	345	14.5
M6	long. edge	360	14.5
M6	long. edge	375	14.5
M2N	long. edge	502.5	14.5
M2N	long. edge	517.5	14.5
M2N	long. edge	532.5	14.5
H2N	long. edge	697.5	14.5
H2N	long. edge	712.5	14.5
H2N	long. edge	727.5	14.5
L2N	center	67.5	7.5
L2N	trans. edge	74.5	7.5
L2N	trans. edge	75.5	7.5
L2N	center	82.5	7.5
L2N	trans. edge	89.5	7.5
L2N	trans. edge	90.5	7.5
L2N	center	97.5	7.5
L2N	trans. edge	104.5	7.5
L2N	trans. edge	105.5	7.5
L6	center	112.5	7.5
L6	trans. edge	119.5	7.5
L6	trans. edge	120.5	7.5
L6	center	127.5	7.5
L6	trans. edge	134.5	7.5
L6	trans. edge	135.5	7.5

TABLE 23. RECOMMENDED LOCATIONS FOR HWD TESTING (CONT.)

Test Cell	Load Position	x-coordinate, ft	y-coordinate, ft
L6	center	142.5	7.5
L6	trans. edge	149.5	7.5
L6	trans. edge	150.5	7.5
L6	center	157.5	7.5
L6	trans. edge	164.5	7.5
L6	trans. edge	165.5	7.5
L6	center	172.5	7.5
L8	trans. edge	179.5	7.5
L6	trans. edge	180.5	7.5
M6	center	330	7.5
M6	trans. edge	337	7.5
M6	trans. edge	338	7.5
M6	center	345	7.5
M6	trans. edge	352	7.5
M6	trans. edge	353	7.5
M6	center	360	7.5
M6	trans. edge	367	7.5
M6	trans. edge	368	7.5
M6	center	375	7.5
M2N	trans. edge	494.5	7.5
M2N	trans. edge	495.5	7.5
M2N	center	502.5	7.5
M2N	trans. edge	509.5	7.5
M2N	trans. edge	510.5	7.5
M2N	center	517.5	7.5
M2N	trans. edge	524.5	7.5
M2N	trans. edge	525.5	7.5
M2N	center	532.5	7.5
H2N	center	697.5	7.5
H2N	trans. edge	704.5	7.5
H2N	trans. edge	705.5	7.5
H2N	center	712.5	7.5
H2N	trans. edge	719.5	7.5
H2N	trans. edge	720.5	7.5
H2N	center	727.5	7.5
H2N	trans. edge	734.5	7.5
H2N	trans. edge	735.5	7.5
L2S	center	67.5	-7.5
L2S	trans. edge	74.5	-7.5

TABLE 23. RECOMMENDED LOCATIONS FOR HWD TESTING (CONT.)

Test Cell	Load Position	x-coordinate, ft	y-coordinate, ft
L2S	trans. edge	75.5	-7.5
L2S	center	82.5	-7.5
L2S	trans. edge	89.5	-7.5
L2S	trans. edge	90.5	-7.5
L2S	center	97.5	-7.5
L2S	trans. edge	104.5	-7.5
L2S	trans. edge	105.5	-7.5
L7	center	112.5	-7.5
L7	trans. edge	119.5	-7.5
L7	trans. edge	120.5	-7.5
L7	center	127.5	-7.5
L7	trans. edge	134.5	-7.5
L7	trans. edge	135.5	-7.5
L7	center	142.5	-7.5
L7	trans. edge	149.5	-7.5
L7	trans. edge	150.5	-7.5
L7	center	157.5	-7.5
L7	trans. edge	164.5	-7.5
L7	trans. edge	165.5	-7.5
L7	center	172.5	-7.5
L8	trans. edge	179.5	-7.5
L7	trans. edge	180.5	-7.5
M7	center	330	-7.5
M7	trans. edge	337	-7.5
M7	trans. edge	338	-7.5
M7	center	345	-7.5
M7	trans. edge	352	-7.5
M7	trans. edge	353	-7.5
M7	center	360	-7.5
M7	trans. edge	367	-7.5
M7	trans. edge	368	-7.5
M7	center	375	-7.5
M2S	trans. edge	494.5	-7.5
M2S	trans. edge	495.5	-7.5
M2S	center	502.5	-7.5
M2S	trans. edge	509.5	-7.5
M2S	trans. edge	510.5	-7.5
M2S	center	517.5	-7.5
M2S	trans. edge	524.5	-7.5

TABLE 23. RECOMMENDED LOCATIONS FOR HWD TESTING (CONT.)

Test Cell	Load Position	x-coordinate, ft	y-coordinate, ft
M2S	trans. edge	525.5	-7.5
M2S	center	532.5	-7.5
H2S	center	697.5	-7.5
H2S	trans. edge	704.5	-7.5
H2S	trans. edge	705.5	-7.5
H2S	center	712.5	-7.5
H2S	trans. edge	719.5	-7.5
H2S	trans. edge	720.5	-7.5
H2S	center	727.5	-7.5
H2S	trans. edge	734.5	-7.5
H2S	trans. edge	735.5	-7.5
L2S	long. edge	82.5	-14.5
L2S	long. edge	97.5	-14.5
L6	long. edge	112.5	-14.5
L6	long. edge	127.5	-14.5
L6	long. edge	142.5	-14.5
L6	long. edge	157.5	-14.5
L6	long. edge	172.5	-14.5
M6	long. edge	330	-14.5
M6	long. edge	345	-14.5
M6	long. edge	360	-14.5
M6	long. edge	375	-14.5
M2S	long. edge	502.5	-14.5
M2S	long. edge	517.5	-14.5
M2S	long. edge	532.5	-14.5
H2S	long. edge	697.5	-14.5
H2S	long. edge	712.5	-14.5
H2S	long. edge	727.5	-14.5
L1S	center	7.5	-15
L1S	trans. edge	14.5	-15
L1S	trans. edge	15.5	-15
L1S	center	22.5	-15
L1S	trans. edge	29.5	-15
L1S	trans. edge	30.5	-15
L1S	center	37.5	-15
L5	trans. edge	187	-15
L5	trans. edge	188	-15
L5	center	195	-15
L5	trans. edge	202	-15

TABLE 23. RECOMMENDED LOCATIONS FOR HWD TESTING (CONT.)

Test Cell	Load Position	x-coordinate, ft	y-coordinate, ft
L5	trans. edge	203	-15
L5	center	210	-15
L5	trans. edge	217	-15
L5	trans. edge	218	-15
H4	trans. edge	382	-15
H4	trans. edge	383	-15
H4	center	390	-15
H4	trans. edge	397	-15
H4	trans. edge	398	-15
H4	center	405	-15
H4	trans. edge	412	-15
H4	trans. edge	413	-15
M1S	center	562.5	-15
M1S	trans. edge	569.5	-15
M1S	trans. edge	570.5	-15
M1S	center	577.5	-15
M1S	trans. edge	584.5	-15
M1S	trans. edge	585.5	-15
M1S	center	592.5	-15
H1S	center	637.5	-15
H1S	trans. edge	644.5	-15
H1S	trans. edge	645.5	-15
H1S	center	652.5	-15
H1S	trans. edge	659.5	-15
H1S	trans. edge	660.5	-15
H1S	center	667.5	-15
H5	trans. edge	817	-15
H5	trans. edge	818	-15
H5	center	825	-15
H5	trans. edge	832	-15
H5	trans. edge	833	-15
H5	center	840	-15
H5	trans. edge	847	-15
H5	trans. edge	848	-15
L2S	long. edge	82.5	-15.5
L2S	long. edge	97.5	-15.5
L7	long. edge	112.5	-15.5
L7	long. edge	127.5	-15.5
L7	long. edge	142.5	-15.5

TABLE 23. RECOMMENDED LOCATIONS FOR HWD TESTING (CONT.)

Test Cell	Load Position	x-coordinate, ft	y-coordinate, ft
L7	long. edge	157.5	-15.5
L7	long. edge	172.5	-15.5
M7	long. edge	330	-15.5
M7	long. edge	345	-15.5
L7	long. edge	360	-15.5
L7	long. edge	375	-15.5
M2S	long. edge	502.5	-15.5
M2S	long. edge	517.5	-15.5
M2S	long. edge	532.5	-15.5
H2S	long. edge	697.5	-15.5
H2S	long. edge	712.5	-15.5
H2S	long. edge	727.5	-15.5
L3S	center	727.5	-18.25
L3S	center	742.5	-18.25
L3S	center	757.5	-18.25
M3S	center	442.5	-18.25
M3S	center	457.5	-18.25
M3S	center	472.5	-18.25
M3S	center	757.5	-18.25
M3S	center	772.5	-18.25
M3S	center	787.5	-18.25
L2S	center	67.5	-22.5
L2S	trans. edge	74.5	-22.5
L2S	trans. edge	75.5	-22.5
L2S	center	82.5	-22.5
L2S	trans. edge	89.5	-22.5
L2S	trans. edge	90.5	-22.5
L2S	center	97.5	-22.5
L2S	trans. edge	104.5	-22.5
L2S	trans. edge	105.5	-22.5
L6	center	112.5	-22.5
L6	trans. edge	119.5	-22.5
L6	trans. edge	120.5	-22.5
L6	center	127.5	-22.5
L7	trans. edge	134.5	-22.5
L7	trans. edge	135.5	-22.5
L7	center	142.5	-22.5
L7	trans. edge	149.5	-22.5
L7	trans. edge	150.5	-22.5

TABLE 23. RECOMMENDED LOCATIONS FOR HWD TESTING (CONT.)

Test Cell	Load Position	x-coordinate, ft	y-coordinate, ft
L7	center	157.5	-22.5
L7	trans. edge	164.5	-22.5
L7	trans. edge	165.5	-22.5
L7	center	172.5	-22.5
L7	trans. edge	179.5	-22.5
L7	trans. edge	180.5	-22.5
M7	center	330	-22.5
M7	trans. edge	337	-22.5
M7	trans. edge	338	-22.5
M7	center	345	-22.5
M7	trans. edge	352	-22.5
M7	trans. edge	353	-22.5
M7	center	360	-22.5
M7	trans. edge	367	-22.5
M7	trans. edge	368	-22.5
M7	center	375	-22.5
M2S	trans. edge	494.5	-22.5
M2S	trans. edge	495.5	-22.5
M2S	center	502.5	-22.5
M2S	trans. edge	509.5	-22.5
M2S	trans. edge	510.5	-22.5
M2S	center	517.5	-22.5
M2S	trans. edge	524.5	-22.5
M2S	trans. edge	525.5	-22.5
M2S	center	532.5	-22.5
H2S	center	697.5	-22.5
H2S	trans. edge	704.5	-22.5
H2S	trans. edge	705.5	-22.5
H2S	center	712.5	-22.5
H2S	trans. edge	719.5	-22.5
H2S	trans. edge	720.5	-22.5
H2S	center	727.5	-22.5
H2S	trans. edge	734.5	-22.5
H2S	trans. edge	735.5	-22.5

10. DATA ANALYSIS PLAN

This chapter presents the project team's thinking on how the data collected during the proposed testing program may be used. This chapter is not intended to be a guide for the data analysis, but rather to reflect the reasoning behind the design of the testing program. The proposed testing program was designed to satisfy the most pressing data needs for improving airport pavement design. This chapter presents an example approach that may be followed to verify or improve current procedures for mechanistic modeling and design of unbonded overlays. Various issues related to data collection are also discussed that are important to ensure reliability and accuracy of the collected data. The following topics are discussed in this chapter:

- Data acquisition QA/QC
- Preliminary data analysis
- Calibration of performance prediction models
- Development of improved structural models

10.1 DATA ACQUISITION QA/QC

The current FAA NAPTF data acquisition QA/QC procedure is recommended for use in the proposed testing program. The research team is satisfied that any systematic errors in data collection can be avoided by following the FAA procedure.

10.2 RELIMINARY DATA ANALYSIS

Although current FAA NAPTF data QA/QC procedure significantly minimizes the possibility of collecting erroneous data, it does not eliminate the need to conduct a comprehensive independent review of the collected information. Preliminary data analysis is recommended for all types of data (e.g., structural response, environmental, pavement performance) that will be collected before initiating any detailed analyses. The purpose of preliminary data analysis is to detect any obvious signs of data problems by reviewing the raw data and conducting simple comparisons that provide a good overview of the data trends. Preliminary data analysis includes the following activities:

- Review data to identify and flag suspicious records
- Develop tables with computed parameters
- Perform side-by-side comparison
- Perform statistical analysis

10.2.1 Data Review

This task involves plotting trends and conducting statistical analysis of records in each group of data to identify any obvious signs of data problems and data trends. Outlier data will be reviewed once the statistics have been determined. Outlier data testing will be performed in accordance with ASTM E-178. An outlying observation may be just an extreme manifestation of the random variability inherent in the data. If this is true, the value should be retained and

processed in the same manner as the other observations in the database. On the other hand, an outlying observation may be the result of gross deviation from prescribed measurement procedure or an error in recording the numerical value. In such a case, the outlier needs to be recognized as probably being from a different population than that of the other observations in that sample.

10.2.2 Development of Computed Parameters Tables

Computed parameters are statistical or mechanistic parameters that adequately represent a much larger number of records to make further data analysis more efficient. This activity requires significant engineering and statistical judgment to find the right balance between reducing the amount of data and retaining sufficient data so as not to skew the analysis outcome. An example of possible computed parameters is the representative maximum computed stresses for each strain sensor and lateral load position for a certain period of time (say, 100 load passes for a particular lateral gear position). Other parameters associated with the computed stress include the following:

- Mean stress
- Maximum stress
- Minimum stress
- Standard deviation in stress
- Total number of observations

With the HWD data, the following parameters should be computed for each deflection basin:

- Normalized deflections
- Backcalculated moduli from HWD deflection basins
- Deflection indexes (AREA, normalized deflection, etc.)
- Radii of relative stiffness

The layer moduli should be determined using both Westergaard- and elastic-layer-based backcalculation programs for comparison. In addition to the basin-by-basin analysis, representative statistical parameters (such as mean, minimum, and maximum values, standard deviation, etc.) should be computed for each test cell for each period for the evaluation of any changes in the support condition over time.

10.2.3 Side-by-side Analysis

Prior to initiating any major data analysis activities, simple side-by side comparison of performance data and structural responses should be performed to evaluate the effect of key design parameters. Examples of some of the proposed comparisons are presented in tables 24 through 31.

TABLE 24. EFFECT OF GEAR CONFIGURATION

Common features	Gear type		
	4 wheels		6 wheels
Low strength subgrade, presence of longitudinal cracks in SL	L1N	Versus	L1S
Low strength subgrade, matched joints, no cracks in SL	L2N	Versus	L2S
Low strength subgrade, shattered SL	L3N	Versus	L3S
Medium strength subgrade, presence of longitudinal cracks in SL	M1N	Versus	M1S
Medium strength subgrade, matched joints, no cracks in SL	M2N	Versus	M2S
Medium strength subgrade, shattered SL	M3N	Versus	M3S
High strength subgrade, presence of longitudinal cracks in SL	H1N	Versus	H1S
High strength subgrade, matched joints, no cracks in SL	H2N	Versus	H2S
High strength subgrade, shattered SL	H3N	Versus	H3S

TABLE 25. EFFECT OF LONGITUDINAL CRACKING IN THE EXISTING PAVEMENT

Common features	Existing pavement condition		
	Longitudinal cracking		No distresses
Low strength subgrade, 6 wheel gear loading	L1N	Versus	L2N
Low strength subgrade, 4 wheel gear loading	L1S	Versus	L2S
Medium strength subgrade, 6 wheel gear loading	M1N	Versus	M2N
Medium strength subgrade, 4 wheel gear loading	M1S	Versus	M2S
High strength subgrade, 6 wheel gear loading	H1N	Versus	H2N
High strength subgrade, 4 wheel gear loading	H1S	Versus	H2S

TABLE 26. EFFECT OF SHATTERED SLABS IN THE EXISTING PAVEMENT

Common features	Existing pavement condition		
	Shattered slabs		No distresses
Low strength subgrade, 6 wheel gear loading	L3N	Versus	L2N
Low strength subgrade, 4 wheel gear loading	L3S	Versus	L2S
Medium strength subgrade, 6 wheel gear loading	M3N	Versus	M2N
Medium strength subgrade, 4 wheel gear loading	M3S	Versus	M2S
High strength subgrade, 6 wheel gear loading	H3N	Versus	H2N
High strength subgrade, 4 wheel gear loading	H3S	Versus	H2S

TABLE 27. EFFECT OF MISMATCHING JOINTS IN THE OVERLAY AND THE EXISTING PAVEMENT

Common features	Existing pavement condition		
	Mismatched joints		Matched joints
Low strength subgrade, 4 wheel gear loading	L5	Versus	L2N
Medium strength subgrade, 4 wheel gear loading	M5	Versus	M2N
High strength subgrade, 4 wheel gear loading	H5	Versus	H2N

TABLE 28. EFFECT OF DOWELS IN OVERLAY JOINTS MISMATCHED WITH JOINTS IN THE EXISTING PAVEMENT

Common features	Existing pavement condition		
	Non-doweled joints		Doweled joints
Low strength subgrade, 4 wheel gear loading	L5	Versus	L4
Medium strength subgrade, 4 wheel gear loading	M5	Versus	M4
High strength subgrade, 4 wheel gear loading	M5	Versus	H4

TABLE 29. EFFECT OF HIGH-SEVERITY TRANSVERSE CRACKING IN THE EXISTING PAVEMENT

Common features	Existing pavement condition		
	Transverse cracking		No distresses
Low strength subgrade, 4 wheel gear loading	L7	Versus	L2N
Medium strength subgrade, 4 wheel gear loading	M7	Versus	M2N

TABLE 30. EFFECT OF SEVERITY LEVEL OF TRANSVERSE CRACKING IN THE EXISTING PAVEMENT

Common features	Existing pavement condition		
	Low severity		High severity
Low strength subgrade, 4 wheel gear loading, transverse cracks in SL	L6	Versus	L7

TABLE 31. EFFECT OF SPALLING OF CRACKS AND JOINTS IN THE EXISTING PAVEMENT

Common features	Existing pavement condition		
	Spalled cracks		No spalling
Low strength subgrade, 4 wheel gear loading, transverse cracks in SL	L8	Versus	L7

Each side-by-side comparisons should include the evaluation of the following, as a minimum:

- Number of load passes until a first crack appears
- Number of load passes when complete failure occurs
- Longitudinal edge stresses in the middle of the longitudinal joints
- Transverse stresses at the middle of transverse joints due to static, slow rolling, and high-speed loading
- Computed FWD deflection indexes

Lessons learned from these comparisons will help to choose the right directions in calibration of both performance prediction and structural response models.

10.2.4 Statistical Analysis

By grouping cells with similar characteristics, statistical analyses can be conducted to evaluate the effects of:

- Subgrade type, gear type, and existing pavement condition on overlay responses
- Existing pavement condition on overlay performance
- Overlay responses on pavement performance

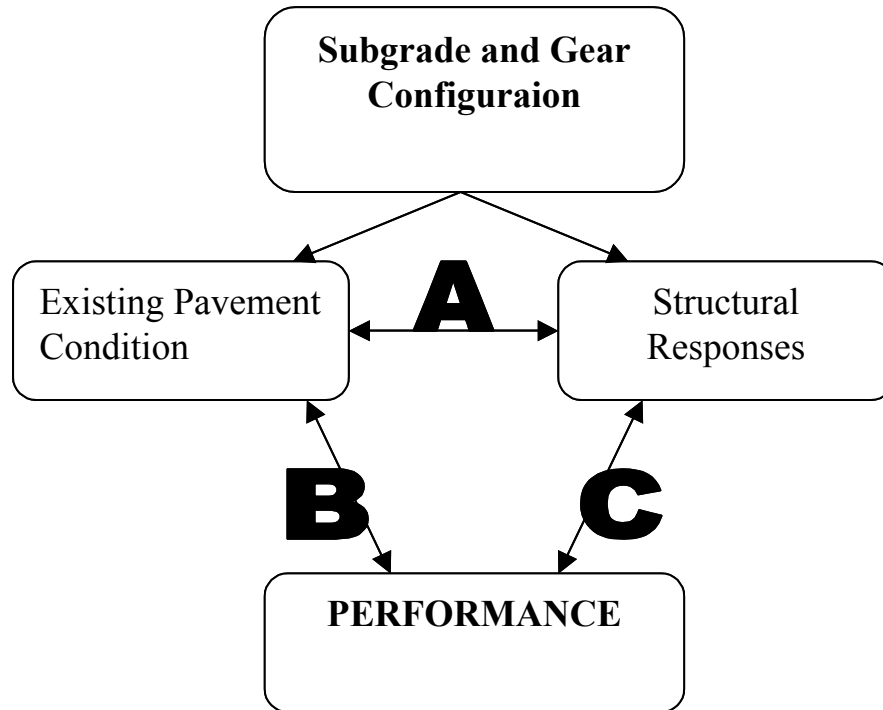


FIGURE 85. BASIC RELATIONSHIPS AFFECTING PAVEMENT BEHAVIOR AND PERFORMANCE

Determining the relative importance of different site conditions is a two-step process:

1. For each combination of site condition, structural response type, and existing pavement distress type, evaluate relationships A, B, and C from figure 85 using bivariate analysis.
2. Refine the results of the bivariate analysis using multivariate analysis to reduce the effects of interaction between different factors.

Each of these subtasks is discussed in detail below.

10.2.4.1 Bivariate Analysis

In this subtask, a simple statistical test (t-test) will be used to determine whether the observed differences in pavement response or performance are attributable to the experimental factors (e.g., condition of the underlying pavement). Being simple in nature, these tests allow quick preliminary assessment of the contribution of individual factors (existing pavement condition, structural responses) to overall pavement behavior. This type of test was used successfully in the recently completed LTPP study “Common Characteristics of Good and Poorly Performing PCC Pavements.”

To conduct this analysis, the test cells are first divided into two groups based on experimental factors. The t-test is then performed for each structural response and performance parameter for each experimental factor. Table 32 presents example groupings of test cells. Note that each row represents a specific comparison (e.g., effects of gear type, subgrade strength, condition of the underlying pavement). The statistical tests are conducted separately for each row.

The test works by taking the ratio of the difference between the two group means (for a specific row) to an appropriate estimate of standard deviation of this difference. If this ratio is large, then the difference of the group means is significant, meaning that the difference is due to something other than chance. If the ratio is small, the difference could be due to chance. For example, if mean transverse overlay stress for sections in group A is lower than that for sections in group B, and the t-test shows this difference is significant, there is strong evidence that this design feature significantly affects the transverse stresses in PCC overlay.

TABLE 32. POSSIBLE DIVISIONS OF EACH SITE CONDITION CELLS INTO TWO SUBGROUPS

Group A	Group B
All subgrades, all existing pavement conditions, six-wheel gear	All subgrades, all existing pavement conditions, four-wheel gear
Low strength subgrade, all cells	Medium strength subgrade, all cells
Medium strength subgrade, all cells	High strength subgrade, all cells
All subgrades, transverse cracks in existing pavement	All subgrades, no distresses/cracks in existing pavement
All subgrades, transverse cracks in existing pavement	All subgrades, longitudinal cracks in existing pavement
Sections with low PCC overlay backcalculated radius of relative stiffness	Sections with high PCC overlay backcalculated radius of relative stiffness
Sections with low PCC overlay longitudinal stress	Sections with high PCC overlay longitudinal stress

The main disadvantage of bivariate analysis is that it does not take into account the effects of other variables, specifically between response, loading, and distress. The confounding effects of other factors can inflate or deflate the results. In this study, confounding effects of site condition factors will be somewhat mitigated (although not completely eliminated) by conducting these

tests separately for each site condition cell. Nevertheless, confounding effect still might be a significant problem. To increase the reliability of the analysis, multivariate tests should be conducted for the cases where sufficient number of tests is available.

10.2.4.2 Multivariate Analysis

The t-test and other bivariate analyses do not take into account the interactions of the different variables and their effects on responses or performance. For example, it could be that the combination of a stiff subgrade and longitudinal cracking in the existing pavement is the cause of the poor performance of PCC. The t-test does not isolate the effect of either of these variables on performance.

A multivariate analysis is needed because of the large number of interactions anticipated between design and construction features and site conditions. The overall objective of the multivariate analysis is to identify key factors from the independent variables and gain an understanding of the interrelationship of these variables. Specific objectives include reducing the number of variables for further evaluation and determining which combinations of variables are the most descriptive and significant. The following relationships should be investigated:

- Relationship between existing pavement condition and performance
- Relationship between existing pavement condition, FWD deflections, and measured strains
- Relationship between existing pavement condition, gear configuration, and measured strains

The last two relationships above will allow a conversion of traffic loading history to strain history.

The analysis methods that may be used for multivariate analysis include the following:

- Regression analysis
- Principle component analysis
- Factor analysis
- Discriminate function analysis

Regression and stepwise regression may be used in an exploratory manner to identify promising combinations of variables. For the standard regression models, the adjusted R-square indicates the amount of variability in the response that is explained by the model after adjusting for the independent parameters. The F-test indicates whether the model is useful for estimating the response. Efforts should be made to find regression models that have the least amount of collinearity. Cook's distance can be used to identify influential points. If any observations significantly altered the parameter estimates, then the model can be refit without the points and the two models compared.

The redundancy tables provide R-squares, partial correlations, and semipartial correlations for the variables in and not in the model. These statistics are based on the regression of each variable onto the variables in the model. Those variables in the model are regressed on the remaining variables in the model. The R-square is a measure of the fit of this regression. The semipartial correlation is found by a second regression of the residuals from these regressions on the raw y values. The partial correlation is found by regressing these first residuals onto the residuals created by regressing y onto the variables in the model. A small semipartial correlation with a relatively large partial correlation indicates a promising variable.

Another guide for selecting variables is the correlation matrix. This matrix contains estimates of the pairwise correlations for two groups of variables. Also included is the p -value, which indicates whether the estimate is significantly different from zero.

One common issue with data collected from a sample is collinearity, which refers to strong correlation among some independent variables. This can be thought of in two ways: one group of variables is nearly a linear function of another group, or as a restricted sample space containing only certain combinations of values of the variables. Models based on collinear variables have a few drawbacks. Collinearity inflates the variance of the regression coefficients, the coefficients are not valid outside the sample space, and the coefficients might not be interpretable. It usually takes a very strong correlation before the effects of collinearity are harmful.

Principal components analysis will also be used to address the collinearity problem. This tool is useful for decomposing a set of k variables into k orthogonal components that capture the cumulative variability of these variables in k dimensions. Each principal component (factor) is a linear combination of the variables that is independent of the other factors. Factor 1 is the linear combination with the most variability; factor 2 is the linear combination that has the most variability of those linear combinations that are orthogonal to factor 1. Factor 3 is the next linear combination with the most variability of those linear combinations that are independent of factors 1 and 2. The later factors explain less and less of the variability. From these principal components, the variables that are correlated with the same components and how much variability these components explain can be noted.

Once the number of variables is narrowed down, a small set of variables can be put into a regression model. This type of model is helpful for thinking about the way the variables interrelate. All the models were developed from the data, so the statistics can only be interpreted in a descriptive or exploratory manner.

Discriminate function analysis is a technique for finding functions of the explanatory variables that fit the groupings provided. Given two or more observed groups, this technique finds a function of the explanatory variables that nearly partitions the most extreme group from the rest. Then the algorithm continues finding functions that partition the remaining groups. By looking at the resulting classification functions, we can try to understand the basis for group membership.

Models produced by the multivariate analysis will be useful for examining the way in which the variables interrelate. However, they will not be validated models and, therefore, can only be interpreted in a descriptive or exploratory manner.

10.3 CALIBRATION OF PERFORMANCE PREDICTION MODELS

The wealth of unbonded overlay performance data collected at the NAPTF will provide numerous opportunities for improving design practices. One possible application is using the full-scale testing data to improve performance prediction within the LEDFAA framework. Another option is to improve unbonded overlay performance prediction using alternative approaches. Both options are briefly discussed below.

10.3.1 Calibration/Verification of LEDFAA

An important application of NAPTF test results will be calibration and verification of LEDFAA. One possible approach for such calibration, described below, consists of two activities:

- Improvement of PCC overlay deterioration model
- Improved characterization of the existing pavement

10.3.1.1 Improvement of PCC Overlay Deterioration Model

The data from the sections with no distresses in the existing pavement can be used for evaluating and improving the PCC overlay deterioration model in LEDFAA. Performance data from six cells (two gear types, three subgrade types) will be available for comparison with LEDFAA predictions. For each cell, two major parameters can be used:

- Passes to the appearance of first crack (SCI=100)
- Passes to the multiple cracks in every slab (SCI=0)

If a significant discrepancy is observed, the following approaches may be used to improve the fit:

- Modification of friction coefficient between the overlay and the PCC pavement—Currently, this interface is assumed fully unbonded. However, JULEA allows for modeling of partial slip. This option should be considered if the observed performance life is much greater than predicted.
- Modification of PCC failure models—Currently, PCC overlay failure models are the same as those for new pavements and have the following form:

$$\frac{R}{c} = 0.5234 + 0.3920 \text{Log} C_0$$

$$\frac{R}{c} = 0.2967 + 0.381 \text{Log} C_f$$

where R is the concrete flexural strength, c is the overlay stress computed using the layered elastic program JULEA, C₀ and C_f are the number of coverages to initiate cracking and

to complete failure, respectively. If the second round of testing of new PCC pavements be completed prior to testing of the overlaid pavements then that performance information should be combined with performance data for the overlays and an attempt to develop new failure models for both new and overlaid pavements should be made. If information for new pavements is not available or a significant difference in performance for new pavements and overlays is observed, a separate failure model for unbonded overlays should be developed.

- Modification of stress adjustment for subgrade type—LEDFAA corrects layered elastic stress prediction for edge effect by applying a correction factor depending on subgrade type. If deviation of predicted performance from observed performance correlates with increase in subgrade strength, a possibility of modification of the stress correction factors can be considered.

10.3.1.2 Improved Characterization of the Existing Pavement

The structural capacity of the existing pavement is a key factor affecting unbonded overlay design. The structural capacity of the existing pavement is characterized using the structural condition index (SCI) in LEDFAA. The SCI is currently the most sophisticated and objective parameter for characterizing the condition of PCC pavements. However, SCI could be improved to better reflect the effects of existing pavement condition and layer interactions on critical stresses in unbonded overlays. The proposed testing program is designed to provide the data needed for accomplishing such a task. The improved SCI will be a key mechanistic parameter for designing unbonded overlays, which makes this task an important step toward improvement of the overlay design procedure in general.

The current procedure assumes that the same deduct values should be used for PCI and SCI calculation. It is quite possible however, that contribution into structural deterioration and loss of serviceability may be different. In part, this possibility is already recognized by excluding some PCI distresses from SCI calculation (mathematically, assuming deduct values for those distresses equal to 0).

The results of the proposed test program will provide crucial information for SCI improvement. The performance of test cells with different distresses (transverse cracking, longitudinal cracking, and shattered slabs) will be compared with the performance of tests cells with no distresses in the existing pavement. Those comparisons will allow for the development of new deduction factors that should be used to estimate structural deterioration of the existing pavement. Based on new deduction factors, a modified procedure for the structural condition index will be developed.

The following example illustrates a possible calibration process. Assume that cell L2S (soft subgrade, no distresses in the underlying pavement) survived 45,000 load applications, whereas cell L5 (high-severity transverse cracking) survived only 16,000 load applications. At the same, according to LEDFAA, cell L2S was supposed to survive only 40,000 load applications. Therefore, it is reasonable to assume that the expected number of load applications for cell L5 is equal to

$$n = \frac{40,000}{45,000} \times 16,000 = 14,000$$

That value of expected number of load repetitions LEDFAA overlay life prediction for corresponds to an SCI of 60. Therefore, the corresponding deduct value for transverse cracking of 100 percent cracked slabs is 40.

Similarly, the deduct values can be determined for other distresses (longitudinal cracking, shattered slabs, joint spalling, low-severity transverse cracking). Since many of these distresses are duplicated for two gear configurations and three subgrade types, the reliability of such analysis can be evaluated.

The result of this calibration will be an improved procedure for determining a very important input parameter into LEDFAA. This will allow significant improvement of the design procedure without major revisions to LEDFAA.

10.3.2 Verification of Gear Configuration Modeling

One of the most important improvements of LEDFAA over the current FAA design procedure is that LEDFAA enables the design of unbonded overlays for dual tridem gear aircraft loading. NAPTF testing will allow for direct comparison of the performance of unbonded overlays under dual tandem and dual tridem gears. If the observed ratio of load repetitions to failure of dual tridem and dual tandem is equal to the ratio of predicted design life from LEDFAA, then no correction will be required. Otherwise, stress predictions for dual tridem gears should be adjusted to provide better correspondence with observed performance.

10.3.3 Calibration of PCC Overlay Fatigue Models

The development of a calibrated mechanistic performance model for predicting slab cracking is another possible use of the data from the full-scale testing to improve the unbonded overlay design process. Fatigue slab cracking is the most important aspect of unbonded overlay performance; therefore, the development of models that predict overlay slab cracking behavior should be a very important aspect of data analysis efforts.

Mechanistic-empirical concepts have been used to model JPCP fatigue cracking of highway pavements since the initial Portland Cement Association (PCA) design procedure was developed in 1966. The first actual model for transverse fatigue cracking was developed in 1977 under the FHWA Zero-Maintenance study (Darter and Barenberg, 1977). This model showed for the first time the relationship between computed fatigue damage and actual transverse cracking in the field.

Of the available cracking models, the ones that are most universally applicable are those that are mechanistic-empirical in nature, relating critical stresses in the pavement slabs to expected levels of slab cracking. Most of these models estimate accumulated damage using Miner's damage

hypothesis. An empirically derived regression model is then used to relate the computed accumulated damage to a set of field cracking data.

One of the most promising field calibrated models for JPCP fatigue cracking was proposed by ERES Consultants (1999) as part of the FHWA-sponsored “Performance Related Specifications” study, which sought to quantify the pavement damage caused by different axle groups for cost allocation purposes. This study produced the following mechanistic-empirical cracking S-shaped model:

$$\% Cracks = \frac{100 FD^{1.52}}{1 + FD^{1.52}}$$

where:

- % Cracks = percent of JPCP panels exhibiting fatigue cracking
- FD = fatigue damage, computed using Miner’s hypothesis = $\sum ni/Ni$
- n_i = number of actual coverages of gear configuration/load combination i
- N_i = number of allowable coverages of gear configuration/load combination i

The shape of this curve is shown in figure 86. This model can also be used explicitly to solve for the amount of slab cracking expected to be associated with any given level of calculated fatigue damage.

It should be noted that the model presented above was developed for new JPCP highway pavements. The behavior of unbonded PCC overlays of airport pavements may be different due to differences in support conditions and geometry and magnitude of gear loading. Therefore, to be applicable for airport overlays, the model has to be recalibrated. The NAPTF test data will provide an excellent opportunity for such calibration.

Due to differences in the existing pavement conditions and subgrade support, it is expected that the overlay slabs will be subjected to a different level of stresses and, therefore, different fatigue damage. Therefore, the experiment should provide sufficient information for the model calibration.

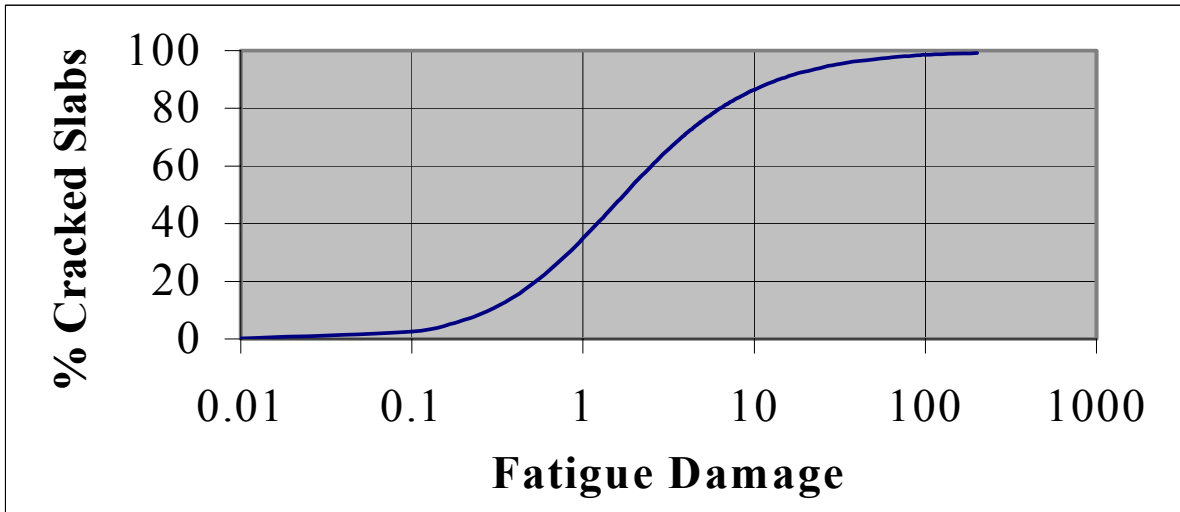


FIGURE 86. TRANSVERSE CRACKING (BOTTOM-UP) VERSUS COMPUTED FATIGUE DAMAGE ILLUSTRATION

Two types of model calibration can be recommended:

- Calibration of the cracking model using NAPTF performance data and damage computed with stresses predicted using layered elastic or finite element models
- Calibration of the cracking model using NAPTF performance data and damage computed with stresses computed from measured strains at the NAPTF

Although the first approach is not as rigorous as the second, it will allow for significant improvement of the current design procedures using available structural models. Therefore, it will permit the development of a new mechanistic-empirical design procedure in a relatively short period of time.

The second approach is more theoretically sound, but if the current structural models do not demonstrate good correspondence with measured overlay structural responses, then the performance model developed using this approach will not be applicable until a significant improvement in structural modeling is made. Nevertheless, development of such a model will provide a long-term opportunity for the improvement of the design procedure and will encourage improvement of structural models. That, in turn, will significantly improve design practice, eliminate unnecessary conservatism in design, and make unbonded overlays more cost competitive design alternative.

10.4 DEVELOPMENT OF IMPROVED STRUCTURAL MODELS

In addition to improving unbonded overlay design procedures, the data from the proposed testing program may be used for improving fundamental understanding of structural behavior of unbonded PCC overlays and for improving structural models.

The pavement response data obtained at the NAPTF will help clarify the following aspects of structural behavior of unbonded overlays:

- Degree of composite behavior (effect of friction) of the unbonded overlay and the existing pavement
- Effect of distresses (cracks and spalls) in the existing pavements on strains in the overlay
- Effect of progressive deterioration of the existing pavement and the overlay on overlay responses (strains and deflections)
- Effect of the overlay curling and warping on the overlay strains

Brief descriptions of possible approaches to investigate these effects are presented below.

10.4.1 Degree of Composite Behavior (Friction)

Traditionally, full slip is assumed between the existing pavement and the overlay. This assumption was also used in the mechanistic analysis presented in chapter 3. At the same time, analysis of FWD deflection data for unbonded PCC overlays of highway pavements performed under the NCHRP 10-41 study showed that many sections exhibit significant bond between the overlay and the existing pavement. Data collected under this study will provide an opportunity to investigate this important subject in great details. The key issues related to layer interaction that require clarification include the following:

- Is bond or significant composite behavior (friction) between the PCC layers present in the beginning of the pavement life, and how long does it lasts?
- Does bond/friction exist on the entire surface or, say, only at slab interior? If only a part of the contact area exhibits high friction, does the size of this area depend on loading conditions
- Does the condition of the existing pavement affect the degree of composite behavior?

PCC strains collected from static, slow rolling, and high-speed tests may be used for interface behavior analysis.

First, the PCC/existing slab bond should be evaluated for test cells that do not have distresses in the existing pavements (L2, M2, and H2). The overlay slabs for these cells will be instrumented

with dynamic strain gages (at the overlay top and bottom surfaces) located on top of strain gages in the existing slab (at the existing slab top and bottom surfaces). If the interface behavior is close to unbonded, the strains at the bottom of the overlay and that at the top of the existing pavement should be of an opposite sign. That is, if the bottom of the overlay is in compression, then the top of the existing slab should be in tension, and vice versa. Moreover, the strains at the top surface of the PCC overlay should have the same magnitude but an opposite sign as the strains at the bottom of the overlay (see figure 87). However, if a perfect bond exists, then the strains at the bottom of the overlay and top of the existing slab will have very close magnitude (and the same sign) and will be much smaller than strains at the top of the overlay or the bottom of the existing pavement. Any strain distribution between these two extremes will indicate the presence of partial bond or friction.

It is important to note that the overlay/existing slab interface condition may not necessarily be uniform throughout the entire slab. The interface may exhibit behavior ranging from full bond to full slip, depending on location (slab interior or slab edges), gear location (significant friction under the load and full slip away from the load and vice versa), and time of measurement. Comparison of strains measured at the center of the slab and the slab longitudinal and transverse edges made at different times of the day and at different stages of overlay life will allow us to answer the following questions:

- Is the behavior of the PCC overlay/slab interface closer to full bond or full slip?
- Does it depend on location?
- Does it change with time of the day?
- Does it change with time?

The interface condition should also be determined for the cells with other conditions of the existing pavement. Although those cells will not have sensors in the existing pavement, the interface condition can be evaluated based on the discrepancy between the magnitude in strains at the top and the bottom surface of the overlay. Significant discrepancy (with a greater absolute value of strain at the top) indicates that the neutral axis is moved down from the mid-depth position which, in turn, indicates the presence of significant friction with the underlying pavement.

Based on this analysis, recommendations for interface condition modeling using a layered elastic program (BISAR or JULEA) or a finite element program (ISLAB2000 and ABAQUS) can be provided. Reliable prediction of the interface condition will allow more accurate prediction of overlay structural responses (stresses and deflections), which is crucial for improvement of mechanistic-empirical design procedures.

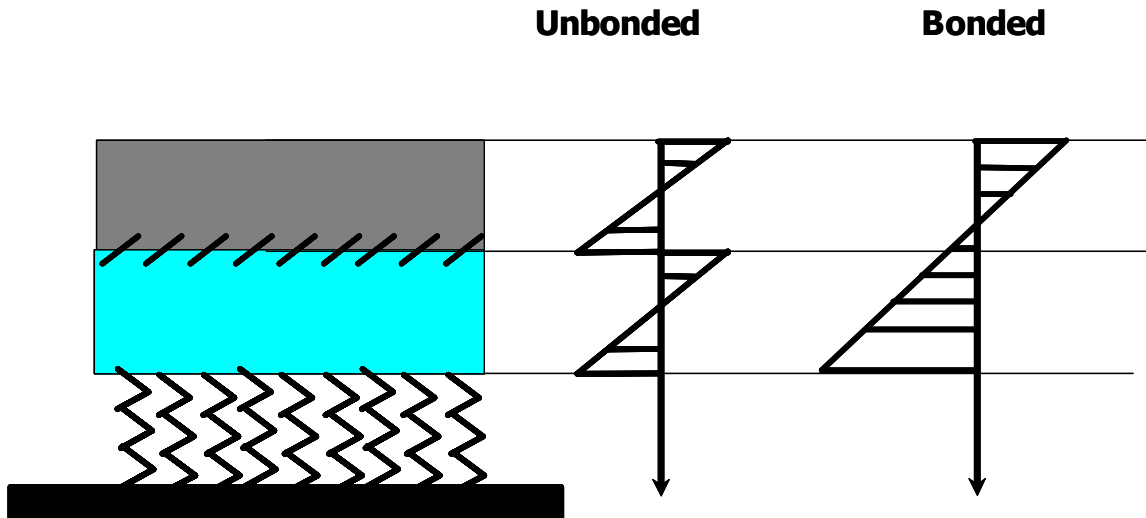


FIGURE 87. EFFECT OF INTERFACE CONDITION ON STRAIN DISTRIBUTION

10.4.2 Effects of Distresses in the Existing Pavements on Overlay Responses

The effect of cracks on the stresses in the overlay is one of the most intriguing problems to be clarified in this study. As shown in chapter 3, finite element models (including ISLAB2000) predict very high localized stresses in the overlay above the cracks in the existing pavement but do not predict a significant change in overlay deflections at the same locations. The structural model adopted by LEDFAA does not predict high stress concentrations but predicts an increase in PCC overlay stresses and deflections compared to the corresponding stresses and deflections of the overlay over an uncracked pavement.

In the proposed study, appropriate longitudinal and transverse strains measured directly above cracks in the existing pavement will be compared with the following strains:

- Strains at the same slab but located 12 in away from the crack (see figure 88)
- Strains in the overlay slab with the same subgrade type and gear loading but existing pavement free from distresses

It is quite possible that a less “rigorous” LEDFAA structural model approach, which uses reduction of stiffness of the underlying pavement due to cracking, will produce a better match with field data than the more sophisticated crack model in ISLAB2000 or other finite element programs. In this case, improved recommendations for stiffness reduction for both layered elastic and finite element models should be developed.

Another perspective on the structural contribution of the existing pavement with different distresses will be obtained from HWD data. HWD deflections of overlay slabs over cracked and uncracked pavements (the same subgrade type and gear loading) may be compared to identify any differences in structural responses. Also, parameters computed from those deflection basins

(such as radii of relative stiffness) can be compared. If cracks in the existing pavement significantly affect the structural behavior of the overlay, the computed radii of relative stiffness for cells with cracked existing pavements will be lower than for the pavements with the same subgrade but uncracked existing pavements.

Deflections from the special FWD tests (conducted at 1-ft intervals) may be used to further investigate the ability of an unbonded overlay to bridge cracks in the existing pavement. The special tests will be conducted on both existing pavements (prior to overlay) on cracked and uncracked cells and at the same locations after the overlay is placed. It is expected that deflections obtained prior to overlay will be different for cracked and uncracked cells. It is not as likely, however, that HWD deflections after the overlay placement will be drastically different. Whatever the actual trends may be, however, it will provide extremely valuable information for validating and improving the structural models for unbonded overlays.

10.4.3 Effects of Joint Mismatching

Another important issue the data from this experiment will help resolve is the effects of joint mismatching on edge stresses in the overlay. Currently, there is no correction factor for adjustment of layered elastic interior stresses for this type of edge effect. Modeling of mismatched joints using finite element programs is a challenging problem. Comparison of edge stresses obtained under matched and mismatched joints will permit the development of another edge stress effect correction factor for the layered elastic model, as well as provide valuable information needed for improvement, validation, and verification of finite element models for joint mismatching.

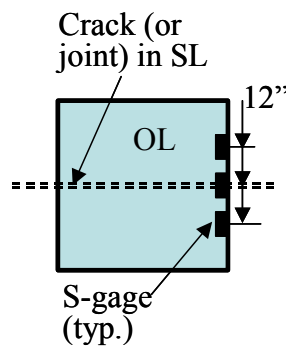


FIGURE 88. STRAIN GAGE ARRANGEMENT TO DETECT STRESS CONCENTRATION IN OVERLAY ABOVE A CRACK IN THE UNDERLYING PAVEMENT

10.4.4 Effect of Slab Curling/Warping

Current design procedures for airport pavements do not consider PCC slab curling and warping directly. However, environmental effects may have a significant effect on PCC overlay performance. Through-thickness differences in temperature and moisture gradients cause

pavement slabs to curl up or down. Curling and warping of concrete slabs can cause different parts of the slabs to lose contact with the foundation. When loads are placed over the unsupported portion of the slab, very high stresses develop. Thus, the contact condition (as affected by slab curling) has a very significant effect on JPCP performance, and it is quite possible that these effects will have to be accounted for in future design procedures.

The NAPTF cannot control temperature conditions, and the pavements are subject to significant temperature variations. In the proposed experiment, PCC temperature and PCC relative humidity throughout the slab thickness will be measured at several locations. This will allow the researchers to evaluate environmental loads on slabs during the experiment. Proper adjustment for the environmental effect will enable researchers to extrapolate the results of the NAPTF tests for different environmental conditions. However, more comprehensive investigation of the environmental effects is needed, and another series of testing dedicated to evaluating the environmental effects is highly recommended. The testing should be conducted at a facility that can simulate the extreme exposure conditions encountered in the field.

Daily variation in PCC overlay curling and warping may result in change in overlay slab support conditions. In this experiment, this effect will be evaluated in two different ways:

- From lift-off gages measurements
- From HWD deflections

Lift-off gage measurements will be evaluated and, if significant vertical movements of overlay slab edges and corners are observed, an attempt will be made to correlate those measurements with temperature gradients.

Another source of information is HWD deflections measured at different times of the day. If a significant difference is observed in normalized deflections and/or backcalculated elastic parameters for certain cells, it is quite likely that the PCC overlay for those cells changes contact condition during the day. Also, HWD corner deflections can be used to detect voids under the overlay corners. Changes in the presence or absence of voids, or changes in void magnitude, also indicate changes in overall contact conditions.

The effect of the existing pavement condition and the effect of joint matching on the PCC overlay curling/warping behavior should also be analyzed. The lift-off gages will be installed on cells with both matched and mismatched joints so that direct comparison will be possible. This comparison, along with HWD data analysis, will clarify whether the stiffness of the existing slab significantly affects the behavior of the overlay subjected to environmental loading only.

The analyses of all strain and deflection data must be made in consideration of the daily and seasonal variations in contact condition. The temperature and moisture data collected throughout the duration of testing can be used to incorporate the effects of slab warping and curling on PCC pavement responses. The effects of another very important aspect of slab curling and warping, built-in curling, are discussed in the following section.

10.4.5 Evaluation of Slab Built-in Curling

The most significant factor that affects the amount of curling in JPCP is temperature gradients, but studies have shown that pavement slabs are not necessarily flat at zero temperature gradient (Eisenmann and Leykauf, 1993; Yu et al., 1998). Other factors, such as moisture gradient and differential shrinkage, can also cause concrete slabs to curl, and a significant amount of curling can be built into a pavement slab. The factors that cause built-in curling in JPCP slabs include the following:

- Temperature gradient at the time of concrete hardening – concrete pavements are exposed to the same climatic conditions during construction as during service. Therefore, concrete slabs can be exposed to a very high temperature gradient while the concrete is still plastic. If a concrete slab hardens while it is exposed to a high positive temperature gradient (slab surface warmer than the bottom), the slab will curl up when the temperature gradient is removed. Thus, any temperature gradient the pavement slab is exposed to during construction will end up as a built-in temperature gradient of the opposite sign but the same magnitude.
- Differential irreversible shrinkage – the concrete near the slab surface tends to dry out more than the bottom. Studies have shown that the moisture level in concrete below about 2 in from the surface remains at constant high level (greater than 80 percent), but the pavement surface can dry out, resulting in differential shrinkage. The effects of differential shrinkage can be represented in terms of equivalent temperature gradient.

The differential shrinkage causes the pavement slabs to curl upward. Because pavements are typically constructed during daytime, the temperature gradients during construction also tend to cause built-in upward curling (effective negative built-in temperature gradient). A recent FHWA-sponsored rigid pavement performance study showed that the magnitude of built-in curling is about 1°F/in on average for pavements in wet-freeze climate (Yu et al., 1998). The combination of built-in curling and actual temperature gradients can cause significant upward curling of the slabs during nighttime hours.

The records of curling deflection movements at slab corners can be used to estimate the amount of built-in curling. The magnitude of built-in curling can be estimated by monitoring curling deflections, because the amount of built-in curling influences the range of curling deflections at slab corners. It is relatively easy for pavement slabs to curl upward because the upward curling is restrained only by the weight of the portion of the slab that is being lifted at the slab corners and edges. However, downward curling is restrained by the weight of almost the entire slab. If significant built-in curling is present (i.e., the slab is curled up significantly at zero temperature gradient), however, the slab can curl downward with almost no resistance until the slab corners are back in contact with the foundation. Thus, the amount of curling movements at slab corners is related directly to the amount of built-in curling, and this relationship can be used to estimate the magnitude of built-in curling in pavement slabs. By observing differences in corner positions from Dipstick measurements, built-in curling maybe estimated (Yu et al., 2002).

Built-in curling and warping are very important components of the total curling and warping that occurs in pavement slabs. Their effects are directly additive to the effects of actual temperature

and moisture gradients, and ignoring the presence of built-in curling will result in a significant discrepancy between measured and analytically predicted pavement responses. Therefore, accurate assessment of the magnitude of built-in curling is critical to obtaining accurate results.

10.5 CONCLUDING REMARKS

Although only a small number of possible scenarios of data analysis are presented in this report, it is clear that the proposed NAPTF testing will provide tremendous opportunities for both short-term improvement of the current design practice and long-term improvement of the fundamental understanding of the overlay behavior and performance.

THIS PAGE INTENTIONALLY LEFT BLANK

11. SUMMARY AND RECOMMENDATIONS

The objective of this study was to develop an experimental design for a large-scale, accelerated testing program for PCC overlays at the NAPTF. Under this study, the research team identified critical factors affecting performance of unbonded PCC overlays, partially bonded PCC overlays, and PCC overlays of AC pavements. The research team evaluated the overall relative importance of testing of different types of PCC overlays at the NAPTF and recommends the following ranking:

- Unbonded PCC overlay – very important
- White topping – important
- Partially bonded PCC overlays – moderately important

It was decided that in the first round of testing at the NAPTF, only unbonded overlays will be tested. The evaluation of the effects of the following critical factors is included in the experimental design for the overlay study:

- Underlying pavement structure and condition: different levels and/or combination of distresses
- Effects of joint mismatching
- PCC joint design (doweled versus undoweled)
- Effects of subgrade type
- Effects of gear geometry
- Effects of traffic wander

To evaluate these factors, a comprehensive experimental program was developed that defines experimental design, construction plan, instrumentation plan, construction scheduler and QA/QC procedure, experimental plan and data analysis roadmap. To ensure that the testing program is implementable, the plan was developed considering the testing capability of the FAA NAPTF, and the plan utilizes the currently available infrastructure of the NAPTF.

The experimental design calls for the construction of unbonded PCC overlay over a specially constructed underlying PCC pavement that has simulated distresses of different type and severity level. The pavement structure test bed takes up the entire width and length of the space available for experimental pavements at NAPTF (900 ft long by 66 ft wide) and is placed on the existing subgrade, which is in three different sections for three different subgrade strengths: low, medium and high. The following pavement parameters were selected:

- Overlay thickness – 9 in
- Overlay joint spacing – 15 ft
- AC separation layer – 2 in
- Existing pavement thickness – 12 in
- Existing pavement joint spacing (uncracked sections) – 15 ft

Although PCC mix design was not a part of this study, it is expected that PCC material properties will be close to properties of the mix used in the 2001–2002 test strip construction (with PCC modulus of rupture exceeding 750 psi). It is also expected that very aggressive PCC curing will be conducted to minimize shrinkage and built-in curling.

A variety of strain gauges, lift-off gauges, thermocouples, PCC humidity gauges, multi-depth deflectometers, and other instrumentation will be installed in both underlying PCC pavement and the PCC overlay. These instruments will provide comprehensive information about the behavior of the unbonded PCC overlay pavement system subjected to different types of gear (static, dynamic, and slow rolling) and temperature loading.

An extensive testing program is proposed for the unbonded overlay testing, which includes the following:

- Subgrade testing
- Laboratory testing of material properties of all constructed layers (underlying pavement, AC interlayer, unbonded overlay)
- Heavy Weight Deflectometer and Dipstick testing
- Gear loading of different gear geometry, load magnitude and rate of loading (static, slow rolling, and high-speed)

The estimated overall cost of the program is \$2,357,529. This includes approximately \$1.40 million for constructing the new overlay pavement sections at the NAPTF, \$485,000 for instrumentation and material testing, and \$470,000 for data analysis.

The proposed series of testing at the NAPTF will be an important step toward improving the current mechanistic-empirical design procedures for unbonded PCC overlays of airport pavements. The data collected from this testing will help develop more reliable and cost-effective design solutions for unbonded PCC overlays by enabling the following:

- Verification of the structural models of unbonded overlays
- Verification of the mechanism of deterioration of unbonded overlays
- Improved characterization of structural contribution of the underlying pavement, including the effect of the existing pavement condition
- Calibration of the performance prediction model
- Development of recommendations for joint mismatching and for use of dowels

Although execution of the proposed testing program and subsequent data analysis will permit immediate improvements of the design procedure for the unbonded PCC overlays, the research team recommends further research in numerous areas, including the following:

- It is highly desirable to investigate the effect of the separation layer features (thickness and material properties) on performance of unbonded PCC overlay. This feature was not

included into final experimental design because the research team recognized that significant laboratory testing should be performed prior to full-scale testing.

- It is desirable to collect information about performance of in-service PCC overlays located in different climatic zones, subgrades, and traffic loading. That information will allow better extrapolation of the results of NAPTF tests. It is highly desirable to collect information about those sections in a unified manner. The collected information should include:
 - Construction records
 - Coring and material testing
 - HWD testing
 - Past traffic information
 - Performance data (preferably, with distress maps)
- Comprehensive evaluation of the effects of environmental factors (temperature and moisture) on PCC pavement performance (new pavement, as well as overlays) is highly desirable. Such testing should be conducted at a facility where the full range of exposure conditions can be simulated (e.g., CRRL).
- If a possibility to perform another round of testing at the NAPTF or another facility comes up, the following factors should be tested:
 - Whitetopping overlays for heavy airfield pavements
 - Partially bonded PCC overlay
 - Unbonded overlays with different interlayer thicknesses with performance of a partially bonded overlays
 - Past traffic information

However, even without these supplemental information, the completion of the proposed testing program will results in significant improvement in rehabilitation practice of PCC pavements.

THIS PAGE INTENTIONALLY LEFT BLANK

12. REFERENCES

1. Betterton, R.M., and M.J. Knutson, "A Five-Year Performance Summary of Fibrous PC Concrete Overlay Research in Greene County, Iowa," Report for Iowa Highway Research Board Project HR-165, 1978.
2. Darter, M.I., and R.J. Roman, General Concepts for Pavement Design, Design Manual NAVFAC DM-21.02. Washington, DC: Department of the Navy, 1989.
3. Darter, M.I., K.T. Hall, and C. Kuo, "Support Under Portland Cement Concrete Pavements," *NCHRP Report 372*, Washington, DC: National Cooperative Highway Research Program, 1995.
4. Dempsey, B.J., W.A. Herlache, and A.J. Patel, *The Climatic-Materials-Structural Pavement Analysis Program User's Manual*, FHWA/RD-82/126. Washington, DC: Federal Highway Administration, 1986.
5. Eisenmann, J., and G. Leykauf, "Effects of Paving Temperatures on Pavement Performance," *Proceedings, 2nd International Workshop on Theoretical Design of Concrete Pavements*, Madrid, Spain, pp. 419-428, 1990.
6. FAA/AC 150/5320-6D, "Airport Pavement Design and Rehabilitation," Federal Aviation Administration Advisory Circular, 1995
7. Guo, E.H., and W. Marsey, "Verification of Curling In PCC Slabs at FAA National Airport Pavement Test Facility," *Proceedings, ASCE Specialty Conference on Advancing Airport Pavements*, Chicago, IL, pp. 15-29, 2001.
8. Gulden, W., and D. Brown, "Overlays for Plain Jointed Concrete Pavements," Final Report, Research Project No. 7502, Georgia Department of Transportation, Forest Park, GA, 1984.
9. Hayhoe, G. F., R.D. McQueen, E.H. Guo, and D.R. Brill, "LEDFAA, The FAA's New Software for Airport Pavement Design," U.S. Department of Transportation report, Office of Aviation Research, Washington D.C., 2002 (in preparation).
10. Hutchinson, R.L., "Resurfacing With Portland Cement Concrete," *NCHRP Synthesis of Highway Practice 99*, 1982.
11. Khazanovich, L. Structural Analysis of Multi-Layered Concrete Pavement Systems. Ph.D. Thesis, University of Illinois, 1994.
12. Khazanovich, L., and T.Yu. "Modeling of Jointed Plain Concrete Pavement Fatigue Cracking in Pavespec 3.0," Transportation Research Record No 1778, pp32-42, 2001.

13. Khazanovich, L., H.T. Yu, S. Rao, K. Galasova, E. Shats, and R. Jones. "ISLAB2000—Finite Element Analysis Program for Rigid and Composite Pavements. User's Guide." ERES Consultants, 2000.
14. Kreger, W.C., "Computerized Aircraft Ground Flotation Analysis – Edge Loaded Rigid Pavement," Research Report No. ERR-FW-572, General Dynamics Corp, 1967.
15. McGhee, K.H., "Portland Cement Concrete Resurfacings," *NCHRP Synthesis of Highway Practice 204*, 1994.
16. McQueen, R.D., J. Rapol, and R. Flynn, "Development of Material Requirements for Portland Cement Concrete Pavements at the U.S. FAA National Airport Pavement Test Facility," Presented at the 2002 FAA Airport Technology Transfer Conference, Atlantic City, New Jersey, 2002.
17. Navy's Military Handbook 1021/4, *Rigid Pavement Design for Airfields*.
18. Packard, R.G. "Design of Concrete Airport Pavement," Portland Cement Association, 1973.
19. Poblete, M.R., R. Salsilli, A.B. Valenzuela, and P. Spratz, "Field Evaluation of Thermal Deformations in Undowelled PCC Pavement Slabs," *Transportation Research Record 1207*, 1989.
20. Rollings, R.S., *Design of Overlays for Rigid Airport Pavements*, FAA Report No. DOT/FAA/PM-87/19, Final Report, 1988.
21. Spellman, D.L., J.H. Woodstrom, and B.F. Neal, *Investigation of Unbonded PCC Overlays*, State of California, Dept. of Public Works, Division of Highways, Material and Research Department, Research Report No. M&R 635165, FHWA D-5-29, 1971.
22. Tabatabaie, A.M., and Barenberg, E.J., "Structural Analysis of Concrete Pavement Systems," ASCE, *Transportation Engineering Journal*, Vol. 106, No. 5, pp. 493-506, 1980.
23. Tayabji, S.D., and P.A. Okamoto, "Thickness Design of Concrete Resurfacing," *Proceedings, 3rd. International Conference on Concrete Pavement Design and Rehabilitation*, Purdue University, pp. 367-379, 1985.
24. Yu, H.T., M.I. Darter, K.D. Smith, J. Jiang, and L. Khazanovich, *Performance of Concrete Pavements, Vol III - Improving Concrete Pavement Performance*, Report No. FHWA-RD-95-111. Washington, DC: Federal Highway Administration, 1988.

25. Yu, T. and L. Khazanovich. (2001). "Effect of Construction Curling on Concrete Pavement Behavior," *Proceedings, Seventh International Conference on Concrete Pavement*, September 9-13, Lake Buena Vista, FL, pp. 55-68, 2001.